## **Calcium signaling in Arabidopsis and potato**

## From Ca<sup>2+</sup> transient to Ca<sup>2+</sup> (in)dependent protein regulation

#### Dissertation

zur

Erlangung des Doktorgrades (Dr. rer. nat.)

der

Mathematisch-Naturwissenschaftlichen Fakultät

der

Rheinischen Friedrich-Wilhelms-Universität Bonn

vorgelegt von

**Annelotte van Dieren** 

aus

Kapelle, Niederlande

# Angefertigt mit Genehmigung der Mathematisch-Naturwissenschaftlichen Fakultät der Rheinischen Friedrich-Wilhelms-Universität Bonn

Gutachterin/Betreuerin: Prof. Dr. Ute Vothknecht

Gutachter: Prof. Dr. Gabriel Schaaf

Gutachterin: Prof. Dr. Veronica G. Maurino

Gutachter: Prof. Dr. Christian März

Tag der Promotion: 29.08.2025

Erscheinungsjahr: 2025

#### **Affirmation**

I hereby declare that I have written this thesis independently and on my own. I have used only the sources listed, and I have clearly indicated where I have quoted or paraphrased material from these sources. I assure that this thesis has not been submitted for examination elsewhere

Bonn, 30.04.2025
Annelotte van Dieren

## **Table of contents**

Αſ	firmation3
Ta	ble of contents4
1.	List of publications 6
2.	Preface7
3.	Introduction8
	3.1 Plant stress
	3.2 Signal transduction in response to stress
	3.3 Plant calcium signaling
	3.4 Calcium signature hypothesis
	3.5 Aequorin-based calcium measurements
	3.6 Calcium channel inhibitors
	3.7 Oxidative stress, ROS and ROS signaling
	3.8 Label-free quantitative proteomics
4.	Results
	4.1. Chapter 1
	Analysis of abiotic and biotic stress-induced Ca <sup>2+</sup> transients in the crop species <i>Solanum tuberosum</i>
	4.2. Chapter 2
	With or without a Ca <sup>2+</sup> signal? A proteomics approach towards Ca <sup>2+</sup> dependent and independent proteome changes in response to oxidative stress in <i>A. thaliana</i>
	4.3. Chapter 3
	Stress Knowledge Map: A knowledge graph resource for systems biology analysis of plant stress responses
5.	Summary36
	Calcium signaling in potato
	Identification of Ca <sup>2+</sup> -dependent proteomics changes
	Stress Knowledge Map – a case study
	Final remarks and outlook
6.	Acknowledgments
7.	References
8.	Appendices

Appendix 1	65
Analysis of abiotic and biotic stress-induced Ca <sup>2+</sup> transients in the crop s	•
Appendix 2	78
With or without a Ca <sup>2+</sup> signal? A proteomics approach towards Ca <sup>2+</sup> independent proteome changes in response to oxidative stress in <i>A. thaliar</i>	•
Appendix 3	113
Stress Knowledge Map: A knowledge graph resource for systems biology a stress responses	

#### 1. List of publications

The following chapters of this thesis have been published in peer-reviewed scientific journals as well as bioRxiv comprising the full extent cumulative thesis.

<u>Chapter 1:</u> van Dieren, A., Schwarzenbacher, R. E., Sonnewald, S., Bittner, A., & Vothknecht, U. C. (2024). Analysis of abiotic and biotic stress-induced Ca2+ transients in the crop species Solanum tuberosum. *Scientific Reports* 14, no. 1 (2024): 27625.

https://doi.org/10.1038/s41598-024-79134-3

<u>Chapter 2:</u> van Dieren, A., Bittner, A., Wurzinger B., Afjehi-Sadat, L., Weckwerth, W., Teige, M., & Vothknecht, U.C. (2025). With or without a Ca<sup>2+</sup> signal; A proteomics approach towards Ca<sup>2+</sup> dependent and independent proteome changes in response to oxidative stress in *A. thaliana*. Preprint in BioRxiv (2025)

https://doi.org/10.1101/2025.03.31.645912

<u>Chapter 3.</u> Bleker, C., Ramšak, Ž., Bittner, A., Podpečan, V., Zagorščak, M., Wurzinger, B., Baebler, Š., Petek, M., Križnik, M., van Dieren, A. and Gruber, J., (2024). Stress Knowledge Map: A knowledge graph resource for systems biology analysis of plant stress responses. *Plant communications*, *5*, no. 6 (2024).

https://doi.org/10.1016/j.xplc.2024.100920

#### 2. Preface

This doctoral thesis titled "Calcium signaling in Arabidopsis and Potato: 'from Ca<sup>2+</sup> transient, to Ca2+ (in)dependent protein regulation," investigates stress-related Ca2+ signaling in the model plant Arabidopsis thaliana and the crop Solanum tuberosum (potato). The focus lies on the early-phase stress response, specifically in the form of a Calcium (Ca<sup>2+</sup>) signaling that arises in the very first seconds following stress perception. The extensive introduction provides a comprehensive overview of Ca<sup>2+</sup> signaling in plant cells, detailing its foundational principles, methodologies and challenges for measuring and interpretation of this response. Additionally, advanced techniques used to investigate the molecular response of Ca2+ signaling are discussed. Following this background, the research findings are presented in a nonchronologically, but content-wise meaningful order. Chapter one describes the research paper where we present the generation and characterization of Solanum tuberosum Ca2+ biosensor lines expressing the genetically encoded Ca2+ biosensor apoaequorin. We measured Ca2+ transients in response to different biotic and abiotic stimuli and made the comparison with the response observed in an established Arabidopsis apoaequorin line. Furthermore, an additional potato sensor line expressing the redox-sensitive Grx1-roGFP2 probe was introduced. This system enabled the analysis of cytosolic redox dynamics in S. tuberosum and facilitated comparative studies with an existing redox-sensitive Arabidopsis sensor line. Chapter two shows a very different approach towards the elucidation of Ca<sup>2+</sup> signaling. Here we performed a full proteome analysis, investigating the effect of Ca<sup>2+</sup> transients induced by an oxidative stress stimulus on protein regulation. To differentiate between Ca<sup>2+</sup>-dependent and Ca<sup>2+</sup>-independent protein responses to oxidative stress, a subset of samples was treated with the Ca<sup>2+</sup> channel inhibitor LaCl<sub>3</sub>, thereby suppressing the transient Ca<sup>2+</sup> signal. Comparative analysis of proteomic data between LaCl<sub>3</sub> treated and non-treated samples provided insights into the distinct regulatory mechanisms associated with oxidative stress. Chapter three extends the findings of chapter two by employing a novel analytical framework, the Stress Knowledge Map (SKM), to further analyse the data. This computational tool compilates existing knowledge of plant stress response mechanisms extracted from published datasets, facilitating a systems-level analysis of stress signaling networks.

#### 3. Introduction

#### 3.1 Plant stress

Plants growing in natural environments are continuously exposed to a wide range of ecological and environmental changes, natural disasters, and interference by humans, animals and pathogens. These environmental variations can impose stress on plants, which refers to any environmental aspect that can be harmful or detrimental adversely affects their growth, development, and survival (Baweja & Kumar, 2020). Stress factors can trigger a cascade of physiological and biochemical responses, leading to reversible and/or irreversible damage. Such stress-induced responses can significantly influence plant growth dynamics, reproduction, and ultimately, crop yield, posing serious concerns for agricultural productivity and global food security (Singla & Krattinger, 2016).

Environmental stress can be broadly categorized into biotic and abiotic stress factors. Biotic stress arises from interactions with living organisms, including herbivory, pathogen infections (bacteria, fungi, viruses), parasitism, and competition with other plants (Singla & Krattinger, 2016). These biological challenges often lead to substantial losses in crop productivity and require complex defence mechanisms from plants to mitigate their impact. Conversely, abiotic stress factors originate from non-living environmental elements, such as extreme temperature fluctuations, drought, excessive or insufficient water availability, soil salinity, heavy metal toxicity, and nutrient deficiencies (Ben-Ari & Lavi, 2012). The negative effect of these different stressors and the suboptimal conditions they provide is highly reflected on crop yield and biodiversity. Studies have shown that more than 50% of the yield in maize, grain yield for wheat and yield of rice plants got lost as a result of the negative effect of drought (Balla et al., 2011; Fahad et al., 2017, 2017). This negative effect on yield losses is only made more significant by the changing climate, resulting in more extreme weather conditions. In addition, these unfavorable environmental conditions could potentially have a catastrophic effect on the biodiversity of ecosystems, putting an additional pressure on plant species and their ecosystems that are already endangered (Bartholomeus et al., 2011). In order to protect ecosystems, biodiversity and farming crops it is important to gain knowledge and information to understand how plants sense and res to different stresses and environmental changes. More specifically, we need a better understanding on how signal transduction pathways are involved in sensing different biotic and abiotic stressors, and how plants are able to regulate a cellular

and molecular response, to defend themselves against challenging environmental circumstances.

#### 3.2 Signal transduction in response to stress

Plants are sessile organisms, meaning they lack the ability to escape in response to adverse environmental conditions. Consequently, they have evolved sophisticated molecular and structural defence mechanisms to detect, respond and mitigate stressors. One prominent physical defence strategy in land plants is the formation of a cuticle, a lipid-based extracellular layer that serves as a barrier against desiccation, pathogens, and airborne pollutants while providing structural reinforcement (Domínguez et al., 2011). Such structural adaptations are complemented by a variety of molecular defence mechanisms that enable plants to sense and respond to environmental stress through intricate signaling pathways (Suzuki et al., 2014).

Higher plants are capable of perceiving external environmental cues such as chemical signals, biotic interactions, and abiotic fluctuations. These signals are internally processed through complex transduction pathways that initiate downstream responses, influencing physiological, biochemical, and developmental processes (Mulligan et al., 1997). Signal transduction pathways involve a complex network of interactions that coordinate biochemical and physiological responses, often as a defence mechanism against a specific stressor. Key signaling molecules, including reactive oxygen species (H<sub>2</sub>O<sub>2</sub>), abscisic acid (ABA), and calcium ions (Ca<sup>2+</sup>), serving as messengers to transmit stress signals within the plant system (Allan et al., 2022; Li et al., 2022a). These signals are perceived by protein kinases such as calciumdependent protein kinases (CDPKs) and transcription factors like dehydration-responsive element-binding factors (DREBs), which then activate stress-responsive genes and metabolic pathways to enhance the plant's defensive capacity (DeFalco et al., 2010; Mohanta et al., 2019a). The downstream molecular responses triggered by these sensing pathways often involve the upregulation of stress-responsive genes and the modulation of enzymatic activity to mitigate damage. Such responses facilitate adaptive modifications in cellular metabolism, osmotic balance, and antioxidant activity, enhancing plant resilience to detrimental conditions (Kissoudis et al., 2014). Moreover, considerable crosstalk exists between different signaling pathways, meaning that multiple pathways can lead to the same effects due to overlapping

mechanisms. This indicates that a single stress response can help the plant protect itself against multiple stressors simultaneously (Kissoudis et al., 2014).

#### 3.3 Plant calcium signaling

Calcium is an essential macronutrient in plants, serving both structural and signaling functions. As a structural component, it plays a critical role in cell wall stability and membrane integrity. In its ionic form (Ca<sup>2+</sup>), calcium acts as a highly dynamic intracellular messenger, mediating signal transduction in response to a wide range of developmental cues and environmental stresses (Kudla et al., 2010a; Thor, 2019). Calcium-based signaling pathways are central to plant adaptive responses, bridging large-scale intercellular signaling with small-scale intracellular mechanisms to coordinate a unified defensive response.

The basic process of Ca<sup>2+</sup> signaling starts when abiotic and biotic stresses, as well as internal stimuli, trigger an increase in calcium ion concentration ([Ca<sup>2+</sup>]). These calcium transients function as encoded messages that are subsequently decoded by calcium sensors, including calmodulins (CaMs), calmodulin-like proteins (CMLs), calcium-dependent protein kinases (CDPKs), and Calcineurin-B-like proteins (CBLs) along with their interacting protein kinases (CIPKs) to mediate downstream signaling events (Edel et al., 2017). Activation of these sensors leads to the modulation of various transcription factors, metabolic enzymes, and ion transporters, thereby orchestrating a well-coordinated cellular response tailored to the specific environmental stimulus. A schematic overview of the core components of calcium signaling in plant stress responses is provided in Figure 2, illustrating the fundamental interactions between calcium sensors, downstream effectors, and cellular responses.

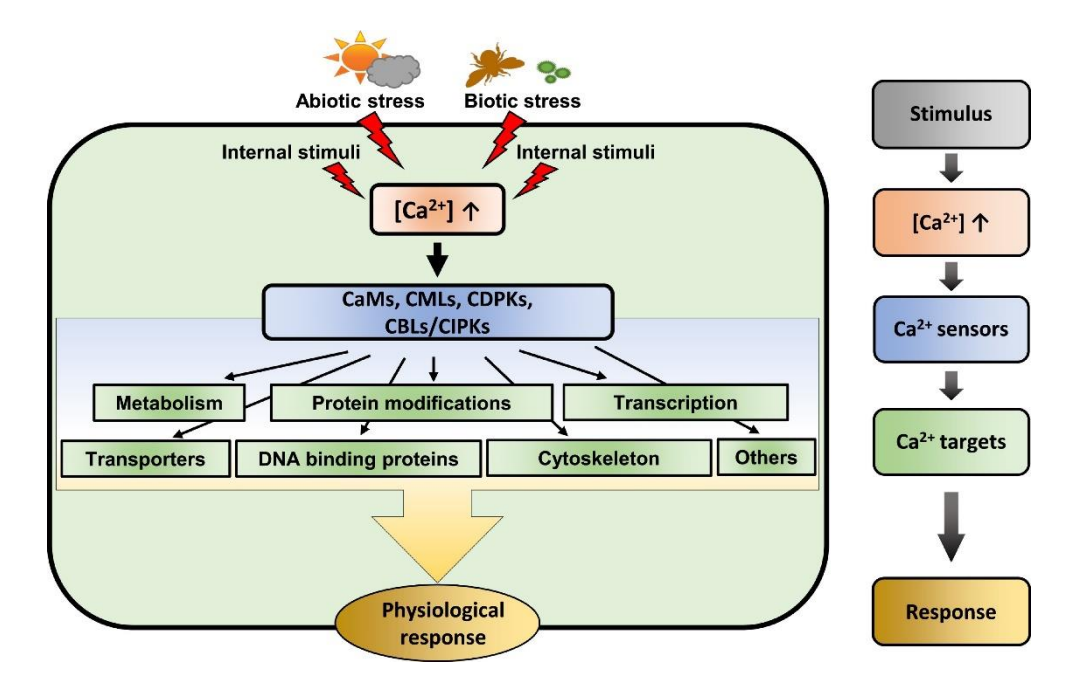
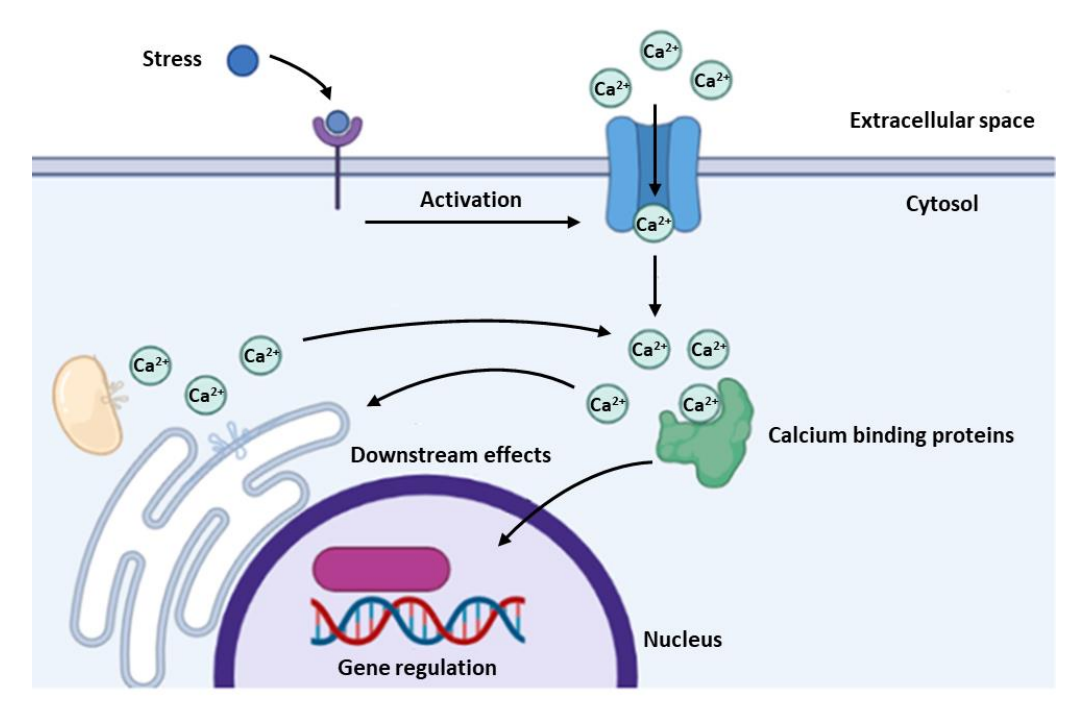


Figure 1: The  $Ca^{2+}$  signaling network in plant cells (Pirayesh et al., 2021). Abiotic and biotic stress, along with internal stimuli, trigger an increase in  $[Ca^{2+}]$ , which is detected by  $Ca^{2+}$  sensors such as calmodulins (CaMs), calmodulin-like proteins (CMLs),  $Ca^{2+}$ -dependent protein kinases (CDPKs), and Calcineurin-B-like proteins (CBLs). These sensors, in turn, activate various downstream processes, leading to a coordinated cellular response that is specific to the initial stimulus and integrates signals from other pathways.

At the cellular level, the process of calcium signaling in response to stress can be described as follows: when receptor proteins embedded in the plasma membrane detect a stress factor, various messenger chemicals, transcription factors, and hormones are activated throughout. A key player in this process are calcium ions (Ca<sup>2+</sup>), which act as a rapid signaling substrate in response to both biotic and abiotic stress factors (Clapham, 2007). Calcium signaling relies on the chemistry affected by the significant electrochemical gradient across cell membranes. This gradient is maintained by proton-ATPases (H<sup>+</sup>-ATPases) and calcium-ATPases (Ca<sup>2+</sup>-ATPases), which use adenosine triphosphate (ATP) as an energy source to transport positively charged ions (including protons) out of the cell against the existing electrochemical gradient. As a result, this movement strengthens the gradient, leading to a rapid influx of Ca<sup>2+</sup> into the cell when a stress response is triggered, thereby initiating a signaling cascade (Demidchik et al., 2018a; Klejchova et al., 2021; Palmgren, 2001). The influx of calcium ions across the cell membrane is visualised in figure 3.



**Figure 2:** Influx of  $Ca^{2+}$  ions across the cell membrane, triggered by a stress factor. After the release,  $Ca^{2+}$  ions bind to calcium binding proteins, which triggers an additional  $Ca^{2+}$  release from vacuoles and the endoplasmic reticulum. In addition, calcium binding proteins trigger downstream effects, such as gene regulation. Adjusted from (Blake Christopher Elliot, 2023)

Free calcium ions (Ca<sup>2+</sup>) act as secondary messengers in plants and other eukaryotes, playing a crucial role in various stress response signaling pathways, as well as in development and growth (Thor, 2019). For Ca<sup>2+</sup> to trigger a defensive response to stress by upregulating related genes, the initial signal must be received and decoded. This process is facilitated by Calmodulins (CaMs), Calmodulin-like proteins (CMLs), and Calcium-dependent Protein Kinases (CDPKs) (Zielinski, 1998). When a stress signal is detected by specialized cellular machinery on the plasma membrane, calcium ion channels open, allowing Ca<sup>2+</sup> ions to flow into the cell. This influx of Ca<sup>2+</sup> generates a wave that is detected by calcium-binding proteins, continuing the signaling cascade and initiating defence responses such as altered gene transcription (Figure 3).

In recent studies, an increase in cytosolic Ca<sup>2+</sup> has been observed in response to various external stimuli, such as pathogen elicitors and drought stress (H. Knight et al., 1997a; Thor & Peiter, 2014; Chi et al., 2021). Pathogen elicitors are molecules produced by pathogens that trigger a defence response in plants (Gill et al., 2016). This fluctuation in cytoplasmic Ca<sup>2+</sup> activates various calcium-binding proteins (CBPs) that facilitate rapid signaling processes throughout plant tissues (Bergey et al., 2014). The most common and well-known CBPs are

Calmodulin (CaM) and Calmodulin-like (CML) proteins, which act as sensors that detect increases in Ca<sup>2+</sup> during abiotic and biotic stress (Aldon et al., 2018). CaM and CML proteins bind to Ca<sup>2+</sup>, forming a complex that triggers subsequent mechanisms in the signaling pathway, such as the phosphorylation of NADPH oxidase proteins, which leads to an increase in hydrogen peroxide (H<sub>2</sub>O<sub>2</sub>). H<sub>2</sub>O<sub>2</sub> is a well-researched stress signaling molecule in plants and works in conjunction with Ca<sup>2+</sup> (Pandey et al., 2011). Additionally, increased cytosolic Ca<sup>2+</sup> has various other effects, including coordination with plant hormones and specialized enzymes, and, most significantly, the regulation of gene expression. The activation or upregulation of gene elements aids plant defence and can result in widespread changes in gene expression throughout the plant's tissues (Bowler & Fluhr, 2000).

#### 3.4 Calcium signature hypothesis

A critical feature of calcium signaling is its spatiotemporal specificity. Distinct stressors elicit unique calcium signatures, characterized by variations in amplitude, duration, and frequency of [Ca²+] fluctuations. These unique signatures contribute to the specificity of the response, allowing plants to distinguish between different environmental challenges and activate appropriate defensive strategies (Li et al., 2022a). Furthermore, crosstalk between calcium signaling and other signal transduction pathways, such as those involving reactive oxygen species (ROS) and phytohormones (e.g., abscisic acid), enables plants to integrate multiple stress signals, ensuring a robust and adaptive response to complex environmental conditions (Ranty et al., 2016).

A variety of biotic and abiotic stresses, along with several developmental processes, lead to an increase in cytosolic calcium ion concentration ([Ca<sup>2+</sup>]<sub>cyt</sub>). This increase occurs through a regulated influx of Ca<sup>2+</sup> from both external sources and internal stores into the cytosol (McAinsh & Pittman, 2009; Kudla et al., 2010a) The rise in [Ca<sup>2+</sup>]<sub>cyt</sub> varies in its spatio-temporal characteristics, including amplitude, frequency, and specific location, depending on the type of stimulus. These distinct patterns of [Ca<sup>2+</sup>]<sub>cyt</sub> changes, often referred to as "calcium signatures," (Allen et al., 2001) are crucial for the specificity of calcium signaling and contribute to varied and appropriate cellular responses to different stimuli. Each calcium signature results from a complex interaction between various Ca<sup>2+</sup> influx channels and efflux transporters that are located in the plasma membrane and the membranes of cellular organelles (McAinsh &

Pittman, 2009; Demidchik et al., 2018a). Stimulus-specific Ca<sup>2+</sup> signals are typically detected and decoded by various Ca<sup>2+</sup> sensors, including calmodulin (CaM), calmodulin-like proteins (CMLs), Ca<sup>2+</sup>-dependent protein kinases (CDPKs), as well as calcineurin B-like proteins (CBLs) and their interacting protein kinases (CIPKs) (Mohanta et al., 2019a; DeFalco et al., 2010). These Ca<sup>2+</sup> sensors are encoded by extensive gene families in plants. While CaM is found in all eukaryotes, the other sensor families are plant- specific. The huge diversity and abundance of these Ca<sup>2+</sup> sensors are thought to enhance the specificity and flexibility of signal processing in response to various stimuli, depending on the tissue type and developmental stage.

The calcium signal hypothesis posits that these spatio-temporal dynamics of free calcium ions encode various stimuli (McAinsh & Hetherington, 1998). These calcium signatures can be decoded by specific calcium machinery (Hashimoto & Kudla, 2011; Lenzoni et al., 2018). Differences in the proteomes of various cell types, potential cell clusters, and different organs will influence how cells receive, transduce, and translate these signals (Fig. 4 adjusted (Martins et al., 2019)). For instance, the presence or absence of stimulus-specific calcium channels will affect cellular responses. Therefore, decoding involves more than just understanding the signatures of the code. The role of calcium as a signaling molecule is deeply connected to calcium-binding proteins, calcium channels, and transporters. As mentioned earlier, these components are crucial for creating specific signatures in response to both internal changes and environmental cues. Calcium-binding proteins facilitate the transduction and translation of the signal. In all scenarios, cell-specific expression patterns likely contribute to functional and distinctive signaling and decoding processes. Calcium-binding proteins typically contain an EF-hand motif responsible for calcium binding. Examples of these proteins include calmodulin (CaM), calmodulin-like proteins (CML), calcium-dependent protein kinases (CDPK), and calcineurin B-like (CBL) proteins (Miller et al., 2014).

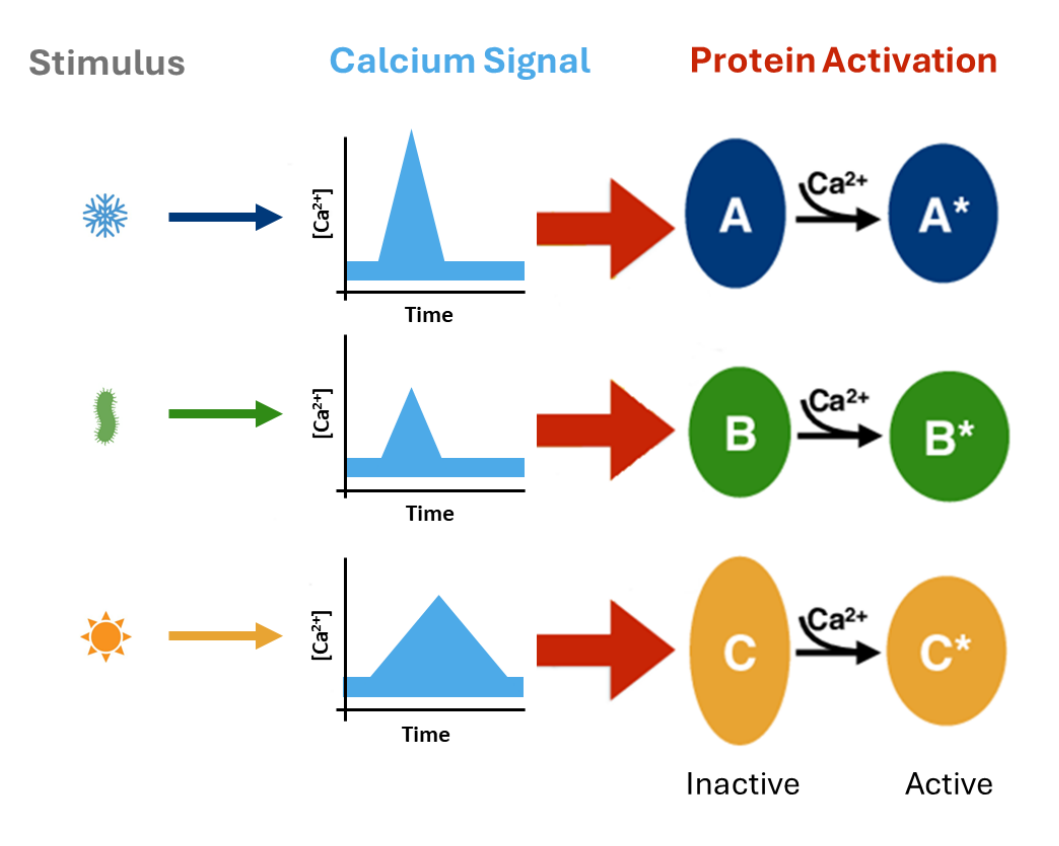


Figure 3: The calcium signature hypothesis states the information encoded in the spatiotemporal pattern of free calcium ions leads to differential activation of downstream targets. Stimulus specificity resides in specific calcium signals that can vary in amplitude, duration and shape. Due to the specificity of the signal, proteins and pathways are activated that are required to initiate the appropriate response (figure adjusted from Martins et al., 2019)

#### 3.5 Aequorin-based calcium measurements

Visualizing Ca<sup>2+</sup> signatures in a living organism requires specialized techniques that provide information on the location and quantity of Ca<sup>2+</sup> in various areas while minimizing invasiveness. This approach allows researchers to observe signals that accurately represent natural conditions. The tools used to indicate calcium localization in these imaging techniques are known as calcium sensors.

The earliest calcium sensor developed was Aequorin, a bioluminescent protein consisting of a single polypeptide chain of 22 kDa, isolated from the jellyfish Aequorea victoria (Shimomura et al., 1962). Apoaequorin interacts with a low-molecular-weight luminophore, coelenterazine, to generate functional aequorin through a biochemical process known as reconstitution. This reaction necessitates the presence of molecular oxygen. Structurally, aequorin exhibits similarity to the calcium-binding protein calmodulin, possessing three EF-hand calcium-binding domains, in contrast to the four EF-hand motifs present in calmodulin. Additionally,

aequorin contains a binding site for both coelenterazine and molecular oxygen. Upon calcium ion (Ca²+) binding, coelenterazine is oxidised into coelenteramide, leading to a conformational change in the protein, converting it into a luciferase, accompanied by the release of carbon dioxide (CO₂) and the emission of blue light at a wavelength of 462 nm (Shimomura, 1995). Aequorin displays high selectivity for Ca²+, as other divalent and monovalent cations such as magnesium (Mg²+) and potassium (K⁺) do not trigger luminescence. However, these ions can modulate the sensitivity of aequorin to Ca²+ by reducing its responsiveness (Thomas, 1982). The functional range of aequorin enables the detection of free intracellular calcium concentrations up to  $100 \, \mu\text{M}$ , though in practice, most experimental measurements fall within the range of  $100 \, \text{nM}$  to  $10 \, \mu\text{M}$  (Mithöfer & Mazars, 2002a).

As an indicator of cytosolic calcium concentration ([Ca<sup>2+</sup>] <sub>cyt</sub>), aequorin has several advantages over conventional fluorescent dyes. Luminescence-based measurements usually exhibit a high signal-to-noise ratio, as endogenous luminescence is typically minimal under optimal conditions. Nonetheless, it is essential to account for endogenous chemiluminescence, which can constitute up to 30% of the total signal in plant cells (Gilroy et al., 1989). Aequorin, being a naturally occurring protein, is presumed to be non-toxic and is expected to localize within the cytoplasm unless specifically directed to alternative cellular compartments. Furthermore, its luminescence remains unaffected at pH values exceeding 7, and its application circumvents photodamage associated with fluorescence-based excitation illumination. The availability of apoaequorin has significantly improved following the successful cloning of the aequorin gene (Inouye et al., 1985; Prasher et al., 1985). However, despite these advancements, the essential cofactor coelenterazine remains costly, posing a limitation to widespread use.

Aequorin can be introduced into the cytoplasm of plant cells through recombinant DNA technology, enabling stable transformation with the cDNA encoding the apoprotein (H. Knight & Knight, 1995a). In transgenic plants, aequorin can be reconstituted in vivo by exogenous application of coelenterazine, facilitating the production of sufficient luminescence to allow reliable quantitative measurements without necessitating cellular disruption. Since all cells inherently generate their own calcium indicator, dynamic fluctuations in intracellular Ca<sup>2+</sup> concentrations can be monitored in intact, living plants and samples taken from these plants. Stable transformation of the apoaequorin gene has been successfully achieved in several plant species, including Arabidopsis thaliana (H. Knight et al., 1996), Nicotiana tabacum (M. R. Knight

et al., 1991a), and the moss Physcomitrella patens (Russell et al., 1996), and more recently in the crop species barley (Giridhar et al., 2022a) and potato (A. Van Dieren et al., 2024a) as well.

A commercially available plasmid (Molecular probes), designated pMAQ2, contains the cloned apoaequorin gene within a binary vector. This plasmid encodes a constitutively expressed cytosolic form of apoaequorin, regulated by the cauliflower mosaic virus (CaMV) promoter, this is the most commonly used form in plant-based aequorin studies. Beyond its cytosolic expression, aequorin has also been successfully targeted to various subcellular compartments through the incorporation of specific targeting sequences. These sequences may consist of either peptide leader motifs or complete polypeptides corresponding to proteins that naturally localize to the desired subcellular domain. Engineered forms of apoaequorin have been developed for targeted expression in distinct organelles within plant cells. For instance, variants have been constructed to localize within the chloroplast (Johnson et al., 1995) via the plasmid pMAQ6 (Molecular probes). Additionally, apoaequorin has been directed to the nucleus (Van Der Luit et al., 1999) and the cytosolic surface of the vacuolar membrane (H. Knight et al., 1996). All of these plasmid constructs include a selectable marker conferring kanamycin resistance, facilitating the identification of transformed plant cells through antibiotic selection.

The intensity of light emission produced by recombinant aequorin has been quantified at approximately  $4.30-5.16 \times 10^{15}$  photons per milligram of aequorin (Shimomura, 1991). However, the levels of aequorin that can be effectively expressed in plant tissues remain relatively low, typically amounting to only a few picograms of protein per milligram of fresh tissue weight. Consequently, the detection of the blue light emitted in response to intracellular calcium fluctuations requires the use of highly sensitive photon-counting instrumentation. An effective luminescence detector must be capable of capturing light signals spanning a wide range, varying by several orders of magnitude in intensity, ranging from only a few photons per second to several million photons per second. Furthermore, in addition to possessing high sensitivity, such a detector must provide adequate temporal resolution to accurately record dynamic changes in luminescence over time (Halliwell, 1989). The ability to resolve these rapid fluctuations is critical for precise measurement of transient calcium signaling events within living plant cells.

Each Aequorin-based experiment to measure intracellular calcium levels begins with the reconstitution of apoaequorin. The optimal duration of reconstitution varies depending on the experimental conditions; however, for cytosolic aequorin-expressing plants, a reconstitution period of 6 to 18 hours is generally sufficient. Following this period, aequorin levels remain high for at least 24 hours (M. R. Knight et al., 1991a). The amount of aequorin reconstituted is positively correlated with the concentration of coelenterazine, with levels increasing as coelenterazine concentration rises, at least up to 10 µM (M. R. Knight et al., 1991a). Once reconstitution is complete, the actual measurement of calcium dynamics can begin. The first step in the measurement process involves recording the total luminescence emitted throughout the experiment. At the end of each experiment, any remaining aequorin within the sample must be fully discharged to account for the total luminescent capacity of the system. This is achieved by applying a discharge solution containing a high concentration of Ca<sup>2+</sup> along with ethanol. A commonly used discharge solution consists of 1 M CaCl<sub>2</sub> and 10% ethanol (Fricker et al., 1999). Following the application of this solution, photon emission continues to be recorded for an additional 1-2 minutes or until the luminescence signal declines to approximately one-thousandth of the maximum value observed during the experiment. To accurately determine the intracellular calcium concentration ([Ca<sup>2+</sup>]), raw luminescence measurements must be adjusted for background fluorescence originating from non-transgenic (wild type) material. Additionally, the rate constant, k, at any given time point within the experiment is determined by calculating the ratio of the photon counts at that specific time to the total photon counts recorded throughout the entire experiment, including the final aequorin discharge phase. This calculation is expressed by the following equation:

$$k = \frac{luminescence\ counts\ s^{-1}}{total\ luminescence\ counts}$$

Where *luminescence counts s*<sup>-1</sup> represents the photon counts at a given time point, and *total luminescence counts* denotes the total photon counts over the course of the experiment, including those obtained during aequorin discharge. To convert luminescence data into actual calcium concentrations, an empirically derived calibration formula is applied. This formula was

originally developed by Cobbold and Rink (Cobbold & Rink, 1987), the equation for calcium concentration is as follows:

$$pCa = 0.332588(-logk) + 5.5593$$

Where pCa represents the negative logarithm of the free calcium ion concentration. It is important to note that these calibration coefficients were determined under controlled experimental conditions at 25°C. Since the luminescence properties of aequorin are temperature-dependent, different calibration values are required for experiments conducted at alternative temperatures. This temperature sensitivity presents a challenge when performing experiments that involve thermal perturbations, such as cold-shock treatments, as variations in temperature may affect the accuracy of calcium measurements.

#### 3.6 Calcium channel inhibitors

Blocking Ca<sup>2+</sup> channel activity is a valuable approach for investigating calcium-dependent processes in plant cells. Ca<sup>2+</sup> channels mediate the release of stored Ca<sup>2+</sup> into the cytoplasm upon signaling, allowing Ca<sup>2+</sup> to move down its electrochemical gradient, a crucial mechanism for the change in cellular Ca<sup>2+</sup> ([Ca<sup>2+</sup>]) functioning as a secondary messenger. Lanthanum chloride (LaCl<sub>3</sub>) is an inorganic compound and a well-known Ca<sup>2+</sup> channel inhibitor (Tracy et al., 2008a). La<sup>3+</sup> ions interfere with various Ca<sup>2+</sup>-dependent processes in both plant and animal systems by interacting with binding sites within Ca<sup>2+</sup> channels or stimulating Ca<sup>2+</sup>-ATPases, thereby preventing the rise of [Ca<sup>2+</sup>] (Bush, 1995; Belyavskaya, 1996). Due to its high positive charge, LaCl<sub>3</sub> is believed to be unable to cross the plasma membrane (Evans, 1990), effectively blocking extracellular Ca<sup>2+</sup> influx by preventing Ca<sup>2+</sup> from entering the cell via the plasma membrane.

In plant biology, LaCl<sub>3</sub> has been employed to elucidate the role of calcium signaling in various stress responses. For instance, a study in rice shows that LaCl<sub>3</sub> strongly inhibited most of the Ca<sup>2+</sup> increase in response to NaCl (Zhang et al., 2015a). For tea plants (*Camellia sinensis*) exogenous application of LaCl<sub>3</sub> under cold stress conditions disrupted calcium signaling

pathways, leading to impaired physiological responses (Chen et al., 2024). Similarly, in snapdragon (Antirrhinum majus L.) spikes, LaCl<sub>3</sub> inhibited gravitropic bending by preventing gravity-dependent processes such as chloroplast sedimentation and the establishment of ethylene gradients across the stem-bending zone. These findings imply that the gravitropic response in shoots may be mediated through a calcium-dependent pathway involving modulation of cytosolic calcium at various stages (Friedman et al., 1998). In barley leaf and root tips it was shown that La<sup>3+</sup> strongly inhibited the [Ca<sup>2+</sup>]<sub>cyt</sub> response induced by NaCl, H<sub>2</sub>O<sub>2</sub>, flg22 and mannitol indicating a critical role of extracellular Ca<sup>2+</sup> in the induction of stress-associated Ca<sup>2+</sup> signatures in barley (Giridhar et al., 2022a). Also, for *Arabidopsis*, the inhibitory effect of LaCl<sub>3</sub> was described, Ca<sup>2+</sup> transients triggered by H<sub>2</sub>O<sub>2</sub> treatment were significantly inhibited upon LaCl<sub>3</sub> incubation (Rentel & Knight, 2004a). These studies demonstrate that LaCl<sub>3</sub> functions as a calcium channel inhibitor across a wide diversity of plant species, tissues and upon differently induced Ca<sup>2+</sup> transients.

#### 3.7 Oxidative stress, ROS and ROS signaling

Reactive oxygen species (ROS), including superoxide anion (O<sub>2</sub> \*-), hydrogen peroxide (H<sub>2</sub>O<sub>2</sub>), and hydroxyl radicals (OH\*), are partially reduced or excited forms of atmospheric oxygen (Halliwell, 1989). In plants they are continuously produced as unavoidable byproducts of aerobic metabolism, but in addition they function as signaling molecules (König et al., 2012a; Foyer & Noctor, 2013; Vaahtera et al., 2014; Mignolet-Spruyt et al., 2016). Cells likely first utilized ROS as signaling molecules to detect hazardous atmospheric oxygen levels or monitor metabolic reactions. Over time, they have evolved to regulate nearly every aspect of life in plants, animals, and most eukaryotic organisms (Mittler et al., 2011). In higher plants, ROS have been shown to regulate development, differentiation, redox balance, stress signaling, interactions with other organisms, systemic responses, and cell death (Mittler et al., 2011; Foyer & Noctor, 2013; Vaahtera et al., 2014; König et al., 2012a; Mignolet-Spruyt et al., 2016).

As toxic byproducts of aerobic metabolism, ROS are mainly generated in chloroplasts, mitochondria, and peroxisomes, where electron transport chains (ETC) generate superoxide radicals (Møller, 2001; Takahashi & Badger, 2011). However, they can be formed in any other cellular compartment containing proteins and molecules with a high enough redox potential to transfer or donate an electron to atmospheric oxygen. To prevent excessive ROS

accumulation, plants use antioxidant systems to neutralize and detoxify the cells. Enzymatic scavengers include superoxide dismutase (SOD), ascorbate peroxidase (APX), and catalase (CAT), while non-enzymatic molecules such as ascorbic acid (AsA) and glutathione (GSH) play crucial roles in ROS detoxification (Apel & Hirt, 2004; Ahmad et al., 2010). The continuous production of ROS as a byproduct of aerobic metabolism, along with their removal by cellular antioxidative mechanisms, helps to mitigate their potential toxic effects, such as oxidation and damage to DNA, RNA, proteins, and membranes, collectively known as oxidative stress (Mittler, 2017). Cellular antioxidative systems maintain ROS at a basal, non-toxic level, and any disruption of this balance can serve as a trigger for ROS-mediated signaling reactions (Mignolet-Spruyt et al., 2016; Mittler et al., 2004; Vaahtera et al., 2014).

As signaling molecules, ROS exhibit remarkable versatility due to their diverse properties, including distinct levels of reactivity, sites of production, and the potential to cross biological membranes (Foyer & Noctor, 2013; König et al., 2012a; Mignolet-Spruyt et al., 2016). Low concentrations of ROS can activate various signaling cascades, including redox-sensitive receptors (NPR1, Heat Shock Factors), redox-regulated ion channels, ROS-sensitive phosphatases, histidine kinases, and ROS-sensitive phosphatases (Apel & Hirt, 2004; Demidchik & Maathuis, 2007; Foyer & Noctor, 2013; Sierla et al., 2013). ROS-mediated signaling is also closely linked to various signaling cascades that involve secondary messengers such as nitric oxide, phytohormones, and Ca<sup>2+</sup> dynamics. As described before in this thesis, calcium plays a crucial role in regulating numerous developmental processes and responses to environmental stressors. ROS- and Ca<sup>2+</sup> signaling have in common that they both are influencing various cellular processes, including the regulation of gene transcription and the activation of downstream responses (Ren et al., 2023).

Various studies support the existence of a crosstalk between  $Ca^{2+}$  and  $H_2O_2$  signaling pathways in response to both abiotic and biotic stress factors (Marcec et al., 2019; Ravi et al., 2023). Multiple studies suggest that  $Ca^{2+}$  acts as an upstream regulator in  $H_2O_2$  signaling by modulating its production. In plants, respiratory burst oxidase homologs (RBOHs) contain a cytosolic N-terminal regulatory domain equipped with  $Ca^{2+}$ -binding EF-hand motifs and  $Ca^{2+}$ -dependent phosphorylation sites, which serve as targets for CDPKs or CPKs and are required for RBOH activation (Kobayashi et al., 2007; Ogasawara et al., 2008; Dubiella et al., 2013). Conversely, other findings indicate that  $H_2O_2$  functions as an upstream signal that triggers

 $[Ca^{2+}]_{cyt}$  transients, facilitating plant responses such as stomatal closure, programmed cell death, and other stress adaptation mechanisms.  $H_2O_2$ -induced  $Ca^{2+}$ -release is thought to be mediated by the direct activation of  $Ca^{2+}$ -permeable channels. Several candidate proteins, including annexins, cyclic nucleotide-gated channels (CNGCs), and mechanosensitive ion channels (MSLs), have been proposed to act as  $H_2O_2$ -activated  $Ca^{2+}$  channels that mediate  $Ca^{2+}$  influx into the cytosol (Demidchik et al., 2018a; Fichman et al., 2022)

A notable development in this area was the identification of a plant-specific  $H_2O_2$  sensor,  $H_2O_2$ -INDUCED  $Ca^{2+}$ INCREASES 1 (HPCA1), which mediates  $H_2O_2$ -induced  $Ca^{2+}$  channel activation in guard cells, leading to elevated  $[Ca^{2+}]_{cyt}$  levels and subsequent stomatal closure (Wu et al., 2020). Notably, HPCA1 has also been implicated in systemic ROS and  $Ca^{2+}$  cell-to-cell signaling. This mechanism involves the  $Ca^{2+}$ -permeable channel MSL3, along with the  $Ca^{2+}$  sensor CBL4 and its interacting protein kinase CIPK26 (Fichman et al., 2022). Nonetheless, despite the growing knowledge of the  $Ca^{2+}$ -  $H_2O_2$  crosstalk, several fundamental questions remain unsolved. It is still unclear how  $H_2O_2$  and  $Ca^{2+}$  signals precisely regulate each other, what determines the directionality of their crosstalk, and how both signaling pathways integrate to produce a coordinated and synergistic response.

#### 3.8 Label-free quantitative proteomics

Label-free quantitative proteomics has emerged as a powerful tool in plant biology, enabling the detailed analysis of proteomes without the need for isotopic or chemical labelling. This approach relies on mass spectrometry to quantify proteins based on their intrinsic properties, offering invaluable insights into plant physiology, development, and responses to environmental stimuli. As plants constantly adapt to their surroundings, their proteomes undergo dynamic changes, and label-free methods provide a means to analyse these shifts with precision. The main focus of label-free quantification (LFQ) lies in the direct measurement of protein abundance from mass spectrometric data. Without external labelling, researchers rely on two primary strategies: spectral counting and peptide signal intensity (Zhu et al., 2010; Blein-Nicolas & Zivy, 2016). Spectral counting quantifies proteins by counting the number of tandem mass spectra (MS/MS) identified for each protein, operating under the assumption that higher-abundance proteins generate more detectable peptides and thus more spectra. While straightforward, this method has limitations, particularly in detecting low-abundance

proteins, as it is influenced by factors such as peptide detectability and ionization efficiency. In contrast, peptide signal intensity-based quantification measures the abundance of a protein by integrating the area under the chromatographic peak corresponding to a peptide ion. This approach benefits from high-resolution mass spectrometry, enabling a more accurate and sensitive quantification of proteins.

In recent years, label-free quantitative proteomics has been extensively applied to plant research, providing a deeper understanding of key biological processes. One of its most significant applications lies in studying plant responses to stress. Plants are constantly exposed to abiotic challenges such as drought, salinity, and temperature fluctuations, as well as biotic threats from pathogens and herbivores. To survive, they must rapidly alter their proteomes, upregulating stress-related proteins while suppressing others. LFQ has been instrumental in identifying and quantifying these differentially expressed proteins, shedding light on molecular mechanisms underlying stress tolerance. For example, a recent study on Elaeagnus angustifolia seedlings subjected to salt stress utilized LFQ to reveal key proteins involved in ion transport, antioxidant defence, and metabolic adjustment (Chang et al., 2023a). Beyond stress responses, LFQ has played a crucial role in uncovering the proteomic changes associated with plant growth and development (Jones & De Smet, 2023). By comparing protein abundancy profiles at different developmental stages or in distinct tissues, researchers have identified regulatory proteins and metabolic enzymes that drive growth. Similarly, studies on plant metabolic pathways have benefited from label-free approaches, as they allow the quantification of key enzymes involved in primary and secondary metabolism (Garcia et al., 2024; Song et al., 2022). Such insights are essential for improving traits such as crop yield, nutritional content, and resistance to environmental challenges.

One of the key advantages of LFQ is its cost-effectiveness and broad applicability, compared to label-based methods. Without the need for expensive isotopic or chemical labelling, this technique is accessible for large-scale studies, making it a valuable tool for plant research. Additionally, its versatility allows for the analysis of diverse plant species, tissues and experimental conditions without the constraints of prior labelling steps (Välikangas et al., 2016). However, despite these strengths, LFQ is not without challenges. Variability in sample preparation, instrument performance, and data processing can introduce inconsistencies, necessitating stringent standardization and quality control measures. Moreover, the dynamic

range of proteomic analysis remains a limiting factor, as detecting low-abundance proteins against a background of highly abundant ones remains difficult. Nevertheless, advancements in mass spectrometry technology and data processing algorithms continue to enhance the sensitivity and accuracy of label-free quantification.

The field of label-free proteomics is rapidly evolving, with new methodologies and analytical strategies pushing the boundaries of what is possible. Recent improvements in data acquisition and processing have expanded proteome coverage, enabling more comprehensive analyses of plant systems. Looking ahead, the integration of LFQ with other omics technologies, such as genomics and metabolomics, holds immense potential for providing a holistic view of plant biology. Moreover, emerging applications in single-cell proteomics promise to unravel cellular heterogeneity within plant tissues, offering unprecedented insights into how individual cells respond to their environment.

As our understanding of plant proteomes deepens, label-free quantitative proteomics continues to stand at the front line of scientific discovery. By capturing the intricate protein networks that govern plant function and adaptation, this approach paves the way for innovations in agriculture, crop improvement, and environmental sustainability. With ongoing technological advancements, the future of plant proteomics is poised to unlock even greater insights into the molecular intricacies of life.

#### 4. Results

The result section is divided into three chapters, each corresponding to a fully published article in a peer-reviewed journal or submitted preprints. A separate Material and Methods section has not been included in this thesis, as each individual publication contains all details on the methodology used. The different chapters are ordered in a non-chronological but content-wise meaningful way to ensure a logical flow of information.

The following Results sections provide concise summaries of all three publications. For further details, readers of this thesis are referred to the original publications, which can be found in the appendix (Chapters 1–3 correspond to Appendices 1–3, respectively). Additionally, the fully selectable and copyable portable document format (PDF) versions of these publications can be accessed through the provided Digital Object Identifier (DOI) hyperlinks.

4.1. Chapter 1

Analysis of abiotic and biotic stress-induced Ca2+ transients in the crop

species Solanum tuberosum

Annelotte van Dieren<sup>1</sup>, Ronald E. Schwarzenbacher<sup>2</sup>, Sophie Sonnewald<sup>3</sup>, Andras Bittner<sup>1</sup>, Ute

C. Vothknecht<sup>1</sup>.

<sup>1.</sup> Institute for Cellular and Molecular Botany, University of Bonn, Kirschallee 1, 53115,

Bonn, Germany

<sup>2.</sup> Department of Biosciences, Durham University, South Road, Durham, DH1 3LE, UK

3. Department of Biology, Chair of Biochemistry, Friedrich-Alexander-University

Erlangen-Nuremberg, Staudtstraße 5, Erlangen, 91058, Germany

Scientific Reports 14, no. 1 (2024): 27625

https://doi.org/10.1038/s41598-024-79134-3

Analysis of abiotic and biotic stress-induced Ca<sup>2+</sup> transients in the crop species *Solanum* 

tuberosum" was published in 2024 in Scientific Reports (Springer Nature Portfolio). The

original publication can be found as Appendix 1. The following abstract summarises the

publication and highlights my personal contribution.

This publication, of which I am the sole first as well as co-corresponding author, analyses

transgenic S. tuberosum lines generated in the laboratory of Dr. S. Sonnewald (FAU Erlangen).

These lines express the genetically encoded Ca<sup>2+</sup> biosensor apoaequorin under the control of

the constitutive 35S promoter. This system enabled us to quantify cytosolic free Ca<sup>2+</sup> ([Ca<sup>2+</sup>]<sub>cyt</sub>)

dynamics in response to a range of abiotic and biotic stress stimuli. Direct comparisons

between stress-induced Ca<sup>2+</sup> transients in potato and those in *Arabidopsis* allowed us to assess

species-specific variations in Ca<sup>2+</sup> signals kinetics and amplitudes. By characterizing these

26

differences, we aimed to expand the understanding of calcium-mediated stress responses in crop plants and provide a foundation for improving stress tolerance in potato.

I conducted all the experimental work presented in this manuscript, which included growth and maintenance of plant material, phenotypic analysis, and immunodetection of the aequorin and roGFP proteins via Western blotting. Additionally, I developed and optimized the protocol for measuring Ca<sup>2+</sup> transients in the newly established sensor lines, especially for soilgrown plants, carried out Ca<sup>2+</sup> measurements, performed data analysis and visualization, and assessed Grx1-roGFP2 fluorescence using confocal microscopy. The experimental design and data interpretation were discussed in collaboration with Drs. A. Bittner, R. Schwarzenbacher, and U.C. Vothknecht. I prepared the initial draft of the manuscript under the supervision of A. Bittner and R. Schwarzenbacher, and the final version was refined under the guidance of U.C. Vothknecht.

Plants continuously encounter various environmental stress factors, both biotic and abiotic, which necessitate rapid and specific cellular responses to ensure survival and adaptation. Among the key signaling molecules involved in these responses, calcium ions (Ca<sup>2+</sup>) act as universal secondary messengers that transduce environmental cues into appropriate downstream regulatory mechanisms. The specificity of a given stress response is encoded in the unique spatial and temporal patterns of Ca<sup>2+</sup> transients, known as calcium signatures. While much of the current understanding of stress-induced Ca<sup>2+</sup> signaling has been derived from studies on the model plant *Arabidopsis thaliana*, there remains a critical gap in knowledge concerning calcium signaling in crop species such as *Solanum tuberosum* (potato) which we address in this research paper.

The first set of experiments examined  $[Ca^{2+}]_{cyt}$  fluctuations in response to three abiotic stress factors: salinity (NaCl), osmotic stress (mannitol), and oxidative stress ( $H_2O_2$ ). NaCl treatments induced a dose-dependent  $Ca^{2+}$  response in both species, but the kinetics differed significantly. Specifically, Arabidopsis showed a concentration dependent shift of the peak of the  $Ca^{2+}$  transients, whereas the response time in potato was not concentration dependent. Moreover, approximately double the NaCl concentration was required in potato to reach a similar amplitude of the response as in Arabidopsis. These results suggest that potato may have a higher threshold for sodium perception or that downstream regulatory mechanisms modulate  $Ca^{2+}$  influx differently than in Arabidopsis. By contrast, osmotic stress induced by mannitol

triggered only negligible Ca<sup>2+</sup> transients in Arabidopsis. However, in potato, high concentrations of mannitol elicited clear Ca<sup>2+</sup> signals, suggesting that osmotic stress perception mechanisms may also differ between these two species.

Oxidative stress responses were investigated using  $H_2O_2$  treatments, a well-established inducer of reactive oxygen species (ROS)-associated signaling pathways. In Arabidopsis, a rapid and dose-dependent  $Ca^{2+}$  transient was observed, with peak values of  $[Ca^{2+}]_{cyt}$  occurring within 15–30 seconds after stimulus application. In contrast, the potato response exhibited a biphasic pattern, with a delayed secondary peak that was absent in *Arabidopsis*. This biphasic response could indicate additional regulatory steps in ROS-induced  $Ca^{2+}$  signaling in potato, potentially linked to differences in redox homeostasis or oxidative burst kinetics. To further explore the redox environment in potato, I analysed a transgenic potato line expressing the redox-sensitive Grx1-roGFP2 sensor, which was kindly generated by SOLANA GmbH (Germany). The analysis revealed that potato exhibits a higher basal level of glutathione oxidation compared to Arabidopsis, which may contribute to its distinct  $Ca^{2+}$  signaling response to oxidative stress.

In addition to abiotic stress, we examined Ca<sup>2+</sup> transients in response to pathogen-associated molecular patterns (PAMPs), i.e. flg22 (derived from *Pseudomonas syringae* flagellin) and Pep-13 (a peptide motif from *Phytophthora infestans*). In Arabidopsis, flg22 triggered a moderate and slower Ca<sup>2+</sup> transient, peaking at approximately 160 seconds post-application. In potato, the flg22 response was even more delayed, with maximal [Ca<sup>2+</sup>]<sub>cyt</sub> increase occurring at around 300 seconds. The Pep-13 response, however, differed markedly between species. While Arabidopsis exhibited only a weak [Ca<sup>2+</sup>]<sub>cyt</sub> increase, potato responded with a significantly higher Ca<sup>2+</sup> transient, suggesting a heightened sensitivity to *P. infestans*-related elicitors. This finding is particularly relevant given that *P. infestans* is the causative agent of late blight, the most devastating disease affecting potato crops worldwide. Furthermore, an additional potato sensor line expressing the redox-sensitive Grx1-roGFP2 probe was introduced. This system enabled the analysis of cytosolic redox dynamics in *S. tuberosum* and facilitated comparative studies with an existing redox-sensitive *Arabidopsis* sensor line. We observed that potato has a higher basal oxidative state compared to Arabidopsis, which may explain the differences in their Ca<sup>2+</sup> signature in response to H<sub>2</sub>O<sub>2</sub>.

Collectively, our results demonstrate that potato and Arabidopsis exhibit distinct calcium signaling patterns in response to abiotic and biotic stressors. These differences may be

attributed to variations in Ca<sup>2+</sup> channel composition, differences in downstream signal transduction pathways, or species-specific adaptations to environmental conditions. The identification of these divergent Ca<sup>2+</sup> signaling mechanisms underscores the importance of studying crop species independently from model plants to develop targeted approaches for improving stress resilience in crop species.

#### **4.2. Chapter 2**

With or without a Ca<sup>2+</sup> signal? A proteomics approach towards Ca<sup>2+</sup> dependent and independent proteome changes in response to oxidative stress in *A. thaliana* 

Annelotte van Dieren<sup>1</sup>, Andras Bittner<sup>1</sup>, Bernhard Wurzinger<sup>2</sup>, Leila Afjehi-Sadat<sup>3</sup>, Wolfram Weckwerth<sup>2,4</sup>, Markus Teige<sup>2</sup> and Ute C. Vothknecht<sup>1</sup>

- Institute for Cellular and Molecular Botany, University of Bonn, Kirschallee 1, 53115
   Bonn, Germany
- Molecular Systems Biology (MOSYS), Department of Functional & Evolutionary Ecology, University of Vienna, Djerassiplatz 1, 1030 Vienna, Austria
- Mass Spectrometry Unit, Research Support Facilities, University of Vienna, Djerassiplatz 1, 1030 Vienna, Austria
- Vienna Metabolomics Center (VIME), University of Vienna, Djerassiplatz 1, 1030 Vienna, Austria

Preprint in BioRxiv (2025)

https://doi.org/10.1101/2025.03.31.645912

 $Ca^{2+}$  and ROS are central secondary messengers in plant stress signaling, mediating responses to abiotic and biotic stimuli. Stress-induced  $H_2O_2$ , a reactive oxygen species (ROS), has been shown to generate distinct  $Ca^{2+}$  signaling patterns. However, a comprehensive understanding of this response at the proteome level is missing. Furthermore, the interplay between  $Ca^{2+}$  and ROS in regulating proteome-wide changes remains largely unexplored. In this publication, of which I am the sole first author, we employ a label-free quantitative (LFQ) proteomics approach to delineate  $Ca^{2+}$ -dependent and independent proteomic alterations in *Arabidopsis* 

thaliana leaves subjected to oxidative stress induced by hydrogen peroxide ( $H_2O_2$ ). By inhibiting  $H_2O_2$ -induced  $Ca^{2+}$  transients with  $LaCl_3$ , a plasma membrane  $Ca^{2+}$  channel blocker, we study the role of  $Ca^{2+}$  in modulating proteome dynamics after 10 and 30 minutes of  $H_2O_2$  treatment.

The experimental parameters, such as the concentration of  $H_2O_2$  used to induce a  $Ca^{2+}$  signal and the concentration of  $LaCl_3$  that was needed to inhibit this signal under the chosen experimental conditions was tested by me. In addition, I tested the method for protein extraction and quantification, to ensure that enough protein extract for the LC-MS/MS analysis would be obtained. I performed the sample treatment together with Andras Bittner. I then prepared extracted and precipitated protein samples for LC-MS analysis, which was performed at the Vienna Metabolomics Center (VIME) by L. Afjehi-Sadat assisted by A. Bittner and B. Wurzinger. Under supervision of A. Bittner and Bernhard Wurzinger I performed the identification and quantification of peptides and proteins from the LC-MS analysis, and later on I did the analysis of the identified proteins individually.

We identified 581 proteins with high confidence after 10 minutes of treatment and 909 proteins after 30 minutes. Among these, 37 and 57 proteins were significantly responsive to H<sub>2</sub>O<sub>2</sub>, respectively, with distinct subsets classified as strictly Ca<sup>2+</sup>-dependent, partially Ca<sup>2+</sup>-dependent, or Ca<sup>2+</sup>-independent. Notably, strictly Ca<sup>2+</sup>-dependent proteins predominantly exhibited reduced abundance, suggesting a role for Ca<sup>2+</sup> in protein degradation, whereas Ca<sup>2+</sup>-independent proteins largely showed increased abundance, indicating potential upregulation potentially via transcription.

The inhibition of  $Ca^{2+}$  signaling via  $LaCl_3$  significantly attenuated the proteomic response to  $H_2O_2$ , with the combined  $LaCl_3$  and  $H_2O_2$  treatment resulting in substantially higher numbers of differentially abundant proteins (DAPs) than  $H_2O_2$  alone. These findings align with previous transcriptomic analyses, suggesting an antagonistic interaction between  $Ca^{2+}$  and ROS pathways. Hierarchical clustering and principal component analysis (PCA) revealed distinct proteomic signatures across different treatments, with the most pronounced shifts observed in the Inhibitor+Stress condition.

A detailed comparison of the proteomic response at 10- and 30-minutes post-treatment highlighted temporal variations in Ca<sup>2+</sup>-regulated protein abundance. While 10-minute responses were dominated by proteins associated with immediate stress perception and

signaling, later (30 minute) responses encompassed mostly proteins involved in metabolic reprogramming, development, and cellular restructuring. Three proteins—WLIM1, CYP97C1, and AGAP1—exhibited Ca<sup>2+</sup> dependency shifts between the two time points, emphasizing the dynamic nature of Ca<sup>2+</sup>-modulated proteomic changes.

Functional enrichment analysis revealed that ribosomal proteins were significantly enriched among the strictly Ca<sup>2+</sup>-dependent downregulated proteins, indicating a potential Ca<sup>2+</sup>-mediated repression of translation under oxidative stress. Conversely, Ca<sup>2+</sup>-independent proteins were enriched in carbon fixation and metabolic pathways, suggesting their role in stress-induced metabolic adjustments independent of Ca<sup>2+</sup> signaling. These findings suggest a dual regulatory mechanism, where Ca<sup>2+</sup> signaling facilitates selective protein degradation while enabling metabolic shifts to enhance stress resilience.

Western blot validation of selected candidate proteins confirmed the reliability of our proteomic dataset, demonstrating congruent abundance patterns for PHENYLALANINE LYASE 2 (PAL2) and GAMMA TONOPLAST INTRINSIC PROTEIN 2 (TIP2).

In summary, this study provides a first proteomic perspective on the Ca<sup>2+</sup>-dependent and independent regulation of oxidative stress responses in Arabidopsis. The findings highlight the intricate balance between ROS and Ca<sup>2+</sup> signaling pathways, revealing novel targets for future research on plant stress adaptation and resilience. Understanding these molecular mechanisms offers potential applications in improving crop stress tolerance through targeted manipulation of Ca<sup>2+</sup>-mediated regulatory networks. Our study not only enhances the current knowledge of the ROS-Ca<sup>2+</sup> interplay at the proteomic level but also paves the way for integrating multi-omics approaches to dissect complex stress signaling networks in plants.

#### **4.3. Chapter 3**

Stress Knowledge Map: A knowledge graph resource for systems biology analysis of plant stress responses

Carissa Bleker <sup>1</sup>, Živa Ramšak <sup>1</sup>, Andras Bittner <sup>2</sup>, Vid Podpečan <sup>3</sup>, Maja Zagorščak <sup>1</sup>, Bernhard Wurzinger <sup>4</sup>, Špela Baebler <sup>1</sup>, Marko Petek <sup>1</sup>, Maja Križnik <sup>1</sup>, Annelotte van Dieren <sup>2</sup>, Juliane Gruber <sup>4</sup>, Leila Afjehi-Sadat <sup>5</sup>, Wolfram Weckwerth <sup>4</sup>, Anže Županič <sup>1</sup>, Markus Teige <sup>4</sup>, Ute C. Vothknecht <sup>2</sup>, Kristina Gruden <sup>1</sup>

- Department of Biotechnology and Systems Biology, National Institute of Biology, Večna pot 121, 1000 Ljubljana, Slovenia
- Plant Cell Biology, Institute of Cellular and Molecular Botany, University of Bonn, Kirschallee 1, 53115 Bonn, Germany
- Department of Knowledge Technologies, Jožef Stefan Institute, Jamova cesta 39, 1000
  Ljubljana, Slovenia
- Department of Functional & Evolutionary Ecology, University of Vienna, Djerassiplatz
   1, 1030 Vienna, Austria
- 5. Mass Spectrometry Unit, Core Facility Shared Services, University of Vienna, Djerassiplatz 1, 1030 Vienna, Austria

Plant communications 5, no 6 (2024)

https://doi.org/10.1016/j.xplc.2024.100920

"Stress Knowledge Map: A knowledge graph resource for systems biology analysis of plant stress responses" was published in 2024 as a research paper in Plant Communications by Cell press. The original publication can be found as Appendix 3 of this thesis. This publication, of which I am co-author, presents a new developed knowledge graph-based tool that provides a

comprehensive framework for analysing plant stress responses, supporting both qualitative and quantitative systems biology approaches. Understanding plant responses to stress is a critical factor in ensuring global food security, particularly in the face of climate change, the spread of pests, and the increasing demand for agricultural productivity. The ability to model and predict stress responses at a systems level is essential for advancing plant science and crop improvement strategies.

The SKM was developed by our collaborators at the NIB in Slovenia and comprises two distinct but complementary knowledge graphs: (1) the Plant Stress Signaling (PSS) model, which is a manually curated collection of 543 validated reactions involved in stress signaling; and (2) the Comprehensive Knowledge Network (CKN), which compiles over 488390 molecular interactions, providing a broader, data-driven context for understanding stress-related mechanisms. The PSS model, developed through expert curation, includes major signaling pathways involving calcium (Ca<sup>2+</sup>), reactive oxygen species (ROS), mitogen-activated protein kinases (MAPKs), or phytohormone signaling (e.g., abscisic acid (ABA), jasmonic acid (JA), and salicylic acid (SA)). These pathways govern plant responses to biotic and abiotic stressors and provide insight into the balance between growth and defence mechanisms.

To demonstrate the practical application of SKM, two case studies were conducted. The first focused on hormonal crosstalk between ABA, JA, and SA, particularly their combined effect on the transcriptional regulation of the *RESPONSIVE TO DESICCATION 29 (RD29)* gene. Experimental evidence demonstrated that JA and SA attenuate ABA-induced *RD29* expression, highlighting the complexity of hormonal interactions in stress adaptation. Through SKM analysis, a mechanistic hypothesis was generated, suggesting that this regulatory interaction occurs via the MYC2 transcription factor interacting with the ABA receptor PYL6.

The second case study utilised a subset of the data generated in my proteomics study (Chapter 2) investigating calcium-dependent proteomic responses to oxidative stress in *Arabidopsis thaliana*. It further explored the dataset using an alternative analytical approach. Network analysis within SKM of Ca<sup>2+</sup>-dependent H<sub>2</sub>O<sub>2</sub> responsive proteins revealed major regulatory hubs, including calmodulin-dependent signaling pathways, which help to mediate oxidative stress responses. My contributions included the processing of data for the SKM analysis, authoring the Materials and Methods section related to this work, contributing to discussions, and reviewing the manuscript.

The SKM web platform (<a href="https://skm.nib.si">https://skm.nib.si</a>) offers researchers interactive tools for network visualization, hypothesis generation, and systems-level modelling, enabling the integration of experimental data with established plant stress signaling knowledge. The PSS model is available in multiple computational formats, facilitating network analysis, Boolean modelling, and pathway visualization for further hypothesis testing. Moreover, SKM is continuously updated with new experimental data, making it a dynamic and expandable resource for plant biology research. Ultimately, the Stress Knowledge Map (SKM) serves as a fundamental tool for plant systems biology, bridging the gap between high-throughput experimental data and mechanistic insights into stress responses. Its utility in predicting gene functions, identifying regulatory interactions, and guiding experimental design makes it a valuable resource for both fundamental plant research and agricultural applications. Future developments will expand SKM to include additional stress conditions such as cold, salinity, and nutrient deficiencies, further enhancing its role in precision breeding and crop resilience research.

#### 5. Summary

Plants are constantly subjected to a wide array of environmental stressors, both abiotic and biotic, that threaten their growth, development, and overall survival. These stressors—ranging from drought and salinity to oxidative damage and pathogen attacks—trigger intricate molecular signaling cascades that determine whether a plant can successfully adapt or struggle to survive in the challenging environmental conditions. Over the past decades, researchers have achieved significant progress in uncovering the molecular components of plant stress responses, yet many critical questions are not fully answered. How do plants perceive and transmit stress signals at the molecular level? How do these signals translate into physiological and biochemical changes? And, perhaps most importantly, how can this knowledge be harnessed to improve the resilience of crop species that sustain human populations worldwide?

The three studies presented in this thesis, each addressing a different aspect of plant stress biology, provide important insights into these pressing questions. The first explores calcium (Ca<sup>2+</sup>) signaling in potato induced by different stress stimuli, revealing species-specific patterns of stress perception and response. The second study delves into the proteomic changes induced by oxidative stress in Arabidopsis, aiming to discover calcium-dependent and independent changes in protein content at a whole proteome level. The third introduces the Stress Knowledge Map (SKM), an ambitious effort to integrate the large amount of available information on plant stress responses into an interactive knowledge graph that enables complex systems biology analyses. Taken together, these studies significantly expand our understanding of plant stress responses, shedding light on key regulatory mechanisms while also offering practical tools and strategies for future research and agricultural improvement.

#### **Calcium signaling in potato**

Calcium plays a central role in plant stress signaling as a ubiquitous secondary messenger that translates external stimuli into precise intracellular responses. The study on calcium signaling in *Solanum tuberosum*, one of the world's most important food crops, provides a crucial step forward in understanding how crop species perceive and respond to external stimuli at a cellular level. By introducing the genetically encoded Ca<sup>2+</sup> biosensor apoaequorin into potato plants, we were able to measure real-time Ca<sup>2+</sup> fluctuations in response to a variety of

stressors, including NaCl, mannitol,  $H_2O_2$ , and pathogen-associated molecular patterns. The results show stimulus- and species-specific calcium signatures—unique patterns of amplitude, duration, and oscillation that encode information about the nature and severity of the stress.

Interestingly, when comparing these calcium transients to those observed in the model plant Arabidopsis thaliana, distinct differences in kinetics and amplitude were noted, highlighting the species-specific nature of stress perception. Similarly, a study examining calcium dynamics in barley leaf tips, in comparison with Arabidopsis, also identified species-specific responses, further supporting this finding. This divergence highlights a critical gap in our current understanding of plant stress biology: while Arabidopsis serves as a model plant, its responses cannot always be extrapolated to agronomically important crops. The potato study provides a reference point for future investigations into stress tolerance in non-model species, offering a foundational tool for breeding or engineering stress-resilient potato varieties.

While this fundamental research approach is essential for advancing our understanding of plant stress responses and establishing a foundation for future applied studies, it is important to acknowledge that laboratory-grown plants can exhibit significantly different morphological and physiological characteristics compared to those cultivated in outdoor environments. Therefore, in this thesis, all analyses were conducted using soil-grown plants to better approximate natural conditions. However, even under these conditions, discrepancies from the true field environment remain. In the field of Ca<sup>2+</sup> signaling research, most studies focus on young plant material grown on agar medium. In Arabidopsis, seedlings are predominantly used to analyse Ca<sup>2+</sup> signatures in response to various stimuli (H. Knight et al., 1997; Rentel & Knight, 2004; Aboul-Soud et al., 2009; Maintz et al., 2014). Studies on crop species often rely on young plant tissue grown on agar as well (Nagel-Volkmann et al., 2009a; Zhang et al., 2015a) or even on protoplasts (Blume et al., 2000) to investigate Ca<sup>2+</sup> signatures. Such experimental approaches may introduce additional challenges in extrapolating findings to natural plant systems in field conditions.

## Identification of Ca<sup>2+</sup>-dependent proteomics changes

But what happens after the initial calcium signal has been perceived? How does this translate into actual biochemical changes at the protein level? The proteomics study on Arabidopsis provides aims to focus on these questions. By subjecting plants to oxidative stress using hydrogen peroxide  $(H_2O_2)$  treatment and analysing the resulting proteome-wide changes, we identified a set of proteins that exhibited altered abundance in response to stress. Importantly, these proteins were further categorised into three distinct categories: strictly  $Ca^{2+}$ -dependent, partially  $Ca^{2+}$ -dependent, and completely  $Ca^{2+}$ -independent, to further analyse their regulation. This classification was made possible by pre-treating plants with  $LaCl_3$ , a well-known  $Ca^{2+}$  channel inhibitor, which effectively blocked calcium transients and revealed which proteins were truly reliant on  $Ca^{2+}$  signaling for their stress-induced abundance changes.

One of the most interesting observations is that strictly Ca<sup>2+</sup>-dependent proteins are more frequently observed with reduced abundance, whereas Ca<sup>2+</sup>-independent H<sub>2</sub>O<sub>2</sub>-responsive proteins tend to show increased abundance. Given the experiment's timeframe, it is likely that protein loss is primarily driven by degradation rather than reduced transcription, while the increase in protein levels results from enhanced transcription and/or translation. These results suggest a potential regulatory mechanism in which Ca<sup>2+</sup> signaling promotes protein destabilization, whereas proteins lacking strict Ca<sup>2+</sup> dependence may undergo increased synthesis in response to oxidative stress. This observation and the associated hypothesis could be further investigated through transcript analysis of individual proteins or a comprehensive transcriptome analysis using the same experimental set up. Since transcriptomics generally captures a faster response to changes compared to proteomics, due to the time required for protein synthesis and post-translational modification (Bathke et al., 2019; Ghazalpour et al., 2011) . Such an approach could provide valuable insights into the regulatory mechanisms and the role of Ca<sup>2+</sup> underlying these changes.

## Stress Knowledge Map – a case study

Our studies clearly reinforce the fact plant stress responses are highly interconnected, with multiple layers of regulations and interactions to shape the final response. One of the major challenges is to integrate these different data into a cohesive framework that allows researchers to explore how different molecular components interact within the broader signaling network. This is precisely where the Stress Knowledge Map (SKM) comes into play. As a publicly available resource containing two complementary knowledge graphs—one focused on highly curated plant stress signaling pathways and the other providing a comprehensive network of nearly 500,000 molecular interactions—SKM represents a big step forward in systems biology approaches to plant stress research.

By aggregating information from diverse literature sources and established biological databases, SKM provides a central access point for exploring plant stress responses. It allows researchers to visualize and model stress signaling cascades, identify key regulatory nodes, and even generate hypotheses for experimental validation. The case studies presented in the SKM paper demonstrate its practical utility, showing how it can be used to investigate hormone crosstalk in stress responses or analyse proteomics data within the broader context of known signaling pathways. One particularly exciting aspect of SKM is its ability to facilitate the development of "digital twins"—computational models that simulate plant stress responses under different environmental conditions, potentially accelerating crop improvement efforts.

Although SKM demonstrated to be a useful generator of potential mechanistic explanations for the observed data in both case studies. As with any hypothesis, further validation is needed, and some may not prove as valid. The next step in the analysis would involve confirming the identified mechanisms through functional analysis experiments such as knockout experiments, to verify the role of the proposed regulatory network.

## Final remarks and outlook

It is important to recognize that a comprehensive understanding of plant stress responses requires a whole-organism approach. Plants do not respond to stress only at the leaf level; rather, their responses involve complex systemic signaling that integrates inputs from roots, stems, leaves, and reproductive structures. The decision to exclusively focus on leaf material in this thesis was made due to technical constraints and time limitations. To ensure that the findings of this research are applicable to real-world agricultural practices, future studies should aim to validate these results at the whole-plant level.

Furthermore, future research on calcium signaling and proteomic changes in response to stress would greatly benefit from field experiments. Such experiments would provide a more realistic context for understanding plant responses and offer insights into how environmental variability influences signaling pathways. This is particularly relevant for crop species like potatoes, which are primarily cultivated for food production. Conducting studies on field-grown plants under realistic agricultural conditions would enhance the translational value of the findings, making them more applicable to improving stress resilience in commercial crop production.

When considered as a whole, these three studies draw a clear picture of how plants integrate calcium signaling, proteomic adjustments, and network-wide regulatory interactions to cope with stress. The insights gained from these studies have profound implications for agriculture. Understanding the species-specific nature of calcium signatures in crop plants can provide knowledge and insides for breeding programs aimed at improving stress tolerance. The identification of key Ca<sup>2+</sup>-dependent and independent proteins provides potential targets for genetic engineering or chemical interventions. And the development of SKM as a systems biology tool sets the foundation for a more holistic, data-driven approach to improving crop resilience. Moving forward, several exciting research directions emerge from these findings. Expanding the SKM database to include additional crop species will further enhance its applicability in agricultural settings. Functional validation of the key proteins identified in the Arabidopsis proteomics study will provide deeper insights into their precise roles in stress adaptation. Integrating transcriptomics, metabolomics, and phenomics data with calcium signaling and proteomic analyses will offer a more complete picture of how plants respond to stress at multiple levels. And perhaps most importantly, applying these insights in real-world agricultural scenarios—whether through precision breeding, genome editing, biotechnological interventions—has the potential to revolutionize how we cultivate crops in an era of increasing climate instability.

# 6. Acknowledgments

First and foremost, I would like to express my sincere gratitude to Prof. Dr. Ute C. Vothknecht for giving me the opportunity to be part of the Plant Cell Biology. Her invaluable guidance, continuous support and patience during my doctoral research have been fundamental in my growth as a researcher. Through the opportunities she provided—shaping my own project, attending conferences and supervising courses—I was able to broaden my knowledge and refine my skills. Her vast expertise, extensive experience, and strong network in the field of plant (calcium) signaling, a field that was relatively new to me, have been very helpful in shaping my development and led me to thesis I present here. I would also like to express my gratitude to Dr. Andras Bittner, for the insightful discussions during the first two years of my PhD, as well as to Dr. Fatima Chigri and Dr. Susann Frank for their valuable advice and support along the way. My appreciation extends to Claudia Heym and Ursula Mettbach, who provided technical assistance, and to Gelareh and Sandra for their help with administrative matters.

I am very thankful for the ADAPT (Accelerated Development of multiple-stress tolerant Potato) consortium, for the interdisciplinary collaboration and funding on this project, I sincerely value the contributions and the positive working relationship we have had, both online and in person on the yearly meetings.

I would like to thank my fellow PhD colleagues. Their collective support has played a vital role in my research journey, and I am truly thankful for their contributions. Nilou Pirayesh, although we had only a short time working together, you greatly helped me in getting me started with the experimental work during the challenging COVID-19 period, when hardly anyone was around. Later on, you also became a wonderful friend for which I am truly grateful. Felipe Yamashita, despite the differences in our research focus, I always appreciated our insightful discussions on data analysis, figure preparation and of course, recommendations for great places to visit in Germany. Sabarna Bhattacharyya, thank you for always being helpful and for your willingness to answer and discuss any scientific questions and doubts I had, your support was invaluable. Yasira Shoaib, after being alone in the office for a long time, I was grateful when you joined, together we created a much better working environment than I would have had on my own, something I am very thankful for, and I know you will do great during you remaining time in the lab.

Moving from professional acknowledgements to the more personal acknowledgment, there is this one hybrid person, that has played a significant role in my PhD journey., Maria del Pilar Martinez. We started at the institute around the same time, and beyond our shared passion and fascination for science, we quickly discovered many common interests, from enjoying sunshine and ice cream, to spending time outdoors and cooking together. Additionally, during moments when I felt like nothing was working as it should, you always helped me find something positive in the situation, additionally we could celebrate nice results and achievements together. I truly hope you will keep this uplifting mindset and boundless energy forever, and that you continue to share it with many more people.

I would like to express my heartfelt gratitude to Thijs, for being a patient, endless and unconditionally source of support throughout every stage of this journey and life in general. Thank you for always listening to my concerns, helping me navigate moments of doubt and uncertainty and, most importantly, for planning wonderful bike tours through the beautiful Bonn area, giving me the perfect way to unwind on the weekends and discovering the best Kaffee und Kuchen places together.

I would like to thank my family - my father, for always supporting me in every life choice I make, prioritizing my happiness above all else; my siblings, who may not fully understand what I do but never fail to ask the obligatory question how my potato plants are doing, before effortlessly steering the conversation towards the humour and nonsense we all love to share. Mom and Dirk who have been on my mind the most over the past few years, regularly reminding me to put things into perspective, live in the moment and appreciate what truly matters. For them, obtaining an additional degree holds no real significance, they have taught me that happiness and health are life's most valuable gifts, that should never be taken for granted.

My friends in Netherlands, who despite the distance, always make me feel welcome, whether by visiting me, hosting me with open arms, or planning wonderful outdoor activities together.

Last but not least, I am grateful to my teammates from the PSV Bonn triathlon team, for providing me an escape from the academic bubble, whether by running in circles, swimming lanes, or occasionally getting lost in the Eifel or stuck at another Baustelle. Your company and support did not only make doing sports even more enjoyable but also helped me to improve my German language skills along the way.

# 7. References

Aboul-Soud, M. A. M., Aboul-Enein, A. M., & Loake, G. J. (2009). Nitric oxide triggers specific and dose-dependent cytosolic calcium transients in Arabidopsis. *Plant Signaling & Behavior*, *4*(3), 191–196. <a href="https://doi.org/10.4161/psb.4.3.8256">https://doi.org/10.4161/psb.4.3.8256</a>

Ahmad, P., Jaleel, C. A., Salem, M. A., Nabi, G., & Sharma, S. (2010). Roles of enzymatic and nonenzymatic antioxidants in plants during abiotic stress. *Critical Reviews in Biotechnology*, 30(3), 161–175. <a href="https://doi.org/10.3109/07388550903524243">https://doi.org/10.3109/07388550903524243</a>

Albert, M., Van Der Krol, S., & Kaldenhoff, R. (2010). *Cuscuta reflexa* invasion induces Ca <sup>2+</sup> release in its host. *Plant Biology*, *12*(3), 554–557. <a href="https://doi.org/10.1111/j.1438-8677.2010.00322.x">https://doi.org/10.1111/j.1438-8677.2010.00322.x</a>

Aldon, D., Mbengue, M., Mazars, C., & Galaud, J.-P. (2018). Calcium Signalling in Plant Biotic Interactions. *International Journal of Molecular Sciences*, *19*(3), 665. <a href="https://doi.org/10.3390/ijms19030665">https://doi.org/10.3390/ijms19030665</a>

Aleman, F., Yazaki, J., Lee, M., Takahashi, Y., Kim, A. Y., Li, Z., Kinoshita, T., Ecker, J. R., & Schroeder, J. I. (2016). An ABA-increased interaction of the PYL6 ABA receptor with MYC2 Transcription Factor: A putative link of ABA and JA signaling. *Scientific Reports*, *6*(1), 28941. <a href="https://doi.org/10.1038/srep28941">https://doi.org/10.1038/srep28941</a>

Ali, A., Petrov, V., Yun, D.-J., & Gechev, T. (2023). Revisiting plant salt tolerance: Novel components of the SOS pathway. *Trends in Plant Science*, *28*(9), 1060–1069. <a href="https://doi.org/10.1016/j.tplants.2023.04.003">https://doi.org/10.1016/j.tplants.2023.04.003</a>

Allan, C., Morris, R. J., & Meisrimler, C.-N. (2022). Encoding, transmission, decoding, and specificity of calcium signals in plants. *Journal of Experimental Botany*, 73(11), 3372–3385. <a href="https://doi.org/10.1093/jxb/erac105">https://doi.org/10.1093/jxb/erac105</a>

Allen, G. J., Chu, S. P., Harrington, C. L., Schumacher, K., Hoffmann, T., Tang, Y. Y., Grill, E., & Schroeder, J. I. (2001). A defined range of guard cell calcium oscillation parameters encodes stomatal movements. *Nature*, *411*(6841), 1053–1057. <a href="https://doi.org/10.1038/35082575">https://doi.org/10.1038/35082575</a>

Aller, I., Rouhier, N., & Meyer, A. J. (2013). Development of roGFP2-derived redox probes for measurement of the glutathione redox potential in the cytosol of severely glutathione-deficient rml1 seedlings. *Frontiers in Plant Science*, 4. https://doi.org/10.3389/fpls.2013.00506

Apel, K., & Hirt, H. (2004). REACTIVE OXYGEN SPECIES: Metabolism, Oxidative Stress, and Signal Transduction. *Annual Review of Plant Biology*, *55*(1), 373–399. <a href="https://doi.org/10.1146/annurev.arplant.55.031903.141701">https://doi.org/10.1146/annurev.arplant.55.031903.141701</a>

Aric Renieris & Schult. (2024). PyGraphviz [Computer software]. https://pygraphviz.github.io

Arvidsson, S., Kwasniewski, M., Riaño-Pachón, D. M., & Mueller-Roeber, B. (2008). QuantPrime – a flexible tool for reliable high-throughput primer design for quantitative PCR. *BMC Bioinformatics*, *9*(1), 465. <a href="https://doi.org/10.1186/1471-2105-9-465">https://doi.org/10.1186/1471-2105-9-465</a>

Ayash, M., Abukhalaf, M., Thieme, D., Proksch, C., Heilmann, M., Schattat, M. H., & Hoehenwarter, W. (2021). LC–MS Based Draft Map of the Arabidopsis thaliana Nuclear Proteome and Protein Import in Pattern Triggered Immunity. *Frontiers in Plant Science*, *12*, 744103. <a href="https://doi.org/10.3389/fpls.2021.744103">https://doi.org/10.3389/fpls.2021.744103</a>

Baebler, Š., Svalina, M., Petek, M., Stare, K., Rotter, A., Pompe-Novak, M., & Gruden, K. (2017). quantGenius: Implementation of a decision support system for qPCR-based gene quantification. *BMC Bioinformatics*, 18(1), 276. <a href="https://doi.org/10.1186/s12859-017-1688-7">https://doi.org/10.1186/s12859-017-1688-7</a>

Baker, S. S., Wilhelm, K. S., & Thomashow, M. F. (1994). The 5?-region of Arabidopsis thaliana cor15a has cis-acting elements that confer cold-, drought- and ABA-regulated gene expression. *Plant Molecular Biology*, *24*(5), 701–713. <a href="https://doi.org/10.1007/BF00029852">https://doi.org/10.1007/BF00029852</a>

Balci, H., Siper, M. C., Saleh, N., Safarli, I., Roy, L., Kilicarslan, M., Ozaydin, R., Mazein, A., Auffray, C., Babur, Ö., Demir, E., & Dogrusoz, U. (2021). Newt: A comprehensive web-based tool for viewing, constructing and analyzing biological maps. *Bioinformatics*, *37*(10), 1475–1477. https://doi.org/10.1093/bioinformatics/btaa850

Balla, K., Rakszegi, M., Li, Z., Békés, F., Bencze, S., & Veisz, O. (2011). Quality of winter wheat in relation to heat and drought shock after anthesis. *Czech Journal of Food Sciences*, *29*(2), 117–128. https://doi.org/10.17221/227/2010-CJFS

Barberini, M. L., Sigaut, L., Huang, W., Mangano, S., Juarez, S. P. D., Marzol, E., Estevez, J., Obertello, M., Pietrasanta, L., Tang, W., & Muschietti, J. (2018). Calcium dynamics in tomato pollen tubes using the Yellow Cameleon 3.6 sensor. *Plant Reproduction*, *31*(2), 159–169. https://doi.org/10.1007/s00497-017-0317-y

Bartholomeus, H., Kooistra, L., Stevens, A., Van Leeuwen, M., Van Wesemael, B., Ben-Dor, E., & Tychon, B. (2011). Soil Organic Carbon mapping of partially vegetated agricultural fields with imaging spectroscopy. *International Journal of Applied Earth Observation and Geoinformation*, 13(1), 81–88. <a href="https://doi.org/10.1016/j.jag.2010.06.009">https://doi.org/10.1016/j.jag.2010.06.009</a>

Bathke, J., Konzer, A., Remes, B., McIntosh, M., & Klug, G. (2019). Comparative analyses of the variation of the transcriptome and proteome of Rhodobacter sphaeroides throughout growth. *BMC Genomics*, *20*(1), 358. <a href="https://doi.org/10.1186/s12864-019-5749-3">https://doi.org/10.1186/s12864-019-5749-3</a>

Baweja, P., & Kumar, G. (2020). Abiotic Stress in Plants: An Overview. In B. Giri & M. P. Sharma (Eds.), *Plant Stress Biology* (pp. 1–15). Springer Singapore. <a href="https://doi.org/10.1007/978-981-15-9380-2">https://doi.org/10.1007/978-981-15-9380-2</a> 1

Belyavskaya, N. A. (1996). Free and membrane-bound calcium in microgravity and microgravity effects at the membrane level. *Advances in Space Research*, *17*(6–7), 169–177. <a href="https://doi.org/10.1016/0273-1177(95)00631-N">https://doi.org/10.1016/0273-1177(95)00631-N</a>

Ben-Ari, G., & Lavi, U. (2012). Marker-assisted selection in plant breeding. In *Plant Biotechnology and Agriculture* (pp. 163–184). Elsevier. <a href="https://doi.org/10.1016/B978-0-12-381466-1.00011-0">https://doi.org/10.1016/B978-0-12-381466-1.00011-0</a>

Berardini, T. Z., Reiser, L., Li, D., Mezheritsky, Y., Muller, R., Strait, E., & Huala, E. (2015). The arabidopsis information resource: Making and mining the "gold standard" annotated reference plant genome. *Genesis*, *53*(8), 474–485. <a href="https://doi.org/10.1002/dvg.22877">https://doi.org/10.1002/dvg.22877</a>

Bergey, D. R., Kandel, R., Tyree, B. K., Dutt, M., & Dhekney, S. A. (2014). The Role of Calmodulin and Related Proteins in Plant Cell Function: An Ever-Thickening Plot. *Springer Science Reviews*. <a href="https://doi.org/10.1007/s40362-014-0025-z">https://doi.org/10.1007/s40362-014-0025-z</a>

Bergmann, F. T., Czauderna, T., Dogrusoz, U., Rougny, A., Dräger, A., Touré, V., Mazein, A., Blinov, M. L., & Luna, A. (2020). Systems biology graphical notation markup language (SBGNML) version 0.3. *Journal of Integrative Bioinformatics*, 17(2–3), 20200016. https://doi.org/10.1515/jib-2020-0016

Bhattacharyya, S., Bleker, C., Meier, B., Giridhar, M., Rodriguez, E. U., Braun, A. M., Peiter, E., Vothknecht, U. C., & Chigri, F. (2025). Ca2+-dependent H2O2 response in roots and leaves of barley—A transcriptomic investigation. *BMC Plant Biology*, *25*(1), 232. <a href="https://doi.org/10.1186/s12870-025-06248-9">https://doi.org/10.1186/s12870-025-06248-9</a>

Bienert, G. P., Møller, A. L. B., Kristiansen, K. A., Schulz, A., Møller, I. M., Schjoerring, J. K., & Jahn, T. P. (2007). Specific Aquaporins Facilitate the Diffusion of Hydrogen Peroxide across Membranes. *Journal of Biological Chemistry*, *282*(2), 1183–1192. https://doi.org/10.1074/jbc.M603761200

Bittner, A., Cieśla, A., Gruden, K., Lukan, T., Mahmud, S., Teige, M., Vothknecht, U. C., & Wurzinger, B. (2022). Organelles and phytohormones: A network of interactions in plant stress responses. *Journal of Experimental Botany*, 73(21), 7165–7181. <a href="https://doi.org/10.1093/jxb/erac384">https://doi.org/10.1093/jxb/erac384</a>

Blake Christopher Elliot. (2023, March). *Investigation of the effects of Mannitol-induced osmotic stress on calcium signalling in Arabidopsis thaliana*. The University of Canterbury, Christchurch, New Zealand.

Blein-Nicolas, M., & Zivy, M. (2016). Thousand and one ways to quantify and compare protein abundances in label-free bottom-up proteomics. *Biochimica et Biophysica Acta (BBA) - Proteins and Proteomics*, 1864(8), 883–895. <a href="https://doi.org/10.1016/j.bbapap.2016.02.019">https://doi.org/10.1016/j.bbapap.2016.02.019</a>

Bleker, C., Ramšak, Ž., Bittner, A., Podpečan, V., Zagorščak, M., Wurzinger, B., Baebler, Š., Petek, M., Križnik, M., Van Dieren, A., Gruber, J., Afjehi-Sadat, L., Weckwerth, W., Županič, A., Teige, M., Vothknecht, U. C., & Gruden, K. (2024). Stress Knowledge Map: A knowledge graph resource for systems biology analysis of plant stress responses. *Plant Communications*, 100920. <a href="https://doi.org/10.1016/j.xplc.2024.100920">https://doi.org/10.1016/j.xplc.2024.100920</a>

Blume, B., Nürnberger, T., Nass, N., & Scheel, D. (2000a). Receptor-Mediated Increase in Cytoplasmic Free Calcium Required for Activation of Pathogen Defense in Parsley. *The Plant Cell*, 12(8), 1425–1440. <a href="https://doi.org/10.1105/tpc.12.8.1425">https://doi.org/10.1105/tpc.12.8.1425</a>

Blume, B., Nürnberger, T., Nass, N., & Scheel, D. (2000b). Receptor-Mediated Increase in Cytoplasmic Free Calcium Required for Activation of Pathogen Defense in Parsley. *The Plant Cell*, 12(8), 1425–1440. <a href="https://doi.org/10.1105/tpc.12.8.1425">https://doi.org/10.1105/tpc.12.8.1425</a>

Bornstein, B. J., Keating, S. M., Jouraku, A., & Hucka, M. (2008). LibSBML: An API Library for SBML. *Bioinformatics*, *24*(6), 880–881. <a href="https://doi.org/10.1093/bioinformatics/btn051">https://doi.org/10.1093/bioinformatics/btn051</a>

Boulware, M. J., & Marchant, J. S. (2008). Timing in Cellular Ca2+ Signaling. *Current Biology*, 18(17), R769–R776. <a href="https://doi.org/10.1016/j.cub.2008.07.018">https://doi.org/10.1016/j.cub.2008.07.018</a>

Bourke, A., Hill, J. R., & Ó Gráda, C. (1993). *The visitation of God? The potato and the great Irish famine*. Lilliput Press.

Bowler, C., & Fluhr, R. (2000). The role of calcium and activated oxygens as signals for controlling cross-tolerance. *Trends in Plant Science*, *5*(6), 241–246. <a href="https://doi.org/10.1016/S1360-1385(00)01628-9">https://doi.org/10.1016/S1360-1385(00)01628-9</a>

Bush, D. S. (1995). Calcium Regulation in Plant Cells and its Role in Signaling. *Annual Review of Plant Physiology and Plant Molecular Biology*, 46(1), 95–122. https://doi.org/10.1146/annurev.pp.46.060195.000523

Caspi, R., Foerster, H., Fulcher, C. A., Kaipa, P., Krummenacker, M., Latendresse, M., Paley, S., Rhee, S. Y., Shearer, A. G., Tissier, C., Walk, T. C., Zhang, P., & Karp, P. D. (2007). The MetaCyc Database of metabolic pathways and enzymes and the BioCyc collection of Pathway/Genome Databases. *Nucleic Acids Research*, *36*(Database), D623–D631. <a href="https://doi.org/10.1093/nar/gkm900">https://doi.org/10.1093/nar/gkm900</a>

Chang, W., Zhang, Y., Ping, Y., Li, K., Qi, D.-D., & Song, F.-Q. (2023a). Label-free quantitative proteomics of arbuscular mycorrhizal Elaeagnus angustifolia seedlings provides insights into salt-stress tolerance mechanisms. *Frontiers in Plant Science*, *13*, 1098260. <a href="https://doi.org/10.3389/fpls.2022.1098260">https://doi.org/10.3389/fpls.2022.1098260</a>

Chang, W., Zhang, Y., Ping, Y., Li, K., Qi, D.-D., & Song, F.-Q. (2023b). Label-free quantitative proteomics of arbuscular mycorrhizal Elaeagnus angustifolia seedlings provides insights into salt-stress tolerance mechanisms. *Frontiers in Plant Science*, *13*, 1098260. <a href="https://doi.org/10.3389/fpls.2022.1098260">https://doi.org/10.3389/fpls.2022.1098260</a>

Chen, Q., & Yang, G. (2020). Signal Function Studies of ROS, Especially RBOH-Dependent ROS, in Plant Growth, Development and Environmental Stress. *Journal of Plant Growth Regulation*, 39(1), 157–171. https://doi.org/10.1007/s00344-019-09971-4

Chen, S., Wang, L., Kang, R., Liu, C., Xing, L., Wu, S., Wang, Z., Wu, C., Zhou, Q., & Zhao, R. (2024). Exogenous Calcium Alleviates the Photosynthetic Inhibition and Oxidative Damage of the Tea Plant under Cold Stress. *Horticulturae*, *10*(7), 666. <a href="https://doi.org/10.3390/horticulturae10070666">https://doi.org/10.3390/horticulturae10070666</a>

Cheng, C., Krishnakumar, V., Chan, A. P., Thibaud-Nissen, F., Schobel, S., & Town, C. D. (2017). Araport11: A complete reannotation of the *Arabidopsis thaliana* reference genome. *The Plant Journal*, 89(4), 789–804. <a href="https://doi.org/10.1111/tpj.13415">https://doi.org/10.1111/tpj.13415</a>

Chi, Y., Wang, C., Wang, M., Wan, D., Huang, F., Jiang, Z., Crawford, B. M., Vo-Dinh, T., Yuan, F., Wu, F., & Pei, Z. (2021). Flg22-induced Ca <sup>2+</sup> increases undergo desensitization and resensitization. *Plant, Cell & Environment, 44*(12), 3793–3805. https://doi.org/10.1111/pce.14186

Chinnusamy, V., Jagendorf, A., & Zhu, J. (2005). Understanding and Improving Salt Tolerance in Plants. *Crop Science*, 45(2), 437–448. <a href="https://doi.org/10.2135/cropsci2005.0437">https://doi.org/10.2135/cropsci2005.0437</a>

Chow, C.-N., Lee, T.-Y., Hung, Y.-C., Li, G.-Z., Tseng, K.-C., Liu, Y.-H., Kuo, P.-L., Zheng, H.-Q., & Chang, W.-C. (2019). PlantPAN3.0: A new and updated resource for reconstructing transcriptional regulatory networks from ChIP-seq experiments in plants. *Nucleic Acids Research*, 47(D1), D1155–D1163. <a href="https://doi.org/10.1093/nar/gky1081">https://doi.org/10.1093/nar/gky1081</a>

Clapham, D. E. (2007). Calcium Signaling. *Cell*, *131*(6), 1047–1058. <a href="https://doi.org/10.1016/j.cell.2007.11.028">https://doi.org/10.1016/j.cell.2007.11.028</a>

Clayton, H., Knight, M. R., Knight, H., McAinsh, M. R., & Hetherington, A. M. (1999). Dissection of the ozone-induced calcium signature. *The Plant Journal*, *17*(5), 575–579. https://doi.org/10.1046/j.1365-313X.1999.00411.x

Cline, M. S., Smoot, M., Cerami, E., Kuchinsky, A., Landys, N., Workman, C., Christmas, R., Avila-Campilo, I., Creech, M., Gross, B., Hanspers, K., Isserlin, R., Kelley, R., Killcoyne, S., Lotia, S., Maere, S., Morris, J., Ono, K., Pavlovic, V., ... Bader, G. D. (2007). Integration of biological networks and gene expression data using Cytoscape. *Nature Protocols*, *2*(10), 2366–2382. https://doi.org/10.1038/nprot.2007.324

Cobbold, P. H., & Rink, T. J. (1987). Fluorescence and bioluminescence measurement of cytoplasmic free calcium. *Biochemical Journal*, 248(2), 313–328. <a href="https://doi.org/10.1042/bj2480313">https://doi.org/10.1042/bj2480313</a>

Costa, A., Navazio, L., & Szabo, I. (2018). The contribution of organelles to plant intracellular calcium signalling. *Journal of Experimental Botany*, 69(17), 4175–4193. <a href="https://doi.org/10.1093/jxb/ery185">https://doi.org/10.1093/jxb/ery185</a>

Cusack, S. A., Wang, P., Lotreck, S. G., Moore, B. M., Meng, F., Conner, J. K., Krysan, P. J., Lehti-Shiu, M. D., & Shiu, S.-H. (2021). Predictive Models of Genetic Redundancy in *Arabidopsis thaliana*. *Molecular Biology and Evolution*, *38*(8), 3397–3414. <a href="https://doi.org/10.1093/molbev/msab111">https://doi.org/10.1093/molbev/msab111</a>

DeFalco, T. A., Bender, K. W., & Snedden, W. A. (2010). Breaking the code: Ca2+ sensors in plant signalling. *Biochemical Journal*, 425(1), 27–40. <a href="https://doi.org/10.1042/BJ20091147">https://doi.org/10.1042/BJ20091147</a>

Demidchik, V., & Maathuis, F. J. M. (2007). Physiological roles of nonselective cation channels in plants: From salt stress to signalling and development. *New Phytologist*, *175*(3), 387–404. https://doi.org/10.1111/j.1469-8137.2007.02128.x

Demidchik, V., Shabala, S., Isayenkov, S., Cuin, T. A., & Pottosin, I. (2018a). Calcium transport across plant membranes: Mechanisms and functions. *New Phytologist*, *220*(1), 49–69. <a href="https://doi.org/10.1111/nph.15266">https://doi.org/10.1111/nph.15266</a>

Demidchik, V., Shabala, S., Isayenkov, S., Cuin, T. A., & Pottosin, I. (2018b). Calcium transport across plant membranes: Mechanisms and functions. *New Phytologist*, *220*(1), 49–69. <a href="https://doi.org/10.1111/nph.15266">https://doi.org/10.1111/nph.15266</a>

Dodd, A. N., Kudla, J., & Sanders, D. (2010). The Language of Calcium Signaling. *Annual Review of Plant Biology*, 61(1), 593–620. <a href="https://doi.org/10.1146/annurev-arplant-070109-104628">https://doi.org/10.1146/annurev-arplant-070109-104628</a>

Domínguez, E., Cuartero, J., & Heredia, A. (2011). An overview on plant cuticle biomechanics. *Plant Science*, *181*(2), 77–84. <a href="https://doi.org/10.1016/j.plantsci.2011.04.016">https://doi.org/10.1016/j.plantsci.2011.04.016</a>

Dubiella, U., Seybold, H., Durian, G., Komander, E., Lassig, R., Witte, C.-P., Schulze, W. X., & Romeis, T. (2013). Calcium-dependent protein kinase/NADPH oxidase activation circuit is required for rapid defense signal propagation. *Proceedings of the National Academy of Sciences*, 110(21), 8744–8749. https://doi.org/10.1073/pnas.1221294110

Eckardt, N. A. (2015). *The Plant Cell* Reviews Dynamic Aspects of Plant Hormone Signaling and Crosstalk. *The Plant Cell*, 27(1), 1–2. <a href="https://doi.org/10.1105/tpc.115.136291">https://doi.org/10.1105/tpc.115.136291</a>

Edel, K. H., Marchadier, E., Brownlee, C., Kudla, J., & Hetherington, A. M. (2017). The Evolution of Calcium-Based Signalling in Plants. *Current Biology*, *27*(13), R667–R679. <a href="https://doi.org/10.1016/j.cub.2017.05.020">https://doi.org/10.1016/j.cub.2017.05.020</a>

Edmonds, J., & Karp, R. M. (1972). Theoretical Improvements in Algorithmic Efficiency for Network Flow Problems. *Journal of the ACM*, 19(2), 248–264. <a href="https://doi.org/10.1145/321694.321699">https://doi.org/10.1145/321694.321699</a>

Evans, C. H. (1990). Biochemical Techniques Which Employ Lanthanides. In C. H. Evans, *Biochemistry of the Lanthanides* (pp. 47–84). Springer US. <a href="https://doi.org/10.1007/978-1-4684-8748-0">https://doi.org/10.1007/978-1-4684-8748-0</a> 3

Fahad, S., Bajwa, A. A., Nazir, U., Anjum, S. A., Farooq, A., Zohaib, A., Sadia, S., Nasim, W., Adkins, S., Saud, S., Ihsan, M. Z., Alharby, H., Wu, C., Wang, D., & Huang, J. (2017). Crop Production under Drought and Heat Stress: Plant Responses and Management Options. *Frontiers in Plant Science*, *8*, 1147. <a href="https://doi.org/10.3389/fpls.2017.01147">https://doi.org/10.3389/fpls.2017.01147</a>

Fichman, Y., Zandalinas, S. I., Peck, S., Luan, S., & Mittler, R. (2022). HPCA1 is required for systemic reactive oxygen species and calcium cell-to-cell signaling and plant acclimation to stress. *The Plant Cell*, *34*(11), 4453–4471. <a href="https://doi.org/10.1093/plcell/koac241">https://doi.org/10.1093/plcell/koac241</a>

Foix, L., Nadal, A., Zagorščak, M., Ramšak, Ž., Esteve-Codina, A., Gruden, K., & Pla, M. (2021). Prunus persica plant endogenous peptides PpPep1 and PpPep2 cause PTI-like transcriptome reprogramming in peach and enhance resistance to Xanthomonas arboricola pv. Pruni. *BMC Genomics*, 22(1), 360. <a href="https://doi.org/10.1186/s12864-021-07571-9">https://doi.org/10.1186/s12864-021-07571-9</a>

Foyer, C. H., & Noctor, G. (2013). Redox Signaling in Plants. *Antioxidants & Redox Signaling*, 18(16), 2087–2090. https://doi.org/10.1089/ars.2013.5278

Fricker, M. D., Plieth, C., Knight, H., Blancaflor, E., Knight, M. R., White, N. S., & Gilroy, S. (1999). Fluorescence and Luminescence Techniques to Probe Ion Activities in Living Plant Cells. In *Fluorescent and Luminescent Probes for Biological Activity* (pp. 569–596). Elsevier. <a href="https://doi.org/10.1016/B978-012447836-7/50044-0">https://doi.org/10.1016/B978-012447836-7/50044-0</a>

Friedman, H., Meir, S., Rosenberger, I., Halevy, A. H., Kaufman, P. B., & Philosoph-Hadas, S. (1998). Inhibition of the Gravitropic Response of Snapdragon Spikes by the Calcium-Channel

Blocker Lanthanum Chloride. *Plant Physiology*, *118*(2), 483–492. https://doi.org/10.1104/pp.118.2.483

Gansner, E. R., & North, S. C. (2000). An open graph visualization system and its applications to software engineering. *Software: Practice and Experience, 30*(11), 1203–1233. https://doi.org/10.1002/1097-024X(200009)30:11<1203::AID-SPE338>3.0.CO;2-N

Garcia, E., Koh, J., Wu, X., Sarkhosh, A., & Liu, T. (2024). Tissue-specific proteome profile analysis reveals regulatory and stress responsive networks in passion fruit during storage. *Scientific Reports*, *14*(1), 3564. <a href="https://doi.org/10.1038/s41598-024-52557-8">https://doi.org/10.1038/s41598-024-52557-8</a>

Garrett, K. A. (2013). Big data insights into pest spread. *Nature Climate Change*, *3*(11), 955–957. https://doi.org/10.1038/nclimate2041

Ge, S. X., Jung, D., & Yao, R. (2020). ShinyGO: A graphical gene-set enrichment tool for animals and plants. *Bioinformatics*, *36*(8), 2628–2629. <a href="https://doi.org/10.1093/bioinformatics/btz931">https://doi.org/10.1093/bioinformatics/btz931</a>

Ghazalpour, A., Bennett, B., Petyuk, V. A., Orozco, L., Hagopian, R., Mungrue, I. N., Farber, C. R., Sinsheimer, J., Kang, H. M., Furlotte, N., Park, C. C., Wen, P.-Z., Brewer, H., Weitz, K., Camp, D. G., Pan, C., Yordanova, R., Neuhaus, I., Tilford, C., ... Lusis, A. J. (2011). Comparative Analysis of Proteome and Transcriptome Variation in Mouse. *PLoS Genetics*, *7*(6), e1001393. <a href="https://doi.org/10.1371/journal.pgen.1001393">https://doi.org/10.1371/journal.pgen.1001393</a>

Ghosh, S., Bheri, M., Bisht, D., & Pandey, G. K. (2022). Calcium signaling and transport machinery: Potential for development of stress tolerance in plants. *Current Plant Biology*, *29*, 100235. <a href="https://doi.org/10.1016/j.cpb.2022.100235">https://doi.org/10.1016/j.cpb.2022.100235</a>

Gill, S. S., Anjum, N. A., Gill, R., & Tuteja, N. (2016). Abiotic Stress Signaling in Plants—An Overview. In N. Tuteja & S. S. Gill (Eds.), *Abiotic Stress Response in Plants* (1st ed., pp. 1–12). Wiley. <a href="https://doi.org/10.1002/9783527694570.ch1">https://doi.org/10.1002/9783527694570.ch1</a>

Gilroy, S., Białasek, M., Suzuki, N., Górecka, M., Devireddy, A. R., Karpiński, S., & Mittler, R. (2016). ROS, Calcium, and Electric Signals: Key Mediators of Rapid Systemic Signaling in Plants. *Plant Physiology*, *171*(3), 1606–1615. <a href="https://doi.org/10.1104/pp.16.00434">https://doi.org/10.1104/pp.16.00434</a>

Gilroy, S., Hughes, W. A., & Trewavas, A. J. (1989). A Comparison between Quin-2 and Aequorin as Indicators of Cytoplasmic Calcium Levels in Higher Plant Cell Protoplasts. *Plant Physiology*, 90(2), 482–491. <a href="https://doi.org/10.1104/pp.90.2.482">https://doi.org/10.1104/pp.90.2.482</a>

Gilroy, S., Read, N. D., & Trewavas, A. J. (1990). Elevation of cytoplasmic calcium by caged calcium or caged inositol trisphosphate initiates stomatal closure. *Nature*, *346*(6286), 769–771. <a href="https://doi.org/10.1038/346769a0">https://doi.org/10.1038/346769a0</a>

Giridhar, M., Meier, B., Imani, J., Kogel, K.-H., Peiter, E., Vothknecht, U. C., & Chigri, F. (2022a). Comparative analysis of stress-induced calcium signals in the crop species barley and the model plant Arabidopsis thaliana. *BMC Plant Biology*, *22*(1), 447. <a href="https://doi.org/10.1186/s12870-022-03820-5">https://doi.org/10.1186/s12870-022-03820-5</a>

Giridhar, M., Meier, B., Imani, J., Kogel, K.-H., Peiter, E., Vothknecht, U. C., & Chigri, F. (2022b). Comparative analysis of stress-induced calcium signals in the crop species barley and the

model plant Arabidopsis thaliana. *BMC Plant Biology*, 22(1), 447. <a href="https://doi.org/10.1186/s12870-022-03820-5">https://doi.org/10.1186/s12870-022-03820-5</a>

Gry, M., Rimini, R., Strömberg, S., Asplund, A., Pontén, F., Uhlén, M., & Nilsson, P. (2009). Correlations between RNA and protein expression profiles in 23 human cell lines. *BMC Genomics*, *10*(1), 365. https://doi.org/10.1186/1471-2164-10-365

Hagberg, A. A., Schult, D. A., & Swart, P. J. (2008). *Exploring Network Structure, Dynamics, and Function using NetworkX*. 11–15. <a href="https://doi.org/10.25080/TCWV9851">https://doi.org/10.25080/TCWV9851</a>

Halliwell, B. (1989). Chemiluminescence. Principles and applications in biology and medicine: By A.K. Campbell Ellis Horwood; Chichester, 1988 608 pages. £103.00. *FEBS Letters*, 247(2), 497–498. <a href="https://doi.org/10.1016/0014-5793(89)81404-8">https://doi.org/10.1016/0014-5793(89)81404-8</a>

Halliwell, B., & Gutteridge, J. M. C. (2015). *Free Radicals in Biology and Medicine*. Oxford University Press. <a href="https://doi.org/10.1093/acprof:oso/9780198717478.001.0001">https://doi.org/10.1093/acprof:oso/9780198717478.001.0001</a>

Hashimoto, K., & Kudla, J. (2011). Calcium decoding mechanisms in plants. *Biochimie*, *93*(12), 2054–2059. https://doi.org/10.1016/j.biochi.2011.05.019

Hassani-Pak, K., Singh, A., Brandizi, M., Hearnshaw, J., Parsons, J. D., Amberkar, S., Phillips, A. L., Doonan, J. H., & Rawlings, C. (2021). KnetMiner: A comprehensive approach for supporting evidence-based gene discovery and complex trait analysis across species. *Plant Biotechnology Journal*, 19(8), 1670–1678. <a href="https://doi.org/10.1111/pbi.13583">https://doi.org/10.1111/pbi.13583</a>

Hastings, J., Owen, G., Dekker, A., Ennis, M., Kale, N., Muthukrishnan, V., Turner, S., Swainston, N., Mendes, P., & Steinbeck, C. (2016). ChEBI in 2016: Improved services and an expanding collection of metabolites. *Nucleic Acids Research*, *44*(D1), D1214–D1219. <a href="https://doi.org/10.1093/nar/gkv1031">https://doi.org/10.1093/nar/gkv1031</a>

Herwig, R., Hardt, C., Lienhard, M., & Kamburov, A. (2016). Analyzing and interpreting genome data at the network level with ConsensusPathDB. *Nature Protocols*, *11*(10), 1889–1907. <a href="https://doi.org/10.1038/nprot.2016.117">https://doi.org/10.1038/nprot.2016.117</a>

Hoque, T. S., Hossain, M. A., Mostofa, M. G., Burritt, D. J., Fujita, M., & Tran, L.-S. P. (2016). Methylglyoxal: An Emerging Signaling Molecule in Plant Abiotic Stress Responses and Tolerance. *Frontiers in Plant Science*, 7. <a href="https://doi.org/10.3389/fpls.2016.01341">https://doi.org/10.3389/fpls.2016.01341</a>

Hunter, M. C., Smith, R. G., Schipanski, M. E., Atwood, L. W., & Mortensen, D. A. (2017). Agriculture in 2050: Recalibrating Targets for Sustainable Intensification. *BioScience*, *67*(4), 386–391. <a href="https://doi.org/10.1093/biosci/bix010">https://doi.org/10.1093/biosci/bix010</a>

Inouye, S., Noguchi, M., Sakaki, Y., Takagi, Y., Miyata, T., Iwanaga, S., Miyata, T., & Tsuji, F. I. (1985). Cloning and sequence analysis of cDNA for the luminescent protein aequorin. *Proceedings of the National Academy of Sciences*, 82(10), 3154–3158. https://doi.org/10.1073/pnas.82.10.3154

Intergovernmental Panel On Climate Change (Ipcc) (Ed.). (2023). Summary for Policymakers. In *Climate Change 2022—Mitigation of Climate Change* (1st ed., pp. 3–48). Cambridge University Press. <a href="https://doi.org/10.1017/9781009157926.001">https://doi.org/10.1017/9781009157926.001</a>

Jiang, Z., Zhu, S., Ye, R., Xue, Y., Chen, A., An, L., & Pei, Z.-M. (2013). Relationship between NaCland H2O2-Induced Cytosolic Ca2+ Increases in Response to Stress in Arabidopsis. *PLoS ONE*, 8(10), e76130. <a href="https://doi.org/10.1371/journal.pone.0076130">https://doi.org/10.1371/journal.pone.0076130</a>

Johnson, C. H., Knight, M. R., Kondo, T., Masson, P., Sedbrook, J., Haley, A., & Trewavas, A. (1995). Circadian Oscillations of Cytosolic and Chloroplastic Free Calcium in Plants. *Science*, *269*(5232), 1863–1865. <a href="https://doi.org/10.1126/science.7569925">https://doi.org/10.1126/science.7569925</a>

Jones, A. M. E., & De Smet, I. (2023). Editorial: Proteomics of plant development and hormonal responses, volume II. *Frontiers in Plant Science*, *14*, 1340170. <a href="https://doi.org/10.3389/fpls.2023.1340170">https://doi.org/10.3389/fpls.2023.1340170</a>

Juteršek, M., Petek, M., Ramšak, Ž., Moreno-Giménez, E., Gianoglio, S., Mateos-Fernández, R., Orzáez, D., Gruden, K., & Baebler, Š. (2022). Transcriptional deregulation of stress-growth balance in Nicotiana benthamiana biofactories producing insect sex pheromones. *Frontiers in Plant Science*, *13*, 941338. <a href="https://doi.org/10.3389/fpls.2022.941338">https://doi.org/10.3389/fpls.2022.941338</a>

Kamara, A. Y., Menkir, A., Badu-Apraku, B., & Ibikunle, O. (2003). The influence of drought stress on growth, yield and yield components of selected maize genotypes. *The Journal of Agricultural Science*, 141(1), 43–50. <a href="https://doi.org/10.1017/S0021859603003423">https://doi.org/10.1017/S0021859603003423</a>

Kanehisa, M., Sato, Y., Kawashima, M., Furumichi, M., & Tanabe, M. (2016). KEGG as a reference resource for gene and protein annotation. *Nucleic Acids Research*, *44*(D1), D457–D462. <a href="https://doi.org/10.1093/nar/gkv1070">https://doi.org/10.1093/nar/gkv1070</a>

Kaplan, B., Davydov, O., Knight, H., Galon, Y., Knight, M. R., Fluhr, R., & Fromm, H. (2006). Rapid Transcriptome Changes Induced by Cytosolic Ca2+ Transients Reveal ABRE-Related Sequences as Ca2+-Responsive *cis* Elements in *Arabidopsis*. *The Plant Cell*, *18*(10), 2733–2748. <a href="https://doi.org/10.1105/tpc.106.042713">https://doi.org/10.1105/tpc.106.042713</a>

Kärkönen, A., & Kuchitsu, K. (2015). Reactive oxygen species in cell wall metabolism and development in plants. *Phytochemistry*, 112, 22–32. <a href="https://doi.org/10.1016/j.phytochem.2014.09.016">https://doi.org/10.1016/j.phytochem.2014.09.016</a>

Keating, S. M., Waltemath, D., König, M., Zhang, F., Dräger, A., Chaouiya, C., Bergmann, F. T., Finney, A., Gillespie, C. S., Helikar, T., Hoops, S., Malik-Sheriff, R. S., Moodie, S. L., Moraru, I. I., Myers, C. J., Naldi, A., Olivier, B. G., Sahle, S., Schaff, J. C., ... Zucker, J. (2020). SBML Level 3: An extensible format for the exchange and reuse of biological models. *Molecular Systems Biology*, *16*(8), e9110. <a href="https://doi.org/10.15252/msb.20199110">https://doi.org/10.15252/msb.20199110</a>

Kim, Y.-U., & Lee, B.-W. (2019). Differential Mechanisms of Potato Yield Loss Induced by High Day and Night Temperatures During Tuber Initiation and Bulking: Photosynthesis and Tuber Growth. *Frontiers in Plant Science*, *10*, 300. <a href="https://doi.org/10.3389/fpls.2019.00300">https://doi.org/10.3389/fpls.2019.00300</a>

Kissoudis, C., Van De Wiel, C., Visser, R. G. F., & Van Der Linden, G. (2014). Enhancing crop resilience to combined abiotic and biotic stress through the dissection of physiological and molecular crosstalk. *Frontiers in Plant Science*, 5. <a href="https://doi.org/10.3389/fpls.2014.00207">https://doi.org/10.3389/fpls.2014.00207</a>

Klarner, H., Streck, A., & Siebert, H. (2017). PyBoolNet: A python package for the generation, analysis and visualization of boolean networks. *Bioinformatics*, *33*(5), 770–772. <a href="https://doi.org/10.1093/bioinformatics/btw682">https://doi.org/10.1093/bioinformatics/btw682</a>

Klejchova, M., Silva-Alvim, F. A. L., Blatt, M. R., & Alvim, J. C. (2021). Membrane voltage as a dynamic platform for spatiotemporal signaling, physiological, and developmental regulation. *Plant Physiology*, *185*(4), 1523–1541. <a href="https://doi.org/10.1093/plphys/kiab032">https://doi.org/10.1093/plphys/kiab032</a>

Knight, H., & Knight, M. R. (1995a). Chapter 14 Recombinant Aequorin Methods for Intracellular Calcium Measurement in Plants. In *Methods in Cell Biology* (Vol. 49, pp. 201–216). Elsevier. <a href="https://doi.org/10.1016/S0091-679X(08)61455-7">https://doi.org/10.1016/S0091-679X(08)61455-7</a>

Knight, H., & Knight, M. R. (1995b). Chapter 14 Recombinant Aequorin Methods for Intracellular Calcium Measurement in Plants. In *Methods in Cell Biology* (Vol. 49, pp. 201–216). Elsevier. <a href="https://doi.org/10.1016/S0091-679X(08)61455-7">https://doi.org/10.1016/S0091-679X(08)61455-7</a>

Knight, H., & Knight, M. R. (2000). Imaging spatial and cellular characteristics of low temperature calcium signature after cold acclimation in Arabidopsis. *Journal of Experimental Botany*, *51*(351), 1679–1686. <a href="https://doi.org/10.1093/jexbot/51.351.1679">https://doi.org/10.1093/jexbot/51.351.1679</a>

Knight, H., Trewavas, A. J., & Knight, M. R. (1996). Cold calcium signaling in Arabidopsis involves two cellular pools and a change in calcium signature after acclimation. *The Plant Cell*, 8(3), 489–503. <a href="https://doi.org/10.1105/tpc.8.3.489">https://doi.org/10.1105/tpc.8.3.489</a>

Knight, H., Trewavas, A. J., & Knight, M. R. (1997a). Calcium signalling in *Arabidopsis thaliana* responding to drought and salinity. *The Plant Journal*, *12*(5), 1067–1078. <a href="https://doi.org/10.1046/j.1365-313X.1997.12051067.x">https://doi.org/10.1046/j.1365-313X.1997.12051067.x</a>

Knight, H., Trewavas, A. J., & Knight, M. R. (1997b). Calcium signalling in *Arabidopsis thaliana* responding to drought and salinity. *The Plant Journal*, *12*(5), 1067–1078. <a href="https://doi.org/10.1046/j.1365-313X.1997.12051067.x">https://doi.org/10.1046/j.1365-313X.1997.12051067.x</a>

Knight, M. R., Campbell, A. K., Smith, S. M., & Trewavas, A. J. (1991a). Transgenic plant aequorin reports the effects of touch and cold-shock and elicitors on cytoplasmic calcium. *Nature*, *352*(6335), 524–526. <a href="https://doi.org/10.1038/352524a0">https://doi.org/10.1038/352524a0</a>

Knight, M. R., Campbell, A. K., Smith, S. M., & Trewavas, A. J. (1991b). Transgenic plant aequorin reports the effects of touch and cold-shock and elicitors on cytoplasmic calcium. *Nature*, *352*(6335), 524–526. <a href="https://doi.org/10.1038/352524a0">https://doi.org/10.1038/352524a0</a>

Knight, M. R., Smith, S. M., & Trewavas, A. J. (1992). Wind-induced plant motion immediately increases cytosolic calcium. *Proceedings of the National Academy of Sciences*, 89(11), 4967–4971. https://doi.org/10.1073/pnas.89.11.4967

Kobayashi, M., Ohura, I., Kawakita, K., Yokota, N., Fujiwara, M., Shimamoto, K., Doke, N., & Yoshioka, H. (2007). Calcium-Dependent Protein Kinases Regulate the Production of Reactive Oxygen Species by Potato NADPH Oxidase. *The Plant Cell*, *19*(3), 1065–1080. <a href="https://doi.org/10.1105/tpc.106.048884">https://doi.org/10.1105/tpc.106.048884</a>

König, J., Muthuramalingam, M., & Dietz, K.-J. (2012a). Mechanisms and dynamics in the thiol/disulfide redox regulatory network: Transmitters, sensors and targets. *Current Opinion in Plant Biology*, *15*(3), 261–268. https://doi.org/10.1016/j.pbi.2011.12.002

König, J., Muthuramalingam, M., & Dietz, K.-J. (2012b). Mechanisms and dynamics in the thiol/disulfide redox regulatory network: Transmitters, sensors and targets. *Current Opinion in Plant Biology*, *15*(3), 261–268. <a href="https://doi.org/10.1016/j.pbi.2011.12.002">https://doi.org/10.1016/j.pbi.2011.12.002</a>

König, M. (2020). *matthiaskoenig/libsbgn-python: 0.2.2* (Version 0.2.2) [Computer software]. Zenodo. <a href="https://doi.org/10.5281/ZENODO.4171366">https://doi.org/10.5281/ZENODO.4171366</a>

Kudla, J., Batistič, O., & Hashimoto, K. (2010a). Calcium Signals: The Lead Currency of Plant Information Processing. *The Plant Cell*, 22(3), 541–563. https://doi.org/10.1105/tpc.109.072686

Kudla, J., Batistič, O., & Hashimoto, K. (2010b). Calcium Signals: The Lead Currency of Plant Information Processing. *The Plant Cell*, 22(3), 541–563. <a href="https://doi.org/10.1105/tpc.109.072686">https://doi.org/10.1105/tpc.109.072686</a>

Lenzoni, G., Liu, J., & Knight, M. R. (2018). Predicting plant immunity gene expression by identifying the decoding mechanism of calcium signatures. *New Phytologist*, *217*(4), 1598–1609. https://doi.org/10.1111/nph.14924

Li, Y., Liu, Y., Jin, L., & Peng, R. (2022a). Crosstalk between Ca2+ and Other Regulators Assists Plants in Responding to Abiotic Stress. *Plants*, *11*(10), 1351. <a href="https://doi.org/10.3390/plants11101351">https://doi.org/10.3390/plants11101351</a>

Li, Y., Liu, Y., Jin, L., & Peng, R. (2022b). Crosstalk between Ca2+ and Other Regulators Assists Plants in Responding to Abiotic Stress. *Plants*, *11*(10), 1351. https://doi.org/10.3390/plants11101351

Liang, L., Guo, L., Zhai, Y., Hou, Z., Wu, W., Zhang, X., Wu, Y., Liu, X., Guo, S., Gao, G., & Liu, W. (2023). Genome-wide characterization of SOS1 gene family in potato (Solanum tuberosum) and expression analyses under salt and hormone stress. *Frontiers in Plant Science*, *14*, 1201730. <a href="https://doi.org/10.3389/fpls.2023.1201730">https://doi.org/10.3389/fpls.2023.1201730</a>

Lichtenberg, J., Yilmaz, A., Welch, J. D., Kurz, K., Liang, X., Drews, F., Ecker, K., Lee, S. S., Geisler, M., Grotewold, E., & Welch, L. R. (2009). The word landscape of the non-coding segments of the Arabidopsis thaliana genome. *BMC Genomics*, *10*(1), 463. <a href="https://doi.org/10.1186/1471-2164-10-463">https://doi.org/10.1186/1471-2164-10-463</a>

Liu, Y., Beyer, A., & Aebersold, R. (2016). On the Dependency of Cellular Protein Levels on mRNA Abundance. *Cell*, 165(3), 535–550. <a href="https://doi.org/10.1016/j.cell.2016.03.014">https://doi.org/10.1016/j.cell.2016.03.014</a>

Lu, Y.-J., Li, P., Shimono, M., Corrion, A., Higaki, T., He, S. Y., & Day, B. (2020). Arabidopsis calcium-dependent protein kinase 3 regulates actin cytoskeleton organization and immunity. *Nature Communications*, *11*(1), 6234. https://doi.org/10.1038/s41467-020-20007-4

Ludwig, A. A. (2003). CDPK-mediated signalling pathways: Specificity and cross-talk. *Journal of Experimental Botany*, *55*(395), 181–188. <a href="https://doi.org/10.1093/jxb/erh008">https://doi.org/10.1093/jxb/erh008</a>

Maintz, J., Cavdar, M., Tamborski, J., Kwaaitaal, M., Huisman, R., Meesters, C., Kombrink, E., & Panstruga, R. (2014a). Comparative Analysis of MAMP-induced Calcium Influx in Arabidopsis Seedlings and Protoplasts. *Plant and Cell Physiology*, *55*(10), 1813–1825. <a href="https://doi.org/10.1093/pcp/pcu112">https://doi.org/10.1093/pcp/pcu112</a>

Maintz, J., Cavdar, M., Tamborski, J., Kwaaitaal, M., Huisman, R., Meesters, C., Kombrink, E., & Panstruga, R. (2014b). Comparative Analysis of MAMP-induced Calcium Influx in Arabidopsis Seedlings and Protoplasts. *Plant and Cell Physiology*, *55*(10), 1813–1825. <a href="https://doi.org/10.1093/pcp/pcu112">https://doi.org/10.1093/pcp/pcu112</a>

Mandal, S. M., Chakraborty, D., & Dey, S. (2010). Phenolic acids act as signaling molecules in plant-microbe symbioses. *Plant Signaling & Behavior*, *5*(4), 359–368. https://doi.org/10.4161/psb.5.4.10871

Marcec, M. J., Gilroy, S., Poovaiah, B. W., & Tanaka, K. (2019). Mutual interplay of Ca2+ and ROS signaling in plant immune response. *Plant Science*, *283*, 343–354. <a href="https://doi.org/10.1016/j.plantsci.2019.03.004">https://doi.org/10.1016/j.plantsci.2019.03.004</a>

Marcec, M. J., & Tanaka, K. (2021). Crosstalk between Calcium and ROS Signaling during Flg22-Triggered Immune Response in Arabidopsis Leaves. *Plants*, *11*(1), 14. <a href="https://doi.org/10.3390/plants11010014">https://doi.org/10.3390/plants11010014</a>

Martins, T. V., Hammelman, J., Marinova, S., Ding, C. O., & Morris, R. J. (2019). An Information-Theoretical Approach for Calcium Signaling Specificity. *IEEE Transactions on NanoBioscience*, *18*(1), 93–100. <a href="https://doi.org/10.1109/TNB.2018.2882223">https://doi.org/10.1109/TNB.2018.2882223</a>

Mattila, H., Khorobrykh, S., Havurinne, V., & Tyystjärvi, E. (2015). Reactive oxygen species: Reactions and detection from photosynthetic tissues. *Journal of Photochemistry and Photobiology B: Biology*, *152*, 176–214. <a href="https://doi.org/10.1016/j.jphotobiol.2015.10.001">https://doi.org/10.1016/j.jphotobiol.2015.10.001</a>

McAinsh, M. R., Clayton, H., Mansfield, T. A., & Hetherington, A. M. (1996). Changes in Stomatal Behavior and Guard Cell Cytosolic Free Calcium in Response to Oxidative Stress. *Plant Physiology*, 111(4), 1031–1042. https://doi.org/10.1104/pp.111.4.1031

McAinsh, M. R., & Hetherington, A. M. (1998). Encoding specificity in Ca2+ signalling systems. *Trends in Plant Science*, *3*(1), 32–36. <a href="https://doi.org/10.1016/S1360-1385(97)01150-3">https://doi.org/10.1016/S1360-1385(97)01150-3</a>

McAinsh, M. R., & Pittman, J. K. (2009). Shaping the calcium signature. *New Phytologist*, 181(2), 275–294. https://doi.org/10.1111/j.1469-8137.2008.02682.x

Mehlmer, N., Wurzinger, B., Stael, S., Hofmann-Rodrigues, D., Csaszar, E., Pfister, B., Bayer, R., & Teige, M. (2010). The Ca2+-dependent protein kinase CPK3 is required for MAPK-independent salt-stress acclimation in Arabidopsis: CPK3 signalling in plant salt stress. *The Plant Journal*, 63(3), 484–498. https://doi.org/10.1111/j.1365-313X.2010.04257.x

Mignolet-Spruyt, L., Xu, E., Idänheimo, N., Hoeberichts, F. A., Mühlenbock, P., Brosché, M., Van Breusegem, F., & Kangasjärvi, J. (2016). Spreading the news: Subcellular and organellar reactive oxygen species production and signalling. *Journal of Experimental Botany*, *67*(13), 3831–3844. https://doi.org/10.1093/jxb/erw080

Miljkovic, D., Stare, T., Mozetič, I., Podpečan, V., Petek, M., Witek, K., Dermastia, M., Lavrač, N., & Gruden, K. (2012). Signalling Network Construction for Modelling Plant Defence Response. *PLoS ONE*, *7*(12), e51822. <a href="https://doi.org/10.1371/journal.pone.0051822">https://doi.org/10.1371/journal.pone.0051822</a>

Miller, J. B., Pratap, A., Miyahara, A., Zhou, L., Bornemann, S., Morris, R. J., & Oldroyd, G. E. D. (2014). Calcium/Calmodulin-Dependent Protein Kinase Is Negatively and Positively Regulated by Calcium, Providing a Mechanism for Decoding Calcium Responses during Symbiosis Signaling. *The Plant Cell*, 25(12), 5053–5066. <a href="https://doi.org/10.1105/tpc.113.116921">https://doi.org/10.1105/tpc.113.116921</a>

Mithöfer, A., Ebel, J., Bhagwat, A. A., Boller, T., & Neuhaus-Url, G. (1999). Transgenic aequorin monitors cytosolic calcium transients in soybean cells challenged with  $\beta$ -glucan or chitin elicitors. *Planta*, 207(4), 566–574. <a href="https://doi.org/10.1007/s004250050519">https://doi.org/10.1007/s004250050519</a>

Mithöfer, A., & Mazars, C. (2002a). Aequorin-based measurements of intracellular Ca2+-signatures in plant cells. *Biological Procedures Online*, *4*(1), 105–118. <a href="https://doi.org/10.1251/bpo40">https://doi.org/10.1251/bpo40</a>

Mithöfer, A., & Mazars, C. (2002b). Aequorin-based measurements of intracellular Ca2+-signatures in plant cells. *Biological Procedures Online*, *4*(1), 105–118. <a href="https://doi.org/10.1251/bpo40">https://doi.org/10.1251/bpo40</a>

Mittler, R. (2017). ROS Are Good. *Trends in Plant Science*, *22*(1), 11–19. <a href="https://doi.org/10.1016/j.tplants.2016.08.002">https://doi.org/10.1016/j.tplants.2016.08.002</a>

Mittler, R., Vanderauwera, S., Gollery, M., & Van Breusegem, F. (2004). Reactive oxygen gene network of plants. *Trends in Plant Science*, *9*(10), 490–498. <a href="https://doi.org/10.1016/j.tplants.2004.08.009">https://doi.org/10.1016/j.tplants.2004.08.009</a>

Mittler, R., Vanderauwera, S., Suzuki, N., Miller, G., Tognetti, V. B., Vandepoele, K., Gollery, M., Shulaev, V., & Van Breusegem, F. (2011). ROS signaling: The new wave? *Trends in Plant Science*, *16*(6), 300–309. <a href="https://doi.org/10.1016/j.tplants.2011.03.007">https://doi.org/10.1016/j.tplants.2011.03.007</a>

Mohanta, T. K., Yadav, D., Khan, A. L., Hashem, A., Abd\_Allah, E. F., & Al-Harrasi, A. (2019a). Molecular Players of EF-hand Containing Calcium Signaling Event in Plants. *International Journal of Molecular Sciences*, 20(6), 1476. <a href="https://doi.org/10.3390/ijms20061476">https://doi.org/10.3390/ijms20061476</a>

Mohanta, T. K., Yadav, D., Khan, A. L., Hashem, A., Abd\_Allah, E. F., & Al-Harrasi, A. (2019b). Molecular Players of EF-hand Containing Calcium Signaling Event in Plants. *International Journal of Molecular Sciences*, 20(6), 1476. <a href="https://doi.org/10.3390/ijms20061476">https://doi.org/10.3390/ijms20061476</a>

Møller, I. M. (2001). P LANT M ITOCHONDRIA AND O XIDATIVE S TRESS: Electron Transport, NADPH Turnover, and Metabolism of Reactive Oxygen Species. *Annual Review of Plant Physiology and Plant Molecular Biology*, *52*(1), 561–591. <a href="https://doi.org/10.1146/annurev.arplant.52.1.561">https://doi.org/10.1146/annurev.arplant.52.1.561</a>

Moroz, N., & Tanaka, K. (2020). FlgII-28 Is a Major Flagellin-Derived Defense Elicitor in Potato. *Molecular Plant-Microbe Interactions®*, *33*(2), 247–255. <a href="https://doi.org/10.1094/MPMI-06-19-0164-R">https://doi.org/10.1094/MPMI-06-19-0164-R</a>

Mueller, L. A., Zhang, P., & Rhee, S. Y. (2003). AraCyc: A biochemical pathway database for Arabidopsis. *Plant Physiology*, *132*(2), 453–460. <a href="https://doi.org/10.1104/pp.102.017236">https://doi.org/10.1104/pp.102.017236</a>

Mulligan, R. M., Chory, J., & Ecker, J. R. (1997). Signaling in plants. *Proceedings of the National Academy of Sciences*, *94*(7), 2793–2795. <a href="https://doi.org/10.1073/pnas.94.7.2793">https://doi.org/10.1073/pnas.94.7.2793</a>

Mur, L. A. J., Kenton, P., Atzorn, R., Miersch, O., & Wasternack, C. (2006). The Outcomes of Concentration-Specific Interactions between Salicylate and Jasmonate Signaling Include Synergy, Antagonism, and Oxidative Stress Leading to Cell Death. *Plant Physiology*, *140*(1), 249–262. <a href="https://doi.org/10.1104/pp.105.072348">https://doi.org/10.1104/pp.105.072348</a>

Müssel, C., Hopfensitz, M., & Kestler, H. A. (2010). BoolNet—An R package for generation, reconstruction and analysis of Boolean networks. *Bioinformatics*, *26*(10), 1378–1380. https://doi.org/10.1093/bioinformatics/btq124

Nagel-Volkmann, J., Plieth, C., Becker, D., Lüthen, H., & Dörffling, K. (2009a). Cold-induced cytosolic free calcium ion concentration changes in wheat. *Journal of Plant Physiology*, *166*(17), 1955–1960. <a href="https://doi.org/10.1016/j.jplph.2009.05.002">https://doi.org/10.1016/j.jplph.2009.05.002</a>

Nagel-Volkmann, J., Plieth, C., Becker, D., Lüthen, H., & Dörffling, K. (2009b). Cold-induced cytosolic free calcium ion concentration changes in wheat. *Journal of Plant Physiology*, *166*(17), 1955–1960. <a href="https://doi.org/10.1016/j.jplph.2009.05.002">https://doi.org/10.1016/j.jplph.2009.05.002</a>

Nietzel, T., Elsässer, M., Ruberti, C., Steinbeck, J., Ugalde, J. M., Fuchs, P., Wagner, S., Ostermann, L., Moseler, A., Lemke, P., Fricker, M. D., Müller-Schüssele, S. J., Moerschbacher, B. M., Costa, A., Meyer, A. J., & Schwarzländer, M. (2019). The fluorescent protein sensor ro GFP 2-Orp1 monitors *in vivo* H  $_2$  O  $_2$  and thiol redox integration and elucidates intracellular H  $_2$  O  $_2$  dynamics during elicitor-induced oxidative burst in Arabidopsis. *New Phytologist*, *221*(3), 1649–1664. https://doi.org/10.1111/nph.15550

Nikonorova, N., Vu, L. D., Stes, E., Gevaert, K., & De Smet, I. (2018). Proteome Analysis of Arabidopsis Roots. In D. Ristova & E. Barbez (Eds.), *Root Development* (Vol. 1761, pp. 263–274). Springer New York. <a href="https://doi.org/10.1007/978-1-4939-7747-5">https://doi.org/10.1007/978-1-4939-7747-5</a> 20

Nomoto, M., Skelly, M. J., Itaya, T., Mori, T., Suzuki, T., Matsushita, T., Tokizawa, M., Kuwata, K., Mori, H., Yamamoto, Y. Y., Higashiyama, T., Tsukagoshi, H., Spoel, S. H., & Tada, Y. (2021). Suppression of MYC transcription activators by the immune cofactor NPR1 fine-tunes plant immune responses. *Cell Reports*, *37*(11), 110125. <a href="https://doi.org/10.1016/j.celrep.2021.110125">https://doi.org/10.1016/j.celrep.2021.110125</a>

Nürnberger, T., Nennstiel, D., Jabs, T., Sacks, W. R., Hahlbrock, K., & Scheel, D. (1994). High affinity binding of a fungal oligopeptide elicitor to parsley plasma membranes triggers multiple defense responses. *Cell*, 78(3), 449–460. <a href="https://doi.org/10.1016/0092-8674(94)90423-5">https://doi.org/10.1016/0092-8674(94)90423-5</a>

Ogasawara, Y., Kaya, H., Hiraoka, G., Yumoto, F., Kimura, S., Kadota, Y., Hishinuma, H., Senzaki, E., Yamagoe, S., Nagata, K., Nara, M., Suzuki, K., Tanokura, M., & Kuchitsu, K. (2008). Synergistic Activation of the Arabidopsis NADPH Oxidase AtrbohD by Ca2+ and Phosphorylation. *Journal of Biological Chemistry*, 283(14), 8885–8892. https://doi.org/10.1074/jbc.M708106200

Ono, Boucas, Nishida, & Demchak. (n.d.). *Py4cytoscape* [Computer software].

Otasek, D., Morris, J. H., Bouças, J., Pico, A. R., & Demchak, B. (2019). Cytoscape Automation: Empowering workflow-based network analysis. *Genome Biology*, *20*(1), 185. <a href="https://doi.org/10.1186/s13059-019-1758-4">https://doi.org/10.1186/s13059-019-1758-4</a>

Palmgren, M. G. (2001). P LANT P LASMA M EMBRANE H<sup>+</sup> -ATPases: Powerhouses for Nutrient Uptake. *Annual Review of Plant Physiology and Plant Molecular Biology*, *52*(1), 817–845. <a href="https://doi.org/10.1146/annurev.arplant.52.1.817">https://doi.org/10.1146/annurev.arplant.52.1.817</a>

Pandey, D., Gratton, J.-P., Rafikov, R., Black, S. M., & Fulton, D. J. R. (2011). Calcium/Calmodulin-Dependent Kinase II Mediates the Phosphorylation and Activation of NADPH Oxidase 5. *Molecular Pharmacology*, *80*(3), 407–415. https://doi.org/10.1124/mol.110.070193

Payne, S. H. (2015). The utility of protein and mRNA correlation. *Trends in Biochemical Sciences*, 40(1), 1–3. https://doi.org/10.1016/j.tibs.2014.10.010

Pei, Z.-M., Murata, Y., Benning, G., Thomine, S., Klüsener, B., Allen, G. J., Grill, E., & Schroeder, J. I. (2000). Calcium channels activated by hydrogen peroxide mediate abscisic acid signalling in guard cells. *Nature*, *406*(6797), 731–734. <a href="https://doi.org/10.1038/35021067">https://doi.org/10.1038/35021067</a>

Peixoto, T. P. (2017). *The graph-tool python library* (p. 136152697 Bytes) [Dataset]. figshare. https://doi.org/10.6084/M9.FIGSHARE.1164194

Pirayesh, N., Giridhar, M., Ben Khedher, A., Vothknecht, U. C., & Chigri, F. (2021a). Organellar calcium signaling in plants: An update. *Biochimica et Biophysica Acta (BBA) - Molecular Cell Research*, 1868(4), 118948. https://doi.org/10.1016/j.bbamcr.2021.118948

Pirayesh, N., Giridhar, M., Ben Khedher, A., Vothknecht, U. C., & Chigri, F. (2021b). Organellar calcium signaling in plants: An update. *Biochimica et Biophysica Acta (BBA) - Molecular Cell Research*, 1868(4), 118948. <a href="https://doi.org/10.1016/j.bbamcr.2021.118948">https://doi.org/10.1016/j.bbamcr.2021.118948</a>

Plieth, C., Hansen, U., Knight, H., & Knight, M. R. (1999). Temperature sensing by plants: The primary characteristics of signal perception and calcium response. *The Plant Journal*, *18*(5), 491–497. <a href="https://doi.org/10.1046/j.1365-313X.1999.00471.x">https://doi.org/10.1046/j.1365-313X.1999.00471.x</a>

Podpečan, V. (2023). *vpodpecan/pysbgn: V0.2.1* (Version v0.2.1) [Computer software]. Zenodo. <a href="https://doi.org/10.5281/ZENODO.7966410">https://doi.org/10.5281/ZENODO.7966410</a>

Podpečan, V., Ramšak, Ž., Gruden, K., Toivonen, H., & Lavrač, N. (2019). Interactive exploration of heterogeneous biological networks with Biomine Explorer. *Bioinformatics*, *35*(24), 5385–5388. <a href="https://doi.org/10.1093/bioinformatics/btz509">https://doi.org/10.1093/bioinformatics/btz509</a>

Prasher, D., McCann, R. O., & Cormier, M. J. (1985). Cloning and expression of the cDNA coding for aequorin, a bioluminescent calcium-binding protein. *Biochemical and Biophysical Research Communications*, 126(3), 1259–1268. https://doi.org/10.1016/0006-291X(85)90321-3

Prianichnikov, N., Koch, H., Koch, S., Lubeck, M., Heilig, R., Brehmer, S., Fischer, R., & Cox, J. (2020). MaxQuant Software for Ion Mobility Enhanced Shotgun Proteomics. *Molecular & Cellular Proteomics*, *19*(6), 1058–1069. <a href="https://doi.org/10.1074/mcp.TIR119.001720">https://doi.org/10.1074/mcp.TIR119.001720</a>

Price, A. H., Taylor, A., Ripley, S. J., Griffiths, A., Trewavas, A. J., & Knight, M. R. (1994). Oxidative Signals in Tobacco Increase Cytosolic Calcium. *The Plant Cell*, 1301–1310. https://doi.org/10.1105/tpc.6.9.1301

Pylianidis, C., Osinga, S., & Athanasiadis, I. N. (2021). Introducing digital twins to agriculture. *Computers and Electronics in Agriculture*, 184, 105942. <a href="https://doi.org/10.1016/j.compag.2020.105942">https://doi.org/10.1016/j.compag.2020.105942</a>

Ramšak, Ž., Baebler, Š., Rotter, A., Korbar, M., Mozetič, I., Usadel, B., & Gruden, K. (2014). GoMapMan: Integration, consolidation and visualization of plant gene annotations within the MapMan ontology. *Nucleic Acids Research*, *42*(D1), D1167–D1175. https://doi.org/10.1093/nar/gkt1056

Ramšak, Ž., Coll, A., Stare, T., Tzfadia, O., Baebler, Š., Van De Peer, Y., & Gruden, K. (2018). Network Modeling Unravels Mechanisms of Crosstalk between Ethylene and Salicylate Signaling in Potato. *Plant Physiology*, *178*(1), 488–499. <a href="https://doi.org/10.1104/pp.18.00450">https://doi.org/10.1104/pp.18.00450</a>

Ranf, S., Eschen-Lippold, L., Pecher, P., Lee, J., & Scheel, D. (2011). Interplay between calcium signalling and early signalling elements during defence responses to microbe- or damage-associated molecular patterns. *The Plant Journal*, *68*(1), 100–113. https://doi.org/10.1111/j.1365-313X.2011.04671.x

Ranty, B., Aldon, D., Cotelle, V., Galaud, J.-P., Thuleau, P., & Mazars, C. (2016). Calcium Sensors as Key Hubs in Plant Responses to Biotic and Abiotic Stresses. *Frontiers in Plant Science*, 7. <a href="https://doi.org/10.3389/fpls.2016.00327">https://doi.org/10.3389/fpls.2016.00327</a>

Rasmussen, S., Barah, P., Suarez-Rodriguez, M. C., Bressendorff, S., Friis, P., Costantino, P., Bones, A. M., Nielsen, H. B., & Mundy, J. (2013). Transcriptome Responses to Combinations of Stresses in Arabidopsis. *Plant Physiology*, *161*(4), 1783–1794. <a href="https://doi.org/10.1104/pp.112.210773">https://doi.org/10.1104/pp.112.210773</a>

Ravi, B., Foyer, C. H., & Pandey, G. K. (2023a). The integration of reactive oxygen species (ROS) and calcium signalling in abiotic stress responses. *Plant, Cell & Environment*, *46*(7), 1985–2006. https://doi.org/10.1111/pce.14596

Ravi, B., Foyer, C. H., & Pandey, G. K. (2023b). The integration of reactive oxygen species (ROS) and calcium signalling in abiotic stress responses. *Plant, Cell & Environment*, *46*(7), 1985–2006. https://doi.org/10.1111/pce.14596

Ren, H., Zhang, Y., Zhong, M., Hussian, J., Tang, Y., Liu, S., & Qi, G. (2023). Calcium signaling-mediated transcriptional reprogramming during abiotic stress response in plants. *Theoretical and Applied Genetics*, 136(10), 210. <a href="https://doi.org/10.1007/s00122-023-04455-2">https://doi.org/10.1007/s00122-023-04455-2</a>

Rentel, M. C., & Knight, M. R. (2004a). Oxidative Stress-Induced Calcium Signaling in Arabidopsis. *Plant Physiology*, *135*(3), 1471–1479. <a href="https://doi.org/10.1104/pp.104.042663">https://doi.org/10.1104/pp.104.042663</a>

Rentel, M. C., & Knight, M. R. (2004b). Oxidative Stress-Induced Calcium Signaling in Arabidopsis. *Plant Physiology*, *135*(3), 1471–1479. <a href="https://doi.org/10.1104/pp.104.042663">https://doi.org/10.1104/pp.104.042663</a>

Rizhsky, L., Liang, H., Shuman, J., Shulaev, V., Davletova, S., & Mittler, R. (2004). When Defense Pathways Collide. The Response of Arabidopsis to a Combination of Drought and Heat Stress. *Plant Physiology*, *134*(4), 1683–1696. <a href="https://doi.org/10.1104/pp.103.033431">https://doi.org/10.1104/pp.103.033431</a>

Rocha-Sosa, M., Sonnewald, U., Frommer, W., Stratmann, M., Schell, J., & Willmitzer, L. (1989). Both developmental and metabolic signals activate the promoter of a class I patatin gene. *The EMBO Journal*, 8(1), 23–29. <a href="https://doi.org/10.1002/j.1460-2075.1989.tb03344.x">https://doi.org/10.1002/j.1460-2075.1989.tb03344.x</a>

Rosenwasser, S., Rot, I., Meyer, A. J., Feldman, L., Jiang, K., & Friedman, H. (2010). A fluorometer-based method for monitoring oxidation of redox-sensitive GFP (roGFP) during development and extended dark stress. *Physiologia Plantarum*, *138*(4), 493–502. <a href="https://doi.org/10.1111/j.1399-3054.2009.01334.x">https://doi.org/10.1111/j.1399-3054.2009.01334.x</a>

Russell, A. J., Knight, M. R., Cove, D. J., Knight, C. D., Trewavas, A. J., & Wang, T. L. (1996). The moss, Physcomitrella patens, transformed with apoaequorin cDNA responds to cold shock, mechanical perturbation and pH with transient increases in cytoplasmic calcium. *Transgenic Research*, 5(3), 167–170. https://doi.org/10.1007/BF01969705

Scholz, P., Doner, N. M., Gutbrod, K., Herrfurth, C., Niemeyer, P. W., Lim, M. S. S., Blersch, K. F., Schmitt, K., Valerius, O., Shanklin, J., Feussner, I., Dörmann, P., Braus, G. H., Mullen, R. T., & Ischebeck, T. (2025). Plasticity of the Arabidopsis leaf lipidome and proteome in response to pathogen infection and heat stress. *Plant Physiology*, *197*(2), kiae274. https://doi.org/10.1093/plphys/kiae274

Scientific review of the impact of climate change on plant pests. (2021). FAO on behalf of the IPPC Secretariat. <a href="https://doi.org/10.4060/cb4769en">https://doi.org/10.4060/cb4769en</a>

Seaton, D. D., Graf, A., Baerenfaller, K., Stitt, M., Millar, A. J., & Gruissem, W. (2018). Photoperiodic control of the *Arabidopsis* proteome reveals a translational coincidence mechanism. *Molecular Systems Biology*, 14(3), e7962. <a href="https://doi.org/10.15252/msb.20177962">https://doi.org/10.15252/msb.20177962</a>

Sebastian, Nowee, & Carrera. (n.d.).

Seybold, H., Trempel, F., Ranf, S., Scheel, D., Romeis, T., & Lee, J. (2014). Ca <sup>2+</sup> signalling in plant immune response: From pattern recognition receptors to Ca <sup>2+</sup> decoding mechanisms. *New Phytologist*, 204(4), 782–790. https://doi.org/10.1111/nph.13031

Shahwar, D., Deeba, F., Hussain, I., Naqvi, S. M. S., Alatawi, F. S., Omran, A. M. E., Moosa, A., & Zulfiqar, F. (2023). Characterization of the active site of a germin like protein 1 as an oxidative stress defense enzyme in plants. *Plant Gene*, *36*, 100432. <a href="https://doi.org/10.1016/j.plgene.2023.100432">https://doi.org/10.1016/j.plgene.2023.100432</a>

Shannon, P., Markiel, A., Ozier, O., Baliga, N. S., Wang, J. T., Ramage, D., Amin, N., Schwikowski, B., & Ideker, T. (2003). Cytoscape: A Software Environment for Integrated Models of Biomolecular Interaction Networks. *Genome Research*, *13*(11), 2498–2504. https://doi.org/10.1101/gr.1239303

Shimomura, O. (1991). Preparation and handling of aequorin solutions for the measurement of cellular Ca2+. *Cell Calcium*, *12*(9), 635–643. <a href="https://doi.org/10.1016/0143-4160(91)90060-R">https://doi.org/10.1016/0143-4160(91)90060-R</a>

Shimomura, O. (1995). Luminescence of Aequorin Is Triggered by the Binding of Two Calcium Ions. *Biochemical and Biophysical Research Communications*, 211(2), 359–363. <a href="https://doi.org/10.1006/bbrc.1995.1821">https://doi.org/10.1006/bbrc.1995.1821</a>

Shimomura, O., Johnson, F. H., & Saiga, Y. (1962). Extraction, Purification and Properties of Aequorin, a Bioluminescent Protein from the Luminous Hydromedusan, *Aequorea*. *Journal of Cellular and Comparative Physiology*, *59*(3), 223–239. <a href="https://doi.org/10.1002/jcp.1030590302">https://doi.org/10.1002/jcp.1030590302</a>

Sierla, M., Rahikainen, M., Salojärvi, J., Kangasjärvi, J., & Kangasjärvi, S. (2013). Apoplastic and Chloroplastic Redox Signaling Networks in Plant Stress Responses. *Antioxidants & Redox Signaling*, *18*(16), 2220–2239. <a href="https://doi.org/10.1089/ars.2012.5016">https://doi.org/10.1089/ars.2012.5016</a>

Singla, J., & Krattinger, S. G. (2016). Biotic Stress Resistance Genes in Wheat. In *Reference Module in Food Science* (p. B9780081005965002298). Elsevier. <a href="https://doi.org/10.1016/B978-0-08-100596-5.00229-8">https://doi.org/10.1016/B978-0-08-100596-5.00229-8</a>

Song, J., Lu, D., Niu, Y., Sun, H., Zhang, P., Dong, W., Li, Y., Zhang, Y., Lu, L., Men, Q., Zhang, X., Ren, P., & Chen, C. (2022). Label-free quantitative proteomics of maize roots from different root zones provides insight into proteins associated with enhance water uptake. *BMC Genomics*, 23(1), 184. <a href="https://doi.org/10.1186/s12864-022-08394-y">https://doi.org/10.1186/s12864-022-08394-y</a>

Stael, S., Wurzinger, B., Mair, A., Mehlmer, N., Vothknecht, U. C., & Teige, M. (2012). Plant organellar calcium signalling: An emerging field. *Journal of Experimental Botany*, *63*(4), 1525–1542. <a href="https://doi.org/10.1093/jxb/err394">https://doi.org/10.1093/jxb/err394</a>

Stanley Kim, H., Yu, Y., Snesrud, E. C., Moy, L. P., Linford, L. D., Haas, B. J., Nierman, W. C., & Quackenbush, J. (2005). Transcriptional divergence of the duplicated oxidative stress-responsive genes in the Arabidopsis genome. *The Plant Journal*, *41*(2), 212–220. <a href="https://doi.org/10.1111/j.1365-313X.2004.02295.x">https://doi.org/10.1111/j.1365-313X.2004.02295.x</a>

Steinwand, M. A., & Ronald, P. C. (2020). Crop biotechnology and the future of food. *Nature Food*, 1(5), 273–283. https://doi.org/10.1038/s43016-020-0072-3

Stuhlfelder, C. (2002). Purification and partial amino acid sequences of an esterase from tomato. *Phytochemistry*, *60*(3), 233–240. <a href="https://doi.org/10.1016/S0031-9422(02)00126-7">https://doi.org/10.1016/S0031-9422(02)00126-7</a>

Sun, S., Zhang, X., Chen, K., Zhu, X., & Zhao, Y. (2021). Screening for Arabidopsis mutants with altered Ca2+ signal response using aequorin-based Ca2+ reporter system. *STAR Protocols*, *2*(2), 100558. <a href="https://doi.org/10.1016/j.xpro.2021.100558">https://doi.org/10.1016/j.xpro.2021.100558</a>

Suzuki, N., Rivero, R. M., Shulaev, V., Blumwald, E., & Mittler, R. (2014). Abiotic and biotic stress combinations. *New Phytologist*, 203(1), 32–43. <a href="https://doi.org/10.1111/nph.12797">https://doi.org/10.1111/nph.12797</a>

Szklarczyk, D., Kirsch, R., Koutrouli, M., Nastou, K., Mehryary, F., Hachilif, R., Gable, A. L., Fang, T., Doncheva, N. T., Pyysalo, S., Bork, P., Jensen, L. J., & von Mering, C. (2023). The STRING

database in 2023: Protein—protein association networks and functional enrichment analyses for any sequenced genome of interest. *Nucleic Acids Research*, *51*(D1), D638–D646. <a href="https://doi.org/10.1093/nar/gkac1000">https://doi.org/10.1093/nar/gkac1000</a>

Takahashi, F., Kuromori, T., Urano, K., Yamaguchi-Shinozaki, K., & Shinozaki, K. (2020). Drought Stress Responses and Resistance in Plants: From Cellular Responses to Long-Distance Intercellular Communication. *Frontiers in Plant Science*, 11, 556972. <a href="https://doi.org/10.3389/fpls.2020.556972">https://doi.org/10.3389/fpls.2020.556972</a>

Takahashi, S., & Badger, M. R. (2011). Photoprotection in plants: A new light on photosystem II damage. *Trends in Plant Science*, 16(1), 53–60. <a href="https://doi.org/10.1016/j.tplants.2010.10.001">https://doi.org/10.1016/j.tplants.2010.10.001</a>

Tang, R.-J., Wang, C., Li, K., & Luan, S. (2020). The CBL—CIPK Calcium Signaling Network: Unified Paradigm from 20 Years of Discoveries. *Trends in Plant Science*, *25*(6), 604–617. <a href="https://doi.org/10.1016/j.tplants.2020.01.009">https://doi.org/10.1016/j.tplants.2020.01.009</a>

Tao, Y., Wu, L., Volodymyr, V., Hu, P., Hu, H., & Li, C. (2024). Identification of the ribosomal protein L18 (RPL18) gene family reveals that TaRPL18-1 positively regulates powdery mildew resistance in wheat. *International Journal of Biological Macromolecules*, *280*, 135730. https://doi.org/10.1016/j.ijbiomac.2024.135730

Thomas, M. V. (1982). *Techniques in calcium research*. Academic Press.

Thor, K. (2019). Calcium—Nutrient and Messenger. *Frontiers in Plant Science*, 10, 440. https://doi.org/10.3389/fpls.2019.00440

Thor, K., & Peiter, E. (2014). Cytosolic calcium signals elicited by the pathogen-associated molecular pattern flg22 in stomatal guard cells are of an oscillatory nature. *New Phytologist*, 204(4), 873–881. <a href="https://doi.org/10.1111/nph.13064">https://doi.org/10.1111/nph.13064</a>

Tracy, F. E., Gilliham, M., Dodd, A. N., Webb, A. A. R., & Tester, M. (2008a). NaCl-induced changes in cytosolic free Ca<sup>2+</sup> in *Arabidopsis thaliana* are heterogeneous and modified by external ionic composition. *Plant, Cell & Environment, 31*(8), 1063–1073. https://doi.org/10.1111/j.1365-3040.2008.01817.x

Tracy, F. E., Gilliham, M., Dodd, A. N., Webb, A. A. R., & Tester, M. (2008b). NaCl-induced changes in cytosolic free Ca<sup>2+</sup> in *Arabidopsis thaliana* are heterogeneous and modified by external ionic composition. *Plant, Cell & Environment, 31*(8), 1063–1073. <a href="https://doi.org/10.1111/j.1365-3040.2008.01817.x">https://doi.org/10.1111/j.1365-3040.2008.01817.x</a>

Tyanova, S., Temu, T., & Cox, J. (2016). The MaxQuant computational platform for mass spectrometry-based shotgun proteomics. *Nature Protocols*, *11*(12), 2301–2319. <a href="https://doi.org/10.1038/nprot.2016.136">https://doi.org/10.1038/nprot.2016.136</a>

Tyanova, S., Temu, T., Sinitcyn, P., Carlson, A., Hein, M. Y., Geiger, T., Mann, M., & Cox, J. (2016). The Perseus computational platform for comprehensive analysis of (prote)omics data. *Nature Methods*, *13*(9), 731–740. <a href="https://doi.org/10.1038/nmeth.3901">https://doi.org/10.1038/nmeth.3901</a>

United Nations. (2022). *World Population Prospects 2022: Summary of Results*. United Nations. <a href="https://doi.org/10.18356/9789210014380">https://doi.org/10.18356/9789210014380</a>

Vaahtera, L., Brosché, M., Wrzaczek, M., & Kangasjärvi, J. (2014). Specificity in ROS Signaling and Transcript Signatures. *Antioxidants & Redox Signaling*, 21(9), 1422–1441. <a href="https://doi.org/10.1089/ars.2013.5662">https://doi.org/10.1089/ars.2013.5662</a>

Välikangas, T., Suomi, T., & Elo, L. L. (2016). A systematic evaluation of normalization methods in quantitative label-free proteomics. *Briefings in Bioinformatics*, bbw095. <a href="https://doi.org/10.1093/bib/bbw095">https://doi.org/10.1093/bib/bbw095</a>

Van Der Luit, A. H., Olivari, C., Haley, A., Knight, M. R., & Trewavas, A. J. (1999). Distinct Calcium Signaling Pathways Regulate Calmodulin Gene Expression in Tobacco. *Plant Physiology*, *121*(3), 705–714. <a href="https://doi.org/10.1104/pp.121.3.705">https://doi.org/10.1104/pp.121.3.705</a>

Van Dieren, A., Schwarzenbacher, R. E., Sonnewald, S., Bittner, A., & Vothknecht, U. C. (2024a). Analysis of abiotic and biotic stress-induced Ca2+ transients in the crop species Solanum tuberosum. *Scientific Reports*, *14*(1), 27625. <a href="https://doi.org/10.1038/s41598-024-79134-3">https://doi.org/10.1038/s41598-024-79134-3</a>

Van Dieren, A., Schwarzenbacher, R. E., Sonnewald, S., Bittner, A., & Vothknecht, U. C. (2024b). Analysis of abiotic and biotic stress-induced Ca2+ transients in the crop species Solanum tuberosum. *Scientific Reports*, *14*(1), 27625. <a href="https://doi.org/10.1038/s41598-024-79134-3">https://doi.org/10.1038/s41598-024-79134-3</a>

Van Dieren, A. V., Bittner, A., Wurzinger, B., Afjehi-Sadat, L., Weckwerth, W., Teige, M., & Vothknecht, U. C. (2025). With or without a Ca<sup>2+</sup> signal; A proteomics approach towards Ca<sup>2+</sup> dependent and independent proteome changes in response to oxidative stress in A. thaliana. <a href="https://doi.org/10.1101/2025.03.31.645912">https://doi.org/10.1101/2025.03.31.645912</a>

Van Bel, M., Silvestri, F., Weitz, E. M., Kreft, L., Botzki, A., Coppens, F., & Vandepoele, K. (2022). PLAZA 5.0: Extending the scope and power of comparative and functional genomics in plants. *Nucleic Acids Research*, *50*(D1), D1468–D1474. <a href="https://doi.org/10.1093/nar/gkab1024">https://doi.org/10.1093/nar/gkab1024</a>

Wang, C.-F., Han, G.-L., Yang, Z.-R., Li, Y.-X., & Wang, B.-S. (2022). Plant Salinity Sensors: Current Understanding and Future Directions. *Frontiers in Plant Science*, *13*, 859224. <a href="https://doi.org/10.3389/fpls.2022.859224">https://doi.org/10.3389/fpls.2022.859224</a>

Wang, R., Zhou, P., Pan, Y., Zheng, L., Dong, X., Shen, R., & Lan, P. (2023). Label-Free Quantitative Proteomics in Plant. In J. Jeong (Ed.), *Plant Iron Homeostasis* (Vol. 2665, pp. 75–83). Springer US. <a href="https://doi.org/10.1007/978-1-0716-3183-6">https://doi.org/10.1007/978-1-0716-3183-6</a> 7

Whalley, H. J., & Knight, M. R. (2013). Calcium signatures are decoded by plants to give specific gene responses. *New Phytologist*, 197(3), 690–693. <a href="https://doi.org/10.1111/nph.12087">https://doi.org/10.1111/nph.12087</a>

Wilkinson, M. D., Dumontier, M., Aalbersberg, Ij. J., Appleton, G., Axton, M., Baak, A., Blomberg, N., Boiten, J.-W., Da Silva Santos, L. B., Bourne, P. E., Bouwman, J., Brookes, A. J., Clark, T., Crosas, M., Dillo, I., Dumon, O., Edmunds, S., Evelo, C. T., Finkers, R., ... Mons, B. (2016). The FAIR Guiding Principles for scientific data management and stewardship. *Scientific Data*, *3*(1), 160018. https://doi.org/10.1038/sdata.2016.18

World Food and Agriculture – Statistical Yearbook 2021. (2021). FAO. <a href="https://doi.org/10.4060/cb4477en">https://doi.org/10.4060/cb4477en</a>

Wu, F., Chi, Y., Jiang, Z., Xu, Y., Xie, L., Huang, F., Wan, D., Ni, J., Yuan, F., Wu, X., Zhang, Y., Wang, L., Ye, R., Byeon, B., Wang, W., Zhang, S., Sima, M., Chen, S., Zhu, M., ... Pei, Z.-M. (2020). Hydrogen peroxide sensor HPCA1 is an LRR receptor kinase in Arabidopsis. *Nature*, *578*(7796), 577–581. <a href="https://doi.org/10.1038/s41586-020-2032-3">https://doi.org/10.1038/s41586-020-2032-3</a>

Wu, J., Wang, L., & Baldwin, I. T. (2008). Methyl jasmonate-elicited herbivore resistance: Does MeJA function as a signal without being hydrolyzed to JA? *Planta*, *227*(5), 1161–1168. https://doi.org/10.1007/s00425-008-0690-8

Xu, X., Pan, S., Cheng, S., Zhang, B., Mu, D., Ni, P., Zhang, G., Yang, S., Li, R., Wang, J., Orjeda, G., Guzman, F., Torres, M., Lozano, R., Ponce, O., Martinez, D., De la Cruz, G., Chakrabarti, S. K., Patil, V. U., ... Wageningen University & Research Centre. (2011). Genome sequence and analysis of the tuber crop potato. *Nature*, *475*(7355), 189–195. <a href="https://doi.org/10.1038/nature10158">https://doi.org/10.1038/nature10158</a>

Yan, S., Bhawal, R., Yin, Z., Thannhauser, T. W., & Zhang, S. (2022). Recent advances in proteomics and metabolomics in plants. *Molecular Horticulture*, 2(1), 17. https://doi.org/10.1186/s43897-022-00038-9

Yuan, F., Yang, H., Xue, Y., Kong, D., Ye, R., Li, C., Zhang, J., Theprungsirikul, L., Shrift, T., Krichilsky, B., Johnson, D. M., Swift, G. B., He, Y., Siedow, J. N., & Pei, Z.-M. (2014). OSCA1 mediates osmotic-stress-evoked Ca2+ increases vital for osmosensing in Arabidopsis. *Nature*, 514(7522), 367–371. <a href="https://doi.org/10.1038/nature13593">https://doi.org/10.1038/nature13593</a>

Zagorščak, M., Blejec, A., Ramšak, Ž., Petek, M., Stare, T., & Gruden, K. (2018). DiNAR: Revealing hidden patterns of plant signalling dynamics using Differential Network Analysis in R. *Plant Methods*, *14*(1), 78. <a href="https://doi.org/10.1186/s13007-018-0345-0">https://doi.org/10.1186/s13007-018-0345-0</a>

Zandalinas, S. I., Fichman, Y., Devireddy, A. R., Sengupta, S., Azad, R. K., & Mittler, R. (2020). Systemic signaling during abiotic stress combination in plants. *Proceedings of the National Academy of Sciences*, *117*(24), 13810–13820. https://doi.org/10.1073/pnas.2005077117

Zhang, G., Liu, Y., Ni, Y., Meng, Z., Lu, T., & Li, T. (2014). Exogenous Calcium Alleviates Low Night Temperature Stress on the Photosynthetic Apparatus of Tomato Leaves. *PLoS ONE*, *9*(5), e97322. <a href="https://doi.org/10.1371/journal.pone.0097322">https://doi.org/10.1371/journal.pone.0097322</a>

Zhang, N., Zhou, S., Yang, D., & Fan, Z. (2020). Revealing Shared and Distinct Genes Responding to JA and SA Signaling in Arabidopsis by Meta-Analysis. *Frontiers in Plant Science*, *11*, 908. <a href="https://doi.org/10.3389/fpls.2020.00908">https://doi.org/10.3389/fpls.2020.00908</a>

Zhang, Y., Wang, Y., Taylor, J. L., Jiang, Z., Zhang, S., Mei, F., Wu, Y., Wu, P., & Ni, J. (2015a). Aequorin-based luminescence imaging reveals differential calcium signalling responses to salt and reactive oxygen species in rice roots. *Journal of Experimental Botany*, *66*(9), 2535–2545. https://doi.org/10.1093/jxb/erv043

Zhang, Y., Wang, Y., Taylor, J. L., Jiang, Z., Zhang, S., Mei, F., Wu, Y., Wu, P., & Ni, J. (2015b). Aequorin-based luminescence imaging reveals differential calcium signalling responses to salt

and reactive oxygen species in rice roots. *Journal of Experimental Botany*, 66(9), 2535–2545. https://doi.org/10.1093/jxb/erv043

Zhu, W., Smith, J. W., & Huang, C.-M. (2010). Mass Spectrometry-Based Label-Free Quantitative Proteomics. *Journal of Biomedicine and Biotechnology*, 2010, 1–6. <a href="https://doi.org/10.1155/2010/840518">https://doi.org/10.1155/2010/840518</a>

Zhu, X., Taylor, A., Zhang, S., Zhang, D., Feng, Y., Liang, G., & Zhu, J.-K. (2014). Measuring Spatial and Temporal Ca<sup>2+</sup> Signals in Arabidopsis Plants. *Journal of Visualized Experiments*, *91*, 51945. <a href="https://doi.org/10.3791/51945">https://doi.org/10.3791/51945</a>

Zielinski, R. E. (1998). CALMODULIN AND CALMODULIN-BINDING PROTEINS IN PLANTS. *Annual Review of Plant Physiology and Plant Molecular Biology*, 49(1), 697–725. https://doi.org/10.1146/annurev.arplant.49.1.697 8. Appendices

Appendix 1

Chapter 1

Analysis of abiotic and biotic stress-induced Ca2+ transients in the crop

species Solanum tuberosum

Annelotte van Dieren<sup>1</sup>, Ronald E. Schwarzenbacher<sup>2</sup>, Sophie Sonnewald<sup>3</sup>, Andras Bittner<sup>1</sup>, Ute

C. Vothknecht<sup>1</sup>.

<sup>1.</sup> Institute for Cellular and Molecular Botany, University of Bonn, Kirschallee 1, 53115,

Bonn, Germany

<sup>2.</sup> Department of Biosciences, Durham University, South Road, Durham, DH1 3LE, UK

3. Department of Biology, Chair of Biochemistry, Friedrich-Alexander-University

Erlangen-Nuremberg, Staudtstraße 5, Erlangen, 91058, Germany

Scientific Reports 14, no. 1 (2024): 27625

https://doi.org/10.1038/s41598-024-79134-3

65

# scientific reports



# **OPEN**

# Analysis of abiotic and biotic stressinduced Ca<sup>2+</sup> transients in the crop species *Solanum tuberosum*

Annelotte van Dieren<sup>1⊠</sup>, Roland E. Schwarzenbacher<sup>2</sup>, Sophia Sonnewald<sup>3</sup>, Andras Bittner<sup>1</sup> & Ute C. Vothknecht<sup>1⊠</sup>

Secondary messengers, such as calcium ions (Ca<sup>2+</sup>), are integral parts of a system that transduces environmental stimuli into appropriate cellular responses. Different abiotic and biotic stresses as well as developmental processes trigger temporal increases in cytosolic free Ca<sup>2+</sup> levels by an influx from external and internal stores. Stimulus-specificity is obtained by a certain amplitude, duration, oscillation and localisation of the response. Most knowledge on stress-specific Ca<sup>2+</sup> transient, called calcium signatures, has been gained in the model plant *Arabidopsis thaliana*, while reports about stress-related Ca<sup>2+</sup> signalling in crop plants are comparatively scarce. In this study, we introduced the Ca<sup>2+</sup> biosensor apoaequorin into potato (*Solanum tuberosum*, Lcv. Désirée). We observed dosedependent calcium signatures in response to a series of stress stimuli, including H<sub>2</sub>O<sub>2</sub>, NaCl, mannitol and pathogen-associated molecular patterns (PAMPs) with stimuli-specific kinetics. Direct comparison with Arabidopsis revealed differences in the kinetics and amplitude of Ca<sup>2+</sup> transients between both species, implying species-specific sensitivity for different stress conditions. The potato line generated in this work provides a useful tool for further investigations on stress-induced signalling pathways, which could contribute to the generation of novel, stress-tolerant potato varieties.

Keywords Potato, Arabidopsis thaliana, Crops, Calcium signalling, Aequorin, Stress perception

Plants sense and respond to unfavourable environmental conditions to mitigate the negative effects of such stresses. Indeed, each stress type and each stress combination cause a unique molecular footprint, which induces a fine-tuned cellular response<sup>1,2</sup>. For example, unique stress-specific transcriptional changes have been observed in response to heat, drought, high light, or combinations of these treatments in the model plant *A. thaliana*<sup>3,4</sup>. Secondary messengers are involved in transducing a primary stimulus into an appropriate cellular response. In plants, changes in the concentration of free  $Ca^{2+}$  in the cytosol (referred here as  $[Ca^{2+}]_{cyt}$ ), but also in various organelles, have emerged as a universal secondary messenger<sup>5–7</sup>. A wide range of stresses as well as developmental processes trigger temporal increases in  $[Ca^{2+}]_{cyt}$  by an influx of  $Ca^{2+}$  from external and internal stores. The amplitude and timing of  $Ca^{2+}$  influx depends on the type of perturbation, the magnitude of the stress and how often the plant faced such stress conditions in the past<sup>8,9</sup>, resulting in an information encoding 'calcium signature'<sup>10,11</sup>. So far, calcium signatures have been described in Arabidopsis, for instance in response to oxidative stress, biotic elicitors, osmotic stress, salt, cold or touch<sup>9,12–16</sup>.

The use of the genetically encoded  $Ca^{2+}$  indicator (GECI) apoaequorin to determine absolute concentrations of free  $Ca^{2+}$  in plants was established in the 1990s in Arabidopsis<sup>12</sup> and has since been used to investigate  $Ca^{2+}$  changes in many studies<sup>17</sup>. However, only few studies have reported the use of GECIs in crop species, such as  $H_2O_2$  and NaCl responses in rice roots<sup>18</sup>, chilling response in winter wheat<sup>19</sup>, infection with *Cuscuta reflexa* in tomato<sup>20</sup>, and a set of stressors in barley<sup>21</sup>. The comparison of  $Ca^{2+}$  transients between those species revealed tissue- and species-specific calcium signatures in response to different stress stimuli, which might be related to species-specific sensitivity to each stressor or to differences in the down-stream responses.

Plants show different sensitivity to environmental factors depending on their genetic make-up, which defines stress adaptation and acclimation. Potatoes are cultivated in nearly all regions of the world and are an important factor for global nutrition<sup>22</sup>. However, potato plants originate from an area with particular conditions, the high altitudes of the Andes. Based on its origin, potato growth, and by that also tuber yield, is quite sensitive to a wide range of environmental factors, including elevated temperatures<sup>23</sup> and salinity<sup>24</sup>. So far, Ca<sup>2+</sup> signals have only

<sup>1</sup>Institute for Cellular and Molecular Botany, University of Bonn, Kirschallee 1, 53115 Bonn, Germany. <sup>2</sup>Department of Biosciences, Durham University, South Road, Durham DH1 3LE, UK. <sup>3</sup>Department of Biology, Chair of Biochemistry, Friedrich-Alexander-University Erlangen-Nuremberg, Staudtstraße 5, Erlangen 91058, Germany. <sup>™</sup>email: adieren@uni-bonn.de; vothknecht@uni-bonn.de

been investigated in response to flagellin 28 (flg-28) in potato plants $^{25}$ . To obtain a more comprehensive overview, we generated transgenic potato lines expressing apoaequorin under the control of the cauliflower mosaic virus (CaMV) 35S promoter and determined calcium signatures in response to different abiotic and biotic stimuli in leaf tissue of soil-grown plants. We performed direct comparisons with  $Ca^{2+}$  responses in Arabidopsis in order to put the results obtained for potato in context of the vast knowledge available from this model plant.

### Results

## Generation and characterisation of transgenic potato lines expressing apoaequorin

To measure stimuli-induced  $[Ca^{2+}]_{\rm cyt}$  changes in vivo in potato plants, three independent transgenic potato lines (*Solanum tuberosum* L. cv. Désirée) carrying the p35S::apoaequorin construct were created (Fig. 1; Supplementary Fig. S1), referred to hereafter as St-AEQ<sub>cyt</sub>. Protein extracts from all lines showed aequorin luminescence in response to discharge solution (25 mM  $^{\circ}$  CaCl<sub>2</sub>) after overnight reconstitution with coelenterazine (Fig. 1a) indicating expression of the apoaequorin protein. Different luminescence levels were observed among the three St-AEQ<sub>cyt</sub> lines, with #20 showing the highest luminescence level, and this line was therefore used for all further experiments. Functionality of the sensor *in planta* could be confirmed by measuring  $Ca^{2+}$  induced  $Ca^{2+}$  transients (Fig. 1b). Importantly, the insertion of the construct into the genome and expression of apoaequorin did not have any visible impact on growth and development in comparison to wild type plants (Fig. 1c and d). Western Blot analysis confirmed the presence of the apoaequorin protein in leaf extract (Supplementary Fig. S1a). The comparison to a previously described Arabidopsis line carrying the same 35S::apoaequorin construct (At-AEQ<sub>cyt</sub>) showed a lower expression level of apoaequorin (Supplementary Fig. S1a). Accordingly, only about 25% of the aequorin luminescence in response to discharge solution was observed in St-AEQ<sub>cyt</sub> lines compared to At-AEQ<sub>cyt</sub> (Supplementary Fig. S1b).

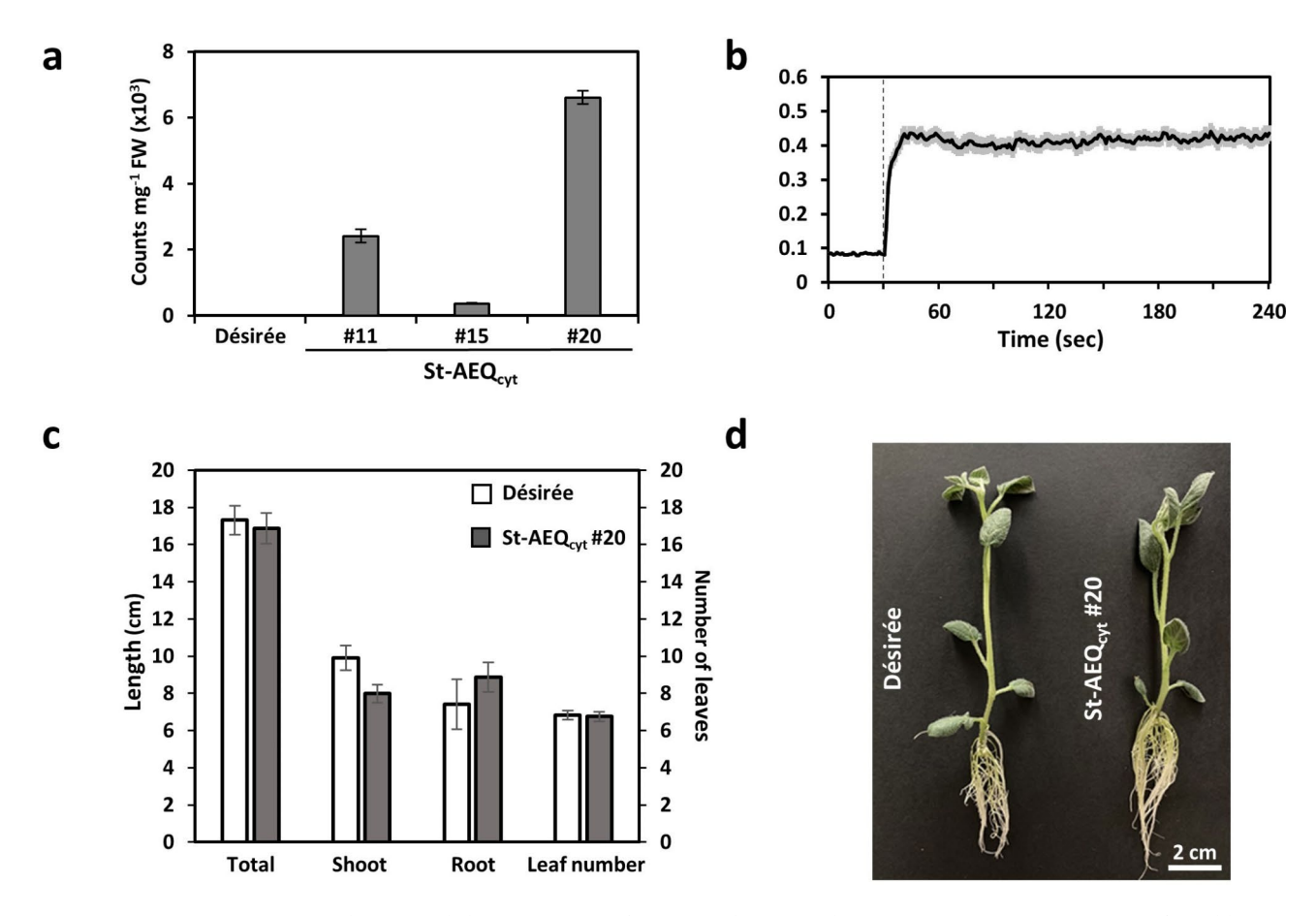


Fig. 1. Selection and characterisation of St-AEQ<sub>cyt</sub> lines. (a) Photon counts (average counts 10 s after adding 50 mM CaCl<sub>2</sub>) were measured in leaf extracts from three independent transgenic potato St-AEQ<sub>cyt</sub> lines after in vitro reconstitution of aequorin with coelenterazine. Untransformed potato cultivar Désirée was used as a negative control (n=9, mean  $\pm$  SE). (b) Time course of changes in  $[{\rm Ca}^{2+}]_{\rm cyt}$  in leaf discs from St-AEQcyt #20 in response to external Ca<sup>2+</sup> application (final concentration 500 mM). (c) Comparison of the total plant length, root length, shoot length, and number of leaves in three-week old St-AEQ<sub>cyt</sub> #20 and wildtype Désirée plants (n=8, mean  $\pm$  SE). (d) Representative picture of three-week old Désirée wild type and St-AEQ<sub>cyt</sub> #20 plant.

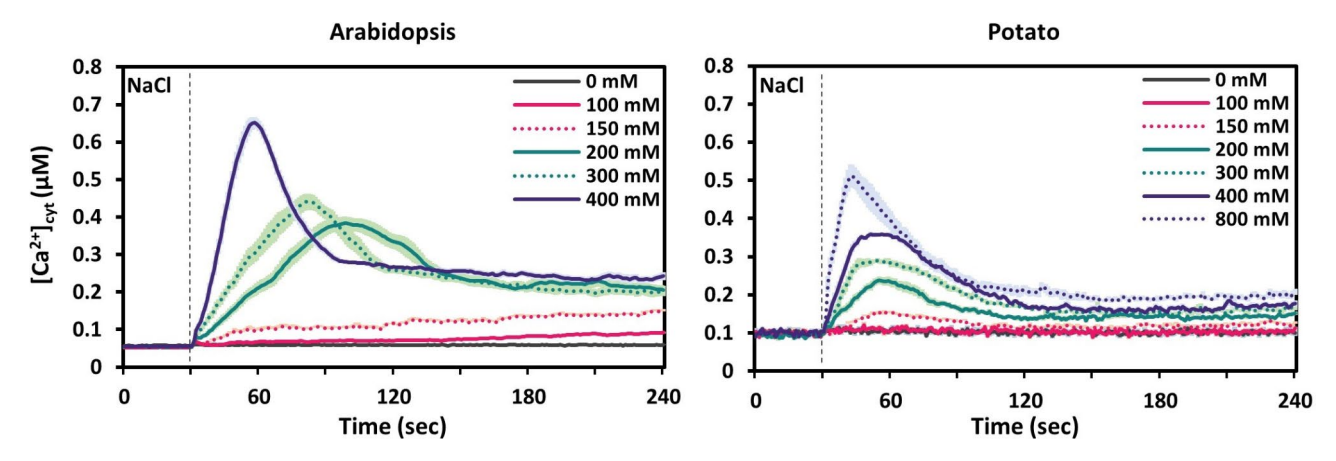
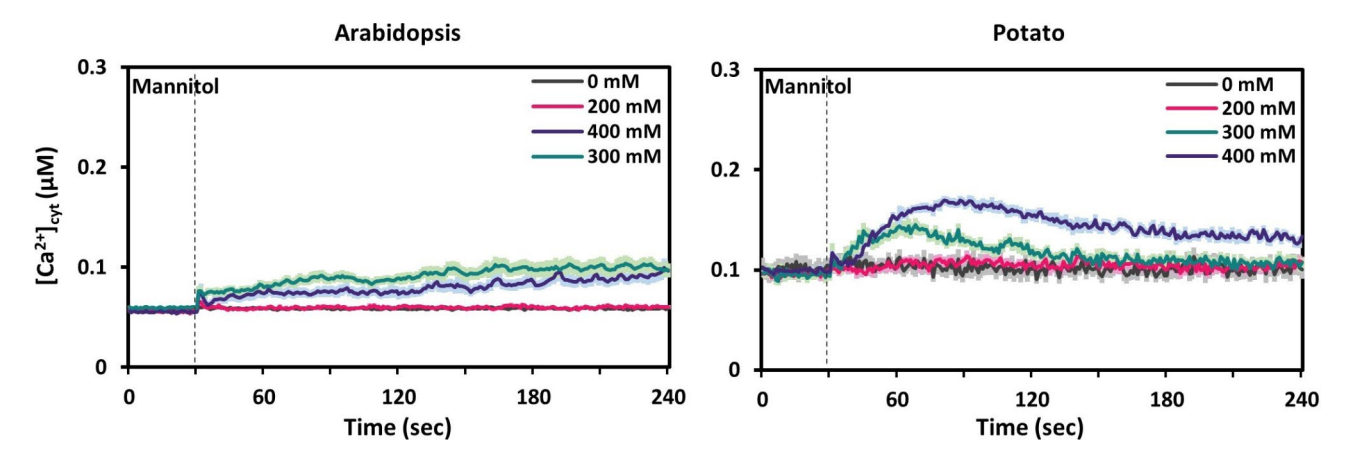


Fig. 2. Time course of changes in  $[Ca^{2+}]_{cyt}$  in response to different concentrations of NaCl in leaf tissue of Arabidopsis (left) and potato (right) plants. Values are shown as mean  $\pm$  SE (n=9). Dashed vertical lines indicate the time point of stimuli application (30 s).



**Fig. 3.** Time course of changes in  $[Ca^{2+}]_{cyt}$  in response to different concentrations of mannitol in leaf tissue of Arabidopsis (left) and potato (right) plants. Values are shown as mean  $\pm$  SE (n=9). Dashed vertical lines indicate the time point of stimuli application (30 s).

### Calcium signatures in Arabidopsis and potato in response to abiotic stimuli

We first analysed stress-induced calcium signatures in leaf discs of Arabidopsis (At-AEQ<sub>cyt</sub>) and potato (St-AEQ<sub>cyt</sub>) in response to the abiotic factors salinity, drought and oxidative stress (Figs. 2, 3 and 4). To that end we treated leaf discs from plants of similar age grown on soil with NaCl, mannitol and  $H_2O_3$ .

#### Salt stress (NaCl)

Initially the salt response was tested in steps of a two-fold increase starting with 100 mM NaCl (Fig. 2). In both species, NaCl elicited a strong response after application of concentrations above 200 mM NaCl, but the kinetics of the response differed between the two species. In Arabidopsis, 200 mM NaCl produced a broad peak occurring at around 70 s after application with a maximum  $\left[\text{Ca}^{2+}\right]_{\text{cyt}}$  amplitude of 0.38  $\mu$ M (Fig. 2, Arabidopsis, green solid line ). Increasing the NaCl concentration to 400 mM further enhanced the amplitude to 0.65  $\mu$ M  $\left[\text{Ca}^{2+}\right]_{\text{cyt}}$  and shifted the time of the maximum peak to around 30 s after application (Fig. 2, Arabidopsis, purple solid line). The shift in the timepoint of the peak value in response to increasing NaCl concentrations made us decide to test the response also to intermediate NaCl concentrations (Fig. 2, Arabidopsis, dotted lines), resulting in true interjacent responses. By testing all these different concentrations, we were able to visualise the dose-dependent shaping of the curve towards a stronger and faster response. Neither time nor amplitude of the maximum peak value did alter any more at concentrations above 400 mM.

In potato, application of NaCl also triggered clear  $Ca^{2+}$  transients (Fig. 2, potato), albeit with a slightly lower amplitude than in Arabidopsis. Also potato showed a dose-dependent increase in the amplitude of the  $[Ca^{2+}]_{cyt}$  peak, however, the timing of the  $[Ca^{2+}]_{cyt}$  peak only showed a very minor shift (Fig. 2, potato). In contrast to Arabidopsis, 800 mM NaCl (Fig. 2, potato, purple dotted line) was needed to induce a maximum response of 0.5  $\mu$ M  $[Ca^{2+}]_{cyt}$ , comparable in height and shape to the response to 400 mM NaCl in Arabidopsis. Overall, these

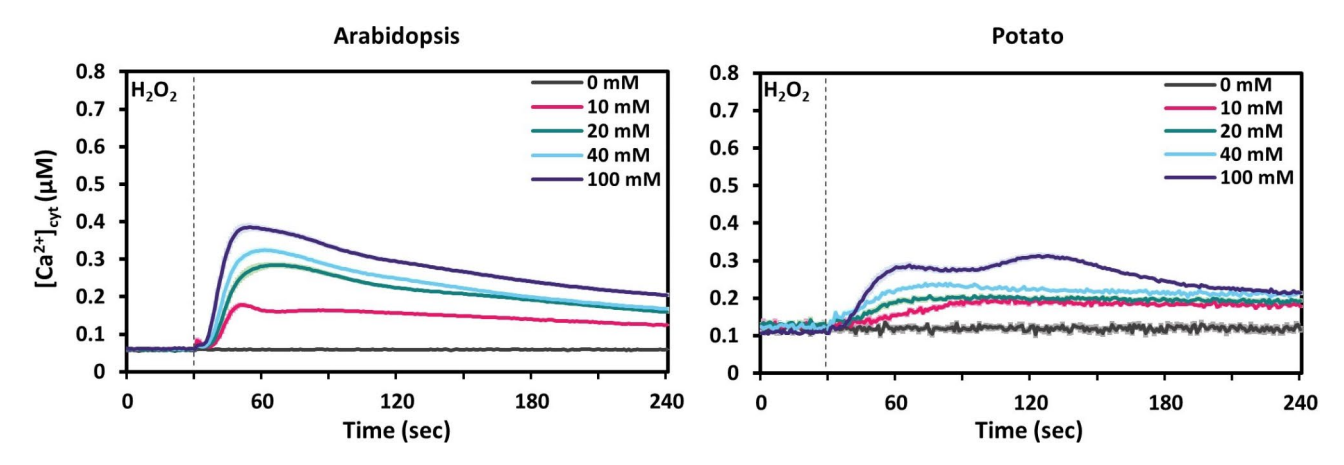


**Fig. 4.** Time course of changes in  $[Ca^{2+}]_{cyt}$  in response to different concentrations of  $H_2O_2$  in leaf tissue of Arabidopsis (left) and potato (right) plants. Values are shown as mean  $\pm$  SE (n=9). Dashed vertical lines indicate the time point of stimuli application (30 s).

data show that dose-dependent NaCl-induced  $Ca^{2+}$  transients occur in both species, but they show differences in their kinetics.

#### Osmotic stress (Mannitol)

To investigate the calcium signature of Arabidopsis and potato in response to acute osmotic changes, we recorded free  $[Ca^{2+}]_{cyt}$  in leaf discs upon application of different concentrations of mannitol (Fig. 3). Because of the crystallizing properties of mannitol at higher concentrations, and the fact that we have to inject a two-fold concentrated stock solution via a narrow syringe system, the concentrations that we could test were limited to a maximum of 400 mM.

In Arabidopsis, a mannitol application with a concentration of 200 mM did not result in any response. Also higher concentrations (300 and 400 mM) did not induced a clear  $Ca^{2+}$  spike but led to a long-lasting minor elevation of  $[Ca^{2+}]_{cyt}$  throughout the whole measurement period (240 s). This elevation started immediately after application of the stimulus and steadily increased to about 0.05  $\mu$ M  $[Ca^{2+}]_{cyt}$  (Fig. 3, Arabidopsis). In contrast to Arabidopsis, we observed a small but clear  $Ca^{2+}$  spike in potato at a concentration of 300 mM with a maximum amplitude of 0.15  $\mu$ M  $[Ca^{2+}]_{cyt}$  at about 30 s after application (Fig. 3, potato). At 400 mM the amplitude of the response increased further, and the peak value was reached later (60 s after application).

## Oxidative stress (H<sub>2</sub>O<sub>2</sub>)

Oxidative stress is a common result of unfavourable growth conditions but also certain biotic stimuli induce an oxidative burst<sup>26</sup>. Hydrogen peroxide  $(H_2O_2)$  is considered as the predominant signalling molecule during oxidative stress, due to its stable nature (half-life > 1 ms) compared to other reactive oxygen species<sup>27</sup>. Therefore, we used  $H_2O_2$  as a stimulus to analyse  $[Ca^{2+}]_{cyt}$  changes in response to oxidative stress (Fig. 4).

In Arabidopsis,  $H_2O_2$  treatment with the lowest tested concentration (10 mM) resulted directly in a clear peak-shaped response with a maximum amplitude of  $0.2~\mu M~[Ca^{2+}]_{cyt}$  just 15 s after application. The peak value of  $[Ca^{2+}]_{cyt}$  increased in a dose-dependent manner with a maximal response of  $0.4~\mu M$  observed at 100 mM (Fig. 4, Arabidopsis, purple line). In potato, 10 mM  $H_2O_2$  did not elicit a clear  $Ca^{2+}$  transient but a slow minor increase (Fig. 4, potato, pink line) similar to what was observed in Arabidopsis in case of mannitol. At 20 mM  $H_2O_2$  a peak-like shape started to appear, which turned into a double-peaked calcium signature at 100 mM  $H_2O_2$  (Fig. 4, potato, purple line). The first peak occurred at around 30 s after application, similar to the peak seen in Arabidopsis, however, its amplitude was much lower ( $0.3~\mu M$ ). The second peak was slightly higher than the first, occurred at around 90 s after application, was not visible in Arabidopsis plants (Fig. 4, Arabidopsis), and was also not seen in barley<sup>21</sup>.

#### Calcium signatures in response to PAMPs

Various studies have demonstrated that  $Ca^{2+}$  signals together with an apoplastic ROS-burst play an important role in activating the plant's pathogen defence system<sup>28,29</sup>. Changes in  $[Ca^{2+}]_{cyt}$  are thus an early and essential element in intracellular signalling networks after perception of pathogen-associated molecular patterns (PAMPs). Due to the observed species-specific  $Ca^{2+}$  transients in response to  $H_2O_2$ , we decided to also analyse  $[Ca^{2+}]_{cyt}$  changes in response to two biotic elicitors (Fig. 5a-b). Compared to the abiotic stimuli, responses to the biotic components were generally slower (Fig. 5c) and measurements were taken for longer periods.

#### Flg22

Flg22 is a 22 amino acid long fragment of the *Pseudomonas syringae* flagellin whose induction of  $Ca^{2+}$  transients and triggering of ROS production has been described in different plant species and tissues<sup>30–32</sup>. While an increase in  $[Ca^{2+}]_{cyt}$  occurred already at 0.5  $\mu$ M flg22 in Arabidopsis, a clear peak was observed with concentrations of 1  $\mu$ M and higher (Fig. 5a, Arabidopsis). A maximal amplitude of less than 0.2  $\mu$ M  $[Ca^{2+}]_{cyt}$  was observed at around

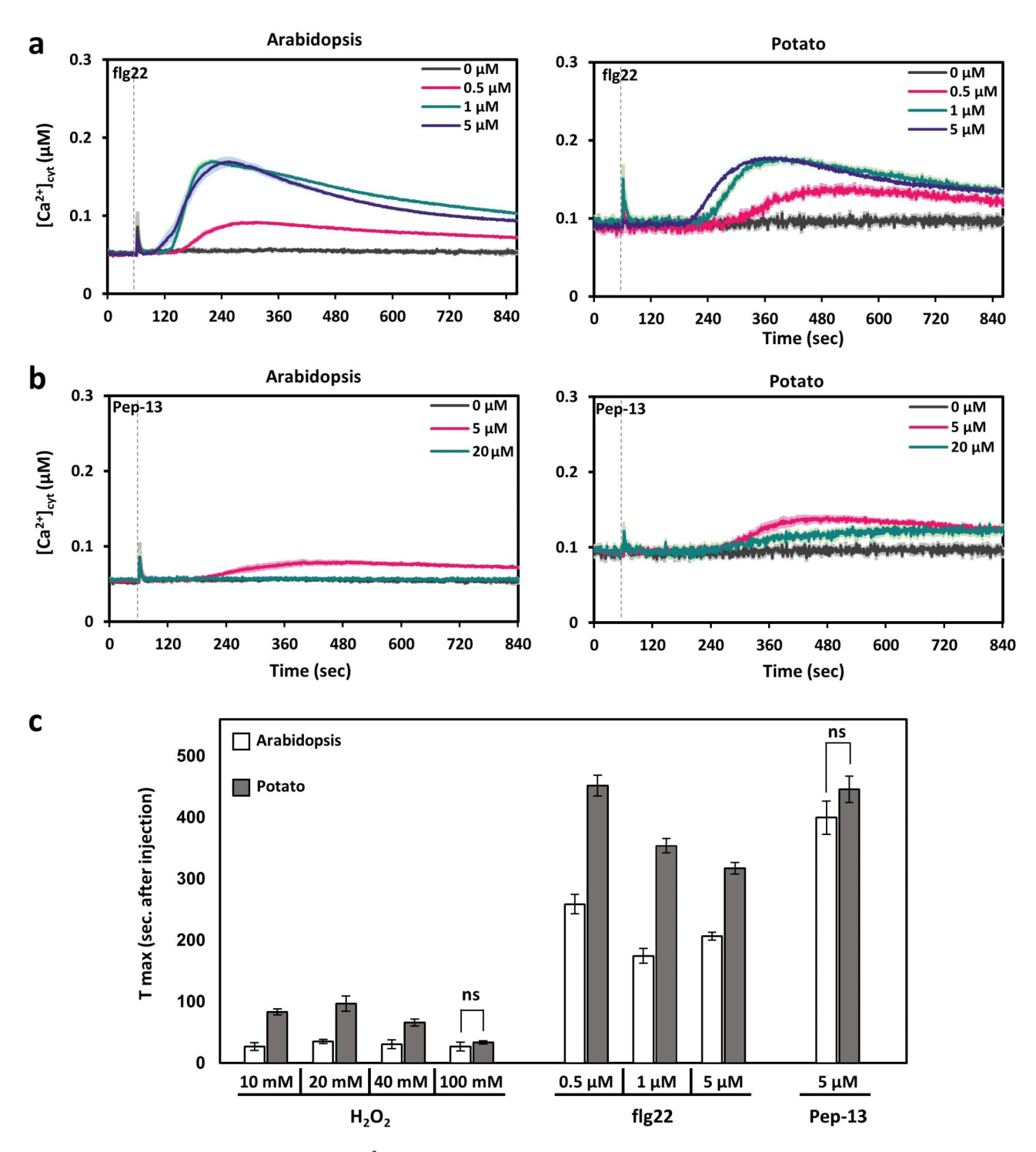


**Fig. 5.** Induction of  $Ca^{2+}$  signals in response to pathogen-associated molecular patterns (PAMPs) in leaf tissue of Arabidopsis and potato. (a) Time course of  $[Ca^{2+}]_{cyt}$  in Arabidopsis (left) and potato (right) in response do different concentrations of flg22. (b) Time course of  $[Ca^{2+}]_{cyt}$  in Arabidopsis (left) and potato (right) in response do different concentrations of Pep-13. Values are shown as mean ± SE (n=9). Dashed lines indicate the time point of PAMP application (60 s). (c) Time to reach the maximal increase of  $[Ca^{2+}]_{cyt}$  ( $T_{max}$ ) after application of flg22 and Pep-13 in comparison to  $H_2O_2$ . Values are derived from the data in Figs. 4 and 5A, and 5B. Treatments that resulted in non-significant differences between the two species are indicated (two tailed student's t-test,  $p \le 0.01$ ).

160 s after application, similar to what has been described earlier in Arabidopsis<sup>21,33</sup> and the peak declined slowly (Fig. 5a, Arabidopsis). The  $[Ca^{2+}]_{cyt}$  transient in potato in response to flg22 looked similar but the response was even slower than in Arabidopsis. Its elevation started only 3 min after application with a peak time around 300s (Fig. 5a, potato and Fig. 5c), which is similar to what was described for barley<sup>21</sup>. In both species, the time it took to reach the maximum amplitude after application of the flg22 stimulus  $(T_{max})$  was much longer than the response to the direct  $H_2O_2$  application (Fig. 4), independent of the concentration tested (Fig. 5c). This could be due to flg22 inducing ROS production which subsequently, and thus time-delayed, triggers a  $Ca^{2+}$  transient.

#### Pep-13

We also tested  $[Ca^{2+}]_{cyt}$  changes in response to Pep-13, a fragment of a glycoprotein from the late blight-causing *Phytophthora infestans*. Arabidopsis showed only a very minor increase in  $[Ca^{2+}]_{cyt}$  of less than 0.04  $\mu$ M with 5  $\mu$ M elicitor and no response at higher concentrations (Fig. 5b, Arabidopsis). The response in potato to 5  $\mu$ M Pep-13 was similar but with a higher amplitude of 0.05  $\mu$ M. At 20  $\mu$ M Pep-13, the response was lower and similar to what was observed in Arabidopsis at 5  $\mu$ M (Fig. 5b, potato). The time to the maximum increase in  $[Ca^{2+}]_{cyt}$  was even longer than with flg-22 and was observed 6 min after application (Fig. 5c). What we did not observe was a slower response of potato compared to Arabidopsis as seen for flg22. (Fig. 5c)

In vivo imaging of H2O<sub>2</sub> induced redox changes using potato biosensor plants

When analysing the Ca<sup>2+</sup> response of Arabidopsis and potato to H<sub>2</sub>O<sub>2</sub> we observed a marked difference in timing and amplitude between the two species (Fig. 4). We were wondering whether this is caused by *bona fide* differences in the molecular response to equivalent redox changes, or whether our treatments induced different redox changes in the two species. To address this question, we expressed the redox-sensitive Grx1-roGFP2 sensor under control of the 35S CaMV promoter in the same cultivar (Désirée) as used for the Ca<sup>2+</sup> analyses (Fig. 6; Supplementary Fig. S2-S4). Several independent lines were obtained that showed a strong and reliable emission at 510 nm upon excitation at 485 nm under reducing conditions (Supplementary Fig. S2). Grx1-roGFP2 line #29 was used for subsequent analysis. It revealed a clear fluorescence signal throughout the leaf with stronger signals in the main leaf veins when imaged under blue light (460–490 nm) using a fluorescence imager (Fig. 6a). Expression of Grx1-roGFP2 had no visible effect on the growth of this line compared to wild type and Western Blot analysis confirmed the presence of the Grx1-roGFP2 protein (Fig. 6b; Supplementary Fig. S3).

Confocal laser scanning microscopy of leaf discs of Grx1-roGFP2 confirmed the cytosolic localisation of the sensor (Fig. 6c). Reducing conditions induced by 100 mM DTT only resulted in minor changes of the fluorescence signals observed at  $535\pm15$  nm after excitation at either 405–485 nm. Oxidation by 100 mM  $\rm H_2O_2$  lowered the emission upon excitation at 485 nm and clearly increased the emission upon excitation at 405 nm (Fig. 6c). Together this shows that the sensor line can be used to assess the cytosolic oxidation status.

Further analyses were performed using the same plate luminometer employed for the aequorin measurements. Comparison of soil grown Grx1-roGFP2 plants from potato with Grx1-roGFP2-expressing Arabidopsis<sup>34</sup> without any stress treatment showed a nearly three times higher ratio of 405/485 nm fluorescence in potato (Fig. 6d, mock). The biosensor is most sensitive for the oxidation status of the small antioxidant glutathione (GSH); thus, the data indicate a higher basal GSH oxidation in potato. Treatment of Arabidopsis and potato with DTT revealed only minor changes in the 405/485 nm ratio with 10 mM DTT and no further decrease with 100 mM DTT or higher (Fig. 6d; Supplementary Fig. S4). This confirms the data from the microscopic analysis of potato (Fig. 6c) and demonstrates that 100 mM DTT fully reduces the leaf cytosolic GSH for both species.

Arabidopsis and potato show slightly differences under treatment with  $\rm H_2O_2$ . Both species reached a maximum 400/485 nm ratio and thus full oxidation of the cytosol at 100 mM  $\rm H_2O_2$ . However, upon treatment with 10 mM  $\rm H_2O_2$ , Arabidopsis leaf cells showed a significant increase in ratio of 405/485 nm fluorescence, while in potato no significant difference to the mock value was observed (Fig. 6d). After treatment with 100 mM  $\rm H_2O_2$ , the ratio of 400/485 nm fluorescence showed a further increase in Arabidopsis and a significant increase in potato. No further increase in ratio was observed with higher  $\rm H_2O_2$  concentrations for either species. Thus, the full dynamic range could be achieved for both species with 10 mM DTT and 100 mM  $\rm H_2O_2$ , however, while in Arabidopsis the ratio of 405/485 nm fluorescence increased from 0.2 to 0.6 (dynamic range of ~3), potato only showed less than a duplicating of the ratio from 0.55 to 0.9 (Fig. 6d). This indicates quite a strong difference in GSH oxidation between Arabidopsis and potato and the high level of GSH oxidation might play a part in the lower  $\rm H_2O_2$ -induced  $\rm Ca^{2+}$  response that we observed in potato (Fig. 4b).

#### Discussion

Transient changes in the concentration of  $[Ca^{2+}]_{cyt}$  are among the earliest responses of plant cells to many environmental stresses. Intriguingly, the exact dynamics of the  $Ca^{2+}$  signature not only differs depending on the stimulus but can also differ between stress acclimated and non-acclimated plants<sup>9</sup>. This raises the exciting possibility that screening of specific  $Ca^{2+}$  signatures could identify promising varieties for improved crop breeding. However, before such an approach could be incorporated into breeding programmes, baseline  $Ca^{2+}$  responses for the desired crop need to be investigated. Considering the importance of  $Ca^{2+}$  signalling as a very early component of plant stress responses, surprisingly few investigations using GECIs have so far been performed with plants other than Arabidopsis<sup>18–21,35</sup>. As part of an large-scale analysis of molecular and phenotypical responses of potatoes to environmental stress (https://adapt.univie.ac.at/), we thus investigated stress-dependent changes in  $[Ca^{2+}]_{cyt}$  in the moderate stress-resistant potato variety Désirée. To better put our data in the context of what is known in the model plant Arabidopsis, we measured all stress responses in parallel between both plants. This avoids as much as possible issues, such as difference in plant age, growth conditions etc. when comparing to already published data. Although the apoaequorin expression level was lower and aequorinderived photon counts in potato reached only about 25% as those observed in Arabidopsis (supplementary Fig.

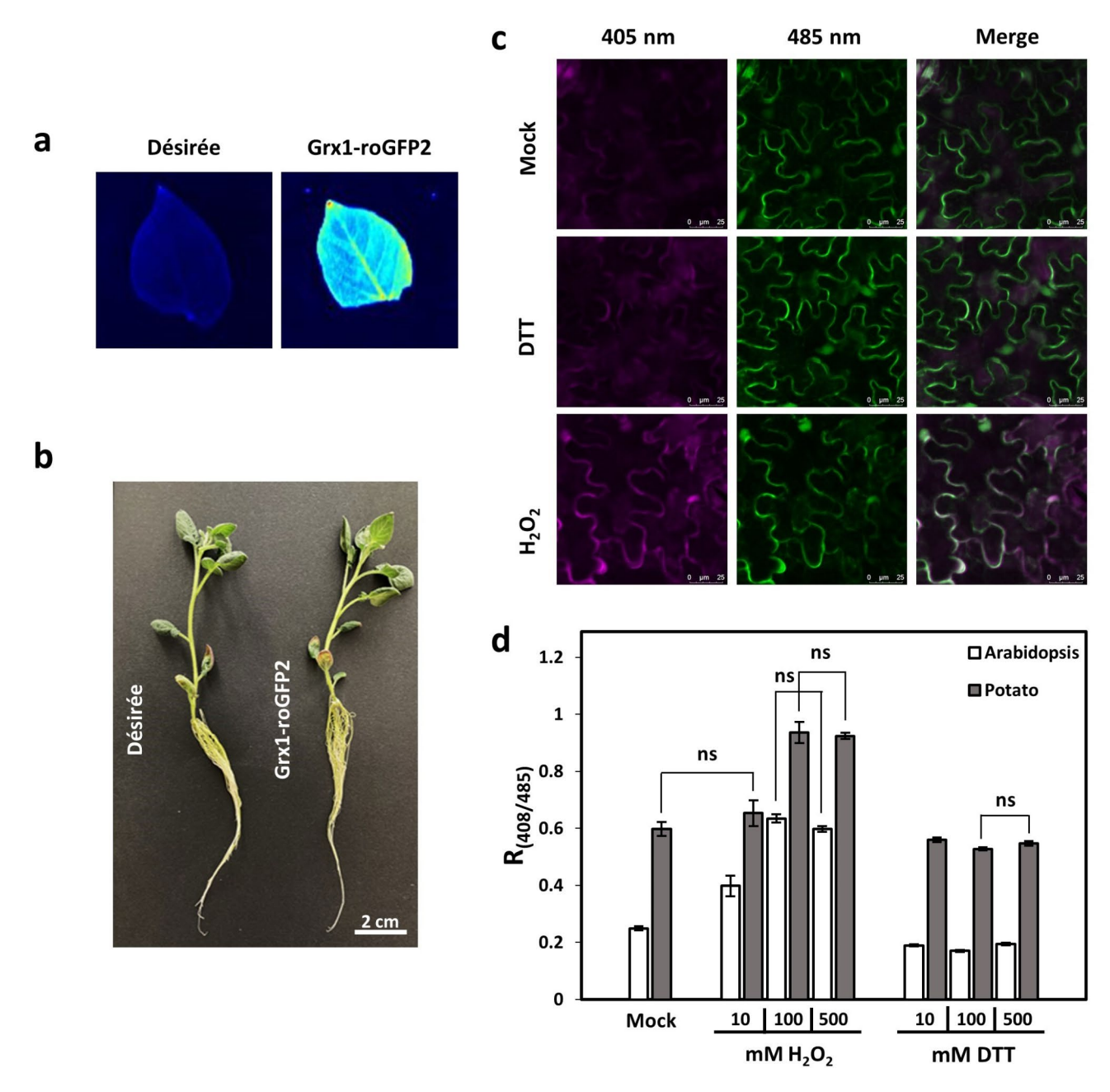


**Fig. 6.** Cytosolic redox status of soil-grown potato and Arabidopsis plants. (a) Image of the abaxial side of full mature leaves of wild type and St-Grx1-roGFP2 plants after excitation with blue light (460–485 nm). (b) Representative picture of three-week old Désirée (wild type) and St-Grx1-roGFP2 potato plants. (c) Confocal images of St-Grx1-roGFP2 plants after sequential excitation at 405 nm, 485 nm, and the merge of both channels. Leaf discs were incubated for 10 min in either mock solution, 100 mM DTT or 100 mM  $\rm H_2O_2$ . (d) Ratiometric measurement of emission at 535 ± 15 nm after sequential excitation at 405 nm and 485 nm. Leaf discs were placed with abaxial side upwards into 96-well plates and emission was measured 10 min after application of imaging buffer (mock),  $\rm H_2O_2$  (10, 100 or 500 mM) or DTT (10, 100 or 500 mM) (n=9, mean ± SE). Treatments that resulted in non-significant differences within the same species are indicated (two tailed student's t-test, p ≤ 0.01).

S1a and b), we could measure well-defined responses in the potato line #20 with stress-induced photon counts well above baseline levels. Thus, we believe that the differences we observed represent species-specific responses of potato and Arabidopsis.

With regards to NaCl, the differences between Arabidopsis and potato mostly pertained to the shape of the response curve at different concentrations (Fig. 2). While both organisms showed a clear dose dependent response to NaCl, Arabidopsis exhibited a strong shift in the maximum peak which was reached earlier with higher concentrations. By contrast, this effect of concentration was very minor in potato. Ultimately, both species reached a similar shape of the response curve, however, potato required about double the NaCl concentration for

a maximal response and even then, a much lower peak value for  $[Ca^{2+}]_{cyt}$  was recorded. The much lower NaCl response in potato is remarkable since potato plants have been described as rather sensitive to salt stress with a soil salinity threshold of  $1.7~dSm^{-1}$ . This is remarkably low in comparison to more NaCl-insensitive crops such as wheat  $(6~dSm^{-1})$  and barley  $(8~dSm^{-1})^{24}$ , the latter of which shows a NaCl-induced  $Ca^{2+}$  transient in its leaves with a maximum amplitude of around  $0.4~\mu M^{21}$ . The salt overly sensitive (SOS) pathway plays a crucial role in the salt tolerance of plants and involves the activation of a  $N^+/H^+$  antiporter by a  $Ca^{2+}$ -dependent sensor-protein kinase complex<sup>36</sup>. Very little is known about the SOS pathway in potato<sup>37</sup>. Whether the lower  $Ca^{2+}$  transient in potato leads to less activation of the SOS pathway and therefore impacts subsequent salt tolerance remains to be tested, especially because Arabidopsis displays a high NaCl-induced  $Ca^{2+}$  transient but is also considered as salt sensitive. While such species-specific sensitivity to salt might have an impact on the  $Ca^{2+}$  responses they are not sufficient to fully explain these observations, especially in light of the fact that salt stress occurs primarily as soil salinity and is sensed in the roots<sup>38</sup>. Consequently, very little is known about salt sensing in leaves and shoots. Another reason for the observed differences in  $Ca^{2+}$  responses could lie in different physical surface properties of the leaves that affect the uptake of NaCl, however NaCl penetration into the tissue cannot be easily accessed experimentally.

In contrast to NaCl, mannitol is a non-ionic, osmotic substance. It is used to mimic drought stress since the latter is often not applicable in experimental set-ups, such as the one used in this study. Increase in  $[Ca^{2+}]_{cyt}$  in response to mannitol has been shown in several previous studies for whole young seedlings of Arabidopsis  $^{13,39,40}$ . However, when roots and shoots were analysed separately, it was shown that the response occurred exclusively in roots while no  $[Ca^{2+}]_{cyt}$  transient could be observed in leaves neither in Arabidopsis nor in barley<sup>21,41</sup>. In this study the lack of response in leaves could be confirmed for Arabidopsis also in case of soil-grown plants (Fig. 3). By contrast, a broad  $[Ca^{2+}]_{cyt}$  transient could be observed in response to 400 mM in the leaf tissue of potato. The underlaying mechanisms for these species-dependent responses to mannitol need to be further investigated at a molecular level.

With regards to H<sub>2</sub>O<sub>2</sub>, it was most remarkable that for both species rather high concentrations were required to elicit a response. In experiments using leaves from young seedlings grown on sterile medium, 10-15 mM H<sub>2</sub>O<sub>2</sub> was sufficient for a maximal response in Arabidopsis and barley<sup>21</sup>, while in the leaves of soil-grown, older plants used in this study the amplitude of  $[Ca^{2+}]_{cvt}$  increased up to 100 mM  $H_2O_2$  for both Arabidopsis and potato. This might be due to a difference in penetration of H<sub>2</sub>O<sub>2</sub> into the tissue of the older, soil-grown plants. Moreover, while Arabidopsis showed response curves with a dose-dependent increase in the maximal amplitude but identical shape, the response curve in potato became biphasic with two overlapping broad peaks of similar amplitude. The timing of the first of these two peaks matched the single peak seen in Arabidopsis indicating that they are caused by the same initial response to  $H_2O_2$ . The second peak in potato could be attributed to secondary responses that are activated by the initial increase in [Ca<sup>2+</sup>]<sub>cvt</sub>. Biphasic signature have been described before also for Arabidopsis in response to ozone or even H<sub>2</sub>O<sub>2</sub><sup>14,42</sup> however, in these studies, whole seedlings including roots were used and the second peak occurs much later (~600s after application) than what we observe with potato. Thus, the molecular basis for the biphasic response of potato is likely different. In this regard, the differences we measured for the basal oxidative state of the cytosol using the GRX1-roGFP2 sensor lines for Arabidopsis and potato (Fig. 6d) is interesting. Our data shows that both species have the potential to reach a similar increase of the oxidative state (+0.4  $R_{405/485}$ ) after being stimulated with 100 mM  $H_2O_2$ . However, the reason behind the higher basal level of  $R_{405/485}$  (0.2 vs. 0.55) in potato remains unclear. Former research with a chloroplast-targeted GRX1-roGFP2 probe in potato<sup>43</sup> revealed that the basal oxidative state of the chloroplast was higher for older leaves compared to younger leaves and they speculated that this may be due to an increase in photosynthesis efficiency and decrease in photoprotection.

Differences between Arabidopsis and potato where also observed for the two PAMPs, flg22 and Pep-13. Most remarkable was the response to Pep-13, which contrary to most other stimuli we tested in the present study, elicited a higher  $[Ca^{2+}]_{cyt}$  increase in potato than in Arabidopsis, suggesting that potato has a higher sensitivity to Pep-13 and thus *Phytophthora infestans*. Indeed, late blight, caused by *Phytophthora infestans*, is the most devastating disease of global potato production<sup>44</sup>. It was however shown before that Pep-13 elicits a defence response against late blight in parsley including a  $[Ca^{2+}]_{cyt}$  transient with a peak of about 0.8  $\mu$ M at around 150 s<sup>45,46</sup>. This response is faster and stronger than what we observed in Arabidopsis and potato (Fig. 5b). This might be the result of the different types of sample tissue used (parsley suspension cells vs. leaf tissue from soil grown plants) or could indicate a high susceptibility of parsley to *Phytophthora*. Indeed, severe yield loss of parsley due to root rot caused by *Phytophthora cryptogea* has been described<sup>47</sup>.

Overall, when comparing the interplay between species- and stimulus-dependent responses, no simple conclusion as to the driving factor of the observed differences can be drawn. While issues such as difference in stimuli-penetration need to be addressed methodically, it can be expected that species-specific differences in  $Ca^{2+}$  transients affect the downstream mechanism of perception and translation of the stimulus into cellular responses. Mechanistically,  $Ca^{2+}$  signatures are shaped by the activity of  $Ca^{2+}$  transporters and channels, as well as  $Ca^{2+}$ -buffering systems<sup>48</sup>.

The phylogenetic relationship between  $Ca^{2+}$  transport proteins across a range of plant species has been determined<sup>49</sup> and based on this analysis, we identified similar sequences in the potato reference genome Phureja DM1-3 v6.1 (Supplementary Table S1). Notably, the potato genome seems to encode more GLRs (27 in potato vs. 20 in Arabidopsis), MCA channels (7 vs. 2) and  $Ca^{2+}$ -ATPases (21 vs. 14). However, given the overall higher number of annotated protein-coding genes in potato compared to the Arabidopsis genome<sup>50</sup> these differences are not significant (chi-square test, p < 0.05). Nevertheless, variance in the  $Ca^{2+}$  toolbox between species might be related to some of the observed difference in stress-induced  $Ca^{2+}$  transients and the functionality of the corresponding gene products and the impact of a putatively increased complexity in potato remain to be studied further. With regard to down-stream mechanisms activated by the  $Ca^{2+}$  transients, an alteration in amplitude

and/or shape could affect how different plants can cope with environmental changes. This could be investigated by analysing the  $Ca^{2+}$  response of different varieties of the same species that are more or less susceptible to a certain stress. In that regard, our data can be used to define which stimuli and stimuli concentrations are useful to trigger cytosolic  $Ca^{2+}$  changes in the moderate stress-resistant potato variety Désirée and by that offers a basis for future  $Ca^{2+}$  related studies in this crop species.

### Methods

### Vector construction and transformation into S. tuberosum (cv. Désirée)

To generate potato lines of the cultivar Désirée with constitutive expression of *apoaequorin* (St-AEQ<sub>cyt</sub>), the pMAQ2 vector carrying the coding region of *apoaequorin* down-stream of the cauliflower mosaic virus (CaMV) 35S promoter was used<sup>12</sup>. For the generation of Désirée lines with constitutive expression of redox-sensitive *roGFP2* fused with human *glutaredoxin* 1 (St-Grx1-roGPF2) a previous described fusion construct<sup>51</sup> was inserted into pBINar upstream of the CaMV 35S promoter. Both constructs were introduced into the potato cultivar Désirée as described previously<sup>52</sup>.

### Plant material and growth conditions

In addition to the transgenic potato plants described above, corresponding transgenic *A. thaliana* plants (Col-0) expressing either cytosolic *apoaequorin* (At-AEQ<sub>cyt</sub>;<sup>12</sup>) or *Grx1-roGFP2* (St-Grx1-roGFP2<sup>53</sup>) under the control of the cauliflower mosaic virus 35S promoter were used.

Potato cuttings/explants were first grown on sterile MS agar (pH 5.7, 2% (w/v) sucrose) for root formation and subsequently transplanted into single pots filled with soil. In case of Arabidopsis, seeds were sown onto the same soil, stratified for 2 days at 4 °C in the dark, and separated after germination into single pots. Potato and Arabidopsis plants were subsequently cultivated side-by-side for 3 weeks in a growth chamber with a temperature of  $20\pm2$  °C at a light intensity of ~150 µmol photons m<sup>-2</sup> s<sup>-1</sup> (Philips TLD 18 W of alternating 830/840 light colour) under long day (16 h light/8 h dark) conditions.

### In vitro aequorin reconstitution and quantification

To quantify apoaequorin expression in transgenic potato plants, aequorin was reconstituted and chemiluminescence was measured in vitro. Leaf discs (Ø 6 mm) were collected from fully expanded leaves of soil-grown St-AEQ cyt plants and the fresh weight was recorded. The tissue was homogenised in 500  $\mu$ L extraction buffer (0.5 M NaCl, 9.547 mM beta-mercaptoethanol, 5 mM EDTA, 0.2% (w/v) gelatine, 10 mM Tris-HCl pH 7.4) and cleared by centrifugation in a bench-top centrifuge at 16,300 g for 10 min. Supernatants were transferred to new tubes and reconstituted with 1  $\mu$ M coelenterazine (Biosynth AG, Switzerland) at room temperature in the dark overnight. The following day, 4  $\mu$ L aliquots were added to 200  $\mu$ L of 200 mM Tris HCl, 0.5 mM EDTA, pH 7.0 in the wells of a 96 well plate. The relative amount of aequorin in each extract was calculated by measuring photon counts over a 10-second period before and after addition of 200 $\mu$ L of 50 mM CaCl<sub>2</sub> (final concentration 25 mM), using a plate luminometer (Tristar 3 Multimode Reader, Berthold GmbH). Aequorin abundance was expressed as relative luminescence / fresh weight (arbitrary units/mg).

### Aequorin and GFP immunodetection

Proteins were isolated from leaves of 3-week-old potato plants using Lacus protein isolation buffer (20 mM Tris pH 7.7, 80 mM NaCl, 0.75 mM EDTA, 1 mM  $\rm CaCl_2$ , 5 mM  $\rm MgCl_2$ , 1 mM DTT, 2% (w/v) SDS). The proteins were separated on a 12% SDS-polyacrylamide gel and transferred to nitrocellulose membrane (0.45 µm pore size). After transfer of the proteins the membrane was stained using 0.1% (w/v) Ponceau S in 5% (v/v) glacial acetic acid. Immunodetection was performed using antibodies against aequorin (Abcam, Berlin, Germany) or GFP (Agrisera, AS20 4443) and an ECL detection system with an anti-rabbit secondary antibody coupled to horseradish peroxidase.

### In planta reconstitution of apoaequorin and stimuli-induced luminescence measurements

One day before measurements were taken, leaf discs ( $\emptyset$  6 mm) were collected from ~3-week-old plants and floated overnight in the dark at 20 °C in 10  $\mu$ M coelenterazine (Biosynth AG, Switzerland) for reconstitution. The following day, the leaf discs were transferred individually into a 96-well plate containing 100  $\mu$ L ddH<sub>2</sub>O. Photon count measurements were performed using a plate luminometer (Tristar 2 Multimode Reader, Berthold GmbH). The basal level of photon counts was measured for 30 s for the abiotic stimuli and 60 s for the PAMPs (Flg22, GenScript Biotech Corporation, The Netherlands; Pep-13, ProteoGenix, France) with an interval of 1 s, followed by application of various stimulants using a stock solution with 2x the final concentration and a volume equal to the starting volume (100  $\mu$ L), with continuous measuring for a minimum of 240 s after application. Subsequently, the remaining aequorin was discharged by adding 1/3 volume of 3 M CaCl<sub>2</sub> in 30% (v/v) EtOH resulting in a final concentration of 1 M CaCl<sub>2</sub> in 10% (v/v) EtOH. Photon counts were then recorded for another 300 s. [Ca<sup>2+</sup>]<sub>Cvt</sub> was calculated based on the photon counts as described previously<sup>54</sup>.

### Measurement of Grx1-roGFP2 fluorescence

To check the expression of Grx1-roGFP2 in leaves of 3-week-old wild type and St-Grx1-roGFP2, plants were imaged via the ChemiDoc MP Imaging System (BioRAD, USA) with a blue light source (460–490 nm) and an exposure time of 0.4 s.

For imaging of Grx1-roGFP2 fluorescence using laser scanning confocal microscopy, leaf discs (Ø 7 mm) of 3-week-old St-Grx1-roGFP2 plants were pre-incubated in imaging buffer (10 mM MES pH 5.8, 10 mM MgCl<sub>2</sub>, 10 mM CaCl<sub>2</sub>, 5 mM KCl) for 30 min and then transferred onto a microscope slide. The samples on the slide were covered with either ddH<sub>2</sub>O, 100 mM H<sub>2</sub>O<sub>2</sub> or 100 mM DTT and mounted into the light pass of a Leica

SP8 lightning (Leica Biosystems, Germany). Images were collected using a 40x lens (HC-PL-APO-C22, Zeiss) in multi-track mode with sequential excitation by 485 nm (1% gain) and 405 nm lasers (5% gain). Emitted roGFP2 fluorescence was detected from 505 to 536 nm 10 min after the treatment started.

roGFP2 fluorescence was further measured in 96 well plates using the Tristar2 LB 942 multimode reader (Berthold, Germany). After cutting the leaf discs (Ø 7 mm) of 3-week-old St-Grx1-roGFP2 and At-Grx1-roGFP2 samples were placed into ddH<sub>2</sub>O for 1 h to rest. For measurements the leaf discs were transferred individually into a 96-well plate containing 100 µL ddH<sub>2</sub>O. Measurements took place with 2-minute intervals for 10 min to measure the basal level of fluorescence, followed by application of different treatments (mock, H<sub>2</sub>O<sub>2</sub> or DTT) using a stock solution with 2x the final concentration and a volume equal to the starting volume ( $100 \,\mu\text{L}$ ), with continuous measuring for a minimum of 70 min after treatment application. Exposure time was set manually to 0.1 s with an alternating excitation at 405 nm (30% lamp energy) and 485 nm (30% lamp energy) using a 535 ± 15 nm emission filter. Redox changes were represented as the ratio of the emission after measurements at both excitation wavelengths (405/485) at 10 min after applying the stimulus.

#### **Statistics**

All Ca<sup>2+</sup> and redox measurements include data from nine individual replicates. For those nine measurements, the plants were grown independently three times and leaf discs were obtained from three independent plants each time. Pairwise comparisons were performed via students t-test with a significance threshold of  $p \le 0.01$ . All data are represented as means ± SE. Details of the statistical analysis are specified in figure legends.

### Data availability

The data used to support the findings of this study are included within the manuscript or supplementary information files.

Received: 8 May 2024; Accepted: 6 November 2024

Published online: 11 November 2024

#### References

- 1. Rizhsky, L. et al. When defense pathways collide. The response of Arabidopsis to a combination of drought and heat stress. Plant Physiology 134, 1683-1696 (2004).
- 2. Takahashi, F., Kuromori, T., Urano, K., Yamaguchi-Shinozaki, K. & Shinozaki, K. Drought stress responses and resistance in plants: From cellular responses to long-distance intercellular communication, Front. Plant Sci. 11, 556972 (2020).
- 3. Rasmussen, S. et al. Transcriptome responses to combinations of stresses in Arabidopsis. Plant Physiology 161, 1783-1794 (2013).
- 4. Zandalinas, S. I. et al. Systemic signaling during abiotic stress combination in plants. Proc. Natl. Acad. Sci. U.S.A. 117, 13810–13820
- 5. Kudla, J., Batistič, O. & Hashimoto, K. Calcium signals: The lead currency of plant information processing. Plant Cell 22, 541-563 (2010).
- 6. Pirayesh, N., Giridhar, M., Ben Khedher, A., Vothknecht, U. C. & Chigri, F. Organellar calcium signaling in plants: An update. Biochimica et Biophysica Acta (BBA) - Molecular Cell Research 1868, 118-948 (2021).
- 7. Ghosh, S., Bheri, M., Bisht, D. & Pandey, G. K. Calcium signaling and transport machinery: Potential for development of stress tolerance in plants. Current Plant Biology 29, 100235 (2022).
- 8. Plieth, C., Hansen, U., Knight, H. & Knight, M. R. Temperature sensing by plants: The primary characteristics of signal perception and calcium response. The Plant Journal 18, 491-497 (1999).
- 9. Knight, H. & Knight, M. R. Imaging spatial and cellular characteristics of low temperature calcium signature after cold acclimation in Arabidopsis. Journal of Experimental Botany 51, 1679-1686 (2000).
- 10. McAinsh, M. R. & Pittman, J. K. Shaping the calcium signature. New Phytologist 181, 275-294 (2009).
- 11. Whalley, H. J. & Knight, M. R. Calcium signatures are decoded by plants to give specific gene responses. New Phytologist 197, 690-693 (2013).
- 12. Knight, M. R., Campbell, A. K., Smith, S. M. & Trewavas, A. J. Transgenic plant aequorin reports the effects of touch and coldshock and elicitors on cytoplasmic calcium. Nature 352, 524-526 (1991).
- 13. Knight, H., Trewavas, A. J. & Knight, M. R. Calcium signalling in Arabidopsis thaliana responding to drought and salinity. The Plant Journal 12, 1067-1078 (1997).
- 14. Rentel, M. C. & Knight, M. R. Oxidative stress-induced calcium signaling in Arabidopsis. Plant Physiology 135, 1471–1479 (2004).
- 15. Jiang, Z. et al. Relationship between NaCl and H<sub>2</sub>O<sub>2</sub>-induced cytosolic Ca<sup>2+</sup> increases in response to stress in Arabidopsis. PLoS ONE 8, e76130 (2013).
- 16. Thor, K. & Peiter, E. Cytosolic calcium signals elicited by the pathogen-associated molecular pattern flg22 in stomatal guard cells are of an oscillatory nature. New Phytologist 204, 873-881 (2014).
- 17. Mithöfer, A. & Mazars, C. Aequorin-based measurements of intracellular Ca<sup>2+</sup>-signatures in plant cells. Biol Proced Online 4, 105-118 (2002).
- 18. Zhang, Y. et al. Aequorin-based luminescence imaging reveals differential calcium signalling responses to salt and reactive oxygen species in rice roots. Journal of Experimental Botany 66, 2535–2545 (2015).
- 19. Nagel-Volkmann, J., Plieth, C., Becker, D., Lüthen, H. & Dörffling, K. Cold-induced cytosolic free calcium ion concentration changes in wheat. Journal of Plant Physiology 166, 1955-1960 (2009)
- 20. Albert, M., Van Der Krol, S. & Kaldenhoff, R. Cuscuta reflexa invasion induces Ca 2+ release in its host. Plant Biology 12, 554-557 (2010).
- 21. Giridhar, M. et al. Comparative analysis of stress-induced calcium signals in the crop species barley and the model plant Arabidopsis thaliana. BMC Plant Biol 22, 447 (2022).
- 22. World Food and Agriculture. Statistical Yearbook 2021 (FAO, 2021). https://doi.org/10.4060/cb4477en.
- 23. Kim, Y.-U. & Lee, B.-W. Differential mechanisms of potato yield loss induced by high day and night temperatures during tuber initiation and bulking: Photosynthesis and tuber growth. Front. Plant Sci. 10, 300 (2019).
- 24. Chinnusamy, V., Jagendorf, A. & Zhu, J. Understanding and improving salt tolerance in plants. Crop Sci. 45, 437-448 (2005).
- 25. Moroz, N. & Tanaka, K. FlgII-28 is a major flagellin-derived defense elicitor in potato. MPMI 33, 247-255 (2020).
- 26. Mittler, R. ROS are good. Trends in Plant Science 22, 11-19 (2017).
- 27. Mattila, H., Khorobrykh, S., Havurinne, V. & Tyystjärvi, E. Reactive oxygen species: Reactions and detection from photosynthetic tissues. Journal of Photochemistry and Photobiology B: Biology 152, 176-214 (2015).

- 28. Ranf, S., Eschen-Lippold, L., Pecher, P., Lee, J. & Scheel, D. Interplay between calcium signalling and early signalling elements during defence responses to microbe- or damage-associated molecular patterns. The Plant Journal 68, 100-113 (2011).
- Seybold, H. et al. Ĉa <sup>2+</sup> signalling in plant immune response: From pattern recognition receptors to Ca <sup>2+</sup> decoding mechanisms. New Phytologist 204, 782-790 (2014).
- 30. Mithöfer, A., Ebel, J., Bhagwat, A. A., Boller, T. & Neuhaus-Url, G. Transgenic aequorin monitors cytosolic calcium transients in soybean cells challenged with β-glucan or chitin elicitors. Planta 207, 566-574 (1999)
- 31. Maintz, J. et al. Comparative analysis of MAMP-induced calcium influx in Arabidopsis seedlings and protoplasts. Plant and Cell Physiology 55, 1813-1825 (2014).
- 32. Marcec, M. J. & Tanaka, K. Crosstalk between calcium and ROS signaling during Flg22-triggered immune response in Arabidopsis leaves. Plants 11, 14 (2021).
- 33. Chi, Y. et al. Flg22-induced Ca<sup>2+</sup> increases undergo desensitization and resensitization. Plant Cell & Environment 44, 3793-3805
- 34. Rosenwasser, S. et al. A fluorometer-based method for monitoring oxidation of redox-sensitive GFP (roGFP) during development and extended dark stress. Physiologia Plantarum 138, 493-502 (2010).
- Barberini, M. L. et al. Calcium dynamics in tomato pollen tubes using the Yellow Cameleon 3.6 sensor. Plant Reprod 31, 159-169
- 36. Ali, A., Petrov, V., Yun, D.-J. & Gechev, T. Revisiting plant salt tolerance: Novel components of the SOS pathway. Trends in Plant Science 28, 1060-1069 (2023).
- 37. Liang, L. et al. Genome-wide characterization of SOS1 gene family in potato (Solanum tuberosum) and expression analyses under salt and hormone stress. Front. Plant Sci. 14, 1201730 (2023).
- 38. Wang, C.-F., Han, G.-L., Yang, Z.-R., Li, Y.-X. & Wang, B.-S. Plant salinity sensors: Current understanding and future directions. Front. Plant Sci. 13, 859224 (2022).
- 39. Yuan, F. et al. OSCA1 mediates osmotic-stress-evoked Ca<sup>2+</sup> increases vital for osmosensing in Arabidopsis. Nature 514, 367–371
- 40. Sun, S., Zhang, X., Chen, K., Zhu, X. & Zhao, Y. Screening for Arabidopsis mutants with altered Ca2+ signal response using aequorin-based Ca<sup>2+</sup> reporter system. STAR Protocols 2, 100558 (2021).
- 41. Zhu, X. et al. Measuring spatial and temporal Ca<sup>2+</sup> signals in Arabidopsis plants. JoVE https://doi.org/10.3791/51945 (2014).
- 42. Clayton, H., Knight, M. R., Knight, H., McAinsh, M. R. & Hetherington, A. M. Dissection of the ozone-induced calcium signature. The Plant Journal 17, 575-579 (1999).
- 43. Hipsch, M. et al. Sensing stress responses in potato with whole-plant redox imaging. Plant Physiology 187, 618-631 (2021).
- 44. Bourke, A., Hill, J. R. & O Gráda, C. The Visitation of God? The Potato and the Great Irish Famine (Lilliput Press, 1993).
- 45. Nürnberger, T. et al. High affinity binding of a fungal oligopeptide elicitor to parsley plasma membranes triggers multiple defense responses. Cell 78, 449-460 (1994).
- 46. Blume, B., Nürnberger, T., Nass, N. & Scheel, D. Receptor-mediated increase in cytoplasmic free calcium required for activation of pathogen defense in parsley. Plant Cell 12, 1425-1440 (2000).
- 47. Davis, R. M. First report of phytophthora root rot of parsley. Plant Dis. 78, 1122D (1994).
- 48. Stael, S. et al. Plant organellar calcium signalling: an emerging field. Journal of Experimental Botany 63, 1525-1542 (2012).
- 49. Demidchik, V., Shabala, S., Isayenkov, S., Cuin, T. A. & Pottosin, I. Calcium transport across plant membranes: Mechanisms and functions. New Phytol 220, 49-69 (2018).
- 50. Xu, X. et al. Genome sequence and analysis of the tuber crop potato. *Nature* 475, 189–195 (2011).
  51. Aller, I., Rouhier, N. & Meyer, A. J. Development of roGFP2-derived redox probes for measurement of the glutathione redox potential in the cytosol of severely glutathione-deficient rml1 seedlings. Front. Plant Sci. 4, 66 (2013).
- 52. Rocha-Sosa, M. et al. Both developmental and metabolic signals activate the promoter of a class I patatin gene. The EMBO Journal 8, 23-29 (1989).
- 53. Nietzel, T. et al. The fluorescent protein sensor ro GFP 2-Orp1 monitors in vivo H<sub>2</sub>O<sub>2</sub> and thiol redox integration and elucidates intracellular H<sub>2</sub>O<sub>2</sub> dynamics during elicitor-induced oxidative burst in Arabidopsis. New Phytologist 221, 1649-1664 (2019).
- 54. Knight, H. & Knight, M. R. Chapter 14 recombinant aequorin methods for intracellular calcium measurement in plants. in Methods in Cell Biology vol. 49 201-216 (Elsevier, 1995).

### **Acknowledgements**

We are grateful to Marc R. Knight (Durham University) for critical assessment of the manuscript. We thank the Solana Research GmbH for generation of the St-Grx1-roGFP2 lines, Stephan Hartmann, who carried out the initial screen to select GRX1-roGFP2 line #29, and Ursula Mettbach for the maintenance of all potato lines. We also thank Jose Ugalde (University of Bonn) and Sakil Mahmud (now University of Missouri) for support with the set-up of the in vivo roGFP2 imaging and Andreas Meyer (University of Bonn) for help with roGFP2 measurements. We acknowledge funding to A.B., R.E.S., S.S., U.C.V. and A.v.D by the EU Horizon 2020 research and innovation project ADAPT (GA 2020 862-858) and to U.C.V by the DFG (INST 217/939-1 FUGG).

### **Author contributions**

A.v.D. contributed to conceptualization, investigation (responsible for most experimental work), formal analysis, validation, visualization, and writing - original draft as well as review & editing; R.E.S. and A.B. contributed to conceptualization, investigation and writing - original draft; S.S. contributed to resources (potato transformation and selection) and writing - review & editing; U.C.V. contributed to conceptualization, formal analysis, validation, funding acquisition, project administration, supervision, and writing - review & editing.

#### Funding

Open Access funding enabled and organized by Projekt DEAL.

### **Declarations**

#### Competing interests

The authors declare no competing interests.

#### **Ethics Declaration**

All methods were carried out in accordance with Cartagena protocol domestic law and related regulations

and followed the instructions given by the providers of the plant material. *Solanum tuberosum* plants (cultivar Désirée) were used in this study. Plants expressing the apoprotein aequorin were created and kindly provided by Dr. Sophia Sonnewald (Department of Biology, Chair of Biochemistry, Friedrich-Alexander-University Erlangen-Nuremberg, Germany) and plants expressing the Grx1-roGFP2 sensor were created and kindly provided by Solana Research GmbH. *Arabidopsis* mutant lines (Col-0) carrying the apoprotein aequorin were kindly provided by Prof. Dr. Marc Knight (Department of Biosciences, Durham University, United Kingdom). *Arabidopsis* mutants expressing the Grx1-roGFP2 sensor were kindly provided by Prof. Dr. Andreas Meyer (Department of Chemical Signalling, Bonn University, Germany).

### Additional information

Supplementary Information The online version contains supplementary material available at https://doi.org/1 0.1038/s41598-024-79134-3.

**Correspondence** and requests for materials should be addressed to A.D. or U.C.V.

Reprints and permissions information is available at www.nature.com/reprints.

**Publisher's note** Springer Nature remains neutral with regard to jurisdictional claims in published maps and institutional affiliations.

**Open Access** This article is licensed under a Creative Commons Attribution 4.0 International License, which permits use, sharing, adaptation, distribution and reproduction in any medium or format, as long as you give appropriate credit to the original author(s) and the source, provide a link to the Creative Commons licence, and indicate if changes were made. The images or other third party material in this article are included in the article's Creative Commons licence, unless indicated otherwise in a credit line to the material. If material is not included in the article's Creative Commons licence and your intended use is not permitted by statutory regulation or exceeds the permitted use, you will need to obtain permission directly from the copyright holder. To view a copy of this licence, visit <a href="https://creativecommons.org/licenses/by/4.0/">https://creativecommons.org/licenses/by/4.0/</a>.

© The Author(s) 2024

**Appendix 2** 

Chapter 2

With or without a Ca<sup>2+</sup> signal? A proteomics approach towards Ca<sup>2+</sup> dependent

and independent proteome changes in response to oxidative stress in A.

thaliana

Annelotte van Dieren<sup>1</sup>, Andras Bittner<sup>1</sup>, Bernhard Wurzinger<sup>2</sup>, Leila Afjehi-Sadat<sup>3</sup>, Wolfram

Weckwerth<sup>2,4</sup>, Markus Teige<sup>2</sup> and Ute C. Vothknecht<sup>1</sup>

<sup>1.</sup> Institute for Cellular and Molecular Botany, University of Bonn, Kirschallee 1, 53115

Bonn, Germany

<sup>2.</sup> Molecular Systems Biology (MOSYS), Department of Functional & Evolutionary Ecology,

University of Vienna, Djerassiplatz 1, 1030 Vienna, Austria

3. Mass Spectrometry Unit, Research Support Facilities, University of Vienna,

Djerassiplatz 1, 1030 Vienna, Austria

<sup>4.</sup> Vienna Metabolomics Center (VIME), University of Vienna, Djerassiplatz 1, 1030

Vienna, Austria

Preprint in BioRxiv (2025)

https://doi.org/10.1101/2025.03.31.645912

78

# With or without a Ca2+ signal?

A proteomics approach towards Ca<sup>2+</sup> dependent and independent proteome changes in response to oxidative stress in *A. thaliana* 

### **Authors:**

Annelotte van Dieren<sup>1</sup>, Andras Bittner<sup>1</sup>, Bernhard Wurzinger<sup>2</sup>, Leila Afjehi-Sadat<sup>3</sup>, Wolfram Weckwerth<sup>2,4</sup>, Markus Teige<sup>2</sup> and Ute C. Vothknecht<sup>1</sup>

### **Affiliations**

<sup>1</sup>Institute for Cellular and Molecular Botany, University of Bonn, Kirschallee 1, 53115 Bonn, Germany

<sup>2</sup> Molecular Systems Biology (MOSYS), Department of Functional & Evolutionary Ecology, University of Vienna, Djerassiplatz 1, 1030 Vienna, Austria

<sup>3</sup> Mass Spectrometry Unit, Research Support Facilities, University of Vienna, Djerassiplatz 1, 1030 Vienna, Austria

<sup>4</sup> Vienna Metabolomics Center (VIME), University of Vienna, Djerassiplatz 1, 1030 Vienna, Austria

Email corresponding author: adieren@uni-bonn.de, vothknecht@uni-bonn.de

Keywords: Calcium signaling, ROS, abiotic stress, proteomics, Arabidopsis thaliana

## Abstract

Calcium (Ca<sup>2+</sup>) and reactive oxygen species (ROS) are key secondary messengers in plant stress signaling, yet their interplay in regulating proteome-wide responses remains poorly understood. In this study, we employed label-free quantitative (LFQ) proteomics to investigate Ca<sup>2+</sup>-dependent and independent changes in the proteome of Arabidopsis thaliana leaves upon oxidative stress induced by hydrogen peroxide (H<sub>2</sub>O<sub>2</sub>). To dissect the role of Ca<sup>2+</sup> signaling, we inhibited H<sub>2</sub>O<sub>2</sub>-induced Ca<sup>2+</sup> transients by pretreatment with LaCl<sub>3</sub>, a plasma membrane Ca<sup>2+</sup> channel blocker. We then analysed the proteome of plants treated with H<sub>2</sub>O<sub>2</sub> or ddH<sub>2</sub>O after 10 and 30 min of treatment and detected 3724 and 3757 proteins, respectively. From these, 581 proteins showed significant changes in abundance after 10 min and 909 proteins after 30 min. Remarkably, the combined LaCl<sub>3</sub> and H<sub>2</sub>O<sub>2</sub> treatment resulted in the highest number of differentially abundant proteins (DAPs), indicating a strong attenuating effect of Ca<sup>2+</sup> signaling on the oxidative stress response. Specifically responsive to only H<sub>2</sub>O<sub>2</sub> were 37 and 57 proteins with distinct subsets of strictly Ca<sup>2+</sup>-dependent, partially Ca<sup>2+</sup>dependent, and Ca<sup>2+</sup>-independent proteins. Notably, Ca<sup>2+</sup>-independent H<sub>2</sub>O<sub>2</sub>-responsive proteins predominantly showed increased abundance, while strictly Ca2+-dependent proteins exhibited decreased abundance, suggesting a role for Ca2+ signaling in protein degradation. Furthermore, three proteins—WLIM1, CYP97C1, and AGAP1—underwent Ca<sup>2+</sup>-dependent shifts between the two time points, pointing to a dynamic nature of Ca<sup>2+</sup>-regulated proteomic changes. This study provides novel insights into short-term Ca<sup>2+</sup>-dependent and independent regulation of the Arabidopsis leaf proteome in response to oxidative stress, identifying key stress-responsive proteins and potential new targets for further research on plant stress resilience mechanisms.

## Introduction

Plants are continuously exposed to various environmental stresses, including drought, salinity, extreme temperatures, and pathogen attacks. These stressors can disrupt cellular homeostasis, leading to the overproduction of reactive oxygen species (ROS), which can cause oxidative damage to cellular components such as lipids, proteins, and nucleic acids (Mittler, 2017). However, plants have evolved sophisticated signaling networks to perceive and respond to oxidative stress, with Ca2+ signaling playing a central role in orchestrating these adaptive responses (Li et al., 2022). Calcium ions (Ca<sup>2+</sup>) serve as a ubiquitous second messenger in plant cells, regulating various physiological and developmental processes. A diverse array of biotic and abiotic stress factors, along with various developmental processes, can induce increases in cytosolic calcium concentration [Ca<sup>2+</sup>]<sub>cvt</sub> through a regulated influx of Ca<sup>2+</sup> from both extracellular sources and intracellular reservoirs into the cytosol (McAinsh & Pittman, 2009; Kudla et al., 2010). These transient elevations in [Ca<sup>2+</sup>]<sub>cvt</sub> exhibit distinct spatio-temporal characteristics, including variations in amplitude, frequency, and subcellular localization, in a manner that is specific to the type of stimulus encountered. The unique patterns of [Ca<sup>2+]</sup><sub>cvt</sub> fluctuations, commonly referred to as "calcium signatures," (Allen et al., 2001; Whalley & Knight, 2013) play a crucial role in ensuring the specificity of calcium-mediated signaling, thereby facilitating context-dependent and stimulus-appropriate cellular responses. Each calcium signature arises from the coordinated and dynamic interplay of multiple calcium influx channels and efflux transporters, which are located within the plasma membrane as well as the membranes of various intracellular organelles (Demidchik et al., 2018). These external stimuli are decoded by calcium-binding proteins, including calmodulins (CaMs), calcium-dependent protein kinases (CDPKs), and calcineurin B-like proteins (CBLs), which send the signal to downstream effectors (Mohanta et al., 2019; Tang et al., 2020). Furthermore, different plant organs and tissues exhibit distinct calcium signatures in response to stress, emphasizing the complexity and specificity of Ca2+-mediated signaling networks (Costa et al., 2018; Giridhar et al., 2022).

After the initial identification of stimulus-specific changes in  $[Ca^{2+}]_{cyt}$ , an increasing number of processes involving  $Ca^{2+}$  signaling have been elucidated, including those related to plant growth and development, such as cell division and organ formation (Zhang et al., 2014). Numerous studies have investigated a variety of calcium inducing stimuli across different plant species, including NaCl, mannitol,  $H_2O_2$ , and Flg22 in barley leaf and root samples (Giridhar et al., 2022), and NaCl, mannitol,  $H_2O_2$  and Pep13 in potato (Van Dieren et al., 2024). Additionally, downstream responses controlled by these specific  $Ca^{2+}$  signals have been described, including the role of  $Ca^{2+}$ -regulated kinases in mediating phosphorylation events that coordinate signaling cascades (Ludwig, 2003) as well as

responses that comprise regulation of gene expression through Ca2+-regulated transcriptional responses (Kaplan et al., 2006) and Ca<sup>2+</sup>-responsive promotor elements (Kudla et al., 2010). Oxidative stress results from an imbalance between ROS production and detoxification. While excessive ROS can be detrimental, controlled ROS production acts as a signaling molecule that activates stress-responsive pathways (Mittler, 2017; Chen & Yang, 2020). Rapid signaling and communication from individual cells that perceive potential threats to their neighbouring cells as well as more distal tissue is vital for plant acclimation and fitness. In this context, it was shown that calcium signaling and ROS interact in a complex feedback loop. ROS can induce Ca2+ influx through plasma membrane and organellar channels, leading to further signal propagation (Li et al., 2022; Ravi et al., 2023). In turn, Ca<sup>2+</sup> signaling modulates ROS-scavenging mechanisms, such as the activation of antioxidant enzymes including superoxide dismutase (SOD), catalase (CAT), and ascorbate peroxidase (APX) (Gilroy et al., 2016). Other studies highlight the role of NADPH oxidases, also known as respiratory burst oxidase homologs (RBOHs), in ROS production upon Ca<sup>2+</sup> signaling activation (Kärkönen & Kuchitsu, 2015). These enzymes facilitate ROS bursts that act as secondary messengers, amplifying stress responses. Moreover, Ca2+ channels such as cyclic nucleotide-gated channels (CNGCs) and glutamate receptor-like channels (GLRs) contribute to ROS-Ca<sup>2+</sup> crosstalk, further fine-tuning the stress response (Gilroy et al., 2016). The interplay between calcium signaling and oxidative stress represents a crucial aspect of plant stress responses. Understanding these mechanisms provides insights into how plants adapt to adverse environmental conditions and could be exploited for the development of stress-resilient crops.

One of the first layers of cellular signaling is the translation of secondary signal components into readjustments of the transcriptional machinery. Consequently, many large-scale approaches to study stress responses analyse changes in gene expression. However, proteins are key players in the structure, function, and regulation of cells, tissues, and organs, and proteome changes can occur independent from transcription by processes such as protein degradation and regulation of translation (Gry et al., 2009; Payne, 2015; Liu et al., 2016). The interplay of ROS and Ca<sup>2+</sup> signaling on transcriptome changes have recently been investigated in barley (Bhattacharyya et al., 2025), however, no investigation has so far described the effect of Ca<sup>2+</sup> signaling on ROS induced changes of proteomes. We thus aimed to elucidate the role of H<sub>2</sub>O<sub>2</sub>-induced Ca<sup>2+</sup> signals on short-term proteome changes observed in Arabidopsis leaf tissue by inhibiting stress induced Ca2+ transients using the established plasma membrane Ca<sup>2+</sup> channel blocker LaCl<sub>3</sub> (Tracy et al., 2008). MS-based proteome analysis identified specific subsets of proteins, whose abundance changed upon 10 and 30 min  $H_2O_2$  application in a Ca<sup>2+</sup>-dependent or -independent manner. However, one of the major challenges in omics is translating high-dimensional data into meaningful biological insights with practical applications. The integration of proteomic data with other omics datasets (e.g., genomics, transcriptomics, and metabolomics) holds great potential for advancing systems biology approaches and improving our  $_{_{\it A}}$  understanding of complex biological processes. This knowledge could be further investigated and applied to future research aiming to enhance stress resistance and optimizing performance and productivity in crop species under increasingly challenging environmental conditions.

**Results** 

 $H_2O_2$  and  $Ca^{2+}$  are secondary messengers that are involved in the mediation of environmental changes into an appropriate cellular response. Temporal increases in these messengers affect various cellular processes including gene transcription or protein activity. Here we employed label free quantitative (LFQ) proteomics to analyse the  $H_2O_2$  induced changes in the leaf proteome of Arabidopsis and the contribution of  $Ca^{2+}$  signals in the  $H_2O_2$  induced changes.

Establishing parameters and experimental design

 $H_2O_2$  induced  $Ca^{2+}$  transients and their inhibition by the  $Ca^{2+}$  channel blocker  $La^{3+}$  have been shown before for Arabidopsis (Giridhar et al., 2022; Rentel & Knight, 2004; Van Dieren et al., 2024). To confirm that these responses also occur under the experimental conditions chosen for the protein isolation, leaf discs from 3-week-old At-AEQ<sub>cyt</sub> plants grown under the same circumstances as wild type plants used for proteomics analysis were analysed. As shown before for soil-grown Arabidopsis plants (Van Dieren et al., 2024), an oxidative stress stimulus of 20 mM  $H_2O_2$  resulted in a well-shaped  $Ca^{2+}$  transient in Arabidopsis leaf tissue, which was inhibited by over 50 % upon pre-treatment with 1 mM LaCl<sub>3</sub> (Fig. 1A).

The workflow of the application of the different treatments before proteomics analyses is schematically displayed in Fig. 1B. Complete rosettes from 3-week-old wild type plants grown on soil were pre-incubated with LaCl<sub>3</sub> (Inhibitor) or ddH<sub>2</sub>O for 60 min. Subsequently, the rosettes were washed carefully and treated with either 20 mM  $H_2O_2$  (Stress) or ddH<sub>2</sub>O for 10 and 30 min. The timing was chosen to elucidate short-term responses to the stress stimulus. The different treatment paths result in the following treatment names used further: Control: pre-incubation in ddH<sub>2</sub>O, treatment with ddH<sub>2</sub>O; Stress: pre-incubation with ddH<sub>2</sub>O, treatment with  $H_2O_2$ ; Inhibitor: pre-incubation with  $H_2O_2$ .

5

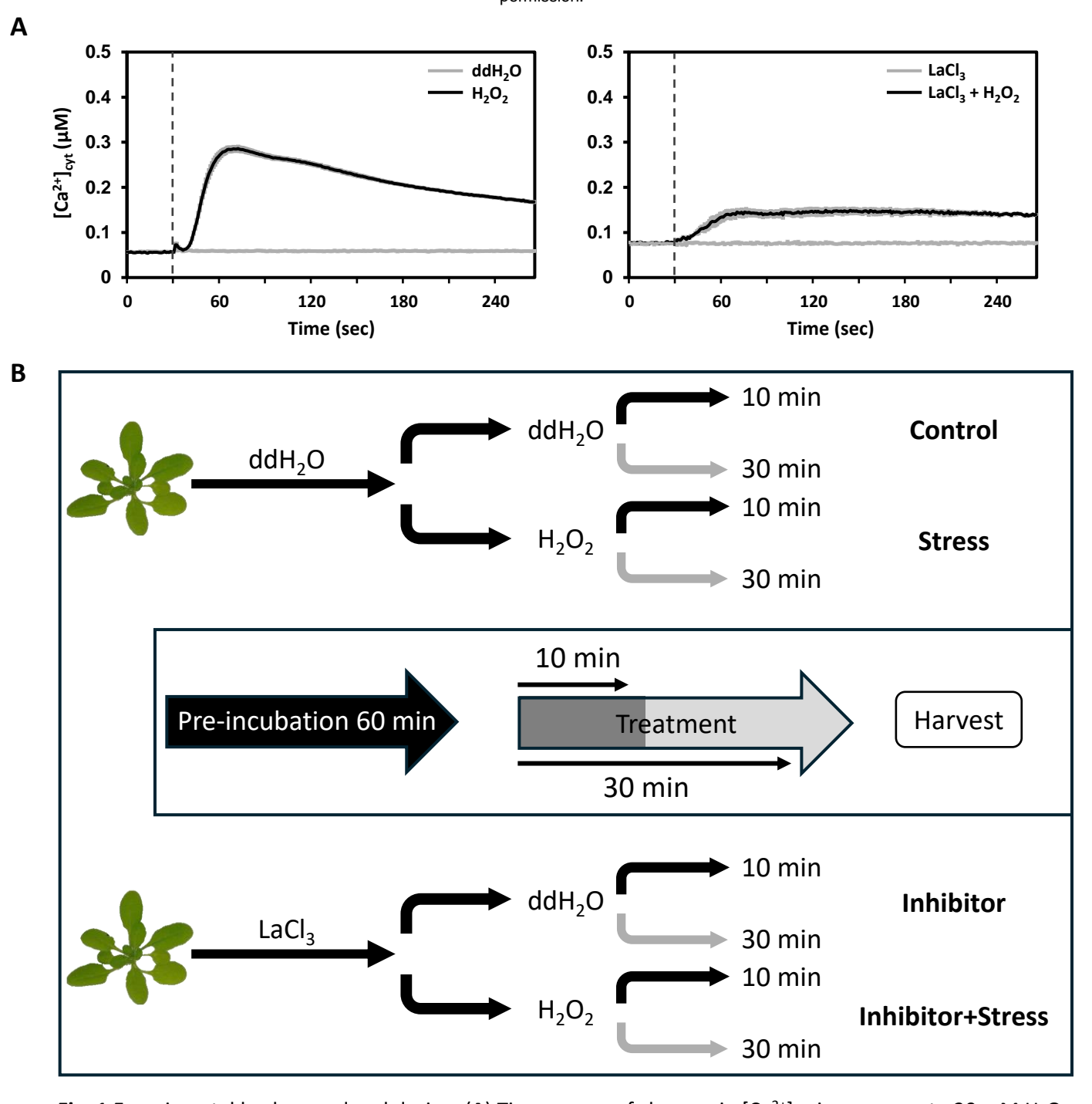


**Fig. 1** Experimental background and design. (**A**) Time course of changes in  $[Ca^{2+}]_{cyt}$  in response to 20 mM  $H_2O_2$  in leaf tissue of Arabidopsis (left) and in response to 20 mM  $H_2O_2$  after 60 min pre-incubation with  $LaCl_3$  (right). Values are shown as mean  $\pm$  SE (n = 6). Dashed vertical lines indicate the time point of stimuli injection (30 sec). (**B**) Overview of treatment application: plants were either pre-incubated in  $ddH_2O$  or 1 mM  $LaCl_3$  (Inhibitor) for 60 min. Half of the plants from both pre-incubations were transferred into a 20 mM  $H_2O_2$  solution (Stress), another half was transferred into fresh  $ddH_2O$ . Half of these plants were harvested after 10 minutes, the other half after 30 minutes and labelled as indicated: Control ( $ddH_2O + ddH_2O$ ), Stress ( $ddH_2O + 20$  mM  $H_2O_2$ ), Inhibitor (1 mM  $LaCl_3 + ddH_2O$ ), Inhibitor + Stress (1 mM  $LaCl_3 + 20$  mM  $H_2O_2$ ) with their corresponding treatment duration (10 or 30 min).

## Initial data analysis

For each of the four different treatments (Control, Stress, Inhibitor and Inhibitor+Stress), five independent biological replicates, each consisting of pooled proteins from 12 rosettes, were analysed.

The proteome analysis of the samples resulted in the identification of 3724 proteins after 10 min and 3757 proteins after 30 min of stress treatment (Fig. 2A). The number of identified proteins is in line with former proteomics analyses in Arabidopsis (Seaton et al., 2018; Ayash et al., 2021; Scholz et al., 2025). For the further analysis we separated the LFQ intensities in two groups: one group representing the samples harvested after 10 min of stress treatment, the other group representing the samples harvested after 30 min of stress treatment. After a quality control step, in which proteins 'only identified by site, reverse sequences, and potential contaminants' were filtered out, 2906 proteins remained for the 10 min samples and 2965 proteins for the 30 min samples (Fig 2A, quality control). After multiple sample ANOVA test (p-value <0.05), 581 proteins remained for the 10 min samples and 909 for 30 min (Fig. 2A, statistical analysis). To ensure biological validity, stringent filtering is applied, leading to significant dataset reduction.

A principal component analysis (PCA) of the LFQ values showed that all replicates clearly fell into their corresponding treatment group (Fig. 2B). PC1 explains more than 34% of the variance within the data for both time points and essentially separating the Inhibitor+Stress treatment from all other treatments, while PC2 (>17 % of the variance for both time points) separates the Control, Stress and Inhibitor treatments. Overall, this analysis indicates clear proteomic changes, especially with regards to the Inhibitor+Stress samples compared to all other treatments. The other treatments cluster closer together but still remain separated from each other.

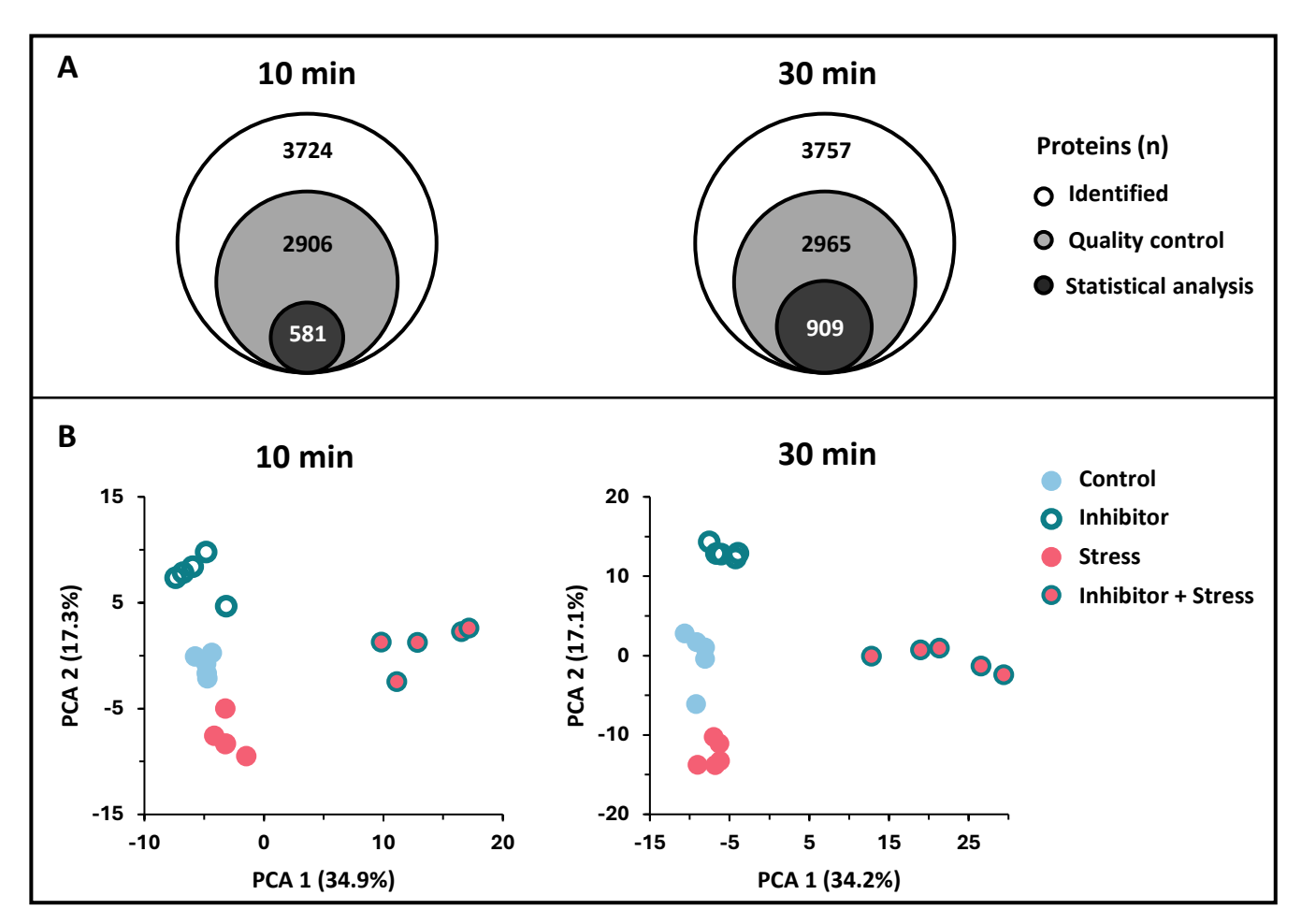
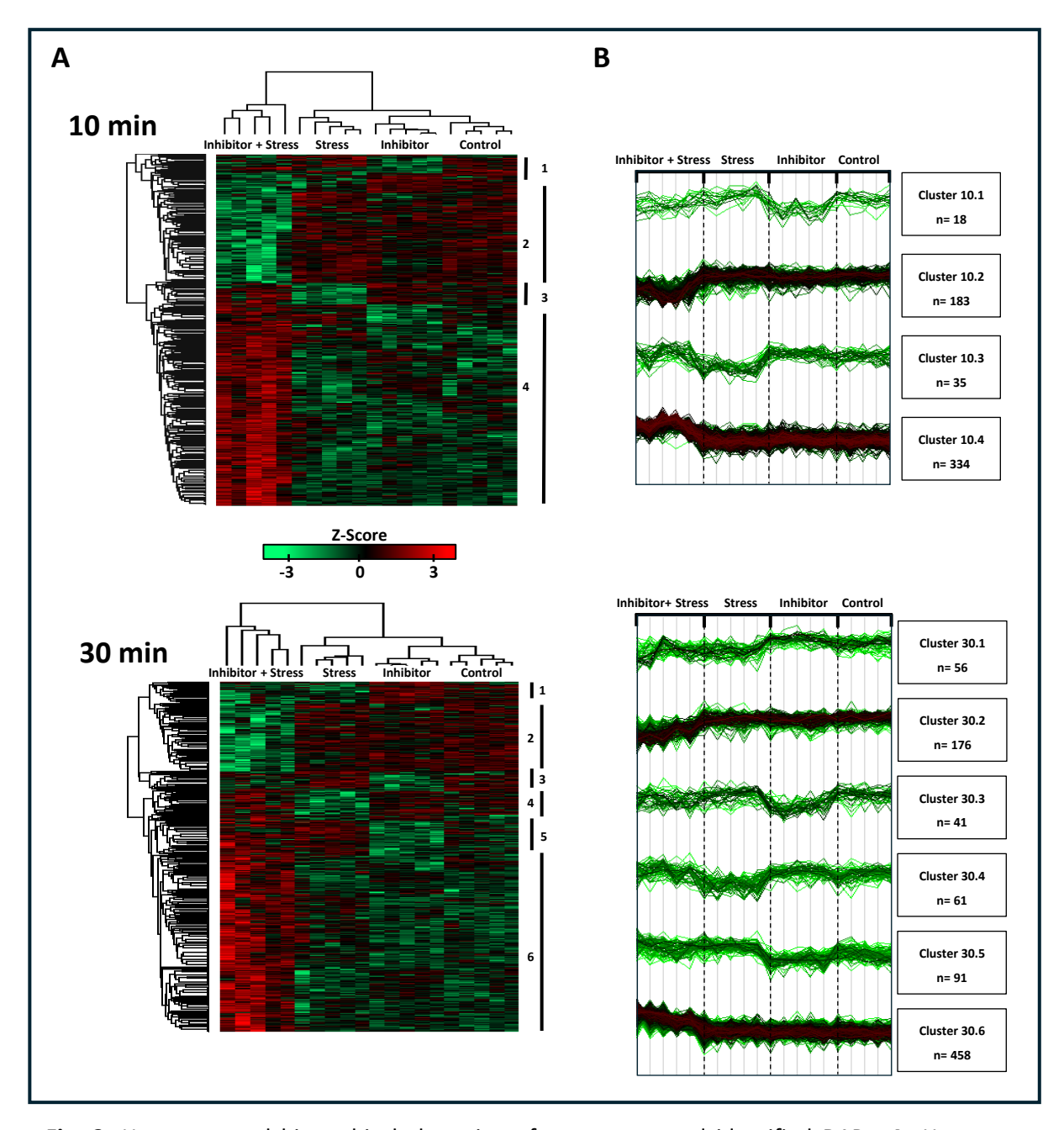


Fig. 2: Overview of the initial data analysis for the 10 min (left) and 30 min (right) samples with (A) showing the numbers of all proteins identified (identified), proteins left after removal of contaminants, proteins only identified by site, and reverse annotated peptides (quality control), and proteins left after statistical analysis (ANOVA,  $p \le 0.05$ ). (B) Principal component analysis (PCA) of the LFQ intensities of the quantified proteins, colours indicate the different treatments: blue fill = Control, magenta cycle = Stress, turquoise fill = Inhibitor and magenta cycle + turquoise fill = Inhibitor+Stress.

## **Clustering analysis**

In line with the PCA analysis, the hierarchical clustering of protein abundance, performed on the Z-scored normalized intensities, showed a clear clustering of all replicates of an individual treatment (Fig. 3A, dendrograms on top of the heatmaps) and therewith the strong similarity in protein abundance among the replicates within one treatment group. All five replicates of the Inhibitor+Stress treatment clustered together as one of two main clusters. In the other main cluster, two subclusters could be observed, with the first one representing the 5 replicates of the Stress treatment, and the second one showing a close relation of the Control and Inhibitor only treatment. This pattern of clustering was observed for both the 10 and the 30 min of stress treatment. It substantiates the strong effect of the Inhibitor+Stress treatment on the proteome, and the slightly milder but clear effect of the Stress treatment alone, while the Inhibitor treatment alone has a lesser effect. It also indicates an attenuating effect of  $Ca^{2+}$  signaling on the  $H_2O_2$ -induced stress response.

Hierarchical clustering further revealed segregation of the proteins into 4 different abundance clusters after 10 min of treatment, and 6 clusters after 30 min of treatments (Fig. 3A, dendrograms on the side of the heatmaps). The differences in protein abundance of the different samples are shown in the heatmap with green colour indicating a decrease and red colour an increase in relative protein abundance (Fig. 3A) as well as profile plots (Fig. 3B). The 10 min clusters were characterized by a lower protein abundance for the Inhibitor and Inhibitor+Stress treatment (cluster 10.1), a lower abundance for the Inhibitor+Stress treatment (cluster 10.2), a lower abundance for the Stress treatment (cluster 10.3) and a lower abundance for all but the Inhibitor+Stress treatment (cluster 10.4). The clusters identified after 30 min of treatment were defined by a lower abundance for the Inhibitor+Stress and the Stress treatment (30.1), a lower abundance for the Inhibitor+Stress treatment (30.2), a lower abundance for the Inhibitor treatment (30.3), a lower abundance for the Stress treatment (30.4), a lower abundance for the Control and Inhibitor treatment (30.5), and a lower abundance for all but the Inhibitor+Stress treatment (30.6). At both time points the clusters containing proteins with different abundance in the Inhibitor+Stress treatment only were the largest clusters, containing 183 and 334 proteins for the 10 min (10.2 and 10.4), and 176 and 458 proteins for the 30 min (30.2 and 30.6).



**Fig. 3:** Heatmaps and hierarchical clustering of treatments and identified DAPs. **A:** Heatmaps showing the z-score overall pattern of relative increased (red) and decreased (green) protein abundance within the samples after 10 (upper panel) and 30 (lower panel) min of treatment. The dendrogram of the columns (top) shows how the four different treatments separate based on Euclidean distance. The dendrogram of the rows (left side) shows the clustering of the protein. Identified protein clusters are indicated with a number on the right side of both heatmaps. **B:** Intensity plots for each cluster from panel A and number of proteins (n) in the specific cluster is indicated.

### Gene Ontology analysis of heatmap clusters

Proteins in each cluster were functionally classified by Gene Ontology (GO) and KEGG term enrichment analysis. Details on the different GO-terms (molecular function and biological process) of all clusters are shown in Table 1 (10 min) and Table 2 (30 min). Enriched terms in three out of four clusters with a relative lower abundance of proteins in the Inhibitor+Stress treatment (10.1, 10.2 and 30.2) included Ribosomal pathways. Cluster 10.2, with lower abundance only for Inhibitor+Stress, also included the KEGG term proteasome. Clusters 10.4, 30.5 and 30.6, all of which comprise a relative higher abundance of proteins in the Inhibitor-Stress treatment, have carbon fixation and other pathways related to carbon metabolisms as the most enriched KEGG terms.

			Enrichment	Protein	Pathway	Fold	
Cluster	Proteins (n)	Analysis	FDR	(n)	protein (n)	Enrichment	Pathways
1	18	KEGG	7.40E-09	7	315	34.1	Ribosome
		GO Molecular function	3.60E-07	7	423	25.4	Structural constituent of ribosome
			1.00E-06	7	545	19.7	Structural molecule activity
			5.00E-05	7	1030	10.4	MRNA binding
		GO Biological Process	5.40E-03	6	934	9.9	Amide biosynthetic proc.
			6.30E-03	6	1086	8.5	Cellular amide metabolic proc.
			8.00E-03	7	1808	5.9	Organonitrogen compound
							biosynthetic proc.
2	183	KEGG	8.90E-38	40	315	19.2	Ribosome
			4.90E-04	5	61	12.4	Proteasome
			3.40E-03	4	53	11.4	Phenylalanine, tyrosine and tryptophan
							biosynthesis
		GO Molecular function	1.20E-05	3	3	151	MAP-kinase scaffold activity
			1.20E-05	3	3	151	Protein kinase C binding
			1.20E-05	3	3	151	Signaling adaptor activity
		<b>GO Biological Process</b>	7.20E-35	54	860	9.5	Translation
			7.20E-35	54	865	9.4	Peptide biosynthetic proc.
			1.90E-34	55	934	8.9	Amide biosynthetic proc.
3	35	KEGG	1.0E-03	2	13	121.4	Sulfur relay system
			2.9E-03	2	25	63.1	Biosynthesis of unsaturated fatty acids
			5.7E-03	2	43	36.7	Alpha-Linolenic acid metabolism
		GO Molecular function	8.7E-04	2	5	315.7	Acetyl-CoA C-acyltransferase activity
			8.7E-04	2	5	315.7	Thiosulfate sulfurtransferase activity
			3.6E-03	2	15	105.2	Sulfurtransferase activity
		GO Biological Process	1.0E-05	4	36	87.7	Cysteine metabolic proc.
			4.5E-06	5	75	52.6	Sulfur amino acid metabolic proc.
			5.6E-05	7	437	12.6	Sulfur compound metabolic proc.
4	334	KEGG	8.00E-26	23	69	27.6	Carbon fixation in photosynthetic organisms
			1.50E-14	16	77	17.2	Glyoxylate and dicarboxylate metabolism
			4.30E-11	12	58	17.1	Pentose phosphate pathway
		GO Molecular function	4.10E-08	6	10	49.6	L-malate dehydrogenase activity
			1.40E-07	7	20	29	Intramolecular oxidoreductase activity,
							interconverting aldoses and ketoses
			1.10E-09	18	180	8.3	Oxidoreductase activity, acting on CH-OH
							group of donors
		<b>GO Biological Process</b>	7.60E-31	44	317	11.5	Response to cadmium ion
			4.70E-18	32	315	8.4	Nucleotide metabolic proc.
			4.30E-36	78	1055	6.1	Carboxylic acid metabolic proc.

**Table 1:** Functional classification of the protein clusters after 10 min of treatment, obtained after hierarchical clustering. For each cluster the top 3 GO-terms (KEGG, molecular function, biological process), selected by FDR and sorted by fold enrichment, are displayed.

permission.  Enrichment Protein Pathway Fold							
Cluster	Proteins (n)	Analysis	FDR	(n)	protein (n)	Enrichment	Pathways
1	56	KEGG	1.90E-03	3	61	24.3	Citrate cycle (TCA cycle)
			1.10E-03	4	119	16.6	Glycolysis / Gluconeogenesis
			1.10E-03	4	120	16.4	Cysteine and methionine metabolism
		GO Molecular function	1.90E-04	8	423	9.3	Structural constituent of ribosome
			1.90E-04	9	545	8.1	Structural molecule activity
			4.70E-04	9	674	6.6	Zinc ion binding
		GO Biological Process	7.90E-04	4	67	29.5	Aspartate family amino acid metabolic proc.
			2.50E-03	6	317	9.3	Response to cadmium ion
			2.50E-03	7	468	7.4	Cellular amino acid metabolic proc.
2	176	KEGG	1.30E-35	38	315	18.9	Ribosome
			1.40E-03	4	41	15.3	Propanoate metabolism
		0014	9.80E-07	9	120	11.8	Cysteine and methionine metabolism
		GO Molecular function	1.90E-19	20	144	21.8	RRNA binding
			3.80E-41	46	423	17.1	Structural constituent of ribosome
		GO Biological Process	3.80E-41	50	545	14.4	Structural molecule activity
		GO biological Process	6.00E-36	54	860	9.9	Translation
			6.10E-36 2.30E-37	54 57	865 934	9.8 9.6	Peptide biosynthetic proc. Amide biosynthetic proc.
3	41	KEGG	4.30E-02	1	3	224.6	Caffeine metabolism
,	71	KEGG	4.30E-02	2	77	17.5	Phagosome
			3.60E-02	3	157	12.9	Endocytosis
		GO Molecular function	1.30E-03	5	211	16	GTPase activity
			3.70E-03	5	303	11.1	GTP binding
			3.70E-03	5	323	10.4	Guanyl nucleotide binding
		GO Biological Process	3.90E-02	2	16	84.2	Mitochondrial fission
			3.90E-02	2	18	74.9	Purine-containing compound catabolic proc.
			3.90E-02	3	97	20.8	Endocytosis
4	61	KEGG	3.30E-03	3	57	23.8	Aminoacyl-tRNA biosynthesis
			9.30E-05	5	98	23.1	Biosynthesis of nucleotide sugars
			1.90E-04	5	131	17.3	Amino sugar and nucleotide sugar metabolism
		GO Molecular function	2.90E-02	3	72	18.9	Aminoacyl-tRNA ligase activity
			2.90E-02	3	72	18.9	Ligase activity, forming carbon-oxygen
							bonds
			2.90E-02	3	76	17.9	Actin filament binding
		GO Biological Process	2.10E-03	3	19	71.5	Pentose metabolic proc.
			7.60E-03	5	188	12	Monosaccharide metabolic proc.
			2.80E-04	9	468	8.7	Cellular amino acid metabolic proc.
5	91	KEGG	5.90E-03	6	269	6.8	Carbon metabolism
			2.40E-03	14	1243	3.4	Biosynthesis of secondary metabolites
		GO Molecular function	8.70E-03	3	29	31.4	Poly(U) RNA binding
			8.70E-03	3	33	27.6	Poly-pyrimidine tract binding
		CO Biological Brasses	8.70E-03	4	82	14.8	NAD binding
		GO Biological Process	1.00E-03	6	144	12.7	Photosynthesis, light reaction
			6.30E-03	7	317	6.7	Response to cadmium ion
			3.90E-04	11	517	6.5	Generation of precursor metabolites and
6	458	KEGG	2.70E-21	22	69	19.3	Carbon fixation in photosynthetic organisms
	333		1.90E-17	20	77	15.7	Glyoxylate and dicarboxylate metabolism
			5.70E-13	15	61	14.9	Citrate cycle (TCA cycle)
		GO Molecular function	7.70E-09	8	17	28.4	Malate dehydrogenase activity
			4.90E-10	14	69	12.3	Protein domain specific binding
			5.70E-08	13	82	9.6	NAD binding
		GO Biological Process	4.40E-38	56	317	10.7	Response to cadmium ion
			9.90E-34	59	433	8.2	Response to metal ion
			1.00E-47	104	1055	6	Carboxylic acid metabolic proc.

**Table 2:** Functional classification of the protein clusters after 30 min of treatment, obtained after hierarchical clustering. For each cluster the top 3 GO-terms (KEGG, molecular function, biological process), selected by FDR and sorted by fold enrichment, are displayed.

## Identification of proteins with significant change in abundance (DAPs)

Quantitative differences occurring among proteome profiles due to the different treatments were detected by comparing the individual protein intensities in each treatment group (Stress, Inhibitor+Stress and Inhibitor) with the control samples. Protein abundance differences were obtained by performing a t-test (p<0.05) on the proteins shown to be significant different in any of the treatments, i.e., 581 proteins after 10 min of treatment and 909 proteins after 30 min of treatment (indicated in Fig.2A) and visualized in volcano plots (Fig. 4A and B). This analysis resulted in 49 DAPs (18 more abundant and 31 less abundant) between Stress treatment and control after 10 min and 65 DAPs (22 more abundant, 43 less abundant) after 30 min. For the Inhibitor only treatment a total of 48 DAPs (7 higher abundant, 41 less abundant) were found after 10 min and 84 DAPs (26 more abundant, 58 less abundant) in the 30 min set. The highest number of differences occurred for the Inhibitor+Stress treatment versus control, with 459 DAPs (287 more abundant, 172 less abundant) after 10 min and 667 DAPs (468 more abundant, 199 less abundant) after 30 min. The DAPs identified for each treatment were further subjected to comparable analysis to categorise them based on whether they require Ca<sup>2+</sup> for their regulation.

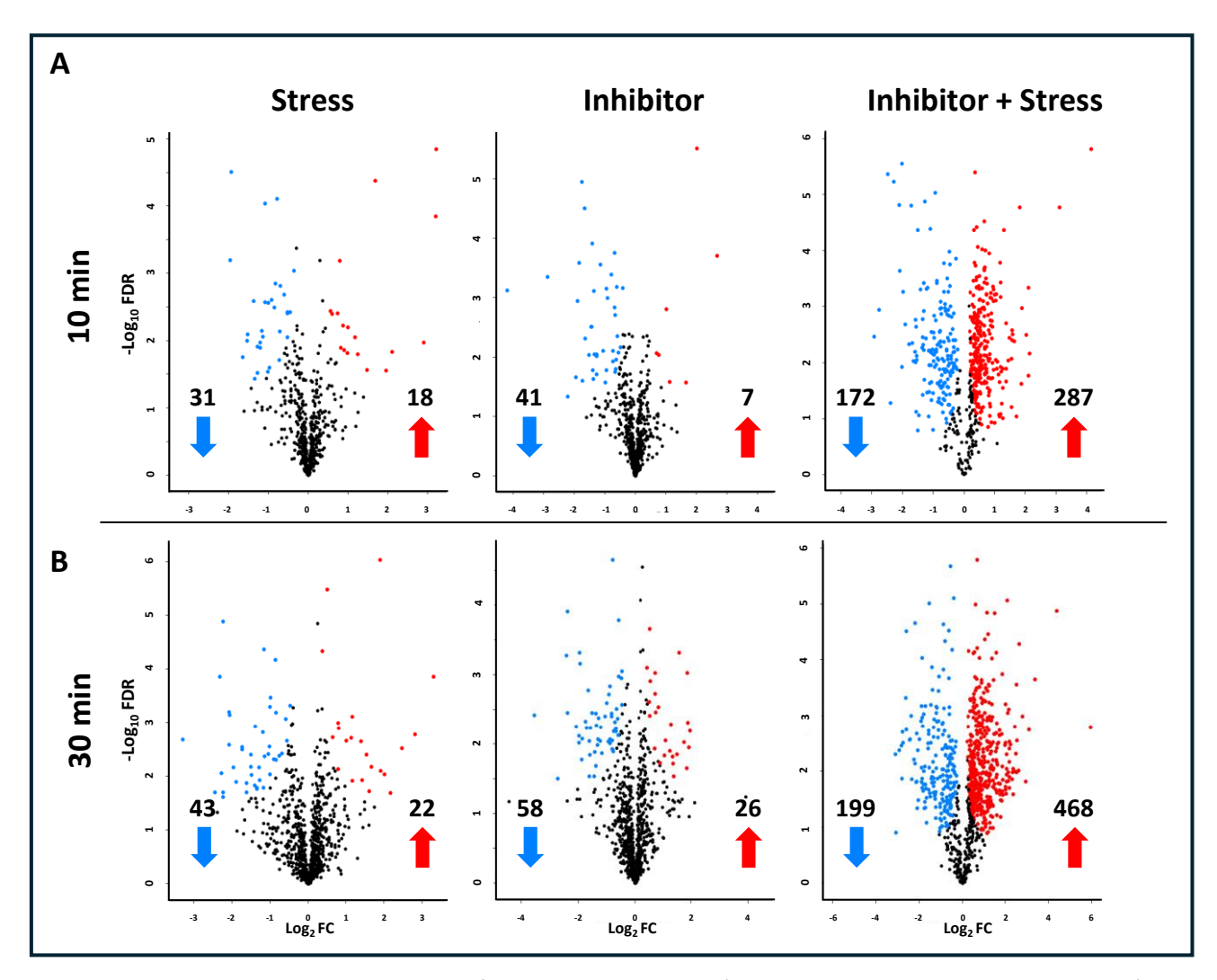


**Fig. 4:** Volcano plots indicating DAPs for three treatments (Stress, Inhibitor and Inhibitor+Stress) in comparison to control (double mock) samples (FDR 0.05) after 10 'min (A) and 30 min (B) of treatment. Proteins were graphed by fold change (x-axis) and the confidence statistic (-log P) on the y-axis. Blue dots represent proteins that show a significant lower abundancy while red dots represent proteins that show a significant higher abundancy for the indicated treatment compared to control samples. Black dots represent the proteins that do not show a significant change in abundance (S0=0.1, FDR= 0.05).

## Comparison of DAPs and identification of Ca2+ dependent and independent proteins

After identification of the DAPs for each treatment vs control at both timepoints (Fig. 4), the DAPs of each treatment were compared to all other treatments of the same timepoint to find overlapping and unique proteins (Fig. 5A). In general, the overlapping numbers were relatively low, indicating that each treatment has an individual effect on the proteome. For both time points the largest overlap was observed between Stress and Inhibitor+Stress as well as Inhibitor and Inhibitor+Stress with a much smaller overlap between Stress and Inhibitor. As the total number of proteins differs between the two time points, we decided to also compare the relative numbers (% from total proteins) of DAPs (suppl. Fig. 1). This comparison shows a very similar pattern between the two time points.

For the further analysis, we wanted to focus on H<sub>2</sub>O<sub>2</sub> responsive proteins, i.e. those proteins that show a difference in abundance between  $H_2O_2$  treatment and control (DAP-Stress, 10 and 30 min). From these sets we omitted the DAPs that showed a different abundance upon treatment with LaCl<sub>3</sub> alone, to avoid effects of the inhibitor that are not related to the reduction of the  $H_2O_2$  induced  $Ca^{2+}$  transient. This resulted in a set of 37 H<sub>2</sub>O<sub>2</sub> responsive proteins after 10 min of treatment and 57 proteins after 30 min of treatment (Fig. 5A, underlined numbers). These stress responsive proteins were further categorised as being Ca<sup>2+</sup>-independent or Ca<sup>2+</sup>-dependent, depending on their abundance in the Inhibitor+Stress treatment. For this categorisation we used the method described by Bhattacharyya et al. (2025). The steps used in this approach are schematically displayed in Fig. 5B. H<sub>2</sub>O<sub>2</sub> responsive proteins that showed an unchanged abundance (UCs) compared to control under Inhibitor+Stress treatment can be considered strictly  $Ca^{2+}$  dependent in their  $H_2O_2$  response (Fig. 5C and D). Proteins that showed a differential abundance upon both Stress vs. control and Stress+Inhibitor vs. control, but their abundance level differed significantly (∆FC ≥1.25, corresponding to a change in protein abundance of at least 25%) between the two treatments, were categorised as being partially Ca<sup>2+</sup> dependent (Fig. 5C and D). This group was further split in two categories, with the lower threshold set to a change in abundance of at least 25% up to 50%, and the higher threshold including all proteins showing a change in abundance of at least 50% (ΔFC ≥1.5). Proteins that showed no differential abundance between Stress and Stress+Inhibitor treatment (ΔFC ≤1.25) were considered Ca<sup>2+</sup>independent in their  $H_2O_2$  response.

This analysis identified a total of 7 Ca<sup>2+</sup>-independent and 30 Ca<sup>2+</sup>-dependent  $H_2O_2$  responsive proteins after 10 min of treatment (Fig. 5C). Among the Ca<sup>2+</sup>-dependent proteins, 17 were classified as strictly Ca<sup>2+</sup>-dependent and 13 partial Ca<sup>2+</sup>-dependent. Of these 13 partial Ca<sup>2+</sup>-dependent proteins, 4 met the threshold of at least a 50% change in abundance ( $\geq$ 2-fold increase or decrease). For the 30 min treatment, 8 Ca<sup>2+</sup>-independent and 49 Ca<sup>2+</sup>-dependent  $H_2O_2$  responsive proteins were identified (Fig.

5D). Within the Ca<sup>2+</sup>-dependent group, 27 proteins were strictly Ca<sup>2+</sup>-dependent, a similar percentage as observed at 10 min, while 22 proteins displayed partial Ca<sup>2+</sup>-dependence. Among the partially Ca<sup>2+</sup>-dependent proteins, 14 met the threshold of at least a 50% change in abundance ( $\geq$ 2-fold increase or decrease). A detailed list of the H<sub>2</sub>O<sub>2</sub> responsive proteins, along with their classification as Ca<sup>2+</sup>-independent, partially Ca<sup>2+</sup>-dependent or strictly Ca<sup>2+</sup>-dependent, is provided in Table 3 for the 10 min and Table 4 for the 30 min data set.

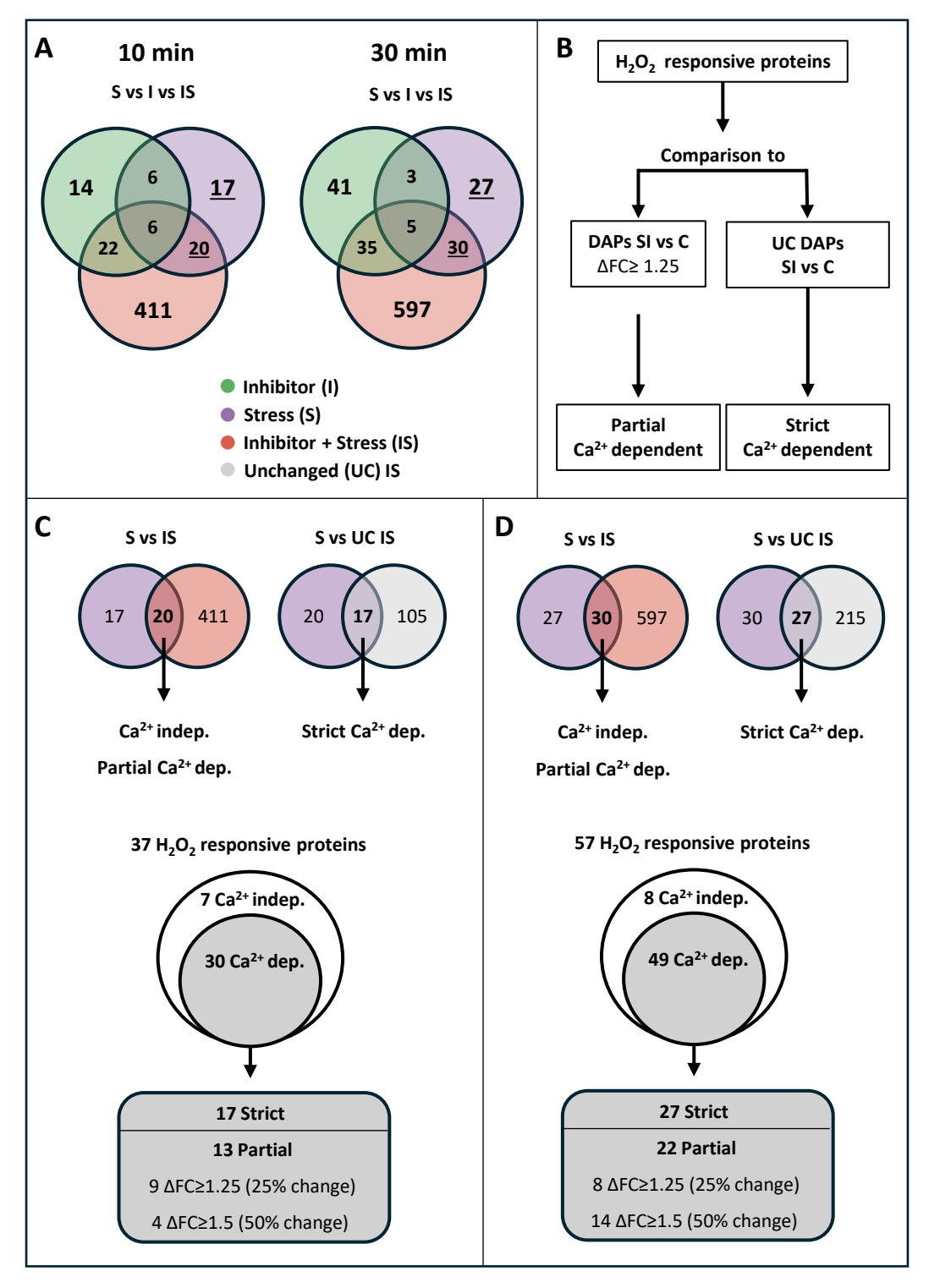


**Fig.5** Identification and categorisation of  $H_2O_2$  responsive proteins. **A:** Venn diagrams showing all identified DAPs and their overlap between the different treatments. Underlined numbers are the  $H_2O_2$  responsive proteins. **B:** Schematic representation of the analysis steps to identify the different levels of  $Ca^{2+}$  dependency for  $H_2O_2$  responsive proteins. **C:** Categorisation of the  $H_2O_2$  responsive proteins after 10 min of stress treatment. **D:** Categorisation of the  $H_2O_2$  responsive proteins after 30 min of stress treatment

		Protein ID	Abundancy (compared to control)	Full name	ΔFC (SvsC-SlvsC)	Symbol
	$\neg$	AT1G16460	Less	Sulfurtransferase 2	(State Sitate)	STR2
Strict Ca <sup>2+</sup> dependent		AT1G48350	More Large ribosomal subunit protein uL18c			RPL18
		AT1G62180	Less 5' adenylylsulfate reductase 2, chlorplastic			APR2
		AT1G72610	More	Germin like protein		GLP1
		AT2G30520	More	Root phototropism protein 2	·	
		AT2G44060	Less	Late embryogenesis abundant protein		RPT2 LEA26
		AT3G07660	Less	Flocculation protein		DUF1296
		AT3G14990	Less	Protein DJ-1 homolog A		DJ1A
		AT3G17880	Less	TPR repeat- containing thioredoxin		TDX
, a		AT3G17900	Less	Heat-inducible transcription repressor		MEB5 12
١ĕ		AT3G45850	Less	Kinesin motor domain- containg protein		KIN5D
Stric		AT3G53260	Less	Phenylalanine ammonia-lyase 2		PAL2
		AT4G28730	Less	Glutaredoxin-C5 chloroplastic		GRXC5
		AT5G06460	Less	Ubiquitin-activating enzym		UBA2
		AT5G21274	Less	Calmodulin		CAM
		AT5G43830	Less	Domain containing protein		DUF3700
		AT5G59890	Less	Actin-depolymerizing factor 4		ADF4
	ΔFC ≥ 1.5	AT1G13750	More	Probable inactive purple acid phosphatase 1	5.37	PAP1
		AT1G20160	More	CO(2)-response secreted protease	2.51	CRSP
l		AT3G49080	Less	Small ribosomal subunit protein uS9m	1.71	RPS9M
Partial Ca <sup>2+</sup> dependent		AT4G38510	More	V-type proton ATPase subunit B2	2.34	VHA-B2
l g	AFC 1.25 - 1.5	AT1G10200	Less	LIM domain-containing protein	1.26	WLIM1
l g		AT1G14030	More	Fructose-bisphosphate aldolase	1.39	LSMT-L
ح   ±		AT1G26460	More	Tetratricopeptide repeat-containing protein	1.32	TPR
e <sup>7</sup>		AT1G70890	Less	MLP-like protein 43	1.45	MLP43
ia.		AT2G20890	More	Thylakoid formation 1	1.29	THF1
art		AT3G53130	More	Carotene epsilon-monooxygenase, chloroplastic	1.29	CYP97C1
-		AT4G11260	Less	SGT1 homolog B	1.40	SGT1B
		AT4G14440	More	Enoyl-CoA delta isomerase 3	1.28	ECI3
		AT4G29510	Less	Protein arginine N-methyltransferase 1.1	1.34	PRMT11
Ca <sup>2+</sup> independent	ΔFC <1.25	AT1G11790	Less	Arogenate dehydratase	1.16	ADT1
		AT2G20900	More	Diacylglycerol kinase 5	1.11	DGK5
		AT2G42690	More	Phospholipase A1-IIdelta	1.07	AGAP1
		AT3G45140	More	Lipoxygenase 2, chloroplastic	1.10	LOX2
	M	AT4G13010	More	Chloroplast envelope quinone oxidoreductase homolog	1.13	CEQORH
	7	AT4G28660	More	Photosystem II reaction center Psb28 protein	1.00	PSB28
		AT5G63870	Less	Serine/threonine-protein phosphatase 7	1.09	PP7

**Table 3:** List of  $H_2O_2$  responsive proteins indicated as strict  $Ca^{2+}$  dependent (dark grey), partial  $Ca^{2+}$  dependent (light grey) and  $Ca^{2+}$  independent (white) after 10 min of treatment. Partial  $Ca^{2+}$  dependent proteins were further divided by a threshold of at least a 50% change in abundance ( $\geq$ 2-fold increase or decrease).

		bioRxiv prepr	int doi: https://doi.org/10	1101/2025.03.31.645912; this version posted April 1, 2025.	The copyright hold	der for
		Protein ib	Abundancy	by peer review) is the author/funder. All rights reserved. No permission.	reuse allowed with	nout Symbol
			(compared to control)	<u> </u>	(SvsC-SIvsC)	
		AT1G43140	Less	Putative cullin-like protein		CUL
1		AT1G10200	Less	LIM domain-containing protein		WLIM1
1		AT1G16340	Less	2-dehydro-3-deoxyphosphooctonate		KDSA2
1		AT1G16460	Less	Sulfurtransferase 2		STR2
1		AT1G21065	Less	Secondary thiamine-phosphate synthase enyzme		T22I11.11
1		AT1G26880	Less	Large ribosomal subunit protein		RPL34A
1		AT1G35580	Less	Alkaline/neutral invertase		CINV1
		AT1G55450	More	Methyltransferase		
		AT1G69250	Less	Nuclear transport factor 2		NTF2
		AT1G75660	Less	5'-3' exoribonuclease 3		XRN3
t		AT2G02100	More	Defensin-like protein 2		PDF2.2
Strict Ca <sup>2+</sup> dependent		AT2G29700	Less	Pleckstrin homology domain-containing protein 1		PH1
š		AT3G15090	Less	GroES-like zinc-binding alcohol dehydrogenase fam.		
ŏ		AT3G16050	Less	Pyridoxal 5'-phosphate synthase-like subunit PDX1.2		PDX12
ද්		AT3G43540	Less	Initiation factor 4F subunit		DUF1350
<u>ម</u>		AT3G54170	Less	FKBP12-interacting protein of 37 kDa		FIP37
Str		AT3G57870	Less	SUMO-conjugating enzyme		SCE1
1		AT4G01883	Less	Polyketide cyclase / dehydrase and lipid transport protein		MLBP1
1		AT4G23650	More	Calcium-dependent protein kinase 3		СРК3
		AT4G36020	Less	Cold shock protein 1		CSP1
		AT5G01600	Less	Ferritin-1, chloroplastic		FER1
		AT5G11810	Less	Rhomboid family protein		T22P22_200
		AT5G18100	Less	Superoxide dismutase		CSD3
		AT5G53530	Less	Vacuolar protein sorting-associated protein 26A		VPS26A
		AT5G57890	Less	Anthranilate synthase beta subunit 2, chloroplastic		ASB2
		AT5G62340	More	Pectin methylesterase inhibitor superfamily protein		MMI9.17
		ATCG00270	More	Photosystem II D2 protein		PSBD
	ΔFC≥ 1.5	AT1G03030	More	RING1B	4.58	-
		AT1G56700	More	Pyrrolidone-carboxylate peptidase	4.81	
		AT1G60950	More	Ferredoxin	1.82	FD2
		AT1G74060	Less	Large ribosomal subunit protein L6y-2	1.71	RPL6B
		AT2G17870	Less	Cold shock domain-containing protein 3	1.66	CSP3
		AT2G18020	Less	Large ribosomal subunit protein uL2z	1.69	RPL8A
		AT2G32500	More	Sucrose-phosphatase	1.66	20/ 1
		AT2G42690	More	Phospholipase A1-IIdelta	2.13	AGAP1
ent		AT3G02830	Less	Zinc finger CCCH domain-containing protein 33	2.46	ZFN1
ğ		AT3G07630	Less	Arogenate prephenate dehydratase 2, chloroplastic	1.58	ADT2
g		AT3G54440	More	Glycoside hydrolase family 2 protein	3.71	7.512
👸		AT4G12730	Less	Fasciclin-like arabinogalactan protein 2	2.04	FLA2
ja <sub>2</sub>		AT4G33220	Less	Probable pectinesterase/pectinesterase inhibitor 44	2.03	PME44
<u>a</u> [		AT5G54430	More	Adenine nucleotide alpha hydrolases-like superfamily	2.14	PHOS32
Partial Ca <sup>2+</sup> depend		A13034430	IVIOIC	protein	2.17	1110332
ے ا		AT1G20110	Less	Protein FREE1	1.49	FREE1
	H	AT1G52380	Less	Nuclear pore complex protein NUP50A	1.27	NUP50A
	1.5	AT1G70890	Less	MLP-like protein 43	1.35	MLP43
	<u>``</u>	AT1G79750	More	NADP-dependent malic enzyme	1.40	NADP-ME4
	1.2	AT2G33040	More	ATP synthase subunit gamma, mitochondrial	1.28	ATPC
	AFC 1.25-	AT3G50440	More	Methylesterase 10	1.47	MES10
	ΔF	AT5G38520	More	Alpha/beta-Hydrolases superfamily protein	1.39	CLD1
		AT5G565320	More	Golgi-localized GRIP domain-containing protein	1.47	GRIP
$\vdash$		AT1G71220	More	UDP-glucose:glycoprotein glucosyltransferases	1.14	UGGT
		AT3G45140	More	Lipoxygenase 2, chloroplastic	1.14	LOX2
int		AT3G43140	More	Carotene epsilon-monooxygenase, chloroplastic	1.06	CYP97C1
l g	25	AT4G01690	More	Protoporphyrinogen oxidase	1.17	PPOX1
je	<1.25	AT4G01690 AT4G02230	Less	Large ribosomal subunit protein eL19y	1.17	RPL19C
Ca <sup>2+</sup> independent	ΔFC «	AT4G02230 AT4G04210	Less	Plant UBX domain-containing protein 4	1.22	PUX4
2 i	۵	AT5G38430	More	Ribulose bisphosphate carboxylase small chain 1B,	1.11	RBCS-1B
ន		A13030430	INIOLG	chloroplastic	1.13	VDC2-1D
		AT5G58060	More	VAMP-like protein YKT61	1.21	YKT61
	ш	V1202000	More	AWINIL-IIVE BLOKEIII LKIOT	1.41	11/1/1

Table 4: List of H<sub>2</sub>O<sub>2</sub> responsive proteins indicated as strict Ca<sup>2+</sup> dependent (dark grey), partial Ca<sup>2+</sup> dependent (light grey) and Ca<sup>2+</sup> independent (white) regulated after 30 min of treatment. Partial Ca<sup>2+</sup> dependent proteins were further divided by a threshold of at least a 50% change in abundance (≥2-fold increase or decrease). 19

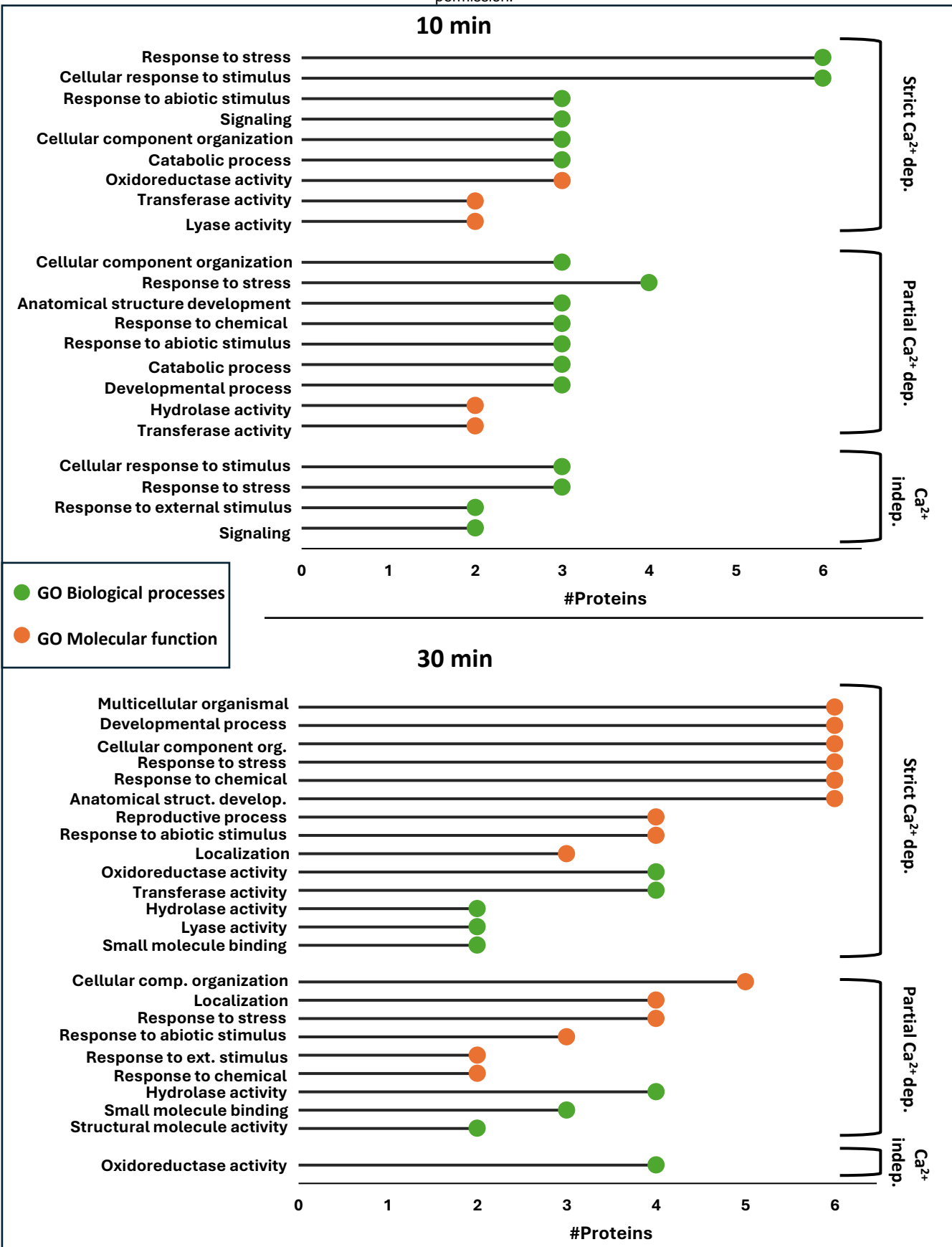


**Fig. 6:** GO-term analysis (Biological Processes and Molecular Function) on the  $H_2O_2$  responsive proteins indicated as strict  $Ca^{2+}$  dependent, partial  $Ca^{2+}$  dependent, and  $Ca^{2+}$  independent regulated after 10 and 30 min of treatment. Numbers represent absolute numbers of proteins that are annotated to functional categories based on high level GO terms.

## Effect of the duration of the stress treatment

As stated above, the largest difference in biological function was observed between the two time points of stress treatment. To further elucidate the effects of stress duration on DAPs, a comparative analysis was conducted using two approaches. First, the absolute numbers of  $H_2O_2$  responsive proteins identified after 10 and 30 min of stress treatment were compared. This comparison, visualized in a Venn diagram (Fig. 7A, upper panel), revealed a duration related increase of  $H_2O_2$  responsive proteins from 37 to 57, with an overlap of only six proteins between the two time points. The latter is in line with the different biological processes observed for the proteins in the two data sets (Fig. 6A and B) and indicates that the duration of the treatment results in a significant different effect on the proteome. The same trend holds true, when proteins were separated based on their  $Ca^{2+}$  dependency (Fig. 7A, lower panel).

We further investigate the effect of stress duration by additionally considering the increase and decrease of proteins abundance (Fig. 7B). Although the total number of DAPs was relatively low, a clear pattern emerged. Proteins that were strictly Ca<sup>2+</sup>-dependent predominantly exhibited a significant decrease in abundance, whereas those that were partially Ca<sup>2+</sup>-dependent or Ca<sup>2+</sup>-independent tended to show increased abundance.

We than had a closer look at the only six  $H_2O_2$  responsive proteins that were found at both timepoints (Fig. 6A, upper panel). Their  $Ca^{2+}$  dependency and changes in abundance were examined across both conditions (Fig. 6C). The analysis revealed that all six proteins exhibited the same change in abundance (either increased or decreased) after both 10 and 30 min of stress treatment. Three of these proteins - WLIM1, CYP97C1, and AGAP1 - displayed a difference in their  $Ca^{2+}$  dependency between the two timepoints.

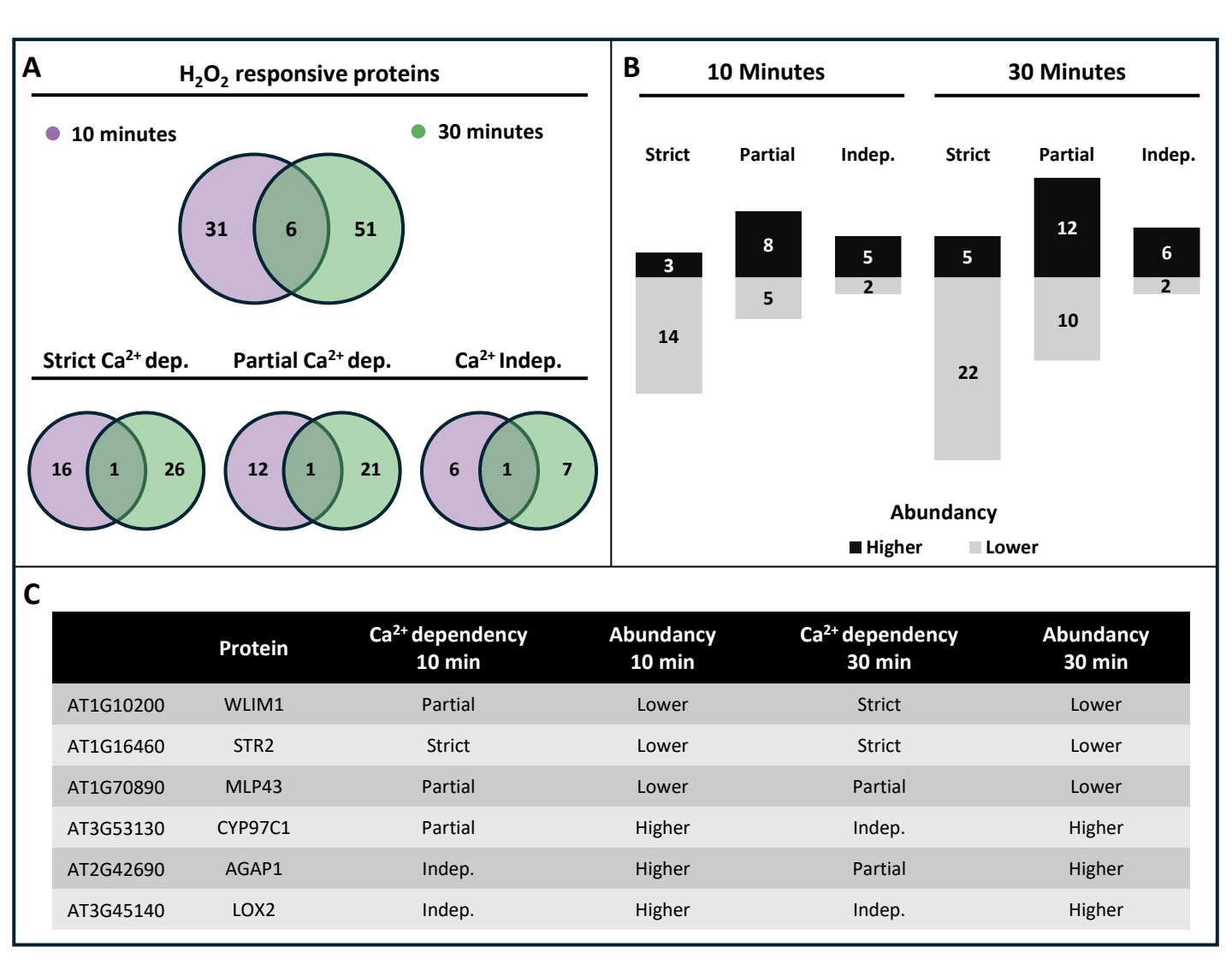


**Fig. 7:** Comparison of the  $H_2O_2$  responsive proteins between 10 and 30 min of stress treatment. **A:** Venn diagrams for comparison of all  $H_2O_2$  responsive proteins identified after 10 min (purple) and 30 min (green) of stress treatment (top part). Comparison of the  $H_2O_2$  responsive proteins after 10 and 30 min of stress treatment, separated for their dependency on  $Ca^{2+}$  (bottom). Values represent absolute number of DAPs in each category. **B:** Bar chart showing absolute numbers of DAPs and their change in abundancy after  $H_2O_2$  treatment separated for the group of  $Ca^{2+}$  dependency they resolve into. **C:** Overview of the  $Ca^{2+}$  dependency and the change in abundancy after stress treatment of the 6  $H_2O_2$  responsive proteins found to be overlapping between 10 and 30 min of stress treatment.

### Validation of the dataset

We tried to assess the accuracy of the Mass spec analysis by comparing the data output (raw average LFQ intensity values) with Western blot analysis for two proteins from our dataset, for which antibodies could be obtained (Fig. 8). PHENYLALANINE LYASE 2 (PAL2), known to be responsive to oxidative stress (Stanley Kim et al., 2005), showed a lower abundance after 10 min of H<sub>2</sub>O<sub>2</sub> treatment (Fig. 8A, upper panel) and was found in the group of strict Ca<sup>2+</sup>-dependent H<sub>2</sub>O<sub>2</sub> responsive proteins (Table 3). This pattern could be confirmed by the Western blot analysis, where the protein band detected in the extracts of stress treated plant material was clearly fainter as for the other treatments (Fig.8A, lower panel). The aquaporin GAMMA TONOPLAST INTRINSIC PROTEIN 2 (TIP2), suspected to be involved in hydrogen peroxide transmembrane transport (Bienert et al., 2007), showed a higher abundance in the 10 min stress treated samples compared to control but is not in Table 4 due to its also higher LFQ-values after inhibitor only treatment (Fig. 8B upper panel). Also, this result could be confirmed by the increased intensity of the reaction in the stress treated and the inhibitor treated samples in the Western blot (Fig.8B, lower panel). Thus, in both cases an agreement between the proteome data (LFQ values) and the Western blot analysis was found.

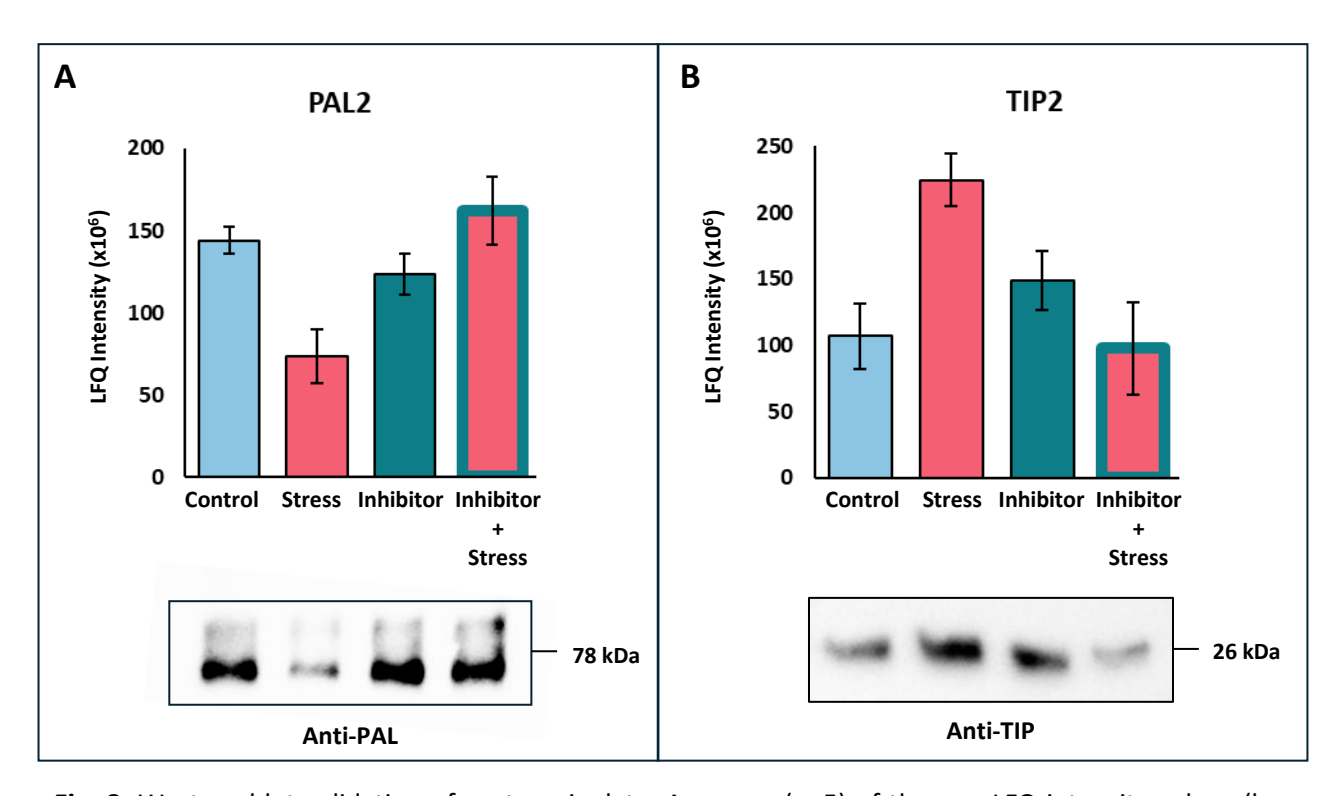


**Fig. 8:** Western blot validation of proteomic data. Averages (n=5) of the raw LFQ intensity values (bar graph) and immunodetection using specific antibodies for (blot) for **A:** PAL2 and **B:** TIP2. Full sized blots are shown in Supplementary Fig. S2

## Discussion

In this study, we employed a pre-treatment with the  $Ca^{2+}$  channel inhibitor  $La^{3+}$  to differentiate between  $Ca^{2+}$ -dependent and  $Ca^{2+}$ -independent changes in protein abundance after treatment with  $H_2O_2$  in *Arabidopsis thaliana* at a proteome-wide scale. Our investigation was focused on short-term responses, therefore we analysed the proteome after 10 and 30 min of treatment with  $H_2O_2$ . We detected 3724 proteins after 10 min and 3757 after 30 min of treatment. From these, 581 and 909 proteins significantly changed abundance, respectively. The much smaller number of proteins used for further analysis is the result of proteomics experiments often generating a large number of low-confidence identifications or proteins with inconsistent quantifications across replicates.

A key initial step in our analysis was the identification of H<sub>2</sub>O<sub>2</sub>-responsive proteins, which resulted in distinct subsets of proteins detected after 10 and 30 min of stress treatment, with only six proteins identified in both sets. This temporal variation in protein abundance highlights the dynamic nature of the oxidative stress response and suggests that the duration of stress exposure significantly influences proteome-wide adaptations. Given that H<sub>2</sub>O<sub>2</sub> is known to induce Ca<sup>2+</sup>signals at the cellular level (Rentel & Knight, 2004), which are then decoded by Ca<sup>2+</sup>-binding proteins to activate downstream molecular processes (Mohanta et al., 2019; Tang et al., 2020), the observed temporal differences are in line with the described spatiotemporal plasticity of Ca<sup>2+</sup>signaling (Boulware & Marchant, 2008). Consequently, it is not unexpected that a threefold increase in stress duration results in distinct proteomic responses, reflecting the dynamic and evolving nature of oxidative stress adaptation at the molecular level.

Following the identification of  $H_2O_2$ -responsive proteins, we further categorized them based on their dependence on  $Ca^{2+}$  for differential abundance regulation. Strict  $Ca^{2+}$  dependency was defined by proteins that exhibited significant changes in abundance upon  $H_2O_2$  treatment but lack this response when pre-incubated with  $LaCl_3$ , indicating a complete reliance on  $Ca^{2+}$  signaling for their regulation. This was the largest group for both the 10 and 30min time point. Partially  $Ca^{2+}$ -dependent proteins showed a difference in abundance both between control and  $H_2O_2$  treatment as well as control and  $H_2O_2$ +La $Cl_3$  treatment, however, the abundance was significantly different between the two treatments.  $Ca^{2+}$  independency was observed for less than 20% and 15% of the  $H_2O_2$ -responsive after 10 and 30 min, respectively, showing the strong impact of  $Ca^{2+}$  signaling on the oxidative stress response that was also observed in a recent transcriptomic analysis on barley (Bhattacharyya et al., 2025). Another notable finding related to this was the high number of DAPs identified when the  $H_2O_2$ -induced  $Ca^{2+}$  transient was blocked by  $LaCl_3$ . With over 400 DAPs at 10 and over 600 DAPs at 30 min, the numbers were about a factor 10 higher than for the stress treatment or inhibitor treatment alone.

The high number of DAPs in response to the combined treatment suggest that  $Ca^{2+}$  signaling can strongly attenuate the  $H_2O_2$  response.

Another interesting result is the observation that much more proteins with a strict  $Ca^{2+}$  dependency show a reduced abundance, while a higher abundance is more often observed for  $Ca^{2+}$  independent  $H_2O_2$ -responsive proteins. Considering the timeframe of the experiment it seems likely that protein loss is mostly driven by degradation (and not reduced transcription) while increase in protein content is the result of increased transcription and/or translation. These findings indicate a potential regulatory mechanism in which protein destabilization is driven by  $Ca^{2+}$  signaling, while proteins without strict  $Ca^{2+}$  dependency may undergo enhanced synthesis under oxidative stress conditions.

Comparison of H<sub>2</sub>O<sub>2</sub>-responsive proteins between 10 and 30 min of treatment revealed only six overlapping proteins, all of which exhibited the same change in abundance at both time points. Notably, three proteins exhibited a shift in Ca<sup>2+</sup> dependency between the two time points. However, they went from partial to strictly Ca<sup>2+</sup> dependent or from partial to Ca<sup>2+</sup> independent, but no protein changed from strictly Ca<sup>2+</sup>-dependent to Ca<sup>2+</sup>-independent. Since the difference in logFC change between the two time points is quite consistent for these three proteins over the five biological replicates analysed, these findings clearly suggest a dynamic nature of Ca<sup>2+</sup> dependent and independent protein regulation in response to oxidative stress.

Overall, it remains challenging to draw a definitive conclusion regarding the precise role of Ca<sup>2+</sup> signaling in shaping proteomic changes from our data. However, we found several candidates with known functions in stress responses among the H<sub>2</sub>O<sub>2</sub>-responsive proteins. In all of these cases single proteins and not proteins groups were identified. The ribosomal protein RPL18, which exhibited higher abundance after 10 min of H<sub>2</sub>O<sub>2</sub> treatment, has been previously described as a positive regulator of powdery mildew resistance in wheat (Tao et al., 2024). The germin-like protein GLP1, which also showed increased abundance after 10 min, has been characterized as an oxidative stress defence enzyme in plants (Shahwar et al., 2023). CPK3, a calcium-dependent protein kinase, displayed higher abundance with strict Ca<sup>2+</sup> dependency after 30 min, aligning with its known role in Ca<sup>2+</sup>-dependent signaling pathways involved in responses to abiotic and biotic stresses (Mehlmer et al., 2010) and plant immunity (Lu et al., 2020). For the identified H<sub>2</sub>O<sub>2</sub>-responsive proteins that lack a well-defined role in plant stress responses, further investigation is required to elucidate their functions in plant defence mechanisms, signaling pathways, ROS homeostasis, and overall plant survival.

## **Conclusion**

Hydrogen peroxide ( $H_2O_2$ ) is a crucial reactive oxygen species (ROS), generated as a toxic by-product of biological metabolic processes while also functioning as a signaling molecule that regulates plant growth and development. Additionally, it interacts with signaling pathways involving second messengers such as  $Ca^{2+}$ . Our findings expand the current knowledge of oxidative stress responses by identifying proteins which are degraded or synthesized in response to  $H_2O_2$  in a  $Ca^{2+}$  dependent manner. In these subsets, proteins were found that are known to play a role in  $Ca^{2+}$  signaling and stress response, but also proteins that were unassociated with stress response pathways before. These novel proteins present potential targets for further investigation into the molecular basis of  $H_2O_2$ - $Ca^{2+}$  interactions. Given that both biotic and abiotic stress factors can induce  $H_2O_2$  accumulation and  $Ca^{2+}$  fluctuations, understanding this crosstalk is essential for deciphering plant stress acclimation mechanisms. The insights gained from Arabidopsis may thus have broader applications, potentially for strategies to enhance stress resilience in economically significant crop species.

## **Material and Methods**

## Plant material and growth conditions

Leaf protein extracts for the proteomics analysis were obtained from *A. thaliana* (ecotype Columbia; Col-0). Seeds were sown on soil, stratified for 2 days at 4°C in the dark, and separated after germination into single pots filled with standard plant potting soil pre-treated with Confidor WG 70 (Bayer Agrar, Germany). Plants were cultivated in a climatized growth chamber with a room temperature of 20  $\pm$  2°C, a light intensity of ~150  $\mu$ mol photons m<sup>-2</sup> s<sup>-1</sup> (Philips TLD 18 W of alternating 830/840 light colour) and long day conditions (16 h light/8 h dark). Pre-experiments to determine the best conditions for the inhibitor treatment and stress stimulus were performed with Arabidopsis plants expressing cytosolic apoaequorin (At-AEQ<sub>cvt</sub>) (M. R. Knight et al., 1991).

## Aequorin reconstitution, luminescence measurements and Ca<sup>2+</sup> concentration calculations

Stimulus-induced Ca<sup>2+</sup> transients were analysed using leaf material of three-week-old At-AEQ<sub>cvt</sub> plants. The day before measurements were taken, leaf discs (Ø 6mm) were collected and incubated overnight in the dark at 20°C in 5 μM coelenterazine (Biosynth AG, Switzerland) for reconstitution of the cytosol targeted apoaequorin to aequorin. After reconstitution, leaf discs were carefully washed (ddH<sub>2</sub>O) and transferred either into 1 mM LaCl<sub>3</sub> solution (inhibitor pre-treatment) or ddH<sub>2</sub>O (mock) for 1 hour. Subsequently, single leaf discs were washed again and transferred individually into a 96-well plate (Lumitrac 600, Greiner Bio-One, Austria), floating in 100 μl ddH<sub>2</sub>O. Photon count measurements were performed using a plate luminometer (Tristar 2 Multimode Reader, Berthold GmbH). First the basal level of photon counts was measured for 30 seconds with an interval of 1 second, followed by the application 20 mM H<sub>2</sub>O<sub>2</sub> using a 40 mM stock solution and a volume equal to the starting volume of the ddH<sub>2</sub>O (100 μl), with continuous measuring of the response for 240 seconds. The remaining aequorin was discharged by adding discharge solution (final concentration of 1 M CaCl<sub>2</sub> in 10% (v/v) EtOH) and photon counts were recorded for another 300 sec. Concentrations of free calcium ions in the cytosol ( $[Ca^{2+}]_{cyt}$ ) were calculated based on the photon counts as described before (H. Knight & Knight, 1995). The measurements were performed with three independent experimental replicates consisting of three technical replicates.

## Sample collection and treatment for proteomics

For proteomics analysis, 12 complete rosettes of three-weeks-old Col-0 plants were incubated in 1 mM LaCl<sub>3</sub> (inhibitor treatment) or  $ddH_2O$  for 1 hour.  $ddH_2O$  and  $LaCl_3$  pre-treated plants were carefully washed and then transferred into either 20 mM  $H_2O_2$  (stress treatment) or  $ddH_2O$  for the control treatment. For each proteomics sample, complete rosettes of 12 plants were harvested after 10 and 30 min of the stress treatment, pooled, immediately frozen in liquid nitrogen, and stored at -80 °C until protein extraction. Within one experiment, plants from all four treatments were harvested for both timepoints (10 and 30 min), and a total of 5 experiments with independently grown plants were performed. For a schematic overview of the protocol see Figure 1.

## Protein isolation, precipitation, lysis and digestion

Frozen plant material was first ground in liquid nitrogen using a pre-cooled mortar and pestle. 500 mg of the ground plant material was mixed with 2 ml ice-cold Lacus protein isolation buffer (20 mM Tris [pH 7.7], 80 mM NaCl, 0.75 mM EDTA, 1 mM CaCl<sub>2</sub>, 5 mM MgCl<sub>2</sub>, 1 mM DTT, 1 mM NaF) containing 4 tablets of protease inhibitor (Roche cOmplete EDTA-free, protease inhibitor cocktail tablets) and 10 tablets of phosphatase inhibitor (Roche PhosSTOP) per 200 ml. Samples were incubated on ice for 10 min followed by centrifugation at 15000 g for 10 min at 4 °C. Supernatants were transferred into a fresh tube. An equal volume of 20 % (w/v) trichloroacetic acid (TCA) was added to the supernatant, and the samples were placed on ice for 30 min. Afterwards, the samples were centrifuged at 15000 g for 10 min at 4 °C and the supernatant removed. The precipitated protein pellets were washed with cold 80% acetone and the samples were vacuum-dried. 50 µl of urea lysis buffer (8 M urea, 150 mM NaCl, 40 mM Tris-HCl pH 8) was added and the protein concentration was determined via the Pierce™ BCA Protein Assay (Thermo Fisher Scientific). Subsequently, 3 mg total protein per sample was reduced in 5 mM DTT and alkylated in 15 mM iodoacetamide for 30 min in the dark at room temperature. The alkylated samples were quenched by adding DTT to a final concentration of 5 mM and mixed with 30 mg carboxylate beads (Sera-Mag<sup>™</sup>, 1:1 ratio of hydrophilic and hydrophobic beads, Cytiva, USA). Proteins attached to the beads were washed four times with 80 % (v/v) ethanol and digested in ammonium bicarbonate buffer (30 mM, pH 8.2) containing 30 µg Trypsin (Promega, WI, USA). Tryptic digestion was performed overnight at 37 °C under constant shaking. The digestion was stopped by the addition of formic acid (final concentration 4%). 100 µg of the digested peptides per sample were transferred into a new reaction tube, vacuum-dried and stored at -20 °C until HPLC-MS analysis.

## LC-MS analysis

Digested peptides were subjected to LC-MS analysis at the Mass Spectrometry unit of the faculty of life sciences at the University of Vienna as described previously (Bleker et al., 2024). In brief: approximately 1 µg of peptide sample was reconstituted in 0.1% (v/v) formic acid and separated using an online reversed-phase high-pressure liquid chromatography (HPLC) system. Separation was performed on a heated C18 analytical column over a 140-minute gradient (5-50%). The eluate was introduced into a Q-Exactive Plus mass spectrometer using an Easy-Spray ion source. Mass spectra were acquired in positive ion mode with a data-dependent acquisition strategy, selecting the top 15 most intense ions for MS analysis. A full MS scan was performed at 70,000 resolution (m/z 200), followed by MS/MS fragmentation at 17,500 resolution using higher-energy collisional dissociation (HCD) at 27% normalized collision energy. Dynamic exclusion was set to 40 seconds, and specific precursor ions (unassigned, +1, +7, +8, and >+8 charge states) were excluded. The analysis was conducted with five independent experimental replicates per sample to ensure reproducibility.

## Peptide identification and quantification

Identities and peptide features were defined by the peptide search engine Andromeda provided by the MaxQuant software (Prianichnikov et al., 2020) and using standard settings (Tyanova et al., 2016). In detail: trypsin-based digestion of the peptides with up to two missing cleavage sites was selected. Methionine oxidation as well as N-terminal acetylation was set as a variable modification for peptide identification. In total, up to three potential modification sites per peptide were accepted. The identified peptide sequences were searched and aligned against the Araport11 reference protein database (Cheng et al., 2017). The false discovery rate cut-off for protein identification and side identification was set to 0.01. The minimum peptide length was set to seven and the maximum length to 40 amino acids. For each identified protein group, label-free quantitation (LFQ) intensities were calculated using the Maxquant software. A protein group contains all proteins and protein isoforms that cannot be unambiguously identified by unique peptides but have shared peptides. We further on refer to protein groups only as 'proteins'.

### Data analysis

For quantitative proteome analyses, the derived LFQ intensities were loaded into the Perseus software (Tyanova et al., 2016) and used for data and statistical analysis, as well as graphics and visualisation of the results. The steps taken to determine which proteins show a differential abundance among the different treatments was based on a method described before (Nikonorova et al., 2018). In short: after

loading the LFQ intensities, a quality control was performed in which protein groups with the indication 'only identified by site' (proteins that are only identified by peptides carrying modified amino acids), reverse sequences (decoy proteins), and potential contaminants (for example, albumin) were filtered out. Biological replicates were grouped, and values were log2 transformed. Protein groups were filtered based on valid values, where the criterium was set to have at least 3 valid values in one group (each treatment group consists of 5 replicates) to remove the low abundant proteins. Remaining missing values (protein group not identified in a run) were imputed with values based on the normal distribution with a width of 0.3 (relative to the standard deviation of the measured values) and a downshift of 1.8. The imputed numbers represent very small values, meaning the identified peptide has a very low abundance. Principal component analysis (PCA) was performed using the Perseus software. Differential abundant proteins were determined by multiple sample ANOVA test (p-value < 0.05). P-values were corrected for multiple testing using Benjamin-Hochberg rule (adjusted P-value). All ANOVA significant proteins were z-score normalized and used for supervised hierarchical clustering to produce a heatmap, using Euclidean distance and average linkage. Pairwise Student's t-tests (pvalue < 0.05) were performed on the non-z-scored values to determine differences in protein abundance between two treatments. Volcano plots were generated using the Perseus software, by plotting log<sub>2</sub> fold-change values on the x-axis against the -log p values on the y-axis, cut-off was set by nonlinear volcano lines based on SO = 0.1 adjusted p-value. Protein groups showing different abundance among the treatments were analysed for overlapping groups between treatments and time points. Gene ontology (GO) enrichment analysis (KEGG, biological processes, molecular function) was performed on the major protein clusters identified by hierarchical clustering, and on the identified H<sub>2</sub>O<sub>2</sub> responsive proteins using ShinyGO, which uses the annotations of Ensembl and STRING-db (Ge et al., 2020). An error probability according to Fisher's' t-test of <0.05 and a false-discovery rate (FDR) of <0.01 was selected for enriched GO-Terms.

## **Immunodetection**

For immunodetection, proteins were isolated from the plant material that was used for the MS-analysis using the same Lacus protein isolation buffer and isolation protocol (described above). The proteins were separated on a 12% SDS-polyacrylamide gel and transferred to nitrocellulose membrane (0.45µm pore size; Bio-Rad Laboratories). After transfer of the proteins, the membrane was stained using 0.1% (w/v) Ponceau S in 5% (v/v) glacial acetic acid. Immunodetection was performed using antibodies against Anti-PAL 1-4 (dilution 1:2000) and Anti-TIP 1;1-2 (dilution 1:1000) (Agrisera, AS214614 and AS22 4844). Blots were incubated with the matching secondary antibody (anti-rabbit IgG horse radish peroxidase conjugated, AS09602, dilution 1:25000) and developed with the AgriseraBright (AS16 ECL-N-10) detection reagent.

# Data availability statements

The authors upon reasonable request can provide the data presented in this study

# **Declaration of competing interest**

The authors declare no competing interests

# **Author contributions**

A.v.D. contributed to conceptualization, investigation, formal analysis, validation, visualization, and writing - original draft as well as review & editing; A.B. and B.W. contributed to conceptualization and sample preparation for LC-MS measurements; L.A. contributed to LC-MS analysis and writing the corresponding method; W.W contributed to supervision; M.T. contributed to conceptualization, supervision and writing — review editing; U.C.V. contributed to conceptualization, formal analysis, validation, funding acquisition, project administration, supervision, and writing — review & editing.

# References

Allen, G. J. *et al.* A defined range of guard cell calcium oscillation parameters encodes stomatal movements. *Nature* **411**, 1053–1057 (2001).

Ayash, M. et al. LC–MS Based Draft Map of the Arabidopsis thaliana Nuclear Proteome and Protein Import in Pattern Triggered Immunity. Front. Plant Sci. 12, 744103 (2021).

Bhattacharyya, S. et al. Ca2+-dependent H2O2 response in roots and leaves of barley - a transcriptomic investigation. *BMC Plant Biol* **25**, 232 (2025).

Bienert, G. P. *et al.* Specific Aquaporins Facilitate the Diffusion of Hydrogen Peroxide across Membranes. *Journal of Biological Chemistry* **282**, 1183–1192 (2007).

Bleker, C. et al. Stress Knowledge Map: A knowledge graph resource for systems biology analysis of plant stress responses. *Plant Communications* 100920 (2024)

Boulware, M. J. & Marchant, J. S. Timing in Cellular Ca2+ Signaling. *Current Biology* **18,** R769–R776 (2008).

Chen, Q. & Yang, G. Signal Function Studies of ROS, Especially RBOH-Dependent ROS, in Plant Growth, Development and Environmental Stress. *J Plant Growth Regul* **39**, 157–171 (2020).

Cheng, C. *et al.* Araport11: a complete reannotation of the *Arabidopsis thaliana* reference genome. *The Plant Journal* **89,** 789–804 (2017).

Costa, A., Navazio, L. & Szabo, I. The contribution of organelles to plant intracellular calcium signalling. *Journal of Experimental Botany* **69**, 4175–4193 (2018).

Demidchik, V., Shabala, S., Isayenkov, S., Cuin, T. A. & Pottosin, I. Calcium transport across plant membranes: mechanisms and functions. *New Phytologist* **220**, 49–69 (2018).

Ge, S. X., Jung, D. & Yao, R. ShinyGO: a graphical gene-set enrichment tool for animals and plants. *Bioinformatics* **36**, 2628–2629 (2020).

Gilroy, S. *et al.* ROS, Calcium, and Electric Signals: Key Mediators of Rapid Systemic Signaling in Plants. *Plant Physiol.* **171,** 1606–1615 (2016).

Giridhar, M. et al. Comparative analysis of stress-induced calcium signals in the crop species barley and the model plant Arabidopsis thaliana. *BMC Plant Biol* **22**, 447 (2022).

Gry, M. et al. Correlations between RNA and protein expression profiles in 23 human cell lines. BMC Genomics 10, 365 (2009).

Kaplan, B. *et al.* Rapid Transcriptome Changes Induced by Cytosolic Ca2+ Transients Reveal ABRE-Related Sequences as Ca2+-Responsive *cis* Elements in *Arabidopsis*. *The Plant Cell* **18**, 2733–2748 (2006).

Kärkönen, A. & Kuchitsu, K. Reactive oxygen species in cell wall metabolism and development in plants. *Phytochemistry* **112**, 22–32 (2015).

Knight, H. & Knight, M. R. Chapter 14 Recombinant Aequorin Methods for Intracellular Calcium Measurement in Plants. in *Methods in Cell Biology* vol. 49 201–216 (Elsevier, 1995).

Knight, M. R., Campbell, A. K., Smith, S. M. & Trewavas, A. J. Transgenic plant aequorin reports the effects of touch and cold-shock and elicitors on cytoplasmic calcium. *Nature* **352**, 524–526 (1991).

Kudla, J., Batistič, O. & Hashimoto, K. Calcium Signals: The Lead Currency of Plant Information Processing. *Plant Cell* **22**, 541–563 (2010).

Li, Y., Liu, Y., Jin, L. & Peng, R. Crosstalk between Ca2+ and Other Regulators Assists Plants in Responding to Abiotic Stress. *Plants* **11**, 1351 (2022).

Liu, Y., Beyer, A. & Aebersold, R. On the Dependency of Cellular Protein Levels on mRNA Abundance. *Cell* **165**, 535–550 (2016).

Lu, Y.-J. *et al.* Arabidopsis calcium-dependent protein kinase 3 regulates actin cytoskeleton organization and immunity. *Nat Commun* **11**, 6234 (2020).

Ludwig, A. A. CDPK-mediated signalling pathways: specificity and cross-talk. *Journal of Experimental Botany* **55**, 181–188 (2003).

McAinsh, M. R. & Pittman, J. K. Shaping the calcium signature. New Phytologist 181, 275–294 (2009).

Mehlmer, N. et al. The Ca2+-dependent protein kinase CPK3 is required for MAPK-independent salt-stress acclimation in Arabidopsis: CPK3 signalling in plant salt stress. *The Plant Journal* **63**, 484–498 (2010).

Mittler, R. ROS Are Good. Trends in Plant Science 22, 11–19 (2017).

Mohanta, T. K. *et al.* Molecular Players of EF-hand Containing Calcium Signaling Event in Plants. *IJMS* **20**, 1476 (2019).

Nikonorova, N., Vu, L. D., Stes, E., Gevaert, K. & De Smet, I. Proteome Analysis of Arabidopsis Roots. in *Root Development* (eds. Ristova, D. & Barbez, E.) **vol. 1761** 263–274 (Springer New York, 2018).

Payne, S. H. The utility of protein and mRNA correlation. *Trends in Biochemical Sciences* **40**, 1–3 (2015).

Prianichnikov, N. *et al.* MaxQuant Software for Ion Mobility Enhanced Shotgun Proteomics. *Molecular & Cellular Proteomics* **19,** 1058–1069 (2020).

Ravi, B., Foyer, C. H. & Pandey, G. K. The integration of reactive oxygen species (ROS) and calcium signalling in abiotic stress responses. *Plant Cell & Environment* **46**, 1985–2006 (2023).

Rentel, M. C. & Knight, M. R. Oxidative Stress-Induced Calcium Signaling in Arabidopsis. *Plant Physiology* **135**, 1471–1479 (2004).

Scholz, P. et al. Plasticity of the Arabidopsis leaf lipidome and proteome in response to pathogen infection and heat stress. *Plant Physiology* **197**, kiae274 (2025).

Seaton, D. D. et al. Photoperiodic control of the *Arabidopsis* proteome reveals a translational coincidence mechanism. *Molecular Systems Biology* **14**, e7962 (2018).

Shahwar, D. et al. Characterization of the active site of a germin like protein 1 as an oxidative stress defense enzyme in plants. Plant Gene **36**, 100432 (2023).

Stanley Kim, H. *et al.* Transcriptional divergence of the duplicated oxidative stress-responsive genes in the Arabidopsis genome. *The Plant Journal* **41,** 212–220 (2005).

Tang, R.-J., Wang, C., Li, K. & Luan, S. The CBL–CIPK Calcium Signaling Network: Unified Paradigm from 20 Years of Discoveries. *Trends in Plant Science* **25**, 604–617 (2020).

Tao, Y. *et al.* Identification of the ribosomal protein L18 (RPL18) gene family reveals that TaRPL18-1 positively regulates powdery mildew resistance in wheat. *International Journal of Biological Macromolecules* **280**, 135730 (2024).

Tracy, F. E., Gilliham, M., Dodd, A. N., Webb, A. A. R. & Tester, M. NaCl-induced changes in cytosolic free Ca<sup>2+</sup> in *Arabidopsis thaliana* are heterogeneous and modified by external ionic composition. *Plant Cell & Environment* **31**, 1063–1073 (2008).

Tyanova, S., Temu, T. & Cox, J. The MaxQuant computational platform for mass spectrometry-based shotgun proteomics. *Nat Protoc* **11**, 2301–2319 (2016).

Tyanova, S. *et al.* The Perseus computational platform for comprehensive analysis of (prote)omics data. *Nat Methods* **13**, 731–740 (2016).

Van Dieren, A., Schwarzenbacher, R. E., Sonnewald, S., Bittner, A. & Vothknecht, U. C. Analysis of abiotic and biotic stress-induced Ca2+ transients in the crop species Solanum tuberosum. *Sci Rep* **14**, 27625 (2024).

Whalley, H. J. & Knight, M. R. Calcium signatures are decoded by plants to give specific gene responses. *New Phytologist* **197**, 690–693 (2013).

Zhang, G. *et al.* Exogenous Calcium Alleviates Low Night Temperature Stress on the Photosynthetic Apparatus of Tomato Leaves. *PLoS ONE* **9**, e97322 (2014).

Appendix 3

Chapter 3

Stress Knowledge Map: A knowledge graph resource for systems biology

analysis of plant stress responses

Carissa Bleker <sup>1</sup>, Živa Ramšak <sup>1</sup>, Andras Bittner <sup>2</sup>, Vid Podpečan <sup>3</sup>, Maja Zagorščak <sup>1</sup>, Bernhard

Wurzinger <sup>4</sup>, Špela Baebler <sup>1</sup>, Marko Petek <sup>1</sup>, Maja Križnik <sup>1</sup>, Annelotte van Dieren <sup>2</sup>, Juliane

Gruber <sup>4</sup>, Leila Afjehi-Sadat <sup>5</sup>, Wolfram Weckwerth <sup>4</sup>, Anže Županič <sup>1</sup>, Markus Teige <sup>4</sup>, Ute

C. Vothknecht <sup>2</sup>, Kristina Gruden <sup>1</sup>

1. Department of Biotechnology and Systems Biology, National Institute of Biology, Večna

pot 121, 1000 Ljubljana, Slovenia

2. Plant Cell Biology, Institute of Cellular and Molecular Botany, University of Bonn,

Kirschallee 1, 53115 Bonn, Germany

3. Department of Knowledge Technologies, Jožef Stefan Institute, Jamova cesta 39, 1000

Ljubljana, Slovenia

<sup>4.</sup> Department of Functional & Evolutionary Ecology, University of Vienna, Djerassiplatz

1, 1030 Vienna, Austria

<sup>5.</sup> Mass Spectrometry Unit, Core Facility Shared Services, University of Vienna,

Djerassiplatz 1, 1030 Vienna, Austria

Plant communications 5, no 6 (2024)

https://doi.org/10.1016/j.xplc.2024.100920

113



# Stress Knowledge Map: A knowledge graph resource for systems biology analysis of plant stress responses

Carissa Bleker<sup>1,6,\*</sup>, Živa Ramšak<sup>1,6</sup>, Andras Bittner<sup>2</sup>, Vid Podpečan<sup>3</sup>, Maja Zagorščak<sup>1</sup>, Bernhard Wurzinger<sup>4</sup>, Špela Baebler<sup>1</sup>, Marko Petek<sup>1</sup>, Maja Križnik<sup>1</sup>, Annelotte van Dieren<sup>2</sup>, Juliane Gruber<sup>4</sup>, Leila Afjehi-Sadat<sup>5</sup>, Wolfram Weckwerth<sup>4</sup>, Anže Županič<sup>1</sup>, Markus Teige<sup>4</sup>, Ute C. Vothknecht<sup>2</sup> and Kristina Gruden<sup>1,\*</sup>

https://doi.org/10.1016/j.xplc.2024.100920

#### **ABSTRACT**

Stress Knowledge Map (SKM; https://skm.nib.si) is a publicly available resource containing two complementary knowledge graphs that describe the current knowledge of biochemical, signaling, and regulatory molecular interactions in plants: a highly curated model of plant stress signaling (PSS; 543 reactions) and a large comprehensive knowledge network (488 390 interactions). Both were constructed by domain experts through systematic curation of diverse literature and database resources. SKM provides a single entry point for investigations of plant stress response and related growth trade-offs, as well as interactive explorations of current knowledge. PSS is also formulated as a qualitative and quantitative model for systems biology and thus represents a starting point for a plant digital twin. Here, we describe the features of SKM and show, through two case studies, how it can be used for complex analyses, including systematic hypothesis generation and design of validation experiments, or to gain new insights into experimental observations in plant biology.

Key words: knowledge graph, plant stress responses, plant signaling, systems biology, plant digital twin

Bleker C., Ramšak Ž., Bittner A., Podpečan V., Zagorščak M., Wurzinger B., Baebler Š., Petek M., Križnik M., van Dieren A., Gruber J., Afjehi-Sadat L., Weckwerth W., Županič A., Teige M., Vothknecht U.C., and Gruden K. (2024). Stress Knowledge Map: A knowledge graph resource for systems biology analysis of plant stress responses. Plant Comm. 5, 100920.

# **INTRODUCTION**

The already apparent effects of climate change on agriculture (Shukla et al., 2022), the spread of pests into new regions (Garrett, 2013; IPPC Secretariat, 2021), and rapid population growth (United Nations Department of Economic and Social Affairs Population Division, 2022) present immediate challenges to global food security (Steinwand and Ronald, 2020). Projections show that an increase of up to 75% in crop production is required to meet the 2050 demand (Hunter et al., 2017). This can be achieved with yield improvements through development of stress-resilient crops, a process that requires a holistic understanding of the effects of stressors on plants. The

rapid development of modern "omics" technologies enables the generation of large and complex datasets characterizing system-wide responses. To understand the biological meaning of these large-scale datasets and generate meaningful hypotheses, contextualization within current knowledge is needed. We have assembled an integrated resource for plant signaling, Stress Knowledge Map (SKM; https://skm.nib.si), which provides a single, up-to-date entry point for plant-response investigations.

Published by the Plant Communications Shanghai Editorial Office in association with Cell Press, an imprint of Elsevier Inc., on behalf of CSPB and CEMPS, CAS.

<sup>&</sup>lt;sup>1</sup>Department of Biotechnology and Systems Biology, National Institute of Biology, Večna pot 121, 1000 Ljubljana, Slovenia

<sup>&</sup>lt;sup>2</sup>Plant Cell Biology, Institute of Cellular and Molecular Botany, University of Bonn, Kirschallee 1, 53115 Bonn, Germany

<sup>&</sup>lt;sup>3</sup>Department of Knowledge Technologies, Jožef Stefan Institute, Jamova cesta 39, 1000 Ljubljana, Slovenia

<sup>&</sup>lt;sup>4</sup>Department of Functional & Evolutionary Ecology, University of Vienna, Djerassiplatz 1, 1030 Vienna, Austria

<sup>&</sup>lt;sup>5</sup>Mass Spectrometry Unit, Core Facility Shared Services, University of Vienna, Djerassiplatz 1, 1030 Vienna, Austria

<sup>&</sup>lt;sup>6</sup>These authors contributed equally to this article.

<sup>\*</sup>Correspondence: Carissa Bleker (carissa.bleker@nib.si), Kristina Gruden (kristina.gruden@nib.si)

SKM integrates knowledge on plant molecular interactions and stress-specific responses from a wide diversity of sources, combining recent discoveries from journal articles with knowledge present in established resources such as KEGG (Kanehisa et al., 2016), STRING (Szklarczyk et al., 2023), MetaCyc (Caspi et al., 2016), and AraCyc (Mueller et al., 2003). SKM extends other aggregated resources (listed in Supplemental Table 1), including the heterogeneous knowledge graphs of KnetMiner (Hassani-Pak et al., 2021), Biomine Explorer (Podpečan et al., 2019), and ConsensusPathDB (Herwig et al., 2016), in that it enables conversion of biochemical knowledge to diverse mathematical modeling formalisms and integration with multi-omics experiments, in addition to enabling interactive exploration of current knowledge that is constantly reproducibly updated. SKM is a versatile resource that assists diverse users, from plant researchers to crop breeders, in investigating current knowledge and contextualizing new datasets in existing plant research. A number of tools have been developed within the SKM environment to support this aim and enable efficient linking to complementary tools.

# **RESULTS**

SKM is a resource that combines two knowledge graphs resulting from the integration of dispersed published information on current biochemical knowledge: the Plant Stress Signaling model (PSS) and the Comprehensive Knowledge Network (CKN) of plant molecular interactions. SKM enables interactive exploration of its contents and represents a basis for diverse systems biology modeling approaches, from network analysis to dynamical modeling.

#### The Plant Stress Signaling model

PSS is an ongoing endeavor to assemble an accurate and detailed mechanistic model of plant stress signaling by extracting validated molecular interactions from published resources (Miljkovic et al., 2012; Ramšak et al., 2018). Currently, PSS covers the complete stress response cascade within the plant cell (Figure 1), initiating with abiotic (heat, drought, and waterlogging) and biotic stressors (extracellular pathogens, intracellular pathogens, and necrotrophs; Layer 1). Perception of these stressors through diverse receptors (Layer 2) initiates Ca<sup>2+</sup>, reactive oxygen species (ROS), and MAPK signaling cascades, as well as phytohormone biosynthesis and signaling pathways (abscisic acid [ABA], jasmonic acid [JA], salicylic acid [SA], ethylene, auxin, gibberellins, and cytokinins; Layer 3). These translate perception into a cellular response, resulting in activation of processes that execute protection against stress (Layer 4). Within and across these layers, relevant transcriptional (transcription factors known to act downstream of phytohormones) and posttranscriptional (e.g., small-RNA-transcript regulation known to participate in stress signaling) regulation is included. To capture the relationships between stress responses and growth and development, PSS also contains the major known regulators of growth (target of rapamycin signaling and the above-mentioned hormones) and major primary metabolism processes. Finally, tuberization signaling from potato is included as an example for evaluating potential effects on crop yields.

PSS is based primarily on the model plant *Arabidopsis* thaliana and also contains pertinent information from several

crop species, predominantly potato (Solanum tuberosum). It currently includes 1425 entities and 543 reactions, a substantial update from the preceding model with 212 entities and 112 reactions (Ramšak et al., 2018). PSS entities include genes and gene products (proteins, transcripts, small RNAs), complexes, metabolites, and triggers of plant stress. Genetic redundancy (Cusack et al., 2021) is incorporated using the concept of functional clusters—groups of genes (possibly across species) that are known to mediate the same functions. Functional clusters can be used to obtain a list of candidate genes linked to a particular use case. For further analysis, individual genes within the functional clusters can be prioritized on the basis of context-specific experimental data (e.g., results transcriptomics or proteomics analysis). Interactions between these entities include protein-DNA (e.g., transcriptional regulation), non-coding RNA-transcript, and protein-protein interactions, as well as enzymatic catalysis and transport reactions. The majority of these interactions were compiled from peerreviewed articles with targeted experimental methodology, giving them a high degree of confidence. PSS also contains relevant signaling-associated pathways from KEGG (Kanehisa et al., 2016) and AraCyc (Mueller et al., 2003).

#### The Comprehensive Knowledge Network

Complementary to PSS, CKN is a large-scale condition-agnostic assembly of current knowledge, offering broader insights into not only stress signaling but also any other plant process. CKN is a network of experimentally observed physical interactions between molecular entities, encompassing protein–DNA interactions, interactions of non-coding RNA with transcripts, posttranslational modifications, and protein–protein interactions (Table 1) in *A. thaliana*. Here we present an update of the previous version, which involved 20 012 entities and 70 091 interactions (Ramšak et al., 2018), to the current version, which provides 30% more entities (26 234 entities) and an almost seven-fold increase in the number of molecular interactions (488 390 unique interactions, Table 1). Entities in CKN include 24 829 of 38 202 genes registered in Araport11 (Cheng et al., 2017).

During the update, only STRING was found to have been altered since 2018 (updated to v.11.5 in 2021) and was thus reintegrated. In addition, nine novel sources of information were added, bringing the total number of sources integrated into CKN to 25 (Supplemental Table 2). Interactions are annotated with the interaction type and whether the interaction has directionality (e.g., undirected binding vs. transcription factor regulation). A ranking system for the interaction reliability (Table 1 legend) enables researchers to evaluate the biological credibility and relevance of individual interactions. CKN includes all relevant reactions from PSS to enable direct comparison of results obtained through both networks.

#### SKM environment and features

To enable accessibility and exploitation of the resources within SKM, we have developed an encompassing environment (Figure 2). The main features include content exploration and visualization, access to various export formats, and the ability to contribute improvements based on novel biological knowledge. The SKM webpage is publicly available at https://skm.nib.si/.

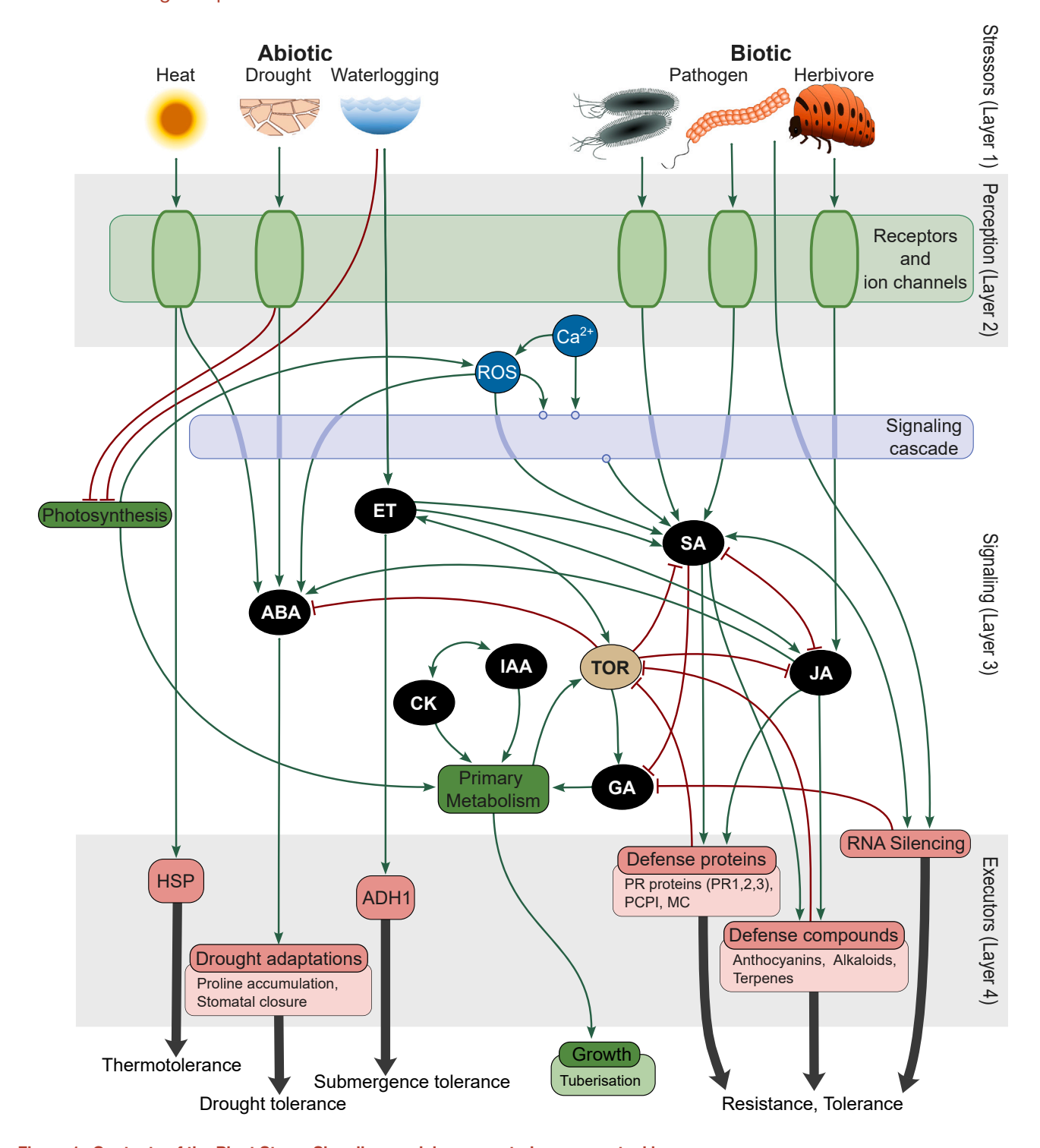


Figure 1. Contents of the Plant Stress Signaling model represented as conceptual layers.

From top to bottom: stressors (Layer 1) acting on the plant are first perceived (Layer 2), resulting in a signaling (Layer 3) cascade that leads to plant defense and/or adaptive changes in the form of executor molecules and processes (Layer 4, examples listed below each group). ABA, abscisic acid; *ADH1*:, alcohol dehydrogenase 1; CK, cytokinin; ET, ethylene; GA, gibberellic acid; *HSP*:, heat shock protein; IAA, indole-3-acetic acid (auxin); JA, jasmonic acid; *MC*:, multi-cystatin; *PCPI*:, potato cysteine proteinase inhibitor; *PR*:, pathogenesis related; ROS, reactive oxygen species; SA, salicylic acid; TOR, target of rapamycin.

# Exploration

SKM provides a number of options for the exploration of its contents, including interactive network visualizations of both PSS (PSS Explorer, Figure 2C) and CKN (CKN Explorer, Figure 2F),

offering neighborhood extraction of selected entities, shortestpath detection between multiple entities of interest, and on-thefly exports. Both explorers provide direct references to the object provenance, as well as links for the corresponding A.

		Rank					
Interaction type	No. of resources	0	1	2	3	4	Total
Binding	13	650	24 054	30 442	343 401	31 253	429 800
Transcription factor regulation	9	480	1442	8567	174	11 869	22 532
Non-coding RNA interactions <sup>a</sup>	3	-	48	41	34 059	-	34 148
Posttranslational modification	2	754	393	192	-	-	1339
Other <sup>b</sup>	1	571	_	_	-	-	571
Total	25°	2455 <sup>d</sup>	25 937	39 243	377 634	43 122	488 390

Table 1. Counts of unique CKN interactions by type and reliability ranking.

Rank meanings: 0, manually curated interactions from PSS; 1, literature-curated interactions detected using multiple complementary (mostly targeted) experimental methods (e.g., luciferase reporter assay, co-immunoprecipitation, and enzymatic assays); 2, interactions detected solely using highthroughput technologies (e.g., high-throughput yeast two hybrid assay, chromatin immunoprecipitation sequencing, and degradome sequencing); 3, interactions extracted from the literature (co-citation, excluding text mining) or predicted in silico and additionally validated with data; 4, interactions predicted using purely in silico binding-prediction algorithms. See Supplemental Table 2 for a detailed list of sources.

thaliana genes within the KnetMiner knowledge base (Hassani-Pak et al., 2021), providing even broader context. An additional visualization of the complete PSS model, showing biological pathways, is available in the Newt Viewer (Figure 2D). A separate search interface using internal and external database identifiers (e.g., DOI, KEGG) is also available for PSS.

#### Modeling and analysis support

PSS is available for download in a number of domain-standard formats (Figure 2H; summarized in Table 2) enabling further visualizations, analysis, and dynamical modeling. A suite of tools implemented in Python (SKM-tools, Figure 2I) has been developed to support additional network analysis of CKN and PSS (described in Table 3).

### Extending and improving SKM

The contribution interface of PSS enables constant updates based on novel discoveries (Figure 2B). Registered users can add new entities and interactions to PSS through guided steps, and expert curators are able to make corrections. For major updates to PSS, a batch upload option is also available. The contribution interface automatically retrieves GoMapMan (Ramšak et al., 2014) gene descriptions and short names, as well as article metadata via DOI or PubMed ID, simplifying the contribution process.

#### **FAIRness**

SKM has been developed with the FAIR principles (Findable, Accessible, Interoperable, and Reusable) (Wilkinson et al., 2016) at the forefront. SKM is indexed in FAIDARE (FAIR Datafinder for Agronomic Research; https://urgi.versailles.inra.fr/ faidare/search?db=SKM), listed in both bio.tools (https://bio. tools/skm) and FAIRsharing.org (https://fairsharing.org/4524), and registered at identifiers.org (https://registry.identifiers.org/ registry/skm). Aside from the downloads, a GraphQL endpoint is available for programmatic access to PSS. SKM also makes use of stable reaction and functional cluster identifiers. Data provenance is maintained by storing links to input data through DOIs and external database references (Figure 2G).

#### **Case studies**

To showcase the benefits of SKM, we present two case studies demonstrating the use of SKM for contextualization of experimental results within prior knowledge networks. The first case study concerns jasmonates (JA) and SA interference with ABAmediated activation of RESPONSIVE TO DESICCATION 29 (RD29) transcription, and the second, a proteomics analysis of Ca<sup>2+</sup>-dependent redox responses.

# Case study 1: Interaction of ABA, JA, and SA in the activation of RD29 transcription

In A. thaliana, the RESPONSIVE TO DESICCATION 29 A gene (AtRD29A) plays a pivotal role in stress acclimation (Baker et al., 1994) and is transcriptionally regulated via several promoter elements, including the ABA-responsive binding motif ABRE (ACGTG), located close to the transcription initiation site. The 1-kb upstream region of the potato StRD29 transcription initiation site also contains ABRE and several other abiotic-stressresponsive binding elements (Supplemental Figure 1).

ABA treatment of leaf discs from tobacco plants transiently transformed with pStRD29::fluc and from transgenic potato plants (cv. Désirée) carrying the pStRD29::mScarlet-I (Supplemental Figure 2) construct strongly induced pStRD29 activity, which reached its highest amplitude after approximately 4 h in the ABA solution (Figure 3A). Treatments with either jasmonates (JA/MeJA) or SA alone did not lead to an increase in pStRD29 activity. However, combined treatments of ABA with JA or ABA with SA attenuated the ABA-induced activation of pStRD29, revealing a negative effect of both these phytohormones on ABA-dependent StRD29 transcription (Figure 3A). We subsequently constructed transgenic potato plants (cv. Désirée) carrying the pStRD29::fluc construct to confirm the negative effect of MeJA and SA on ABA-responsive promoter activity in planta (Figure 3B). The effect of MeJA on ABA activation of both RD29s was further analyzed in potato and A. thaliana by quantitative real-time PCR. The data revealed attenuation of ABA induction of RD29A/RD29 by jasmonates in both species (Figure 3C).

We first tried to explain the observed effect of jasmonates and SA on ABA-dependent RD29 activation through promoter motif analysis, but no SA- or JA-signaling-related motifs were identified in

<sup>&</sup>lt;sup>a</sup>Currently only miRNA interactions are included in CKN.

<sup>&</sup>lt;sup>b</sup>Includes interactions from PSS that do not fall into the previous categories.

<sup>&</sup>lt;sup>c</sup>Some resources contain multiple interaction types.

<sup>&</sup>lt;sup>d</sup>Includes interactions expanded from 335 PSS functional clusters to 2253 individual genes.

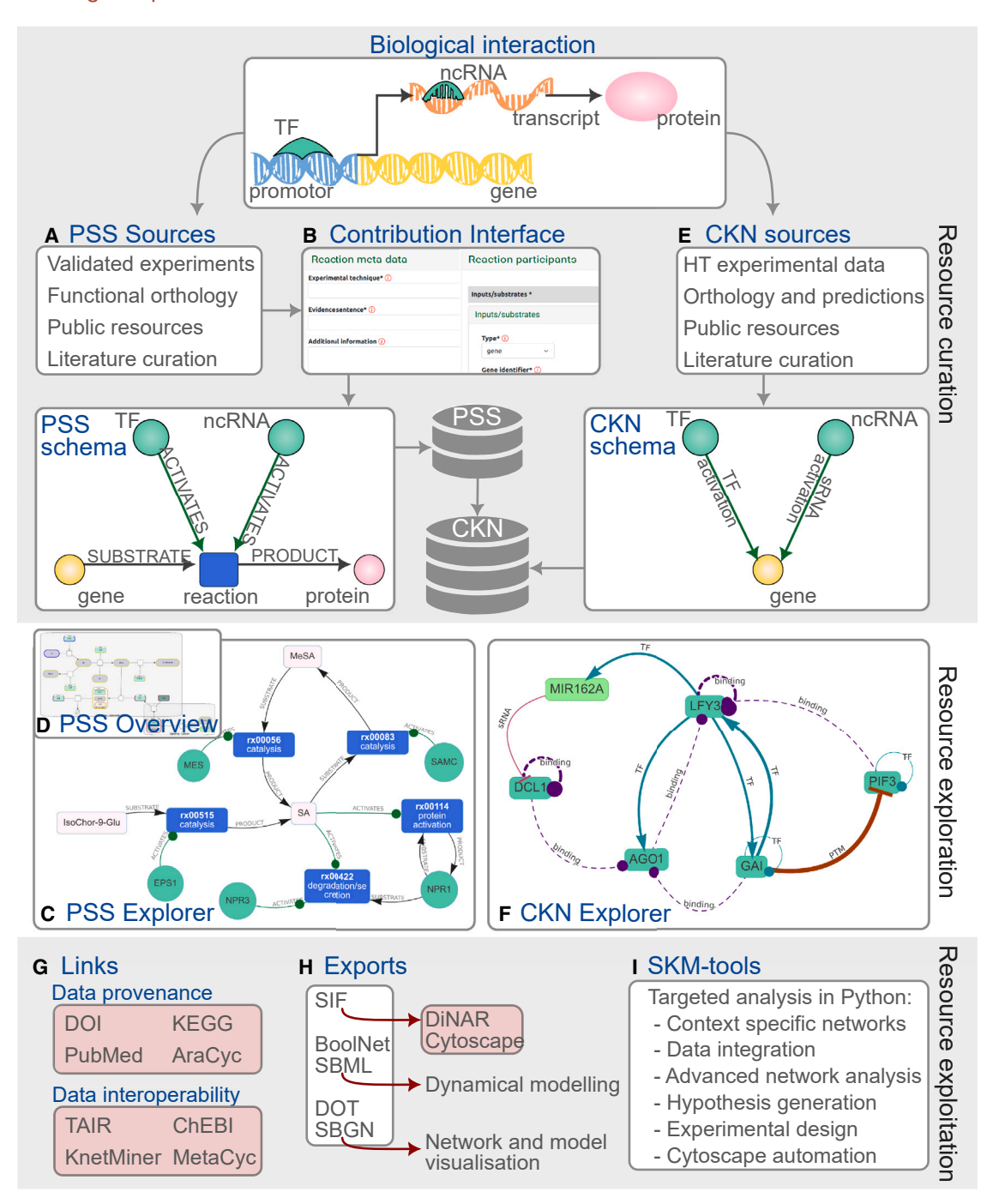


Figure 2. Stress Knowledge Map environment and features.

New validated biological interactions (e.g., transcriptional and translational regulation of a target gene) from various sources (A) can be added to PSS through the guided contribution interface (B) and are consolidated according to the PSS schema. The contents of PSS can be explored through interactive search and visualization provided by both the PSS Explorer (C) and the PSS overview in Newt (D). Correspondingly, sources for CKN interactions (E) are integrated and consolidated into the CKN schema through batch scripts and are accessible for exploration through the CKN Explorer (F), which provides interactive search and visualization of CKN interactions. Data provenance and interoperability links (G) provide context for SKM contents. Exports of PSS and CKN (H) enable various additional analysis and modeling approaches, including through the Python functions provided in the SKM-tools resource (I). Links to specific external resources and tools are highlighted in red. HT, high throughput; PSS, Plant Stress Signaling network; CKN, Comprehensive Knowledge Network; TF, transcription factor; ncRNA, non-coding RNA (currently only miRNAs are included); DOT/SBGN/SBML/SIF, systems biology data formats, see Table 3 for details.

Format	Description	Available for
SBGN-ML	Systems Biology Graphical Notation XML format, enabling graphical visualization of models (Bergmann et al., 2020)	PSS
SBML	Systems Biology Markup Language XML format, enabling mechanistic modeling (Keating et al., 2020)	PSS
DOT	Graph description language compatible with Graphviz applications (Gansner and North, 2000; graphviz.org)	PSS
SIF/LGL	Simple interaction format/large graph format compatible with Cytoscape (Shannon et al., 2003) and DiNAR (Zagorščak et al., 2018)	PSS, CKN
boolnet	Boolean network format for logical modeling compatible with pyboolnet (Klarner et al., 2017) and BoolNet (Müssel et al., 2010), among others	PSS

Table 2. Supported exports of SKM knowledge graphs.

the potato promoter sequence (Supplemental Figure 1). We therefore hypothesized that the signaling pathways interact upstream of actual transcriptional activation. Owing to the complexity of several phytohormone pathway interactions, this was a good case study for the hormone-centric and expertcurated PSS model. We performed a triple shortest-path analysis to identify potential mechanisms of studied crosstalk. This analysis revealed an intersection of JA signaling with the ABA pathway through a protein-protein interaction of the JAresponsive MYC-like transcription factor 2 (MYC2) with the ABA receptor PYRABACTIN RESISTANCE-LIKE 6 (PYL6; Figure 3D). This reaction entry (rx00459) is based on experimental in vitro and in vivo interaction studies of PYL6 and MYC2 in A. thaliana (Aleman et al., 2016). It is conceivable that this interaction depletes PYL, thereby limiting ABA perception (Aleman et al., 2016), which could explain the lower activation of the ABA pathway in the presence of jasmonates. The SA pathway was found to converge with the ABA pathway through the JA pathway with a protein-protein interaction between the SA receptor NPR1 and MYC2 (rx00432) (Nomoto et al., 2021), and this might influence the interaction of MYC with PYL. To verify the hypothesis of direct synergism between JA and SA in attenuation of the ABA response, we performed titration experiments of combined JA and SA treatment on ABAdependent StRD29 induction, which was confirmed (Figure 3E; Supplemental Table 3).

Case study 2: Effect of the Ca<sup>2+</sup> channel inhibitor LaCl<sub>3</sub> on proteome-wide peroxide responses

Secondary messengers such as Ca2+ and H2O2 are important in the translation of many perceived environmental changes towards a cellular response (Kudla et al., 2010; Pirayesh et al., 2021). It is still a challenge to disentangle and understand the principles of specificity and information flow in such networks. Lanthanide ions are known to block anion channels and inhibit the flux of Ca<sup>2+</sup> across the plasma membrane (Knight et al., 1992; Tracy et al., 2008). Thus, they can be used to identify Ca<sup>2+</sup>-dependent plant responses. H<sub>2</sub>O<sub>2</sub> is known to induce Ca<sup>2+</sup> transients (Rentel and Knight, 2004). In this case study, we analyzed the proteome of A. thaliana rosettes treated with either H<sub>2</sub>O<sub>2</sub> or a combination of H<sub>2</sub>O<sub>2</sub> and LaCl<sub>3</sub> to identify the components of H<sub>2</sub>O<sub>2</sub> signaling that are Ca<sup>2+</sup> dependent. We initially identified 119 proteins whose abundance changed significantly in response to H<sub>2</sub>O<sub>2</sub> compared with the mock treatment after 10 or 30 min of treatment. Of these, 49 proteins did not respond significantly in the same manner upon pretreatment with LaCl<sub>3</sub>

(Supplemental Table 4), indicating that a significant number of H<sub>2</sub>O<sub>2</sub>-induced changes in protein abundance required a Ca<sup>2+</sup> signal (Ca<sup>2+</sup>-dependent redox-responsive proteins).

In the guest to identify mechanistic explanations for these results, CKN provides a universal resource for large-scale hypothesis generation. The largest connected component of CKN contains 98% of the nodes and 99% of the edges, indicating its high connectivity; thus, the analysis was performed on this part of CKN only. Using CKN prefiltered to only leaf-expressed genes, we searched for directed shortest paths from known Ca2+signaling-related proteins (source set) to the Ca2+-dependent redox-responsive proteins identified by the proteomics approach (target set). The final source set of 53 genes included mainly calmodulins, Ca<sup>2+</sup>-dependent protein kinases, and calcineurin B-like proteins (Supplemental Table 4). Of the 49 Ca<sup>2+</sup>-dependent redox-responsive target proteins, 41 were present in CKN. All of these proteins either could be connected to the source set of Ca<sup>2+</sup>-signaling-related proteins, directly or through an up-to-four-step pathway (Figure 4A), or were in the source set themselves. Combining all the detected shortest paths (all sources to all targets) into a single network (Figure 4A) revealed major network hubs-connected to multiple known Ca2+ signaling genes and potentially regulating multiple targets. For example, the analysis revealed an intricate network of calmodulin-dependent regulation of downstream targets in A. thaliana (CAM2,3,5,6,7, Figure 4B). Another example of such a hub is Floricaula/leafy-like transcription factor 3 (LFY3), shown in Figure 4C, which integrates paths originating from four source nodes and in turn potentially regulates four downstream targets.

The next step in the analysis would be confirmation of the identified mechanisms by functional analysis experiments, e.g., knockout experiments to confirm the role of the proposed regulatory network. The design of such experiments is, however, not always trivial; thus, we designed the CUT-tool within SKM-tools to aid experimentalists. This analysis reveals the minimum interactions that must be severed ("cut-set") to separate the upstream regulators from the downstream targets. The cut-set to disrupt the regulation of all targets is shown in Figure 4A. As an example, the cut-set of one target, glutamine-dependent asparagine synthase 1 (ASN1), is shown in Figure 4C, revealing that deregulation of ASN1 would require knockout of both LFY3 and A. THALIANA NAC DOMAIN CONTAINING PROTEIN 29 (NAP) genes.

Functionality	Description		
Load	Directly create networkX (Hagberg et al., 2008) graph objects for PSS or CKN, thus providing access to the multitude of graph analysis and graph operations available in the library		
Node filter	For PSS and CKN, filter on node type or node origin (plant or foreign), and additionally for CKN filter nodes based on tissue specificity, creating a network specific to the biological question at hand		
Edge filter	Filter CKN edges by rank, removing less reliable edges as the situation requires		
Network analysis	Standard node-based analysis approaches, such as neighborhood extraction (identifying the immediate interactors of a node) and shortest-path analysis (identifying directed or undirected paths between source and target nodes of interest)		
CUT-tool	CUT-tool provides information on which genes must be perturbed (knockout, knockdown, or overexpression) to modulate the response of the network		
Cytoscape automation	Loading of networks and subnetworks into Cytoscape (Otasek et al., 2019); functionalities include providing default styling; node, edge, and path highlighting; network layout from coordinates; and pdf exporters		
Multi-omics data visualization	Import of multi-omics experimental data tables (e.g., logFC and <i>p</i> values) as context to the networks and functionality to visualize experimental data associated with nodes in the network, through rendering of PNGs (e.g., heatmaps) per node in the Cytoscape view		
Link to DiNAR	Instructions for the use of CKN or PSS as the prior knowledge network for integration and visualization of multiple-condition high-throughput data in the DiNAR application (Zagorščak et al., 2018)		

Table 3. Features of SKM-tools.

# DISCUSSION

Plant stress signaling pathways are connected by synergistic and antagonistic interactions in a complex network that checks and balances the plant's response to its environment and its growth/development (Eckardt, 2015; Bittner et al., 2022). To understand the functioning of these complex processes, novel approaches are required. Knowledge graphs, such as those provided by SKM, provide powerful and accessible tools to integrate and simplify interpretations within curated published knowledge, as well as providing a basis for a plant digital twin and all the advantages of *in silico* simulation experiments it enables. A number of tools have been developed within the SKM environment to support this and also enable efficient linking to complementary tools.

To showcase the applicability of SKM, we investigated two distinct experimental datasets. In the first, our experiments provided evidence that jasmonate and SA treatment attenuates ABA-activated transcription of RD29 in both the crop plant potato and the model plant A. thaliana through hormonal signaling cross-talk (Figure 3). A manual attempt to extract known information on the crosstalk between ABA and JA with a search in PubMed ((JA OR jasmon\*) AND (ABA OR abscisic) AND (plant)) resulted in over 2000 published items. With the wealth of data generated these days, it would be laborious for an individual researcher to perform a thorough literature survey: instead, interrogation of SKM provided a mechanistic hypothesis that explained the experimental results within hours. The hypothesis was empirically supported by further experiments and provides an explanation for the synergistic action of jasmonates and SA that is sometimes argued for in the literature (Mur et al., 2006; Zhang et al., 2020). However, additional experiments are needed to determine (and potentially confirm) whether the exact synergistic mechanism lies in the NPR1-MYC2-PYL6 interaction. Although knowledge compiled in SKM is predominately based on A. thaliana, this use case clearly shows its applicability to other species. Through orthology tools

such as PLAZA (Van Bel et al., 2022), the knowledge graphs in SKM can be translated to other species, as was done with the previous version of CKN for *Prunus persica* (Foix et al., 2021), *S. tuberosum* (Ramšak et al., 2018), and *Nicotiana benthamiana* (Juteršek et al., 2022). This way, canonical principles of plant signaling networks can be assessed across species.

Our second case study showed that SKM is not only helpful in revealing mechanisms in complex pathways for a single target but also can be used to identify regulators using a large number of targets, as is commonly the case with interpretation of large omics datasets. Using network analyses, arguably the simplest qualitative modeling approach, we identified hubs involved in complex redox-Ca<sup>2+</sup> signaling interconnectedness. By identifying connections from known Ca2+-related proteins to our experimentally derived target list, we were able to prioritize certain processes and hypotheses in an informed manner. The majority of our targets were found to have only one or two intermediary nodes between them and the upstream Ca2+related proteins. Paths with many intermediary nodes are less likely to be valid sources of regulation; however, examples of longer paths such as these are known to be functional in the cell, e.g., MAPK signaling cascades. One of the SKM-tools features, the CUT-tool, was designed to help in the next step of research: validation of generated hypotheses. It enables the design of complex functional validation experiments (e.g., gene knockout or overexpression) identifying the genes whose activity should be modulated to achieve a desired effect, taking network redundancy into account.

Overall, in both case studies, SKM proved to be a useful generator of potential mechanistic explanations for the observed data. As with any hypothesis, further validation is needed and some may not prove as valid. More likely hypotheses for further research can be prioritized by weighing the interaction reliability (edge ranks) and exploring the linked content in other resources.

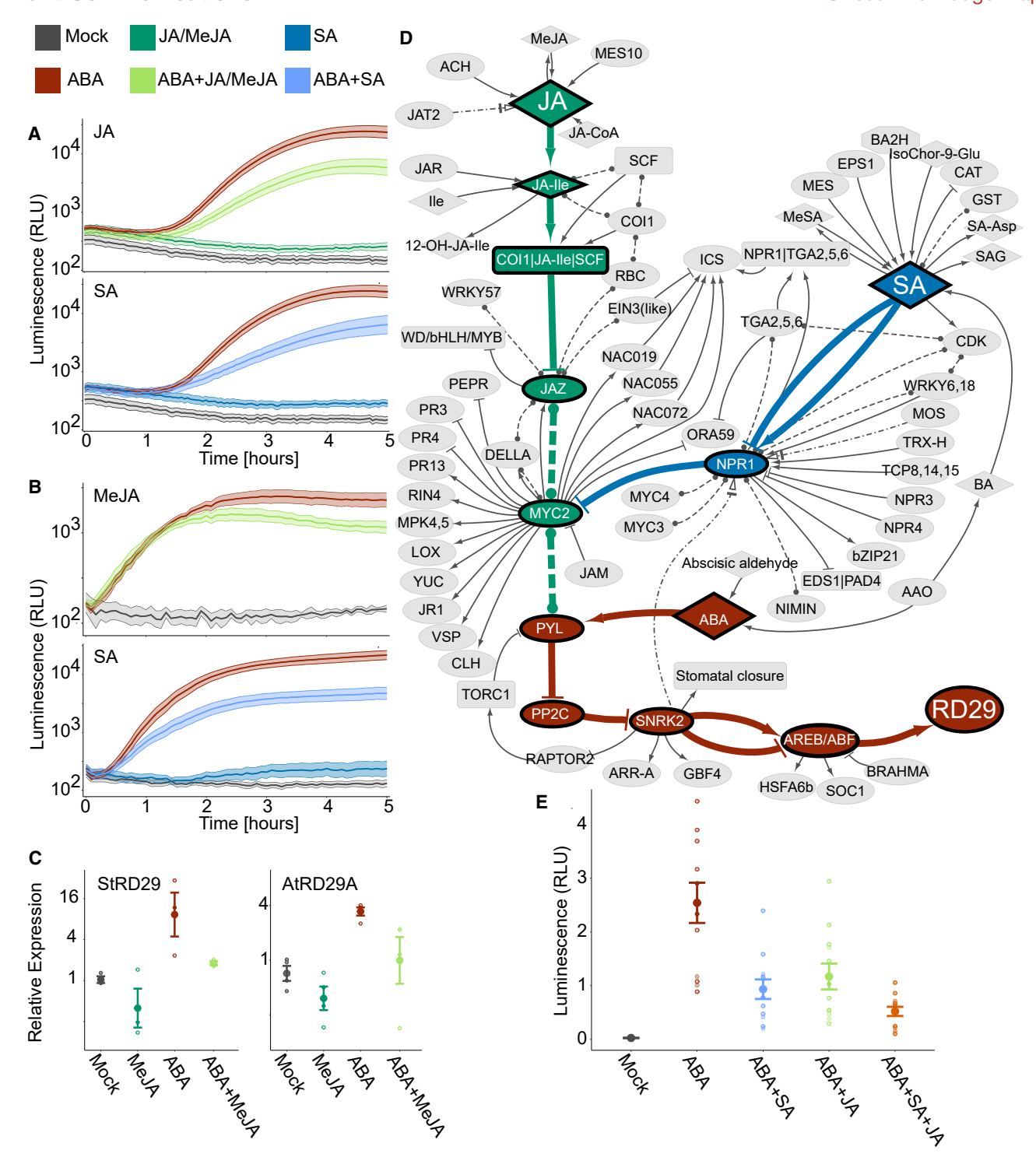


Figure 3. Elucidating connections from JA and SA to ABA-mediated regulation of RD29 expression in potato.

(A and B) Expression of firefly luciferase driven by the StRD29 promoter (pStRD29::fluc) in (A) transiently transformed tobacco leaves treated with the indicated hormones (25  $\mu$ M JA, 50  $\mu$ M ABA, and 50  $\mu$ M SA) and (B) transgenic potato leaves treated with the indicated hormones (50  $\mu$ M MeJA, 50  $\mu$ M ABA, and 50  $\mu$ M SA). Values are shown as mean  $\pm$  SE. Data are provided in Supplemental Table 3.

(C) Relative transcript abundance of StRD29 (left) and AtRD29A (right) 6 h after application of 50  $\mu$ M ABA, 50  $\mu$ M MeJA, or a combination of both, analyzed by quantitative real-time PCR. Bars represent mean values  $\pm$  SE of three or four independent biological replicates.

(D) PSS node-induced subnetwork of shortest paths and immediate neighbors. Paths are directed from the hormones (source) to RD29 (target). Nodes and edges are colored by the path source: ABA (brown), JA (green), and SA (blue). Edges to first neighbors, edges not on the directed shortest paths, and

# Stress Knowledge Map

Plant digital twins, virtual replicas of physical systems, are expected to provide a revolutionary platform for modeling the effect of crop management systems and environmental changes in agriculture (Pylianidis et al., 2021). Digital twins can be used to perform *in silico* experiments that guide or replace lab and field experiments. The detail that digital twins provide, combined with fast computational methodologies, enables efficient planning of experiments and will thus speed up our understanding of plant function and provide information for more effective breeding. Aside from being a tool for the interpretation of experimental data, SKM also provides a starting point for the integration of stress signaling and growth trade-offs in digital twins.

SKM will be continuously updated, keeping abreast of the latest developments in the field. Future plans include extending the repertoire of stressors to include additional factors such as cold, salinity, or nutrient deficiencies. We believe the integrated knowledge in SKM will help in understanding plant interactions with the environment by enabling exploration of knowledge and by supporting diverse mechanistic modeling approaches. This is of interest to the wider plant scientific community, enabling the informed design of experiments and, in the long term, contributing to the breeding of improved varieties and precision agriculture.

#### **METHODS**

#### **PSS** construction

From the predecessor model (PIS v.2; Ramšak et al., 2018), numerous improvements, additions, and reformulations were carried out, resulting in the current PSS. In addition to intracellular pathogens (potyviruses), we extended PSS to also contain perception of extracellular pathogens (*Pseudomonas* sp.) and insect pests, as well as heat, drought, and waterlogging stress. Downstream of perception, PSS now includes Ca<sup>2+</sup> signaling, ROS signaling, and the MAPK signaling cascade, as well as the synthesis and signaling of all major phytohormones. We also added the synthesis of actuator molecules and processes, as well as known regulators of growth and major processes leading to growth.

PSS is implemented as a Neo4j graph database. The types of nodes and edges (relationships) in the database are summarized in Supplemental Table 5. Genes and gene products are represented by functional cluster nodes, including protein and non-coding RNA nodes. Functional clusters enable the representation of genetic redundancy. These groups were defined using sequence similarity among genes (orthologs and paralogs) and experimental data that confirmed functional overlap. The functional cluster concept includes groupings of enzyme-coding genes (similar to the EC number system), as well as genes involved in transcriptional and translational regulation. Users can access the same information in PSS at the gene level by utilizing the gene-level representation of PSS interactions in CKN. Groups of metabolites with the same biological function are also represented as metabolite families. Nodes also include more abstract entities, such as known but unidentified gene products and plant processes. Finally, foreign entities, such as biotic or abiotic stressors, are also included as nodes.

In addition to biological entities, molecular interactions are also represented by nodes in PSS and are categorized into 10 formal reaction types

#### **Plant Communications**

(e.g., protein activation or catalysis, Supplemental Table 5). Reaction participant nodes are connected to the reaction nodes by relationships, with the type of relationship representing the role of the participant (e.g., SUBSTRATE, ACTIVATES), as demonstrated in Figure 2B. These relationships are annotated with the subcellular location and the form of the participant when involved in the reaction (e.g., "cytoplasm" or "nucleus" and "gene" or "protein").

Where applicable, nodes are annotated with their provenance (e.g., a DOI) and additional information such as biological pathways, gene identifiers, descriptions and annotations (TAIR [Berardini et al., 2015] and GoMapMan [Ramšak et al., 2014]), references to external resources (DOI, PubMed, KEGG [Kanehisa et al., 2016], MetaCyc [Caspi et al., 2016], AraCyc [Mueller et al., 2003], and ChEBI [Hastings et al., 2016]), and explanatory statements (such as a quote from the article and the experimental techniques used in the original experiments).

PSS is available in a number of standard systems biology formats, including SBML (using libSBML [Bornstein et al., 2008]), SBGN (using libSBGN [König, 2020] and pySBGN [Podpečan, 2023] libraries), DOT (using pygraphviz [Aric et al., 2024] and pydot [Sebastian et al., 2023]), and a Boolean formulation in boolnet format. SKM also supplies several generalized formats of PSS in JSON and TSV, enabling multiple formulations of the network model.

All updates to PSS are immediately available in the various interfaces and in all download formats (https://skm.nib.si/downloads). A frozen version (PSS v.1.0.0) is also available in all export formats, and a database dump with detailed deployment instructions can be accessed at GitHub (https://github.com/NIB-Sl/skm-neo4j). All sources and resources used to create PSS v.1.0.0 are available in Supplemental Table 6.

#### **CKN** construction

The second edition of CKN (CKN v.2) was created by merging pairwise interactions from 25 public resources (details in Supplemental Table 2). Additional filtering was performed on the STRING v.11.5 network (Szklarczyk et al., 2023), where the requirement was to only include physical interactions confirmed by experimental data or existence in a database. As Table 2 summarizes, five reliability ranks were designed to describe the reliability of the interactions across the diversity of the various sources. All interactions were then integrated, resulting in a single network of 574 538 interactions. The network was then condensed by collapsing multiple interactions of the same type between a pair of interactors into a single edge. In this process, the highest ranked interaction took precedence to define the interaction type, but all sources that contained any interaction between the pair were retained in the edge attributes.

All gene loci nodes were annotated using Araport11 (Cheng et al., 2017) downloaded from TAIR in June 2023 (Berardini et al., 2015). Gene loci that had been merged or made obsolete were renamed or removed, respectively. Genes are also annotated with Plant Ontology annotations from TAIR (Berardini et al., 2015) (based on gene expression patterns reported in publications), enabling the extraction of tissue-specific interaction networks.

CKN v.2 is available as part of the SKM application and on the downloads page (https://skm.nib.si/downloads).

shared neighborhood nodes are indicated in gray. Solid edges indicate activation (arrowhead) or inhibition (T head), dashed edges represent binding, and dot-dash edges indicate transport.

(E) Verification of the hypothesis presented in (D). Concentrations of hormones are 50 µM ABA, 15 µM JA, and 30 µM SA. Luciferase activity at 5 h is shown (see Supplemental Table 3 for complete response curves). The results show that SA and jasmonates indeed act synergistically on attenuation of ABA signaling, as the addition of SA and JA has a stronger effect than the addition of each hormone individually.

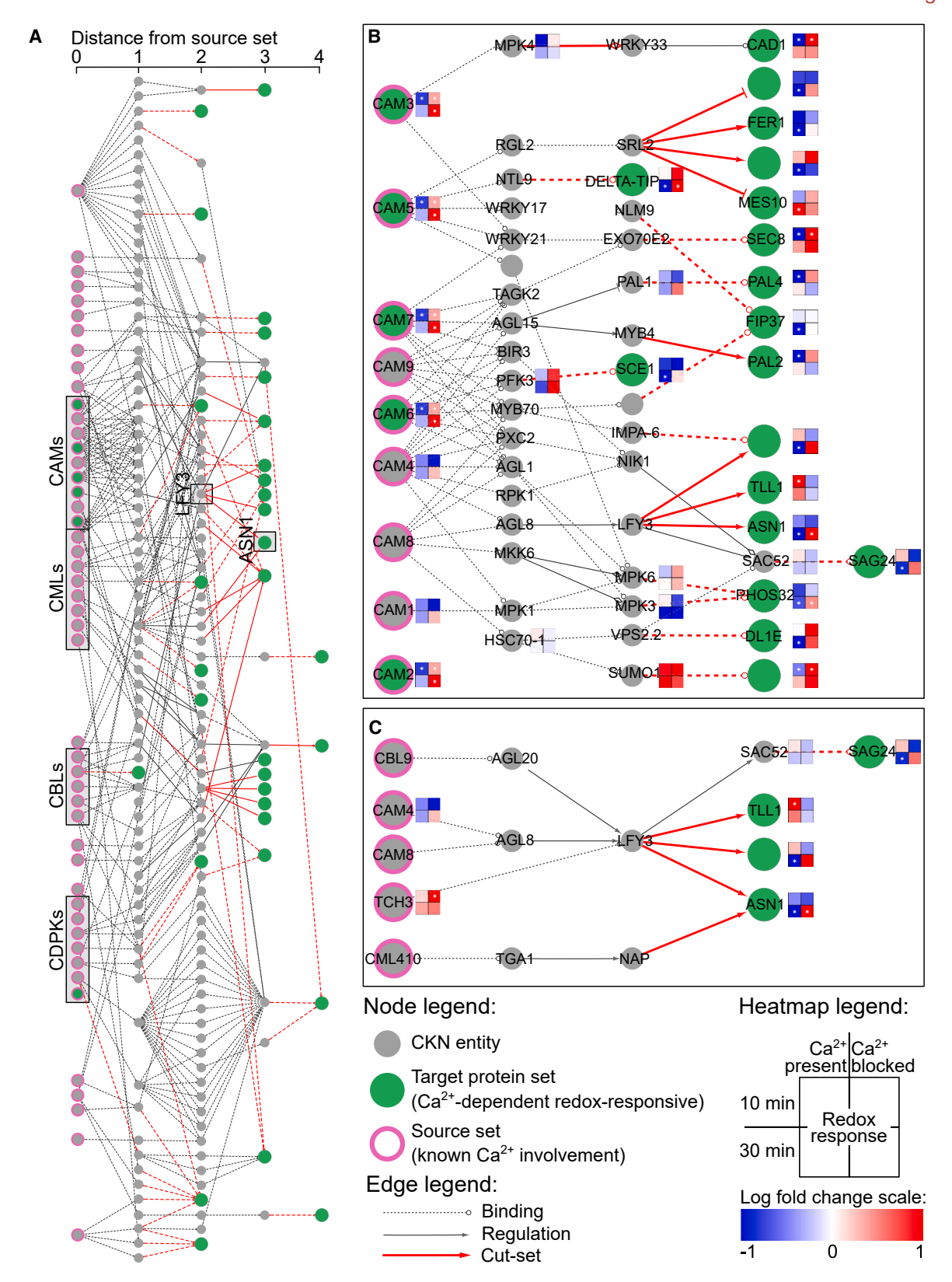


Figure 4. Deciphering the Ca<sup>2+</sup>-dependent network in peroxide signaling.

(A) All shortest paths identified in CKN leading from known Ca<sup>2+</sup>-related proteins (sources, pink-bordered nodes) to Ca<sup>2+</sup>-dependent redox-responsive proteins identified by proteomics (targets, green-filled nodes) using rank 0, rank 1, and rank 2 edges (as described in the Table 1 legend), merged into a single network. The excerpts show (B) a subnetwork with a focus on calmodulins and (C) a subnetwork with a focus on LFY3 and ASN1. Solid edges with (legend continued on next page)

#### Stress Knowledge Map

# Plant Communications

#### SKM environment

The SKM web application is implemented in Python using the microframework Flask. The interactive visualizations of PSS and CKN are based on Biomine Explorer (Podpečan et al., 2019) implemented using vis.js and open-source Python libraries (including networkX [Hagberg et al., 2008] and graph-tools [Peixoto, 2014]) and are freely available on GitHub at <a href="https://github.com/NIB-SI/ckn\_viz">https://github.com/NIB-SI/ckn\_viz</a> and <a href="https://github.com/NIB-SI/pss\_viz">https://github.com/NIB-SI/pss\_viz</a>, respectively. The mechanistic interface to PSS is provided through an instance of the Newt Editor (Balci et al., 2021) using the SBGN standard.

#### SKM-tools

SKM-tools (https://github.com/NIB-SI/skm-tools) is a collection of Python scripts and notebooks, incorporating network analysis and visualization tools, that facilitates interrogation of CKN and PSS with targeted questions beyond the scope of the web application. Included functionalities are described in Table 3. The tools are developed using the networkX (Hagberg et al., 2008) and py4cytoscape (One et al., 2021) libraries.

The CUT-tool makes use of the max-flow min-cut (Edmonds and Karp, 1972) algorithm, which determines the minimum edges that must be severed ("cut-set") to separate the upstream sources from the downstream targets. A max-flow min-cut analysis of multiple sources to an individual target reveals the minimum cut-set needed to disrupt all signaling to the target. To calculate the max-flow min-cut across multiple sources, a dummy node connected with arbitrarily high capacity to all original sources is introduced, and the calculation is performed using the dummy node as the source.

#### Case studies

#### Promoter analysis

Predicted *cis*-regulatory motifs within the 1-kb promoter sequences of *AtRD29A* and *StRD29* were identified with the Atcis database of the *A. thaliana* Gene Regulatory Information Server (Lichtenberg et al., 2009). In addition, we used PlantPAN 3.0 (Chow et al., 2019) to identify *StRD29*-specific motifs that were not previously identified in *AtRD29A*. *Plant material and growth conditions* 

S. tuberosum (cv. Désirée) plants were propagated by cuttings from sterile-grown plants. After 7 days of sterile growth on  $^{1}\!/_{2}$  MS medium (pH 5.7, 2% [w/v] sucrose) to initiate root growth, plantlets were transferred to individual pots filled with soil (9 parts soil, 1 part Perligran). A. thaliana (ecotype Col-0) seeds were sown directly onto soil and transferred into individual pots after 4–6 days. All experiments used leaves from 18- to 21-day-old plants grown in climate chambers (20°C  $\pm$  2°C) under long-day conditions (16 h light/8 h dark) with a light intensity of 120  $\mu$ mol photons  $m^{-2}$  s $^{-1}$  (Philips TLD 18W alternating 830/840 light color temperature).

For promoter reporter assays of transiently transformed *N. benthamiana* leaves, seeds were germinated on Profi substrate (Gramoflor). Five days after germination, seedlings were separated into pots of 15.5 cm diameter  $\times$  12 cm height filled with substrate (3 parts Profi substrate, 1 part vermiculite, 1.5 kg Osmocote Start/m³). Plants were grown in a greenhouse under long-day conditions (16 h light at 28°C/8 h dark at 22°C) with an average light intensity of  $\sim\!\!250~\mu\text{E}$  and 80% relative humidity.

Soltu.DM.03G017570 was identified as the orthologous locus of A. thaliana RD29A in S. tuberosum cultivar DM1-3 using the DM v.6.1 database (http://spuddb.uga.edu/). To generate the gene reporter lines in the potato cultivar

Désirée, 1158 bp of the 5' UTR directly upstream of the start codon region was amplified by PCR and either the firefly luciferase (fluc) or the *mScarlet-l* (*mScar*) gene in a custom variant of the pBIB Hyg vector carrying hygromycin resistance for selection in plants. The complete sequences of both vectors, including annotations, can be found in Supplemental Figure 4. Both constructs were introduced into the potato cultivar Désirée as described previously (Rocha-Sosa et al., 1989).

#### Plate-reader-based luciferase assays

Agrobacteria carrying the pBIN-StRD29::fluc or pBIN-AtRD29A::fluc plasmid were grown in LB liquid medium supplemented with the respective antibiotics. Overnight cultures were diluted to OD600 = 0.1 with fresh LB medium and grown to OD600 = 0.8. Cells were harvested by centrifugation (22°C, 15 min, 4000 g) and resuspended in 5% sucrose solution in  $H_2O$  to OD600 = 0.2. The agrobacterium suspension was infiltrated into leaves 6, 7, and 8 of 4-week-old N. benthamiana plants. Care was taken that the N. benthamiana plants selected for infiltration and measurement were not suffering an obvious pathogen attack before infiltration and during the transformation period, hormone treatment, and measurement. After 48 h, leaf discs (ø 6 mm) of infiltrated plants were transferred into 96-well plates containing 100 µl buffered MS (5 mM MES [pH 5.8]) supplemented with 1% sucrose (w/v) and incubated for 2 h under greenhouse growth conditions. Immediately before measurement, luciferin, to a final concentration of 30  $\mu$ M, and the hormones, to the final concentrations indicated in the text, were added to each respective well. For all combinatorial hormone treatments, the different hormones were applied at the same time to the indicated final concentrations. Fluc luminescence was recorded in a multi-mode microplate reader (TECAN Spark multimode microplate reader, serial no. 2301004717) in a window from 550 to 700 nm for 2 s every 5 min for each well. During the measurement period, the leaf discs were kept in darkness at a constant temperature of 22°C.

For luminescence measurements of *S. tuberosum StRD29::fluc* plants, leaf discs (ø 6 mm) were placed in 96-well plates containing 100  $\mu l$  of 30  $\mu M$  luciferin dissolved in  $^{1}\!/_{2}$  MS. After 2 h of preincubation, the solution was replaced by 100  $\mu l$  of 30  $\mu M$  luciferin containing various effectors (50  $\mu M$  ABA, 50  $\mu M$  MeJA, or both). Since MeJA is rapidly hydrolyzed to JA (Stuhlfelder et al., 2002; Wu et al., 2008), JA and MeJA treatments are comparable when eliciting a jasmonate response. Luminescence was measured every 5 min for up to 12 h using a TriStar2 LB 492 multimode reader (Berthold Technologies, Germany). During the measurement period, the leaf discs were kept in darkness. All luminescence analysis was performed with at least five independent experimental replicates. Luminescence data are available in Supplemental Tables 3 and 7.

#### Transcript analysis

For analysis of StRD29 and AtRD29A transcripts, S. tuberosum or A. thaliana plants were treated with water (mock),  $50~\mu\text{M}$  ABA,  $50~\mu\text{M}$  MeJA, or a combination of both for 6 h in three or four independent biological replicates. Total RNA was extracted from 100 mg of leaf material using the Gene Matrix Universal RNA Purification Kit (Roboklon, Germany) according to the manufacturer's instructions. RNA integrity was assessed by agarose electrophoresis and RNA quantity and purity with a UV-vis spectrophotometer (Eppendorf, Germany). For quantitative real-time PCR, RNA was transcribed into cDNA using the RevertAid First Strand cDNA Synthesis Kit (Thermo Scientific, Germany). The reaction was stopped by a 5-min incubation at  $75^{\circ}\text{C}$ .

Where applicable, all primers were designed to span exon-intron borders using QUANTPRIME (Arvidsson et al., 2008) (gene identifiers and primer

arrowheads indicate directed, regulatory interactions (see Table 1), whereas dashed edges indicate undirected binding. Red edges are part of the merged cut-set. Nodes with proteomics measurements are annotated with a heatmap indicating the change in protein abundance after 10 min (top row) and after 30 min (bottom row) between H<sub>2</sub>O<sub>2</sub>- and mock-treated samples (left column) and between Ca<sup>2+</sup> blocker treatment and H<sub>2</sub>O<sub>2</sub> and Ca<sup>2+</sup> blocker treatment (right column). Significant changes in abundance are marked with a white asterisk in the center of the square. Red, increase in treatment compared with control; blue, decrease in treatment compared with control. Nodes are labeled with their short names, where available. The complete network is provided in Supplemental Figure 3, and all source and target nodes are listed in Supplemental Table 4.

Plant Communications Stress Knowledge Map

sequences in Supplemental Table 8). Quantitative real-time PCR was performed with three technical replicates for each sample in 96-well plates using a CFX96 real-time thermal cycler system (Bio-Rad, Germany). Each reaction contained 1× SYBR Green master mix (Thermo Fisher), 2 ng/μl cDNA, and the respective forward + reverse primers at 10 μM each. The specificity of each product was assessed on the basis of melting curves after 40 cycles of amplification. All transcript levels were normalized against the geometric mean of the transcript abundances of the reference genes YLS8 and CYP5 for A. thaliana and YLS8 and ACT7 for potato. Target relative copy numbers were calculated using quantGenius (http://quantgenius.nib.si/; Baebler et al., 2017), provided in Supplemental Table 9.

#### PSS network analysis

We identified the pathway between ABA and *RD29* by querying for all directed shortest paths from ABA to *RD29* in the reaction participant bipartite projection of PSS. We then extracted all directed shortest paths from JA and SA to *RD29* that partially overlapped with the ABA-to-*RD29* path. For added context to these results, we expanded the network induced by the shortest paths to include the first neighbors of all nodes (Figure 3E).

Analysis was performed in Python using the networkX library (Hagberg et al., 2008) and visualized in Cytoscape (Cline et al., 2007) using the py4cytoscape library (Ono et al., 2021). All code is available in the SKM-tools repository (https://github.com/NIB-SI/skm-tools).

#### Proteomic analysis

Complete rosettes of 3-week-old A. thaliana plants were incubated in 1 mM LaCl $_3$  solution or ddH $_2$ O for 1 h. Afterward, plants were transferred into either 20 mM H<sub>2</sub>O<sub>2</sub> or ddH<sub>2</sub>O and harvested after 10 or 30 min of incubation. Complete rosettes of 12 plants per treatment were pooled and immediately frozen in liquid nitrogen. Frozen plant material was homogenized using a precooled mortar and pestle and stored at -80°C. For peptide isolation, 500 mg of frozen plant material was mixed with 2 ml Lacus buffer (20 mM Tris [pH 7.7], 80 mM NaCl, 0.75 mM EDTA, 1 mM CaCl<sub>2</sub>, 5 mM MgCl<sub>2</sub>, 1 mM DTT, 1/200 mM NaF) containing 4 tablets of protease inhibitor (Roche cOmplete, EDTA-free, Protease inhibitor cocktail tablets) and 10 tablets of phosphatase inhibitor (Roche PhosSTOP) per 200 ml. Samples were incubated for 10 min on ice and then centrifuged at 15 000 g for 10 min at 4°C. The supernatant was transferred to a new tube, adjusted to 20% (v/v) trichloroacetic acid, and incubated overnight at -20°C. The precipitated samples were stored until preparation for mass spectrometry analysis.

Samples were centrifuged at 15 000 g, vacuum-dried, and eluted in urea lysis buffer (8 M urea, 150 mM NaCl, and 40 mM Tris-HCl [pH 8]). Protein concentration was determined via BCA assay (Thermo Fisher). In total, 3 mg of protein per sample was first reduced in 5 mM DTT and then alkylated in 15 mM iodoacetamide for 30 min at room temperature in the dark. The alkylated samples were quenched by adding DTT to a final concentration of 5 mM and mixed with 30 mg Sera-Mag carboxylate-modified magnetic beads (1:1 ratio of hydrophilic and hydrophobic beads, Cytiva, USA). The peptides attached to the beads were washed four times with 80% (v/ v) ethanol and digested in a 30 mM ammonium bicarbonate buffer (pH 8.2) containing 30 µg trypsin (Promega, WI, USA). Tryptic digestion was performed overnight at 37°C under constant shaking. The digestion was stopped by the addition of formic acid (end concentration, 4%). In total,  $100 \mu g$  of digested peptides per sample was transferred to a new reaction tube, vacuum-dried, and stored at -20°C until high-pressure liquid chromatography-tandem mass spectrometry (MS/MS) analysis.

The purified tryptic peptides were dissolved in 0.1% (v/v) formic acid in high-purity water. Approximately 1  $\mu g$  of peptides was separated by an online reversed-phase high-pressure liquid chromatography apparatus (Thermo Scientific Dionex Ultimate 3000 RSLCnano LC system) connected to a benchtop quadrupole orbitrap (Q-Exactive Plus) mass spectrometer (Thermo Fisher Scientific). The separation was carried out on

an Easy-Spray analytical column (PepMap RSLC C18, 2  $\mu$ m, 100 Å, 75  $\mu$ m i.d. × 50 cm, Thermo Fisher Scientific) with an integrated emitter, and the column was heated to 55°C. The liquid chromatography (LC) gradient was set to a 140-min gradient method, with a flow rate of 300 nl/min. The LC gradient was set to 5%–50% buffer B (v/v) (79.9% ACN, 0.1% formic acid, 20% ultra-high purity H<sub>2</sub>O [MilliQ]) for 125 min and then to 80% buffer B over 5 min.

LC eluent was introduced into the mass spectrometer through an Easy-Spray ion source (Thermo Scientific) with the emitter operated at 1.9 kV. The mass spectra were measured in positive ion mode, applying a top 15 data-dependent acquisition. A full mass spectrum was set to 70 000 resolution at *m/z* 200 (automatic gain control target at 1e6, maximum injection time of 120 ms, and a scan range of 400–1600 [*m/z*]). The mass spectrometry scan was followed by an MS/MS scan at 17 500 resolution at *m/z* 200 (automatic gain control target at 5e4, 1.6 *m/z* isolation window, and maximum injection time of 80 ms). For MS/MS fragmentation, the normalized collision energy for higher-energy collisional dissociation was set to 27%. Dynamic exclusion was set to 40 s, and unassigned and +1, +7, +8, and >+8 charged precursors were excluded. The intensity threshold was set to 6.3e3, and isotopes were excluded. The analysis was performed with five independent experimental replicates for each sample. *Peptide identification and quantification* 

Identities and peptide features were defined by the peptide search engine Andromeda, which was provided by MaxQuant software (v.2.1.3.0, Max Planck Institute of Biochemistry), using standard settings (Tyanova et al., 2016b). In detail, trypsin-based digestion of the peptides with up to two missing cleavage sites was selected. Methionine oxidation as well as N-terminal acetylation was set as a variable modification for peptide identification. In total, up to three potential modification sites per peptide were accepted. The identified peptide sequences were searched and aligned against the Araport11 (Cheng et al., 2017) reference protein database. The false discovery rate cutoff for protein identification and side identification was set to 0.01. The minimum peptide length was 7 amino acids, and the maximum length was 40 amino acids. For each identified protein group, label-free quantitation intensities were calculated and used for further analysis (Supplemental Table 4).

Potential contaminants and reverse-sequenced peptides were removed before statistical analysis. Only proteins that were detected in at least three of five replicates in at least one treatment group were considered for statistical analysis, which was performed using Perseus (v.2.0.7.0) (Tyanova et al., 2016a). Missing values were replaced by sampling from a normal distribution using the default settings. Protein groups with an absolute fold change of greater than 1.5 compared with the control and a false discovery rate value below 0.05 were considered significantly regulated (Supplemental Table 4).

To filter for  $\operatorname{Ca}^{2^+}$ -regulated proteins, significantly up(down)regulated proteins in  $\operatorname{La}^{3^+}$  +  $\operatorname{H}_2\operatorname{O}_2$ -treated samples compared with  $\operatorname{La}^{3^+}$ -only-treated samples were subtracted from the list of significantly up(down)regulated proteins in  $\operatorname{H}_2\operatorname{O}_2$ -treated samples. An additional filtering step was performed to ensure a compelling difference in abundance between the two contrasts. This required that  $\operatorname{abs}(L_1-L_2)\geq 1$ , where  $L_1=\log$  fold change for  $\operatorname{H}_2\operatorname{O}_2$  vs. mock and  $L_2=\log$  fold change for  $\operatorname{La}^{3^+}+\operatorname{H}_2\operatorname{O}_2$  treatment vs.  $\operatorname{La}^{3^+}$  only. For each of the protein groups that passed the filters, we extracted all identifiers in the group. For identifiers that occurred in multiple groups, we removed the identifier from the group where it occurred the least.

#### CKN network analysis

For each Ca<sup>2+</sup>-dependent redox-responsive protein group (target), we identified the closest nodes upstream that had a known Ca<sup>2+</sup>-signaling association (source). This was done by identifying all shortest paths in CKN with the source nodes set as all genes with Ca<sup>2+</sup>-signaling-related GoMapMan (Ramšak et al., 2014) annotations and the target set as the

 $\text{Ca}^{2^+}\text{-dependent}$   $\text{H}_2\text{O}_2\text{-responsive}$  peptides. The GoMapMan annotations considered were "30.3 - signaling.calcium," "34.21 - transport.calcium," and "34.22 - transport.cyclic nucleotide or calcium regulated channels." For each target, we kept the source(s) with the shortest paths to the target (the "closest" upstream potential  $\text{Ca}^{2^+}$  interactor). We used the CUT-tool on the merged network to determine the cut-set between all the source nodes and each target. The capacity on the edges was set as the edge rank + 1 (highly ranked edges are more likely to be in the cut-set).

All source and target nodes are listed in Supplemental Table 4, and the complete network is available to view as a high-quality pdf in Supplemental Figure 3. Analysis was performed in Python using the networkX library (Hagberg et al., 2008) and visualized in Cytoscape (Cline et al., 2007) using the py4cytoscape library (Ono et al., 2021). All code is available in the SKM-tools repository (https://github.com/NIB-SI/skm-tools).

#### Gene identifiers

All genes mentioned in the article are listed with their gene identifiers in Supplemental Table 10.

#### SUPPLEMENTAL INFORMATION

Supplemental information is available at Plant Communications Online.

#### **FUNDING**

SKM was developed with funding from the European Union's Horizon 2020 research and innovation programme under grant agreement 862858 (ADAPT); the Slovenian Research Agency under grant agreements 1000-15-0105, Z7-1888, J4-1777, P4-0165, N4-0199, Z4-50146, and J4-3089; and ELIXIR, the research infrastructure for life science data through the ELIXIR Implementation Study "Increasing plant data findability for ELIXIR and beyond" and ELIXIR-SI. We gratefully acknowledge funding from the Deutsche Forschungsgemeinschaft (DFG) to U.C.V. (INST 217/939-1 FUGG).

#### **AUTHOR CONTRIBUTIONS**

For SKM: software and visualization, C.B. and V.P.; data curation of CKN, Ž.R. and C.B.; data curation of PSS, C.B., Ž.R., M.Z., Š.B., M.P., M.K., A.Ž., and K.G.; supervision, project administration, and funding acquisition, KG. For case studies: methodology, L.A.-S. and W.W.; investigation, A.B., B.W., A.v.D., J.G., and L.A.-S.; formal analysis, A.B. and C.B.; data curation, A.B., B.W., A.v.D., L.A.-S., M.Z., and Š.B.; visualization, C.B., A.B., and M.Z.; supervision, U.C.V., M.T., and K.G.; project administration and funding acquisition, U.C.V., M.T., and K.G. Writing – original draft, C.B., A.B., Ž.R., and K.G. All authors took part in writing – review & editing.

#### **ACKNOWLEDGMENTS**

We would like to acknowledge Solana Research GmbH for producing StRD29::fluc Désirée transgenic potatoes and Nelly Braun for preselection of the StRD29 lines. We would also like to thank the many additional contributors to PSS: Anna Coll, Barbara Jaklič, Christian Bachem, Christian Schuy, Juan Antonio López-Ráez, Katja Stare, Maria Pozo, Mojca Juteršek, Špela Tomaž, Tim Godec, Tjaša Lukan, Tjaša Mahkovec Povalej, Valentina Levak, Vaňková Radka, Vid Modic, and Maroof Shaikh. For support in integration of SKM into FAIDARE, we would like to thank Cyril Pommier. Part of this work was performed during the 2nd BioHackathon Germany in Bielefeld, organized by de.NBI and ELIXIR Germany in December 2023. Finally, we would like to acknowledge Zoran Nikoloski for discussions regarding the CKN analyses. No conflict of interest is declared.

Received: December 28, 2023 Revised: March 28, 2024 Accepted: April 11, 2024 Published: April 15, 2024

#### **REFERENCES**

- Aleman, F., Yazaki, J., Lee, M., Takahashi, Y., Kim, A.Y., Li, Z., Kinoshita, T., Ecker, J.R., and Schroeder, J.I. (2016). An ABA-increased interaction of the PYL6 ABA receptor with MYC2 Transcription Factor: A putative link of ABA and JA signaling. Sci. Rep. 6, 28941.
- **Aric, H., Schult, D., and Renieris, M.** (2024). PyGraphviz [Computer software]. https://pygraphviz.github.io.
- Arvidsson, S., Kwasniewski, M., Riaño-Pachón, D.M., and Mueller-Roeber, B. (2008). QuantPrime a flexible tool for reliable high-throughput primer design for quantitative PCR. BMC Bioinf. 9:465.
- Baebler, Š., Svalina, M., Petek, M., Stare, K., Rotter, A., Pompe-Novak, M., and Gruden, K. (2017). quantGenius: implementation of a decision support system for qPCR-based gene quantification. BMC Bioinf. 18:276.
- Baker, S.S., Wilhelm, K.S., and Thomashow, M.F. (1994). The 5'-region of Arabidopsis thaliana cor15a has cis-acting elements that confer cold-drought- and ABA-regulated gene expression. Plant Mol. Biol. 24:701–713.
- Balci, H., Siper, M.C., Saleh, N., Safarli, I., Roy, L., Kilicarslan, M., Ozaydin, R., Mazein, A., Auffray, C., Babur, Ö., et al. (2021). Newt: a comprehensive web-based tool for viewing, constructing and analyzing biological maps. Bioinformatics 37:1475–1477.
- Berardini, T.Z., Reiser, L., Li, D., Mezheritsky, Y., Muller, R., Strait, E., and Huala, E. (2015). The arabidopsis information resource: Making and mining the "gold standard" annotated reference plant genome. genesis 53:474–485.
- Bergmann, F.T., Czauderna, T., Dogrusoz, U., Rougny, A., Dräger, A., Touré, V., Mazein, A., Blinov, M.L., and Luna, A. (2020). Systems biology graphical notation markup language (SBGNML) version 0.3. J. Integr. Bioinforma 17.
- Bittner, A., Cieśla, A., Gruden, K., Lukan, T., Mahmud, S., Teige, M., Vothknecht, U.C., and Wurzinger, B. (2022). Organelles and phytohormones: a network of interactions in plant stress responses. J. Exp. Bot. **73**:7165–7181.
- Bornstein, B.J., Keating, S.M., Jouraku, A., and Hucka, M. (2008). LibSBML: an API Library for SBML. Bioinformatics **24**:880–881.
- Caspi, R., Billington, R., Ferrer, L., Foerster, H., Fulcher, C.A., Keseler, I.M., Kothari, A., Krummenacker, M., Latendresse, M., Mueller, L.A., et al. (2016). The MetaCyc database of metabolic pathways and enzymes and the BioCyc collection of pathway/genome databases. Nucleic Acids Res. 44:D471–D480.
- Cheng, C.-Y., Krishnakumar, V., Chan, A.P., Thibaud-Nissen, F., Schobel, S., and Town, C.D. (2017). Araport11: a complete reannotation of the Arabidopsis thaliana reference genome. Plant J. 89:789–804.
- Chow, C.-N., Lee, T.-Y., Hung, Y.-C., Li, G.-Z., Tseng, K.-C., Liu, Y.-H., Kuo, P.-L., Zheng, H.-Q., and Chang, W.-C. (2019). PlantPAN3.0: a new and updated resource for reconstructing transcriptional regulatory networks from ChIP-seq experiments in plants. Nucleic Acids Res. 47:D1155–D1163.
- Cline, M.S., Smoot, M., Cerami, E., Kuchinsky, A., Landys, N., Workman, C., Christmas, R., Avila-Campilo, I., Creech, M., Gross, B., et al. (2007). Integration of biological networks and gene expression data using Cytoscape. Nat. Protoc. 2:2366–2382.
- Cusack, S.A., Wang, P., Lotreck, S.G., Moore, B.M., Meng, F., Conner, J.K., Krysan, P.J., Lehti-Shiu, M.D., and Shiu, S.-H. (2021).
  Predictive Models of Genetic Redundancy in Arabidopsis thaliana.
  Mol. Biol. Evol. 38:3397–3414.
- **Eckardt, N.A.** (2015). The Plant Cell Reviews Dynamic Aspects of Plant Hormone Signaling and Crosstalk. Plant Cell **27**:1–2.

- Edmonds, J., and Karp, R.M. (1972). Theoretical Improvements in Algorithmic Efficiency for Network Flow Problems. J. ACM 19:248–264.
- Foix, L., Nadal, A., Zagorščak, M., Ramšak, Ž., Esteve-Codina, A., Gruden, K., and Pla, M. (2021). Prunus persica plant endogenous peptides PpPep1 and PpPep2 cause PTI-like transcriptome reprogramming in peach and enhance resistance to Xanthomonas arboricola pv. pruni. BMC Genom. 22:360.
- **Gansner, E.R., and North, S.C.** (2000). An open graph visualization system and its applications to software engineering. Software Pract. Ex. **30**:1203–1233.
- Garrett, K.A. (2013). Agricultural impacts: Big data insights into pest spread. Nat. Clim. Change 3:955–957.
- Hagberg, A.A., Schult, D.A., and Swart, P.J. (2008). Exploring Network Structure, Dynamics, and Function using NetworkX. In Proceedings of the 7th Python in Science Conference (SciPy 2008) (Pasadena).
- Hassani-Pak, K., Singh, A., Brandizi, M., Hearnshaw, J., Parsons, J.D., Amberkar, S., Phillips, A.L., Doonan, J.H., and Rawlings, C. (2021). KnetMiner: a comprehensive approach for supporting evidence-based gene discovery and complex trait analysis across species. Plant Biotechnol. J. 19:1670–1678.
- Hastings, J., Owen, G., Dekker, A., Ennis, M., Kale, N., Muthukrishnan, V., Turner, S., Swainston, N., Mendes, P., and Steinbeck, C. (2016). ChEBI in 2016: Improved services and an expanding collection of metabolites. Nucleic Acids Res. 44:D1214–D1219.
- Herwig, R., Hardt, C., Lienhard, M., and Kamburov, A. (2016). Analyzing and interpreting genome data at the network level with ConsensusPathDB. Nat. Protoc. 11:1889–1907.
- Hunter, M.C., Smith, R.G., Schipanski, M.E., Atwood, L.W., and Mortensen, D.A. (2017). Agriculture in 2050: Recalibrating targets for sustainable intensification. Bioscience 67:386–391.
- IPPC Secretariat. (2021). Scientific Review of the Impact of Climate Change on Plant Pests – A Global Challenge to Prevent and Mitigate Plant Pest Risks in Agriculture, Forestry and Ecosystems (Rome: FAO on behalf of the IPPC Secretariat).
- Juteršek, M., Petek, M., Ramšak, Ž., Moreno-Giménez, E., Gianoglio, S., Mateos-Fernández, R., Orzáez, D., Gruden, K., and Baebler, Š. (2022). Transcriptional deregulation of stress-growth balance in Nicotiana benthamiana biofactories producing insect sex pheromones. Front. Plant Sci. 13, 941338.
- Kanehisa, M., Sato, Y., Kawashima, M., Furumichi, M., and Tanabe, M. (2016). KEGG as a reference resource for gene and protein annotation. Nucleic Acids Res. 44:D457–D462.
- Keating, S.M., Waltemath, D., König, M., Zhang, F., Dräger, A., Chaouiya, C., Bergmann, F.T., Finney, A., Gillespie, C.S., Helikar, T., et al. (2020). SBML Level 3: an extensible format for the exchange and reuse of biological models. Mol. Syst. Biol. 16, e9110.
- Ono, K., Bouças, J., Nishida, K., and Demchak, B. (2021). py4cytoscape [Computer software]. https://py4cytoscape.readthedocs.io.
- **Klarner, H., Streck, A., and Siebert, H.** (2017). PyBoolNet: A python package for the generation, analysis and visualization of boolean networks. Bioinformatics **33**:770–772.
- Knight, M.R., Smith, S.M., and Trewavas, A.J. (1992). Wind-induced plant motion immediately increases cytosolic calcium. Proc. Natl. Acad. Sci. USA 89:4967–4971.
- König, M. (2020). matthiaskoenig/libsbgn-python: 0.2.2 Advance Access. https://doi.org/10.5281/zenodo.4171366.
- Kudla, J., Batistič, O., and Hashimoto, K. (2010). Calcium Signals: The Lead Currency of Plant Information Processing. Plant Cell 22:541–563.
- Lichtenberg, J., Yilmaz, A., Welch, J.D., Kurz, K., Liang, X., Drews, F., Ecker, K., Lee, S.S., Geisler, M., Grotewold, E., and Welch, L.R.

- (2009). The word landscape of the non-coding segments of the Arabidopsis thaliana genome. BMC Genom. 10:463.
- Miljkovic, D., Stare, T., Mozetič, I., Podpečan, V., Petek, M., Witek, K., Dermastia, M., Lavrač, N., and Gruden, K. (2012). Signalling Network Construction for Modelling Plant Defence Response. PLoS One 7, e51822.
- Mueller, L.A., Zhang, P., and Rhee, S.Y. (2003). AraCyc: A Biochemical Pathway Database for Arabidopsis. Plant Physiol. **132**:453–460.
- Mur, L.A.J., Kenton, P., Atzorn, R., Miersch, O., and Wasternack, C. (2006). The Outcomes of Concentration-Specific Interactions between Salicylate and Jasmonate Signaling Include Synergy, Antagonism, and Oxidative Stress Leading to Cell Death. Plant Physiol. 140:249–262.
- **Müssel, C., Hopfensitz, M., and Kestler, H.A.** (2010). BoolNet an R package for generation, reconstruction and analysis of Boolean networks. Bioinformatics **26**:1378–1380.
- Nomoto, M., Skelly, M.J., Itaya, T., Mori, T., Suzuki, T., Matsushita, T., Tokizawa, M., Kuwata, K., Mori, H., Yamamoto, Y.Y., et al. (2021). Suppression of MYC transcription activators by the immune cofactor NPR1 fine-tunes plant immune responses. Cell Rep. 37, 110125.
- Otasek, D., Morris, J.H., Bouças, J., Pico, A.R., and Demchak, B. (2019). Cytoscape Automation: empowering workflow-based network analysis. Genome Biol. 20:185.
- **Peixoto, T.P.** (2014). The graph-tool python library (*figshare* Advance). https://doi.org/10.6084/m9.figshare.1164194.
- Pirayesh, N., Giridhar, M., Ben Khedher, A., Vothknecht, U.C., and Chigri, F. (2021). Organellar calcium signaling in plants: An update. Biochim. Biophys. Acta Mol. Cell Res. 1868, 118948.
- Podpečan, V. (2023). Vpodpecan/Pysbgn: v0.2.1 Advance Access. https://doi.org/10.5281/zenodo.7966410.
- Podpečan, V., Ramšak, Ž., Gruden, K., Toivonen, H., and Lavrač, N. (2019). Interactive exploration of heterogeneous biological networks with Biomine Explorer. Bioinformatics 35:5385–5388.
- Pylianidis, C., Osinga, S., and Athanasiadis, I.N. (2021). Introducing digital twins to agriculture. Comput. Electron. Agric. 184, 105942.
- Ramsak, Ž., Baebler, Š., Rotter, A., Korbar, M., Mozetič, I., Usadel, B., and Gruden, K. (2014). GoMapMan: integration, consolidation and visualization of plant gene annotations within the MapMan ontology. Nucleic Acids Res. 42:D1167–D1175.
- Ramšak, Ž., Coll, A., Stare, T., Tzfadia, O., Baebler, Š., Van de Peer, Y., and Gruden, K. (2018). Network modeling unravels mechanisms of crosstalk between ethylene and salicylate signaling in potato. Plant Physiol. 178:488–499.
- Rentel, M.C., and Knight, M.R. (2004). Oxidative Stress-Induced Calcium Signaling in Arabidopsis. Plant Physiol. **135**:1471–1479.
- Rocha-Sosa, M., Sonnewald, U., Frommer, W., Stratmann, M., Schell, J., and Willmitzer, L. (1989). Both developmental and metabolic signals activate the promoter of a class I patatin gene. EMBO J. 8:23–29.
- Sebastian, K., Nowee, P., and Carrera, E. (2023). Pydot Advance Access.
- Shannon, P., Markiel, A., Ozier, O., Baliga, N.S., Wang, J.T., Ramage,
   D., Amin, N., Schwikowski, B., and Ideker, T. (2003). Cytoscape: A
   Software Environment for Integrated Models of Biomolecular Interaction Networks. Genome Res. 13:2498–2504.
- (2022). IPCC, 2022: Summary for Policymakers. In Climate Change 2022: Mitigation of Climate Change. Contribution of Working Group III to the Sixth Assessment Report of the Intergovernmental Panel on Climate Change, P.R. Shukla, J. Skea, R. Slade, A. Al Khourdajie, R. van Diemen, D. McCollum, M. Pathak, S. Some, R. Vyas, and M. Fradera, et al., eds. (Cambridge University Press).

- Steinwand, M.A., and Ronald, P.C. (2020). Crop biotechnology and the future of food. Nat. Food 1:273–283.
- **Stuhlfelder, C., Lottspeich, F., and Mueller, M.J.** (2002). Purification and partial amino acid sequences of an esterase from tomato. Phytochemistry **60**:233–240.
- Szklarczyk, D., Kirsch, R., Koutrouli, M., Nastou, K., Mehryary, F., Hachilif, R., Gable, A.L., Fang, T., Doncheva, N.T., Pyysalo, S., et al. (2023). The STRING database in 2023: protein–protein association networks and functional enrichment analyses for any sequenced genome of interest. Nucleic Acids Res. 51:D638–D646.
- Tracy, F.E., Gilliham, M., Dodd, A.N., Webb, A.a.R., and Tester, M. (2008). NaCl-induced changes in cytosolic free Ca2+ in Arabidopsis thaliana are heterogeneous and modified by external ionic composition. Plant Cell Environ. 31:1063–1073.
- Tyanova, S., Temu, T., Sinitcyn, P., Carlson, A., Hein, M.Y., Geiger, T., Mann, M., and Cox, J. (2016a). The Perseus computational platform for comprehensive analysis of (prote)omics data. Nat. Methods 13:731–740.
- **Tyanova, S., Temu, T., and Cox, J.** (2016b). The MaxQuant computational platform for mass spectrometry-based shotgun proteomics. Nat. Protoc. **11**:2301–2319.

- United Nations Department of Economic and Social Affairs, Population Division. (2022). World Population Prospects 2022: Summary of Results.
- Van Bel, M., Silvestri, F., Weitz, E.M., Kreft, L., Botzki, A., Coppens, F., and Vandepoele, K. (2022). PLAZA 5.0: extending the scope and power of comparative and functional genomics in plants. Nucleic Acids Res. 50:D1468–D1474.
- Wilkinson, M.D., Dumontier, M., Aalbersberg, I.J., Appleton, G., Axton, M., Baak, A., Blomberg, N., Boiten, J.-W., da Silva Santos, L.B., Bourne, P.E., et al. (2016). The FAIR Guiding Principles for scientific data management and stewardship. Sci. Data 3, 160018.
- Wu, J., Wang, L., and Baldwin, I.T. (2008). Methyl jasmonate-elicited herbivore resistance: does MeJA function as a signal without being hydrolyzed to JA? Planta 227:1161–1168.
- Zagorščak, M., Blejec, A., Ramšak, Ž., Petek, M., Stare, T., and Gruden, K. (2018). DiNAR: revealing hidden patterns of plant signalling dynamics using Differential Network Analysis in R. Plant Methods 14:78.
- Zhang, N., Zhou, S., Yang, D., and Fan, Z. (2020). Revealing Shared and Distinct Genes Responding to JA and SA Signaling in Arabidopsis by Meta-Analysis. Front. Plant Sci. 11.